16th International Workshop on Inelastic Ion-Surface Collisions (IISC-16)

Schloss Hernstein, A-2560 Hernstein, Austria
September 17 -22, 2006

Book of Abstracts

PFEIFFER VACUUM
Austria & C.E. Europe

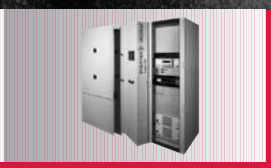

AT THE HEART OF VACUUM TECHNOLOGY.

Vacuum generation technology plays a significant role in many laboratory and manufacturing environments, and lies at the heart of many production processes. The crucial needs are for powerful, stable solutions. Pfeiffer Vacuum offers outstanding vacuum resources ranging from pressure measurement equipment to complete systems, so you always get the perfect results you need.

Pfeiffer Vacuum – the vacuum technology experts.

Pfeiffer Vacuum Austria GmbH
Diefenbachgasse 35 · A-1150 Wien · Phone: +43-1-8941-704 · Fax: +43-1-8941-707 · office@pfeiffer-vacuum.at

16th International Workshop on Inelastic Ion-Surface Collisions (IISC-16)

Schloss Hernstein, A-2560 Hernstein, Austria
September 17 -22, 2006

Book of Abstracts

Conference Chair

F. Aumayr (Austria)

International Scientific Committee

A. Arnau (Spain)
F. Aumayr (Austria)
A. Borisov (France)
V.Kh. Ferleger (Uzbekistan)
A. Hamza (USA)
R. Hoekstra (Netherlands)
D. Jacobs (USA)
T. Koshikawa (Japan)
M.L. Martiarena (Argentina)
K. Morita (Japan)
H. Niehus (Germany)
M. Schleberger (Germany)
I.F. Urazgil'din (Russian Federation)
P.A. Zeijlmans van Emmichoven (Netherlands)

Local Organizing Committee

F. Aumayr (TU Wien)
J. Burgdörfer (TU Wien)
A. Golczewski (TU Wien)
W. Husinsky (TU Wien)
C. Lemell (TU Wien)
M. Marik (TU Wien)
W. Meissl (TU Wien)
K. Schiessl (TU Wien)
B. Solleder (TU Wien)
HP. Winter (TU Wien)

"Institut für Allgemeine Physik" and "Institut für Theoretische Physik"
Technische Universität Wien (Vienna University of Technology)
Wiedner Hauptstr. 8-10, A-1040 Vienna, Austria

Sponsors

The Organizing Committee gratefully acknowledges financial support by

The Government of Lower Austria (Land Niederösterreich)

Austrian Federal Ministry for Education, Science and Culture

Vienna University of Technology

Pfeiffer-Vacuum

Austrian Vacuum Society

Tectra Company

Medieninhaber: F. Aumayr, Institut für Allgemeine Physik, Technische Universität Wien,
Adresse: Wiedner Hauptstr. 8-10/E134, A-1040 Wien
Druck: R. & W. Smutny OEG, A-1110 Wien

PREFACE

Welcome to the 16th International Workshop on Inelastic Ion Surface Collisions (IISC-16)! The history of IISC dates back to the mid 1970s (see table below). This year we are happy to organize IISC for the second time in Austria.

The series of IISC meetings seeks to promote the growth of scientific knowledge and its efficient exchange among scientists in the field of inelastic interactions of particles with surfaces. The meetings provide an informal workshop atmosphere with time for discussions and no parallel sessions. To this purpose the workshops are usually held at a somewhat remote location instead of a big city, and the total number of participants is limited to about 100. Hernstein Palace, a historic chateau once owned by the Habsburg family, has been chosen as the conference location for IISC-16. Located in an idyllic park with a small lake it is situated just 50 km south of Vienna city centre.

We hope that all participants will experience a lively and successful meeting while enjoying the attractive surroundings in this beautiful region of Austria.

Fritz Aumayr
Chair of IISC-16

History of IISC

IISC	Year	Location	Country	Organizers
1	1976	Bell Labs, Murray Hill, NJ	USA	N. Tolk
2	1978	McMaster Univ., Hamilton	Canada	R. Kelly
3	1980	Feldkirchen-Westerham	Germany	E. Taglauer, W. Heiland
4	1982	Hindsgavl Manor, Middelfart	Denmark	P. Sigmund
5	1984	Gold Canyon Ranch, AZ	USA	P. Williams
6	1986	ARNL, Argonne, Illinois	USA	D. Gruen
7	1988	Jagellonian Univ., Krakow	Poland	M. Szymonski
8	1990	Wiener Neustadt	Austria	G. Betz, P. Varga
9	1992	Aussois	France	M. Bernheim, J.P. Gauyacq
10	1994	Grand Targhee, WY	USA	N. Tolk, P. Nordlander
11	1996	Island of Wangerooge	Germany	W. Heiland
12	1998	South Padre Island, Texas	USA	J.W. Rabalais, P. Nordlander
13	2000	San Carlos de Bariloche	Argentina	M. Martiarena, V.H. Ponce
14	2002	Island of Ameland	Netherlands	R. Hoekstra, P. Zeijlmans v. E.
15	2004	Ise-Shima	Japan	K. Morita, T. Koshikawa
16	2006	Hernstein	Austria	F. Aumayr

16th International Workshop on Inelastic Ion-Surface Collisions (IISC-16)

Schloss Hernstein, A-2560 Hernstein, Austria
September 17 -22, 2006

Time Schedule

Sunday, 17 September 2006

15:00 – 20:00 **Registration**

17:30 – 18:30 **Welcome Reception**

18:30 DINNER

Monday, 18 September 2006

08:30 – 08:45 **F. Aumayr**
Welcome and Opening

Session Chair: K. Morita (Japan)

08:45 – 09:30 **Y. Yamazaki** (Japan) PL
Interaction of slow highly charged ions with metals and insulators

09:30 – 10:00 **P. Skog** (Sweden) I
Guiding of highly-charged ions through insulating nano-capillaries

10:00 – 10:20 **K. Schiessl** (Austria) O
Simulation of guiding of multiply charged projectiles through insulating capillaries

10:20 COFFEE

Session Chair: P. A. Zeijlmans van Emmichoven (Netherlands)

10:50 – 11:20 **S. Wethekam** (Germany) I
Auger neutralization of He ions at aluminum surfaces

11:20 – 11:40 **P. Roncin** (France) O
Auger neutralization rates on NaCl (001): final state dependence

11:40 – 12:00 **S. Markin** (Austria) O
Neutralization of low energy He^+ ions by Cu in the Auger regime

12:15 LUNCH

Session Chair: S. Facsko (Germany)

14:00 – 14:30 **M. Tona** (Japan) I
Potential sputtering from a Si surface by very highly charged ion impact

14:30 – 14:50 **A. S. El-Said** (Austria) O
Creation of surface nanostructures on CaF_2 by irradiation with slow highly charged ions

14:50 – 15:20 **Z. Insepov** (USA) I
Surface erosion and modification by ions studied by computer simulation

15:20 – 15:40 **H. Rothard** (France) O
Sputtering by highly charged heavy ions: Application of the xy-TOF technique to secondary ion ejection

15:45 COFFEE

Session Chair: R. Hoekstra (Netherlands)

16:15 – 16:45 **T. D. Märk** (Austria) I
Reactive ion-surface collisions

16:45 – 17:15 **O. Grizzi** (Argentina) I
Direct recoil spectroscopy of alkanethiol-covered surfaces

17:15 – 17:35 **J. Laskin** (USA) O
Interaction of hyperthermal peptide ions with self-assembled monolayer surfaces

17:35 – 17:55 **M. L. Martiarena** (Argentina) O
Ab-initio study of the adsorption of CH_3SH molecule on Au(111)

18:30 DINNER

20:00 **Meeting of International Scientific Committee**
Wappensaal

Tuesday, 19 September 2006

Session Chair: N. Stolterfoht (Germany)

08:30 – 09:15 **P. M. Echenique** (Spain) PL
Dynamic screening, energy loss, and electron dynamics in bulk and at surfaces

09:15 – 09:45 **B. Huber** (France) I
Ion interaction with isolated nano-surfaces

09:45 – 10:15 **D. Vernhet** (France) I
The role of collisional processes in the x-ray emission during laser-cluster interaction

10:15 COFFEE

Session Chair: H. Jouin (France)

10:45 – 11:15 **K. Kimura** (Japan) I
Interactions of C_{60}^{+} ions with a KCl(001) surface under grazing incidence

11:15 – 11:45 **M. S. Gravielle** (Argentina) I
Grazing collisions with insulator surfaces

11:45 – 12:05 **I. Aldazábal** (Spain) O
Convoy electron emission and energy loss of swift protons in grazing collision against LiF(001), KCl(100) and KI(100) surfaces

12:05 – 12:25 **M. Kato** (Japan) O
Energy spectrum shape of low energy ion scattering from insulators and its similarity to asymmetric spectrum shape observed in core level XPS

12:30 LUNCH

Session Chair: J. I. Juaristi (Spain)

14:00 – 14:30 **A. Wucher** (Germany) I
Kinetic excitation of solids: experiment and computer simulation

14:30 – 14:50 **J. Pomeroy** (USA) O
Transport and STM measurements of HCI modified materials

Session Chair: P. Bauer (Austria)

14:50 – 15:50 **Poster Introduction A**

The oral introductions (maximum duration of 2 minutes each) should give the poster presenters a possibility to attract attention to their posters.

W. Meissl (Austria)
Charging and discharging of nano-capillaries during ion-guiding of multiply charged projectiles

Y. Kanai (Japan)
Two dimensional images of slow neon ions guided by nano-capillaries in polymer foils

N. Stolterfoht (Germany)
Scaling laws for ion guiding through nano-capillaries in insulating pet

N. Stolterfoht (Germany)
Electron guiding through nano-capillaries in insulators

R. Vincent (Spain)
Oscillations in the spin polarization of electrons excited by slow ions in a spin-polarized electron gas

P. Bauer (Austria)
Influence of screening length correction on LEIS-spectra

D. Primetzhofer (Austria)
Polar and azimuthal scans for He^+ ions and a Cu(100) surface

K. Khalal-Kouache (Algeria)
Monte Carlo simulation of charge exchange processes in the scattering of 4 KeV He^+ ions by an amorphous silicon surface

A. Duvenbeck (Germany)
On the relative role of electron promotion processes and electronic friction in atomic collision cascades

H. Jouin (France)
Surface-plasmon-assisted electron capture in grazing incidence H^+/Al collisions

H. Winter (Germany)
Energy loss and elecron emission during grazing scattering of fast noble gas atoms from an Al(111)-surface

S. Wethekam (Germany)
Computer simulations of grazing scattering of atomic projectiles from crystal surfaces

I. Aldazabal (Spain)
Time–dependent simulations of electron emission in grazing ion–surface collisions

F. Gou (Netherlands)
Ar scattering from Si(100) surface at grazing incidence: experiment and MD simulation
H. Rothard (France)
Differential multi-electron emission induced by swift highly charged gold ions penetrating carbon foils
T. Kaneko (Japan)
Energy loss of carbon cluster ion impacted on foil
M. Nojima (Japan)
Precise analysis on shave-off depth profiling
K. Morita (Japan)
Temperature dependence of the D-H replacement rates in implanted oxide ceramics exposed to H_2O vapor
S. Nakagawa (Japan)
Antisite defects in a chemical compound crystal caused by ion irradiation
O. Grizzi (Argentina)
Stopping power and final charge fractions in KeV protons traversing thin C and AlF_3 films
W. Rupp (Austria)
Ion beam induced magnetic change of ultrathin Fe films on Cu(100)

15:50 COFFEE

16:00 – 18:30 **Poster Session A**

18:30 DINNER

Special Session Chair: W. Heiland (Germany)
20:00 Special guest speakers:
H. Winter (Germany)
R. Morgenstern (Netherlands)
P. M. Echenique (Spain)

Wednesday, 20 September 2006

Session Chair: C. O. Reinhold (USA)

08:30 – 09:15 **J. Roth** (Germany) PL
Plasma-wall-interaction: important ion induced surface processes and strategy of the EU task force

09:15 – 09:45 **F. W. Meyer** (USA) I
Chemical sputtering of graphite by low energy deuterium projectiles

09:45 – 10:05 **M. Reinelt** (Germany) O
Enhanced room temperature erosion of ultra thin carbon films on titanium, tantalum and beryllium by deuterium ions

10:05 COFFEE

Session Chair: C. Linsmeier (Germany)

10:35 – 11:05 **T. Koshikawa** (Japan) I
Surface and interface structure analysis by using high resolution ion scattering and LEEM/PEEM

11:05 – 11:35 **P. Chakraborty** (India) I
Secondary ion mass spectrometry of MCs_n^+ molecular ion complexes

11:35 – 11:55 **A. Sindona** (Italy) O
Wave packet study of the secondary emission of negatively charged, mono-atomic ions from sputtered metal surfaces

12:15 DEPARTURE OF BUSES FOR CONFERENCE EXCURSION

18:30 VISIT OF A LOCAL "HEURIGEN"

Thursday, 21 September 2006

Session Chair: HP. Winter (Austria)

08:30 – 09:15 **A. M. Wodtke** (USA) PL
Electronic excitations induced by molecule-surface interactions

09:15 – 09:45 **F. B. Dunning** (USA) I
Charge-transfer rates for xenon Rydberg atoms at metal and semiconductor surfaces

09:45 – 10:15 **J-P. Gauyacq** (France) I
Ionisation of Rydberg atoms colliding on metal surfaces

10:15 COFFEE

Session Chair: R. Morgenstern (Netherlands)

10:45 – 11:15 **T. Michely** (Germany) I
Nanostructures by grazing incidence ions: ripple patterns, athermal coarsening and subsurface channeling

11:15 – 11:35 **A. Keller** (Germany) O
Ion-induced nanopatterns on semiconductors: formation and application

11:35 – 12:05 **E. Bertagnolli** (Austria) I
Nanopattern formation with focused ion beams

12:15 LUNCH

Session Chair: B. Ban-d'Etat (France)

14:00 – 14:30 **W. M. Arnoldbik** (Netherlands) I
Nano-scale effects of swift heavy ion irradiation of SiO_x layers and multilayers

14:30 – 14:50 **T. Peters** (Germany) O
SFM investigations of discontinuous ion tracks

14:50 – 15:20 **E. Griesmayer** (Austria) I
The MedAustron project

Session Chair: M. Schleberger (Germany)

15:20 – 16:15 **Poster Introduction B**

The oral introductions (maximum duration of 2 minutes each) should give the poster presenters a possibility to attract attention to their posters.

A. Golczewski (Austria)
Fusion relevant ion - surface collision processes

C. O. Reinhold (USA)
Chemical sputtering of deuterated carbon by D and D_2 impact

N. Endstrasser (Austria)
Ion surface collisions on surfaces relevant for fusion devices

W. Schustereder (Germany)
Sticking coefficient and SIMS of hydrocarbons on fusion relevant plasma sprayed tungsten surfaces

R. Riccardi (Italy)
Angular studies of electron emission in the interaction of slow Na^+ with Al surfaces

W. Meissl (Austria)
Electron emission from insulator surfaces induced by impact of slow highly charged ions

B. Ban-d'Etat (France)
Projectile charge and angle of incidence effect on secondary electron yield

S. Facsko (Germany)
Changing carbon films by highly charged ions

G. Zschornack (Germany)
Production of highly charged ions for ion-surface interaction studies

J. Lenoir (France)
Dynamics of sputtering by highly charged heavy ions investigated by the xy-TOF technique

Y. Sakuma (Japan)
Effect of residual oxygen in Si(111)-7x7 surface on Si^+ and Si^{2+} sputter yields

S. Wethekam (Germany)
Fragmentation of C_{60} ions during grazing scattering from an Al(100) surface

F. B. Dunning (USA)
The dynamics of He^+ ion neutralization at rare gas films: energy- and spin-resolved studies

U. Rasulev (Uzbekistan)
Comparative study of polyatomic secondary ion emission from silicon with Au_m^-, Si_m^- and C_m^- projectiles
U. Rasulev (Uzbekistan)
Sputtering source of cluster ions and surface-ionization source of polyatomic ions of organic compounds
W. Abdallah (Canada)
Asphaltene interaction with metallic surfaces
M. Tomita (Japan)
SIMS depth profile study using metal cluster complex ion bombardment
P. Chakraborty (India)
On the formation mechanism of MCs_2^+ molecular ions under varying oxygen environment
G. Takaoka (Japan)
Interactions of liquid cluster ion beams with metal surfaces
A. Romanyuk (Switzerland)
Ultrasonically-enhanced diffusion and clustering of implanted copper in silica
M. Martiarena (Argentina)
Classical ion trajectory simulation of alkanethiol film growth on Ag(111)
M. S. Gravielle (Argentina)
Impulsive surface-Volkov approach for photoelectron emission from surfaces

16:15 COFFEE

16:30 – 19:00 **Poster Session B**

19:30 CONFERENCE DINNER

Friday, 22 September 2006

Session Chair: H. Winter (Germany)

09:00 – 09:30 **G. Schiwietz** (Germany) I
Auger-electron emission in heavy ion -surface collisions

09:30 – 10:00 **A. M. Borisov** (Russia) I
Ion beam-induced electron emission from carbon-based materials

10:00 – 10:20 **P. Sigmund** (Denmark) O
Electron ejection in collisions between swift heavy ions and atoms

10:20 COFFEE

Session Chair: H. Lebius (France)

10:45 – 11:15 **G. Xiao** (China) I
X-ray emission from hollow atoms

11:15 – 11:45 **M. Unipan** (Netherlands) I
Local spin polarization at surfaces probes by hollow atoms

11:45 – 12:05 **B. Solleder** (Austria) O
Electron emission during scattering of N^{6+} ions from a magnetized iron surface

12:05 CLOSING OF THE WORKSHOP

12:15 LUNCH

DEPARTURE

Contents

Monday, 18.9.2006

INTERACTION OF SLOW HIGHLY CHARGED IONS WITH METALS AND INSULATORS

Y.Yamazaki[1,2 *]

[1] University of Tokyo, 3-8-1 Komaba, Meguro, Tokyo, Japan
[2] RIKEN, 2-1 Hirosawa, Wako, Saitama, Japan

1. INTRODUCTION

Interaction of slow highly charged ions with metallic surfaces has been studied for decades, and various unique features have been discovered [1,2,3,4]. In addition to usual flat surface targets, a thin foil with a multitude of straight holes of ~100nm in diameter (micro-capillary foil) were found to provide unique information on the above surface interaction, where x-rays [5], visible lights [6], charge states of outgoing ions [7], and auger electrons [8] were measured. It is noted that some considerable fraction of ions can pass through the small capillary without suffering violent collisions with the capillary wall but at the same time capturing multiple electrons in their highly excited Rydberg states, i.e., hollow atoms (ions) are extracted in vacuum and their characteristic features such as the electronic states and their decay modes are directly studied.

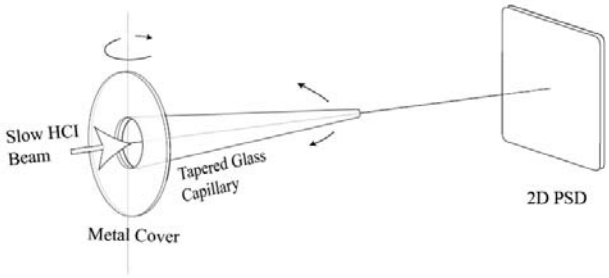

Figure 1: A schematic drawing of the tapered glass capillary setup.

In the case of an insulator micro-capillary foil, when its front and back surfaces are both metal-plated, a so-called guiding effect was observed [9], where slow highly charged ions can transmit through the capillary tunnel keeping their initial charge state even when the capillary axis is tilted against the incident beam. The dynamic feature of the guiding effect including the beginning of the charge up was studied by a 2D PSD (position sensitive detector) [10].

Recently a similar guiding effect was also found for a single tapered glass capillary with its inner diameter varying from ~1mm to ~100nm (see fig.1). The guiding angle was the same as the tilting angle within the experimental accuracy and the transmitted HCIs kept their initial charge states as in the case of refs.9 and 10 [11]. It is expected that such a phenomenon is governed by a self-organized charging and discharging on the inner-

wall of the insulator capillary. Although the interaction of charged particles with insulator surfaces has not been studied very much, such a self-organized charge up is expected to be a general phenomenon, and a new research field might emerge. The prominent feature of this guiding effect with the tapered capillary is the formation of a nano-size beam, which can be applied various field of sciences including biology.

Various aspects of the capillary physics are summarized and future possibilities will be discussed during the talk.

2. REFERENCES

[1] U.A.Arifov et al., Sov. Phys.Tech. Phys. 18, 240 (1973).
[2] J.P.Briand, et al., Phys. Rev. Lett. 65,159 (1990).
[3] J. Burgdoerfer, P.Lerner, F.W.Meyer, Phys. Rev. A44, 5674 (1991).
[4] For recent review works, see F.J. Currell (Ed.), The Physics of Multiply and Highly Charged Ions, Vol. 1 & 2, Kluwer Academic Publishers Group, 2003.
[5] Y. Yamazaki *et al.*, J. Phys. Soc. Jpn. **65**, 1199 (1996), S.Ninomiya et al., 78,4557(1997).
[6] Morishita et al., Phys.Rev.A70, 012902(2004).
[7] D. Murakoshi et al., in XXII ICPEAC Abstracts of Contributed Papers (Santa Fe, USA, 2001), p. 504.
[8] Y.Kanai et al., abstract book of 13th International Conference on the Physics of Highly Charged Ions (Belfast), 2006.
[9] N.Stolterfoht et al.,Phys.Rev.Lett.88, 133201(2002).
[10] Y.Kanai, et al., in XXVI ICPEAC Abstracts of Contributed papers (Rosario, Argentina, 2005).
[11] T.Ikeda et al., in XXVI ICPEAC Abstracts of Contributed papers (Rosario, Argentina, 2005).

* E-mail: yasunori@riken.jp

GUIDING OF HIGHLY-CHARGED IONS THROUGH INSULATING NANO-CAPILLARIES

P. Skog[1,*], *M. B. Sahana*[1], *I. L. Soroka*[1], *Gy. Vikor*[1], *R. T. Rajendra Kumar*[1], *A. Johansson*[2] *and R. Schuch*[1]

[1] Atomic physics, Fysikum, AlbaNova University Centre, S-106 91 Stockholm, Sweden
[2] Dept. of Materials Chemistry, The Ångström Laboratory, Uppsala, Sweden

1. INTRODUCTION

The transmission of highly charged ions (HCI) through nano-capillaries has attracted considerable attention during recent years [1, 2, 3, 4]. In the case of HCI impingent on insulating capillaries at angles larger than the angle given by the aspect ratio, substantial transmission of ions in the initial charge state and at the initial kinetic energy was found.
The transmission of slow HCI through insulating capillaries in PET was first reported by Stolterfoht *et al*. [2]. Here 3 keV Ne^{7+} ions were transmitted at capillary tilt angles of up to 25°, with respect to the incident beam, with a spread of about a factor 10 larger than the aspect ratio. There is a spread in the orientation of the capillary axes in the PET membranes due to the production method; etching of ion tracks formed by fast heavy ions.
The guiding of HCI through insulating capillaries has been attributed to the formation of near-entrance charge patches, preventing incident ions from coming in close contact with the walls [2, 4]. The further propagation of ions, after the first deflection near the entrance, through the capillaries is attributed to guiding by an electric field from all charges deposited on the capillary walls. The angular distributions are then broadened by the inhomogeneous electric field at the capillary exit due to end effects.
The guiding effect is time dependent; ions hitting the capillary walls deposit positive charge, which will deflect ions incident at a later instant. Full transmission is achieved when equilibrium between deposition and diffusion of charge is reached.

2. EXPERIMENTS

To avoid the geometrical uncertainties inherent in the PET membranes, with the orientation of capillaries, our group manufactured highly ordered, parallel, capillaries in Si through electrochemical etching. These capillaries were then thermally oxidized to produce insulating SiO_2 capillaries, 25 μm in length, 100 nm in diameter and with wall thicknesses of 100 nm [5]. We have also produced highly ordered capillaries in Al_2O_3 with diameters of 60 nm, 10 μm in length [6]. We have performed experiments with capillaries of PET (diam.=100 nm, length=10 μm), of SiO_2 (diam. = 100 nm, length = 25 μm) and of Al_2O_3 (diam. = 60 nm, length = 10 μm) using 7 keV Ne^{7+} ions from the 14 GHz ECR ion source located at the Manne Siegbahn Laboratory, Stockholm.
The measured angular distributions and charge state distributions will be discussed in the talk. Figure 1 shows angular distributions of 7 keV Ne^{7+} ions transmitted through Al_2O_3 capillaries.

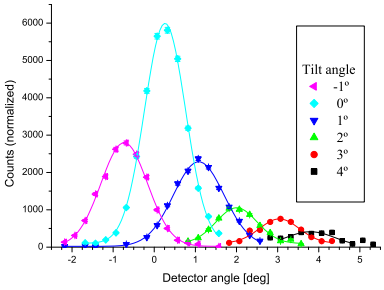

Figure 1: Angular distributions of 7 keV Ne^{7+} ions transmitted through Al_2O_3 capillaries, for capillary tilt angles ranging from -1° to 4°.

3. REFERENCES

[1] S. Ninomiya, Y. Yamazaki, F. Koike, H. Masuda, T. Azuma, K. Komaki, K. Kuroki, and M. Sekiguchi, Phys. Rev. Lett, **78** 4557, (1997).

[2] N. Stolterfoht, J.-H. Bremer, V. Hoffmann, R. Hellhammer, D. Fink, A. Petrov, and B. Sulik, Phys. Rev. Lett., **88** 133201 (2002).

[3] M. B. Sahana, P. Skog, Gy. Vikor, R. T. R. Kumar and R. Schuch, Phys. Rev. A **73** 040901 (2006).

[4] K. Schiessl, W. Palfinger, K. Tksi, H. Nowotny, C. Lemell, and J. Burgdrfer, Phys. Rev. **A 72**, 062902 (2005).

[5] R. T. R. Kumar, X. Badel, G. Vikor, J. Linnros and R. Schuch, Nanotechnology **16** (2005) 1697-1700.

[6] A. Razpet, G. Possnert, A. Johansson, A. Hall and K. Hjort, Nucl. Instr. Meth. B **222** (2004) 593-600.

* E-mail: skog@physto.se

SIMULATION OF GUIDING OF MULTIPLY CHARGED PROJECTILES THROUGH INSULATING CAPILLARIES

K. Schiessl[1,*], *W. Palfinger*[1], *K. Tőkési*[1,2], *H. Nowotny*[1], *C. Lemell*[1], *and J. Burgdörfer*[1]

[1] Institute for Theoretical Physics, Vienna University of Technology, Wiedner Hauptstraße 8-10, A–1040 Vienna, Austria
[2] Institute of Nuclear Research of the Hungarian Academy of Sciences, (ATOMKI), H–4001 Debrecen, P.O.Box 51, Hungary

Recently, capillaries through insulating foils (PET or "Mylar") with aspect ratios $\sim 1:100$ have received interest as a target for beams of slow highly-charged ions (HCIs). Significant transmission probabilities for projectiles in their initial charge state have been measured for incidence angles as large as $\sim 20^\circ$ [1]. Apparently, ions are guided along the capillary axis and do not closely interact with the inner walls of the capillary. More recently, ion guiding could even be observed through macroscopically large, tapered glass capillaries [2]. Key to such processes is a self-organized charge-up of the internal insulator walls due to preceding ion impacts. Ion guiding through the capillary ensues as soon as dynamical equilibrium of the charge-up is established [1].

A theoretical description and simulation of this process poses a considerable challenge in view of the widely disparate time scales present in this problem, ranging from charge transport on the internal capillary wall (hopping time $\tau_h < 10^{-15}$ s) to the average time interval $\overline{\Delta t}$ between two HCIs entering the same capillary which is (for present experimental current densities of nA/mm^2) of the order of $\overline{\Delta t} \approx 0.1$ s. Additionally, characteristic (bulk) discharge times τ_b for Mylar can be estimated from conductivity data to typically exceed $\tau_b \gtrsim 10^3$ s, while discharging arising from surface charge transport is about a factor 100 faster [3]. As a fully microscopic *ab-initio* simulation covering all relevant scales is undoubtedly out of reach, the present approach represents a mean-field classical transport theory, based on a microscopic classical-trajectory Monte Carlo (CTMC) simulation for the transported HCI. Calculation of the ion trajectory is self-consistently coupled to the charge-up of the internal capillary walls, employing appropriate models of charge diffusion [3]. In order to explain certain experimental features such as the transmission function (Fig. 1), we find it crucial to distinguish between fast surface- and slow bulk charge transport. We can also reproduce charging- and discharging characteristics which manifest in a time-dependent HCI transmission function of the capillary.

Experimental data for the angular spread of the transmitted HCIs, which is found to be close to the geometrical opening angle ($\approx 1^\circ$) in our CTMC simulation, varies but reaches several degrees in some experiments close to the geometrical opening angle ($\approx 1^\circ$) in our CTMC simulation, but up to several degrees in some experiments [1]. Phenomenological inclusion of imperfect target preparation (alignment of capillary axis) and multi-capillary effects could offer an explanation for this discrepancy [3].

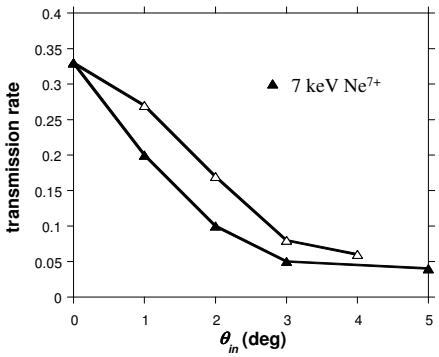

Figure 1: Transmission probability as a function of angle of incidence θ_{in} relative to the mean capillary axis. Full symbols: present CTMC, open symbols: experimental data: 7 keV Ne^{7+} (Vikor et al. [4]). Experimental transmission rates are normalized to CTMC results at $\theta_{in} = 0^\circ$.

1. REFERENCES

[1] N. Stolterfoht, J. Bremer, V. Hoffmann, R. Hellhammer, D. Fink, A. Petrov, and B. Sulik, Phys. Rev. Lett. **88**, 133201 (2002).

[2] T. Nebiki, T. Yamamoto, T. Narusawa, M. Breese, E. Teo, and F. Watt, J. Vac. Sci. Technol. A **21**,1671 (2003).

[3] K. Schiessl, W. Palfinger, K. Tőkési, H. Nowotny, C. Lemell, and J. Burgdörfer, Phys. Rev. A **62**, 042902 (2001).

[4] Gy. Vikor, R. T. Rajendra Kumar, Z.D. Pešić, N. Stolterfoht, and R. Schuch, Nucl. Instr. and Meth. Phys. Res. B **233**, 218 (2005).

* E-mail: klaus@concord.itp.tuwien.ac.at

AUGER NEUTRALIZATION OF He IONS AT ALUMINUM SURFACES

S. Wethekam[*] *and H. Winter*

Institut für Physik der Humboldt-Universität zu Berlin, Newtonstr. 15, D-12489 Berlin, Germany

He atoms and ions are scattered under a grazing angle of incidence from atomically flat and clean Al(111), Al(110), and Al(100) surfaces. By means of a position sensitive micro-channelplate detector, angular and charge state distributions for scattered projectiles are investigated. The system He^+-Al can be considered as model system for the study of Auger neutralization (AN) [1], an inelastic tunneling process where two electrons are involved in the transition.
For incoming He^+ ions we observe defined ion fractions in the scattered beams, whereas for incident He^0 ion fractions are more than one order of magnitude smaller. This observation provides clear evidence for a survival of He^+ over the whole trajectory. From the dependence of ion fractions on the perpendicular energy component we derive neutralization rates as function of distance from the surface.
The analysis of angular distributions for scattered projectiles reveals that the angular shifts between distributions for incident neutral atoms and positive ions show a reversal in sign as function of distance of closest approach to the surface plane. From the data we deduce the energy shift of the He groundstate as function of distance from the surface [2]. The results for the different faces of Al crystals are compared to theoretical calculations [3] and confirm the shift of the reference plane for the neutralization rate observed for Ag(110) and Ag(111) surfaces [4].

In the second part we address the question, to what extent the analysis of fractions of surviving ions can be based on a single neutralization rate. This aspect is of relevance here, because from the work function of an Al surface (about 4.3 eV) transient populations of excited He 2s levels can not be excluded [5] and affect final charge state distributions.
We present studies on AN at Al(100) making use of the different time regimes for scattering of the two stable isotopes ^4He and ^3He. We observe pronounced differences in the fractions of surviving ions for $^3He^+$ and $^4He^+$ ions. We show that this effect is caused by different interaction times for scattering along the same trajectories. The ion fractions for the different isotopes can be well referred to each other in terms of a rate equation approach assuming a single transition rate. This reduction is supposed to fail for a more complex neutralization scenario.
In order to demonstrate our method to distinguish one-step and more complex processes, we have performed measurements on the neutralization of doubly charged He ions. The description as one-step process fails in this case, and an indication for contributions from intermediate states in the neutralization sequence is evident from the interpretation of data.
We conclude that AN into the $1s^2$ ground state of the He atom is the dominant process for neutralization of scattered He^+ ions and determines the resulting fractions of surviving ions [7].

We thank K. Maass, Dr. A. Mertens, A. Schüller (HU Berlin), and G. Adamov (Moscow) for their assistance in the experiments. This work is supported by the Deutsche Forschungsgemeinschaft (DFG) under contract Wi 1336.

[1] R.C. Monreal and F. Flores, Adv. Quantum Chem. **45**, 175 (2004).
[2] S. Wethekam and H. Winter, Surf. Sci. **596**, L319 (2005).
[3] D. Valdés et al., Phys. Rev. B **71**, 245417 (2005).
[4] Yu. Bandurin et al., Phys. Rev. Lett. **92**, 017601-1 (2004).
[5] S. Jequier et al., Surf. Sci. **570**, 189 (2004).
[6] G.E. Makhmetov et al., Surf. Sci. **339**, 182 (1995).
[7] S. Wethekam and H. Winter, Phys. Rev. Lett., in press.

[*] E-mail: stephan.wethekam@physik.hu-berlin.de

AUGER NEUTRALIZATION RATES ON NaCl(001): FINAL STATE DEPENDENCE

*P. Rousseau, H. Khemliche, and P. Roncin**

Laboratoire des collisions atomiques et moléculaires, UMR8625, Fédération LUMAT
Bât. 351,Université Paris Sud 11, F-91405 Orsay Cedex, France

Electron transfer processes, among which Auger-like transitions, are the basis of spectroscopic techniques such as MIES (Metastable Induced Electron spectroscopy) and INS (Ion neutralization spectroscopy). A proper knowledge of these transitions is also essential for the interpretation of LEIS data in surface structure analysis. From the fundamental point of view, calculation of e.g. Auger rates represents a real challenge for theory with the possibility to directly compare the results to the experimentally derived rates [1].

Combining energy loss and electron emission spectroscopies [2], we have measured the neutralization probability of Ne+, He+ and F+ ions on NaCl(001) in keV energy regime and grazing incidence conditions. In spite of the electron localization and high binding energy of the valence electrons, the surviving He ion fractions are on the order of 10^{-4}, very comparable to those observed on metals in similar experimental conditions [3]. For Ne, although the available potential energy is not sufficient to allow a standard Auger neutralization (i.e. with electron ejection), the surviving ion fractions are also equivalent to those observed e.g. on Al(111) [4] in spite of a much lower work function and a more complex electron distribution. Indeed, on ionic cristals neutralization takes place via a *three center transition* since the two electrons involved in the capture belong to adjacent halogen sites [5]. The very high Auger rate measured are thus rather unexpected.

Careful determination of the optical phonon contribution [6] to the energy loss measured for the neutralized projectile suggests that neutralization occurs well before the turning point of the trajectory.

On the basis of the above observations, and with help from trajectory simulations, distance dependent Auger capture rates are derived and compared to values recently published on metals.

In particular the influence of the final state populated on the electron emission yield and on the auger rate is discussed.

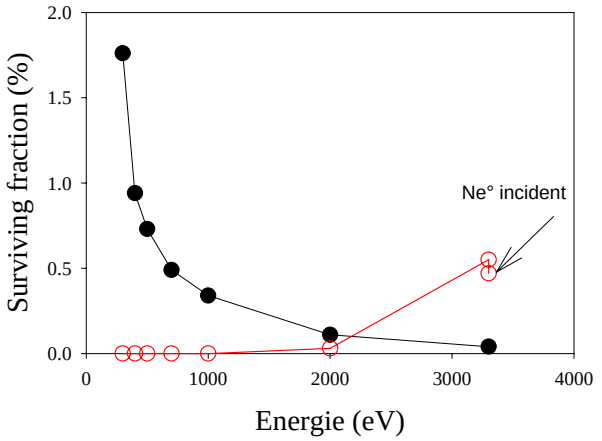

Figure 1: Energy dependence of the outgoing ion fraction following Ne+ (filled circles) and Ne° (circles) scattering from NaCl(001) at grazing incidence.

[1] M.A. Cazalilla et al., Phys. Rev. B **58** (1998) 13991.
[2] P. Roncin et al., Phys. Rev. Lett. **83**, (1999) 864.
[3] S. Wethekam et al., Nucl. Instr. and Meth. in Phys. Res. B **212** (2003) 308
[4] S. Wethekam et al., Nucl. Instr. and Meth. in Phys. Res. B **230** (2005) 305
[5] H. Khemliche et al., Phys. Rev. Lett. **86**, (2001) 5699
[6] A.G. Borisov et al., Phys. Rev. Lett. **83**, (1999) 5378

* E-mail: roncin@lcam.u-psud.fr

NEUTRALIZATION OF LOW ENERGY He^+ IONS BY Cu IN THE AUGER REGIME

S.N. Markin[1,*], *D. Primetzhofer*[1], *J:E. Valdés*[2], *E. Taglauer*[3] *and P. Bauer*[1]

[1] Institut für Experimentalphysik, Johannes Kepler Universität Linz, A-4040 Linz, Austria
[2] Departamento de Física, Universidád Técnica Federico Santa Maria, Valparaíso, Casilla 110-V, Chile
[3] Max-Planck-Institut für Plasmaphysik, EURATOM Association, D-85748 Garching bei München, Germany...

1. INTRODUCTION

Charge exchange of He^+ ions in large angle scattering from Cu(100) and a polycrystalline Cu surface is studied at energies below 2.1 keV, which is the threshold for collision induced neutralization and reionization. In this regime, Auger neutralization is the only relevant charge exchange process. Therefore, only surviving He^+ ions and He^0 are detected.
We examine neutralization at a single crystal with respect to the polycrystalline surface of the same material. The advantage of using a single crystal in channeling/blocking geometry is that scattering is only due to surface atoms; already scattering from the second layer is suppressed due to the large width of the shadow cone. As a consequence, the yields for ions and neutrals, A_+ and A_0, respectively, are obtained as:

$$A_+ = \frac{N_0}{\cos\alpha}\frac{d\sigma}{d\Omega} n_{100} P^+ \cdot \Delta\Omega_+ \eta_+ \qquad (1)$$

$$A_0 = \frac{N_0}{\cos\alpha}\frac{d\sigma}{d\Omega} n_{100} (1 - P^+) \cdot \Delta\Omega_0 \eta_0 \qquad (2)$$

Here, N_0 is the number of primary ions, $d\sigma/d\Omega$ the scattering cross section, n_{100} the surface density of atoms in the (100) plane, $\Delta\Omega_+$ and $\Delta\Omega_0$ the solid angles for ions and neutrals, respectively, η_+ and η_0 are the detection efficiencies for ions and neutrals, respectively. $\Delta\Omega_+$ and $\Delta\Omega_0$ are identical in the set-up used for the present investigation, ACOLISSA. From 1 and 2, the ion fraction is obtained via:

$$\frac{P^+}{1 - P^+} = \frac{A_+ \eta_0}{A_0 \eta_+} \qquad (3)$$

Note that this is much more direct than to deduce P^+ from the ion yield and the height of the neutral spectrum [1]. From direct comparison of the ion yields of the two samples (Cu(100) and Cu_{poly}) one can directly determine the ratio of the corresponding ion fractions P^+_{100}/P^+_{poly} and obtains

$$\frac{P^+_{poly}}{P^+_{100}} = \frac{A_{+,poly}\, n_{100}}{A_{+,100}\, n_{poly}}, \qquad (4)$$

as long as N_0 is identical in both cases.

2. RESULTS AND DISCUSSION

2.1. Cu(100)

For the single crystal, the high quality of the crystal surface was proved by polar and azimuthal scans which showed the expected symmetry with excellent precision. The resulting ion fraction data follow within statistical uncertainties a straight line in a semilog plot of $P^+(1/v_{0\perp} + 1/v_{f\perp})$, with $v_{0\perp}$ and $1/v_{f\perp}$ the perpendicular velocities on incoming and outgoing path, respectively. From this, the characteristic velocity $v_c = 1.72 \cdot 10^5$ m/s is obtained, which is considerably lower than the value obtained in [1] for Cu_{poly}.

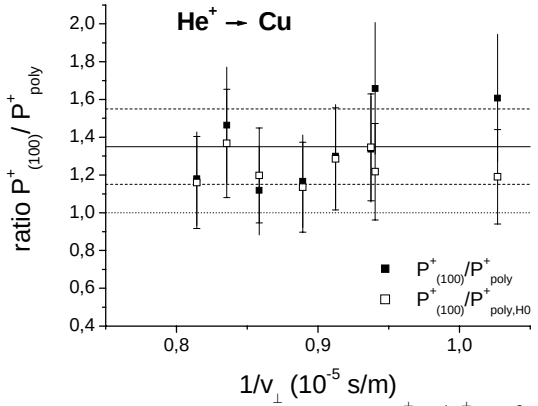

Fig. 1: Ratio P^+_{100}/P^+_{poly} for He^+ ions and Cu (see text).

2.2. Cu(100) versus Cu_{poly}

In an independent experiment, we determined the ratio P^+_{100}/P^+_{poly} in two ways, via 4 and as described in [1]. The result from 4 (1.35 ± 0.2, see also filled symbols in Fig.1) is in accordance with the findings in 2.1. The deduced value P^+_{poly} is in excellent agreement with [1] (see open symbols in Fig.1).

3. REFERENCES

[1] M. Draxler, R. Gruber, H.H. Brongersma and P. Bauer, Phys. Rev. Lett.89 (2002) 263201; M. Draxler, R. Beikler, E. Taglauer, P. Zeppenfeld and P. Bauer, Phys. Stat. Sol. (b) 241 (2004) 2380.

* E-mail: sergej.markin@jku.at

POTENTIAL SPUTTERING FROM A SI SURFACE BY VERY HIGHLY CHARGED ION IMPACT

Masahide Tona[*] *and Shunsuke Ohtani*

Institute for Laser Science and CREST/JST, University of Electro-Communications, Chofu, Tokyo 182-8585, Japan

1. INTRODUCTION

Potential sputtering is induced by the deposition of a large potential energy of a highly charged ion (HCI) onto a surface. The potential energy is defined as the neutralization energy corresponding to the total ionization energy to produce the HCI from an initial neutral atom. In the case of I^{53+}, a fully striped iodine ion used in the present experiment, the potential energy is nearly 200 keV, while that for I^+ is only 10 eV. The sputtering mechanism is thought to be essentially different from kinetic sputtering by the collision of energetic particles with solids. We show here the following features of the potential sputtering; highly secondary positive ion emission yield which was measured with a time of flight secondary ion mass spectrometry (TOF/SIMS) apparatus, and nanometer sized surface modification which was observed with a scanning tunneling microscope (STM). A native SiO_2 thin film on a Si(111) substrate (SiO2/Si: thickness～2 nm), a Si(111)-(7 × 7) surface (Si) and a hydrogen terminated Si(111)-(1 × 1) surface (Si-H) were employed as the representatives of insulator and semiconductor surface materials.

2. EXPERIMENTAL

HCIs were produced in an electron beam ion trap (EBIT) at the University of Electro-Communications. The EBIT was operated with high electron beam energy up to 90 keV. Two collision chambers (base pressure: 2×10^{-8} Pa) along the HCI-beam line were used; one was connected to the observation chamber equipped with the STM apparatus and the other was installed with a low energy electron diffraction optics and the TOF/SIMS apparatus. All of the SIMS measurements were performed for several ten minutes in accumulation time for acquiring TOF/SIMS spectra with a good signal to noise ratio. For the STM observation, an electrically etched tungsten tip was employed. After exposure of HCIs for several hours, the sample was transported to the STM-chamber in the vacuum.

3. RESULTS and DISCUSSION

In a TOF/SIMS spectrum from the SiO_2/Si bombarded with I^{50+}, O^+ ions appear as the larger peak than that of Si^+, and the O^{2+} peak is also observed. O^+ ions, however, are unobservable with low charge state e.g., q=15, impacts, which is analogous to that in the case of irradiation with singly charged ions where kinetically sputtered oxygen ions are ordinarily detected as negative ions rather than positive ones. Furthermore, simultaneous emission of multiple Si^+ ions occurs in an event of a single high q HCI-impact onto the SiO_2/Si although this is not observed in the cases of Si and Si-H targets.

In a TOF/SIMS spectrum from the Si-H bombarded with I^{50+}, the peak of proton appears predominantly, accompanying much weaker peaks of H_2^+, Si^{n+} and Si_2^+. The proton sputtering yield increases strongly with projectile charge q and becomes the value greater than one for I^{q+} impact (q>40), where the multiple H^+ ions are simultaneously emitted from the Si-H surface in a single event of a high q HCI impact. It is found that about ten H^+ ions are emitted at a single I^{50+} ion impact.

The total Si ion yield from the Si surface bombarded I^{50+} is measured to be 0.6. The yields of Si^{n+} (n>3) from the Si surface are in whole ～1.5 times larger than those from the Si-H surface. Such a difference is also observed in the experiments for Si(100)-(2 × 1) and Si(100)-(1 × 1)-H surfaces. The STM observation with atomic resolution for the Si surface reveals that a nanometer sized crater-like structure is created by a single HCI impact, where the size increases rapidly with q. At an I^{50+} impact, ten adatoms are removed and the depth of the crater reaches 0.3 nm corresponding to the height of 1 step of the DAS (Dimer-Adatom-Stacking fault) structure which implies about 90 Si atoms are sputtered by a single I^{50+} impact. It is found from the TOF/SIMS measurement and the STM observation that the sputtering yields of Si ions are two orders of magnitude smaller than those of Si atoms removed. The mechanism for the potential sputtering by HCI-impact is being discussed, based on the "Coulomb explosion" model.

[*] E-mail: tona@ils.uec.ac.jp

CREATION OF SURFACE NANOSTRUCTURES ON CaF_2 BY IRRADIATION WITH SLOW HIGHLY CHARGED IONS

A.S. El-Said[1,*], *W. Meissl*[1], *M.C. Simon*[1], *J.R. Crespo López-Urrutia*[2], *I.C. Gebeshuber*[1], *HP. Winter*[1], *J. Ullrich*[2] *and F. Aumayr*[1]

[1] Institut für Allgemeine Physik, Technische Universität Wien, A-1040 Wien, Austria
[2] EBIT group, Max-Planck Institut für Kernphysik, D-69029 Heidelberg, Germany

1. INTRODUCTION

Upon interaction of highly charged ions (HCI) with solid surfaces a large amount of potential energy is deposited within a very short time (a few femtoseconds) within a nanometer size volume close to the surface [1]. This unique ability of HCI offers a promising way for surface nanostructuring of different materials [2,3]. We present first results on the generation of surface nanostructures by HCI on CaF_2 (111) cleaved surfaces.

2. EXPERIMENTAL RESULTS

The CaF_2 (111) single crystals were irradiated with slow ($v < 1$ a.u.) HCI from the Heidelberg-EBIT. As for other ionic fluoride single crystals, ion-induced surface structures in CaF_2 are known to be stable in atmosphere at room temperature [4,5]. After irradiation, the crystals were investigated by scanning force microscopy in ambient air.

Fig. 1 shows typical AFM topographic images of CaF_2(111) after irradiation with 4.4 keV/amu Xe^{46+} ions. Hillock like nanostructures protruding from the surface are observed. The AFM images were evaluated with respect to hillock height and width distributions. The number of hillocks per unit area is in good agreement with the applied ion fluence.

Measurements for other charge states demonstrate that the mean diameter and height of the hillocks increases with the ion potential energy. Comparison with observations for irradiation of CaF_2 with swift (11.1 MeV/amu) uranium projectiles [5] surprisingly showed that slow Xe^{46+} ions (potential energy of 66.7 keV) generate surface defects with a width larger than for uranium ions with a kinetic energy of 2.6 GeV.

This work has been supported by Austrian Science Foundation FWF (Projects No. M894-N02 and P17449-N02) and was carried out within Association EURATOM-ÖAW. The experiments were performed at the distributed LEIF-Infrastructure at MPI Heidelberg Germany, supported by Transnational Access granted by the European Project HPRI-CT-2005-026015.

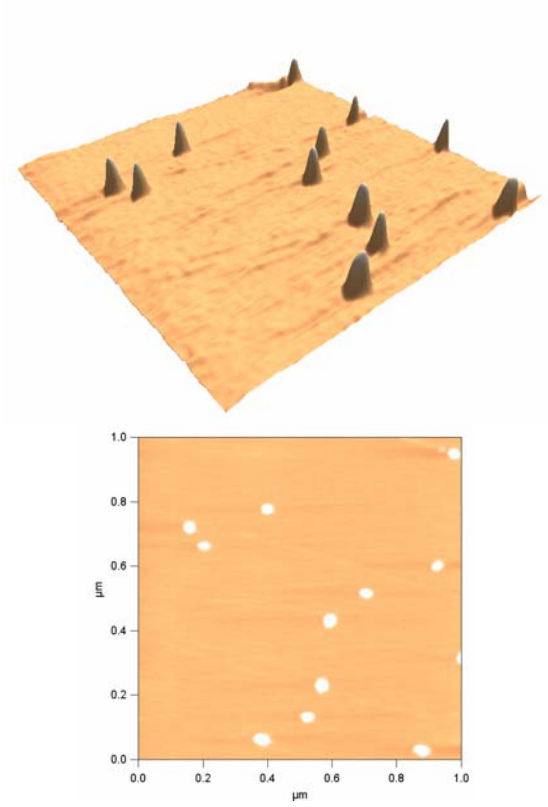

Figure 1: AFM topographic image of a CaF_2 single crystal surface after irradiation with 4.4 keV/amu Xe^{46+} ions.

REFERENCES

[1] F. Aumayr, HP. Winter, Phil. Trans. R. Soc. Lond. A **362** (2004) 77.
[2] Y. Baba, et al., Surf. Sci. **599** (2005) 248.
[3] F. Aumayr and HP. Winter, e-J. Surf. Sci. Nanotechn. **1** (2003) 171
[4] A.S. El-Said , M. Cranney, N. Ishikawa, A. Iwase, R. Neumann, K. Schwartz, M. Toulemonde, C. Trautmann, Nucl. Instr. Meth. B **218**, 492 (2004).
[5] C. Muller, M. Cranney, A. El-Said, N. Ishikawa, A. Iwase, M. Lang, R. Neumann, Nucl. Instr. and Meth. B **191**, 246 (2002).

[*] E-mail: elsaid@iap.tuwien.ac.at

SURFACE EROSION AND MODIFICATION BY IONS STUDIED BY COMPUTER SIMULATION

Z. Insepov[1,*], *D. Swenson*[2], *M. Terasawa*[3], *and A. Hassanein*[1]

[1] Argonne National Laboratory, 9700 South Cass Avenue, Argonne, IL 60439, USA
[2] Epion Corporation, 37 Manning Road, Billerica, MA 01821, USA
[3] University of Hyogo, 3-2-1 Kouto, Kamigori-cho, Ako-gun, Hyogo, 678-1205, Japan

1. INTRODUCTION

Highly-charged ions (HCI) and Gas cluster ion beams (GCIB) are the energetic sources that are capable of surface erosion and modification and can be a promising application tool in many industrial areas.
An emerging EUV-Lithography technology needs highly stable and durable surfaces of condenser optics and surfaces facing the plasma. Highly-charged Xe^{+10} ions (HCI) that are generated in gas discharge or laser plasmas impedes the development of future EUV-lithography sources. [1].
Mitigation of high voltage breakdowns is a major concern in development of higher-field RF cavities for next generation accelerators [2]. Gas Cluster Ion Beam (GCIB) processing of RF cavities is capable of significantly reducing the dark current and enabling operation at higher acceleration gradients [3].
In this paper, various ion energy transfer mechanisms into the solid target, such as hollow atoms (HA) formation, thermal spike, shock wave generation, Coulomb explosion were studied. The following surface erosion and modification pattern are analyzed: surface smoothening and roughening, hillock and crater formation, sputtering yield.

2. COMPUTATIONAL MODELS

HCIs possess very high potential energies characterized by their high charge states. At an impact on a target surface, HCI transfers its potential energy into the target atoms on the surface. Our MD simulation of HA atom formation is based on the COB model [4] and the charge neutralization model is similar to the approach given in [5]. A mechanism for the energy transfer is based on the ''Coulomb explosion'' or ''thermal spike'' models developed in [5]. The potential energy of Xe^{+q} ($q \leq 54$) is calculated by a multi-configuration Dirac–Fock method [6]. Formation of the HA was modeled by switching the interaction potential of Xe ion with the surface atoms. The dynamics of HA formation was studied via visualization of the events by recording movies at various energies and charge states *q*. In molecular dynamics (MD) simulation, the equations of motion of interacting particles are solved numerically. Appropriate initial and boundary conditions are supplied. In mesoscale approach, the dynamics of a non-equilibrium surface profile could be determined from a continuum surface dynamics equation which contains surface tension, viscosity, and evaporation and deposition terms, surface diffusion and a crater formation term.

3. SURFACE EROSION AND MODIFICATION

MD models were applied to erosion of silicon and metal surfaces irradiated by highly-charged Xe^{+q} ions (*q* – the charge of ions) and accelerated gas cluster ions. The sputtering yields of various target materials were calculated and compared with experimental data. The yields of insulators and semiconductors significantly increases with the charge state of the HCI and may lead to surface roughening via crater formation.
Shock wave generation, sputtering and crater formation by HCI and GCIB were studied by MD and the shapes of the craters were compared to AFM, XPS and STM experiments.
Mesoscale simulations were applied for Ag, Cu, Si, and Nb surface modifications by GCIB. Different cluster sizes were modeled, where the total energy of the cluster ion was typical for experiments with cluster ions.
Our experiment showed that the dark current from the Nb surfaces was decreased by GCIB treatment by a factor of 10^6.

4. REFERENCES

[1] J.P. Allain et al., in Emerging lithographic techniques VIII, ed. R. Scott Mackay, Proc. SPIE Vol. 5374 (SPIE, Bellingham, WA, 2004) 112-121 .
[2] Z. Insepov, J. Norem, A. Hassanein, Phys. Rev. ST AB **7**, 122001 (2004).
[3] D.R. Swenson, E. Degenkolb and Z. Insepov, Physica C (to be published, available on-line 27 April, 2006).
[4] J. Burgdörfer, P. Lerner, F.W. Meyer, Phys. Rev. A 44 (1991) 5674.
[5] E.M. Bringa, R.E. Johnson, Phys. Rev. Lett. 88 (2002) 1655011.
[6] T. Sekioka, M. Terasawa, T. Mitamura, M.P. Stockli, U. Lehnert, C. Fehrenbach, Nucl. Instr. and Meth. B 146 (1998) 172, 182 (2001) 121

* E-mail: insepov@anl.gov

SPUTTERING BY HIGHLY CHARGED IONS: APPLICATION OF THE XY-TOF TECHNIQUE TO SECONDARY ION EJECTION

J. Lenoir, P. Boduch, H. Rothard, B.Ban- d'Etat, A. Cassimi, H. Lebius, B. Manil*

Centre Interdisciplinaire de Recherche Ions Laser CIRIL,
UMR 6637 (CEA, CNRS, ENSICAEN, Université de Caen), BP 5133,
Boulevard Henri Becquerel, F-14070 Caen Cedex 05, France

The accelerator facilities SME and ARIBE of GANIL allow to study ion-surface collisions in two different velocity regimes: on the one hand, high velocity heavy ions such as e.g Ca^{17+} at 9 MeV/u, where the electronic energy loss is dominant, can be used. On the other hand, low velocity highly charged ions such as Xe^{21+} at 350 keV are available. In the latter case, nuclear stopping is most important. Possibly, further effects related to the high projectile charge and corresponding high potential energy can occur (potential sputtering).

In order to study whether the physics of energy deposition is different in these two energy regimes, different experiments concerning the sputtering of uranium dioxide (UO_2) were performed at CIRIL-Ganil, both at high energy in the electronic stopping power regime (≈ MeV/u) [1], and with low-energy highly charged ions (≈ q keV) [2,3,4]. In these experiments, either angular distributions of emitted neutrals [1,2,4] or secondary ion mass spectra [3] were measured. From secondary ion mass spectra, in particular, one can obtain information about cluster emission.

We now use a combination of imaging techniques (XY) and time-of-flight (TOF) spectroscopy to measure the complete velocity vector of emitted secondary ions. This technique was applied to sputtering of secondary ions from solid surfaces. First studies were made with UO_2 and with Lithium fluoride LiF.

With the XY-TOF technique, we are now able to obtain the following information from the measurement of the ion position on a channelplate detector and its TOF:

- *identification* of the emitted particle (mass)

- *energy* (or velocity) *distributions*

- *angular distributions* (which can be compared to angular distributions of neutral ejecta)

- a *comparison* of energy and angular distributions for mono-atomic ions versus ejected molecular- and cluster ions

- *correlated detection* of two or more ions.

First results on energy and angular distributions of Li^+ (atomic ions) and $LiFLi^+$ (molecular ions) emitted from LiF will be presented. Also, we compare the angular distributions of Li ions and emitted neutrals.

REFERENCES

[1] S. Bouffard, J.P. Duraud, M. Mosbah, S. Schlutig, Nucl. Instrum. Meth. **B141** (1998) 372

[2] B. Ban d'Etat, F. Haranger, Ph. Boduch, S. Bouffard, H. Lebius, L. Maunoury, J.Y. Pacquet, H. Rothard, C. Clerc, F. Garrido, L. Thomé, R. Hellhammer, Z. Pešić, N. Stolterfoht, Physica Scripta **T110** (2004) 389

[3] S. Boudjadar, F. Haranger, T. Jalowy, A. Robin, B. Ban d'Etat, T. Been, Ph. Boduch, H. Lebius, B. Manil, L. Maunoury, H. Rothard, Eur. Phys. J. **D32** (2005) 19

[3] F. Haranger, B. Ban d'Etat, Ph. Boduch, S. Bouffard, H. Lebius, L. Maunoury, H. Rothard, Eur. Phys. J. **D38** (2006) 501

* E-mail: rothard@ganil.fr

REACTIVE ION SURFACE COLLISIONS

L.Feketeova, V.Grill, F.Zappa, P.Scheier and T.D.Märk[*]

Institut für Ionenphysik und Angewandte Physik, Leopold Franzens Universität, Technikerstr.25, A-6020 Innsbruck

1. INTRODUCTION

The study of ion-surface reactive collisions is a research area, which has undergone rapid growth in the past twenty years. Considerable interest has been devoted to studying selected physical and chemical processes stimulated by the impact of slow ions containing collision energies up to 100 eV [1,2]. In this energy regime the relative collision energy (and the energy transferred) is of the same order of magnitude or somewhat larger than energies observed in chemical bonds. Thus, slow ion-surface interaction studies can provide useful information regarding the nature of both, the projectile and the surface, as well as the characteristics of ion-surface interactions. Reactive collisions of slow ions have been studied here in an effort to characterize molecular ions and to investigate the ion-surface interaction processes, i.e. surface-induced dissociation (SID), charge exchange reactions (CER) and surface-induced reactions (SIR) and the concomitant energy transfer in ion surface collisions.
Besides being of fundamental importance, ion-surface collisions are also relevant in the terrestrial ionosphere and interstellar medium and for technological applications, such as plasma-wall interactions in electrical discharges and fusion plasmas [3]. Hyperthermal plasma particles may collide with solid surfaces such as limiters and divertors in fusion devices, eroding the material by chemical and physical processes. Charged and neutral particles emitted from the surface may interact with the plasma and hit the surfaces again.

2. EXPERIMENTAL

Experiments were carried out with a tandem mass spectrometer apparatus BESTOF described in detail in our earlier paper [4]. It consists of a double focusing two-sector-field mass spectrometer (reversed BE geometry), a Surface chamber combined with a linear Time-Of-Flight mass spectrometer. Projectile ions were produced either in a low-pressure Nier-type electron impact ion source, at elevated pressures in a Colutron gas discharge source or in a cluster source. The ions produced were extracted from the ion source region and accelerated to 3 keV for mass (and energy) analysis by a double-focusing two-sector-field mass spectrometer. After passing the mass spectrometer exit slit, the ions were refocused by an Einzel lens and decelerated to the required collision energy by a system of deceleration lenses before interacting with the target surface. The incident impact angle of the projectile ions was kept at 45^o and the scattering angle (defined as a deflection from the incident beam direction) was fixed at 91^o.
The collision energy of ions impacting on the surface is defined by the potential difference between the ion source and the surface. The potential difference (hence, the collision energy) can be varied from about zero to about 2 keV with a typical resolution of about 200 meV (full width at half maximum) in the case of the Nier type and cluster ion source and of about 1 eV in the case of the Colutron type ion source.
A fraction of the product ions formed at the surface exited the shielded chamber through a 1 mm diameter orifice. The ions were then subjected to a pulsed extraction-and-acceleration field that initiated the time-of-flight analysis of the ions.

3. RESULTS

Results obtained to be presented here include the interaction of various singly and doubly charged hydrocarbon ions (including C_1, C_2 and C_3 group ions) and cluster ions (including carbon aggregates) with a number of targets including stainless steel, carbon tile, and diamond surfaces (O-terminated and H-terminated) maintained under ultra high vacuum conditions (below 10^{-9} Torr) in a bakeable turbo-pump evacuated target collision chamber. Secondary mass spectra at different incident collision energies are converted to collision energy resolved mass spectra (CERMS) plots covering usually the energy range from about 0 to 100 eV thereby yielding after proper analysis desired information on the energetics, kinetics and mechanisms of the various ion surface reactions studied.

4. REFERENCES

[1] R.G.Cooks, T.Ast, and M.D.A.Mabud, Int. J. Mass Spectrom. Ion Process., **100**, 209 (1990).
[2] L. Hanley, ed., *Polyatomic Ion Surface Interactions*, Int. J. Mass Spectrom. Ion Process. **174** (1998).
[3] W. O. Hofer and J. Roth, eds., *Physical Processes of the Interaction of Fusion Plasmas with Solids* (Academic, San Diego, 1996).
[4] A.Qayyum, Z.Herman, T.Tepnual, C.Mair, S.Matt-Leubner, P.Scheier and T.D.Märk, J.Phys.Chem, **108**, 1 (2004).

[*] E-mail: Tilmann.Maerk@uibk.ac.at

DIRECT RECOIL SPECTROSCOPY OF ALKANETHIOL COVERED SURFACES

L. Rodríguez[1], J.E.Gayone[1], E.A. Sánchez[1], O. Grizzi[1], B. Blum[2], R.C. Salvarezza[2]*

[1] Centro Atómico Bariloche, Instituto Balseiro, CNEA, CONICET, 8400 S.C. de Bariloche, Río Negro, Argentina
[2] INIFTA, Depto. de Química, FCE - UNLP, CONICET, CC16, B1904DPI La Plata, Buenos Aires, Argentina

The growth of thin organic layers on surfaces is a field of great interest due to its potential application in areas such as nanolithography, surface pasivation, molecular electronics. The technique of Direct Recoil Spectroscopy with Time of Flight analysis (TOF-DRS) is adequate to study these systems because it provides information that is complementary to that available from electron spectroscopies[2] and other techniques[3]. The main advantages of TOF-DRS are: 1) the high top layer sensitivity, 2) the low damage imparted to the film, and 3) the capability of detecting H. In this report we present a comparative study of the adsorption of alkanethiols (CH_3 $(CH_2)_{n-1}$ SH, with n = 3, 6 and 12, Cn hereafter) on metals (Au(111), Ag(111)) and semiconductors (GaAs(110)). The substrate surfaces were cleaned by grazing sputtering and annealing and the films grown by exposure to the thiol vapours under UHV conditions. TOF-DRS was used to follow the adsorption kinetics in a broad range of exposures (from 10^{-2} to 10^5 Langmuirs). Recoiling atoms from both the molecule and the substrate were followed at a 45 deg scattering angle.

For the metallic surfaces, the shape of the TOF-DRS spectra and the dependence of the recoiling intensity versus dose (Fig.1) present characteristics that can be associated to adsorption in three steps: an initial one at surface defects (inset Fig.1), a slower growth mode that covers the whole surface, and a final, denser layer that can be associated with the self assembled layer. The data show a strong dependence in the sticking coefficient with the surface roughness and the length of the alkyl chain, being smaller for the case of C3. In comparison, adsorption of C6 on GaAs(110) shows a simpler, one step behaviour.

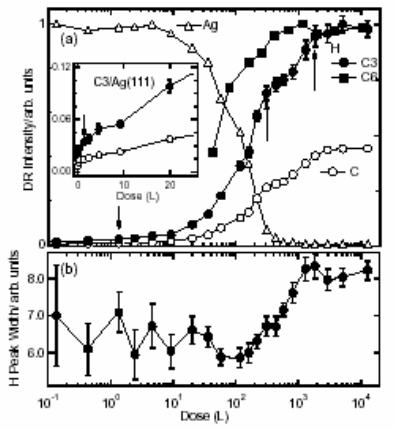

Fig. 1, upper panel: recoil intensities for Ag, H and C vs C3 exposure. Inset: span of the lower range in linear scale [ref 4]. Arrows indicate major changes in sticking. The H recoil intensity during adsorption of C6 is also shown (full squares). Lower panel: width of H recoil peak vs exposure.

Annealing of the films up to temperatures near 500 K resulted in a complete disappearance of the C and H recoil signals and the appearance of small S features. On Ag and Au, the amount of S left at the surface depends on the initial surface roughness. For GaAs it is higher than for both Au and Ag. After the adsorption / desorption cycles, the topography of the Ag substrate changes, giving rise to formation of many small terraces of atomic height. This effect is verified by STM/AFM images. The dependence of the H, C and substrate recoil intensities with sample temperature is different for each substrate, and dependant on the length of the alkyl chain.

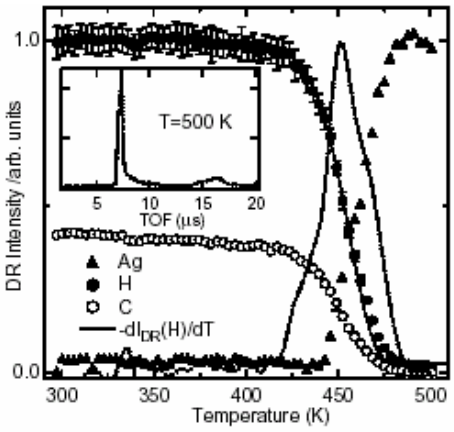

Fig.2: Ag, H and C recoil intensity vs. sample temperature. The full line is a fit to the H recoil intensity with a first order desorption model. The derivative of the H recoil intensity (dotted line) is included.

REFERENCES

[1] J. C. Love, L.A Estroff, J.K. Kriebel, R.G. Nuzzo and G.M. Whitesides *Chem. Rev.* **105** (2005) 1103.
[2] S.S. Duewez J. Electron Spectroscopy and Related Phenomena 134 (2004) 97.
[3] F. Schreiber, Progr. Surf. Sci. 65, 151 (2000). 151.
[4] L.M. Rodríguez, J.E. Gayone, E.A. Sánchez, O. Grizzi, B. Blum and R.C. Salvarezza, J. Phys. Chem. B Lett. 110 (2006) 7095.

* E-mail: grizzi@cab.cnea.gov.ar

INTERACTION OF HYPERTHERMAL PEPTIDE IONS WITH SELF-ASSEMBLED MONOLAYER SURFACES

J. Laskin,[1,*] *O. Hadjar*,[1] *P. Wang*,[1] *J. H. Futrell*,[1] *J. Alvarez*,[2] *J. Green*[2] *and R. G. Cooks*[2]

[1] Pacific Northwest National Laboratory, Fundamental Science Directorate, Richland, Washington 99352
[2] Purdue University, Department of Chemistry, West Lafayette, Indiana 47907

1. INTRODUCTION

Interaction of ions with surfaces is an area of active fundamental research in surface science relevant to a broad range of other scientific disciplines such as materials science, mass spectrometry, imaging and spectroscopy. Our research is focused on fundamental understanding of interaction of hyperthermal (1-100 eV) peptide, protein and polymer ions with organic surfaces under ultrahigh vacuum conditions. Two major processes are dominant for this range of collision energies: reactive and non-reactive scattering of ions and ion loss on the surface as a result of neutralization or soft-landing of projectile ions. SL and a related process of reactive landing (RL) of ions, in which ion is covalently attached to the surface, are unique processes that occur during collisions of low-energy ions with self-assembled monolayer (SAM) surfaces.

2. SCATTERING AND DEPOSITION OF PEPTIDE IONS ON SAM SURFACES

Our research utilizes surface-induced dissociation (SID) as a means for depositing relatively large and controllable amounts of internal energy into large ions on a timescale of several picoseconds. We demonstrated that internal energy distribution functions following ion-surface collision are well-represented by high temperature Maxwell-Boltzmann distributions. [1] A notable discovery was a sharp transition between slow unimolecular decay of large ions at low collision energies and near-instantaneous decomposition (shattering) in higher energy surface collisions. Shattering of ions on surfaces opens up a variety of fragmentation pathways for large complex ions that are not accessible by multiple-collision or multiphoton excitation.

We have recently conducted a first systematic study of several factors that affect SL of peptide ions on inert SAM surfaces.[2] Deposition of peptide ions of different composition and charge state on SAM surfaces was followed by in situ analysis of modified surfaces using 2 keV Cs^+ SIMS inside the FT-ICR mass spectrometer used for SL. Fundamental principles derived from such studies of interaction of protonated peptides with hydrophobic surfaces are relevant to transport of biomolecules through membranes in living organisms. We presented evidence that peptide ions retain at least one proton after SL on FSAM or HSAM surfaces. Quantitative investigation of the effect of the initial kinetic energy of peptide ions on SL demonstrated that in the range of collision energies from 0 to 150 eV SL deposits intact ions on surfaces. Most of our findings such as the decrease in SL efficiency with increase in collision energy and its dependence on the properties of the surface and the charge state of the projectile ion are consistent with an ion-polarizable molecule model for the initial stage of soft landing on SAM surfaces.

This study has been extended to hydrophilic and reactive surfaces such as COOH-terminated SAM or N-hydroxy succinimidyl ester - terminated SAM (NHS-SAM). We were able to demonstrate very strong binding of peptide ions to hydrophilic surfaces and covalent linking of peptides to reactive SAM surfaces via formation of a strong peptide bond (Figure 1).

Figure 1: SIMS spectra of the doubly protonated

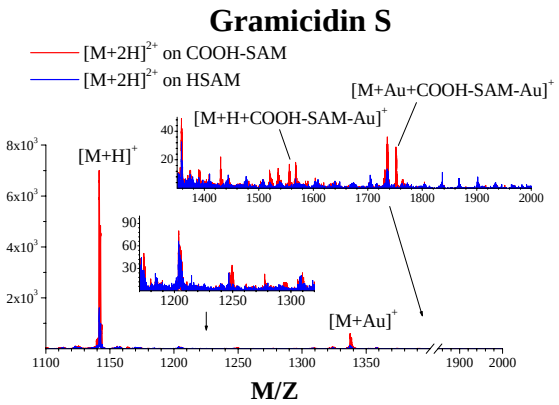

Gramicidin S deposited on SAM surfaces.

3. REFERENCES

[1] J. Laskin and J. H. Futrell, Mass Spectrom. Rev. **24**, 135 (2005)
[2] J. Alvarez, J. H. Futrell, and J. Laskin, J. Phys. Chem. A **110**, 1678 (2006)

* E-mail: Julia.Laskin@pnl.gov

CLASSICAL ION TRAJECTORY SIMULATION OF ALKANETHIOL FILM GROWTH ON AG(111)

P. G. Lustemberg and M. L. Martiarena

Instituto Balseiro - 8400 Bariloche - Argentina
Consejo Nacional de Investigaciones Científicas y Técnicas

The chemisorption of alkanethiol compounds on metal surfaces has been an interesting topic in the past two decades because alkanethiol self-assembled monolayers (SAMs) offer potential applications in many fields, such as corrosion inhibition, wear protection, wetting, lubrication, chemical sensors, molecular electronics [1]. In general, the SAM consists of three parts: a headgroup that strongly binds to the substrate, a surface group that constitutes the outer surface of the molecular layer, and a chain group that connects headgroup and surface groups. The balance between the headgroup-substrate and the intermolecular interactions of chain groups ultimately determines the molecular structure and physical properties of alkanethiols SAMs. The headgroup-substrate interaction plays a predominant role in this balance and the structure of the self-assembled system, which is mainly determined by the choice of the substrate [2].

One of the attractive features of SAMs is the fact that by means of the headgroup and the backbone of the molecule one can anchor virtually any functional group to the surface and thus engineer the properties of the surface. This makes a variety of technological applications possible, ranging from protective surface coatings to ultrathin electronic junctions and to interfacing biological systems.

Despite the apparent simplicity of this system, the adsorption and growth of SAM structures of n-alkanethiolates, on the Au(111) surface have been shown to be very complex, with many controversial results in both theoretical and experimental investigations.

Recently it was reported time-of-flight(TOF) direct recoiling spectroscopy(DRS) to follow propanethiol adsorption from the vapor phase on an Ag(111) surface, for exposures ranging from 10-1 to 105 L. Results show that the adsorption proceeds with changes in the sticking coefficient, consistent with at least three phases [3]. Due to the complex nature of such processes we have used classical ion trajectory simulations in order to understand the relation of the sticking coefficient with molecular geometry as a function of the coverage. Marlowe was used for these simulations.

The adsorption geometry is characterized by four parameters: the surface site above which the head S atom is located; the in-plane direction angle and the tilting angle of the S-C bond; and the rotation angle of the tail molecule in respect to the S-C bond.
Each molecular chain was allowed three degrees of freedom and four inequivalent sites.
The study of adsorption of molecular chains on two substrates, Au(111) and Ag(111), were done in a $3\text{x}2\sqrt{3}$ supercell for Au(111) and $\sqrt{7}\text{x}\sqrt{7}R(19^\circ)$ supercell for Ag(111) as suggested by other structural studies[2].
The ions are expected to substantially probe the subsurface alkanethiols groups below the terminating CH3 groups.
We simulate the experimental spectrum of time-of-flight(TOF) direct recoiling spectroscopy(DRS) to follow propanethiol (C3) adsorption comparing the spectra for clean surfaces with surfaces exposed to C3. The clean surface spectrum shows the peaks of Ar single and multiple scattering of substrate, together with the substrate recoil peak from the outermost layer in good agreement with the experimental data [3]. We present the different characteristic of the spectrum for different coverage and molecular phases (lying-down and standing-up). We follow the appearance of H, C and S recoils and the intensity decreasing of the Ar and substrate peaks. The variation of such peaks allows the deduction of the geometrical configuration of the alkanethiols adsorption process.

1. REFERENCES

[1] J. C. Love, L. A. Estroff, J. K. Kriebel, R. G. Nuzzo, and G. M. Whitesides, Chem. Rev. 105, 1103, (2005)

[2] F.Schreiber, Progress in Surface Scienc 65 (2000) 151.

[3] L. M. Rodriguez, J. E. Gayone, E. A. Sanchez, O. Grizzi, B. Blum and R. C. Salvarezza J. Phys. Chem. B, 110, 7095 (2006)

Tuesday, 19.9.2006

DYNAMIC SCREENING, ENERGY LOSS, AND ELECTRON DYNAMICS IN BULK AND AT SURFACES

P. M. Echenique[1,2,3,*]

[1] Departamento de Física de Materiales, UPV/EHU, 20018 Donostia, Spain.
[2] Donostia International Physics Center DIPC, 20018 Donostia, Spain.
[3] UFM, Centro Mixto CSIC-UPV/EHU, 20018 Donostia, Spain.

The screening response to an external Coulomb field is a fundamental property of electronic media. Screening reduces significantly the interaction range between charged particles and enhances locality in many processes. The understanding of how screening works is basic to interpret the output of many spectroscopies and surface characterization methods, such as Auger spectroscopy, low-energy electron diffraction, and ion beam analysis. The screening of electrons in an interacting Fermi liquid lies behind the concept of quasiparticle, one of the most useful models to describe electronic excitations in solids theoretically. A proper treatment of dynamic screening properties is also required to study the interaction of charges with solids and surfaces.

The rearrangement of electronic charge in the medium, required to create the screening, is not instantaneous but develops in a finite time determined by the electronic density of the medium. In general, standard experimental techniques provide information over time scales for which the screening of charges can be approximated as instantaneous in practice, being much faster than any other measurable process. However, constant improvements in experimental methods, particularly in the field of ultrafast laser spectroscopies, are making possible to access time scales for which the rearrangement of charge is dynamic and the screening is not complete. In this respect, it has become necessary to develop new theoretical approaches to understand how and when the screening is built-up in many-electron systems.

Here, linear and non-linear theories of screening are used to investigate the dynamic screening of charges in different situations. For the short-time regime, TDDFT calculations in finite systems show that the screening is built-up locally on a time scale well below the femtosecond for typical metallic densities. At this time scale, the time evolution of the electronic density is not affected by the system boundary conditions, and the conclusions extracted apply to the infinite system. Universal scaling laws and dimensionality effects in the time-dependent screening of charges are also discussed. For many other situations, the long-time dynamics of screening is needed, and other effects, such as the band structure of the solid, can play a role. Application of our results on the screening response to other problems of interest in the interaction of charges with bulk and surfaces will be also presented.

* E-mail: pedromiguel.echenique@ehu.es

ION INTERACTION WITH ISOLATED NANO-SURFACES

B.A. Huber, E. Giglio, B. Manil, L. Maunoury, J. Rangama

Centre Interdisciplinaire de Recherche Ions Lasers (CIRIL), BP 5133, F-14070 Caen Cedex, France

Studies of ion interactions with nano- or microparticles in the gas phase do have the advantage that the projectile ions can be analysed easily after the collision with respect to different properties like energy loss, scattering angle and the number of captured and stabilised electrons, without being buried in the deeper layers of a macroscopic solid material. For small particles the fraction of atoms being at the surface is rather large, therefore, in general, the interaction occurs predominantly with so-called 'surface-atoms'. It has been shown that under certain collision conditions (impact parameters), the observed phenomena strongly resemble those being observed in ion-surface collisions concerning electron multiplicities, particle neutralisation in front of a metal surface or even negative ion yields, measured when positive F^{q+} ions are colliding with these objects.

However, due to the finite size of the object the number of electrons being available for the interaction with a charged particle is limited. Therefore, one might expect phenomena as observed for ion interactions with insulating surfaces, in particular, as the finite size system is charging up during the collision due to multi-electron capture and ionisation processes.

On the other hand, experiments with 'nano-surfaces' allow to study in more detail the kinematics of surface instabilities and surface deformations under the influence of a Coulombic excess charge and more specifically the role of a finite charge conductivity.

In the present contribution, we will discuss phenomena observed in the interaction of multiply charged ions with 'nano-surfaces' like large molecules, fullerenes and clusters as well as surface instabilities of charged microsystems. Of particular interest will be the aspect of charge localisation and charge mobility.

Figure 1: Fullerenes as perfect nano surfaces.

Figure 2: Charge-deformed micro-droplet

THE ROLE OF COLLISIONAL PROCESSES IN THE X-RAY EMISSION DURING LASER-CLUSTER INTERACTION

E. Lamour[1], *C. Prigent*[1], *J.-P. Rozet*[1], *and D. Vernhet*[1,*]

[1] INSP, CNRS UMR 7588,Universités Paris 6 et Paris 7, Campus Boucicaut, 75015 Paris, France, EU

Similarly to slow highly charged ion-surface interaction, X-ray spectra characteristic of the formation of "hollow atoms" are observed when large rare-gas clusters of nanometric size are submitted to intense femtosecond laser pulses. Correspondingly, the X-ray emission, which tags on inner-shell ionized atoms, gives access to the dynamical evolution of the irradiated cluster on a time scale comparable to that of the laser pulse duration, whereas the spectroscopy of the emitted ions and electrons extracts information from the system a few microseconds after the femtosecond laser pulse and the cluster disintegration.

A fascinating feature of intense laser-matter interaction is its efficiency for converting photons in the eV range to X-rays in the keV. It is now well known that large clusters, similarly to solids, couple very efficiently to intense subpicosecond laser pulses. A highly ionized and excited medium is formed on a cluster scale of a few ten nanometers. Highly charged ions with energies reaching the MeV, electrons with energies up to a few keV, and UV and keV X-ray photons from inner-shell ionized atoms are emitted. As the inner-shell vacancies are produced by electron-impact ionization, X-ray spectroscopy can provide deeper insight into the electron dynamics which are a central element to a more detailed understanding of laser-cluster interaction. In that respect, we have measured absolute x-ray yields and charge state distributions under well controlled conditions as a function of several physical parameters governing the interaction; namely laser intensity, pulse duration, wavelength or polarization state of the laser light, the size and the species of the clusters (Ar, Kr, Xe).

Recently, we show evidence for a very low laser intensity threshold in the x- ray production, well below the laser intensity where the ponderomotive energy of the electrons is sufficient to create inner-shell vacancies. We found typically 1.2 10^{15} W/cm^2 for a pulse duration of 150 fs, down to 3 10^{14} W/cm^2 for 610 fs, in the case of Ar clusters. None of the previously proposed theoretical models provides a satisfactory explanation for a high electron temperature at such moderate intensities. Within a Classical Trajectory Monte Carlo simulation to describe the dynamics of the electrons in the cluster, we developed a model showing that beside the field induced by the build-up of an overall charge of the cluster due to electrons leaving the cluster, elastic electron-ion scattering plays an essential role in the heating process. The resulting high-energy tail of the electron distribution is sufficient to produce K-shell vacancies and we find a good quantitative agreement with the measured effective x-ray yields [2].

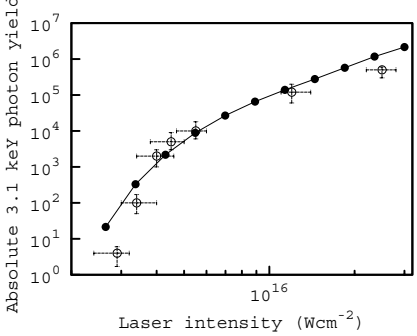

Figure 1: Absolute X-ray yields as a function of laser intensity for argon clusters with N = 2.8 10^5 atoms, excited by 60 fs, λ = 800nm laser pulses. Experimental results (o), simulation including elastic electron-ion scattering (•)

Nevertheless, the efficient depletion of L-shell, which gives rise to the experimentally observed high ionic charge states (~13+), is not yet reproduced, even though the mean charge state rapidly increases to ~7+. In particular the charge-state distribution in the cluster may play a role. To vary the contribution of the surface compared to the bulk, we have investigated the cluster size dependence in the range of 10^5 to 10^7 atoms/cluster. In contradiction with the well-known plasma codes [3, 4], a saturation in the x-ray emission probabilities has been found above a critical cluster size while the mean charge state still increases. Within the CTMC simulation we have developed, additional investigations are under progress, especially concerning the in-situ charge-state distribution.

REFERENCES

[1] Prigent, PhD Thesis, Paris (2004); Prigent *et al.*, Euro Phys Letters (submitted)
[2] Deiss *et al.*, Phys. Rev. Lett. **96**, 013203 (2006)
[3] Ditmire *et al.*, Phys. Rev. A **53** (1996) 3379
[4] Megi *et al.*, J. Phys. B **36** (2003) 27

* E-mail: dominique.vernhet@insp.jussieu.fr

INTERACTIONS OF C_{60}^+ IONS WITH A KCl(001) SURFACE UNDER GRAZING INCIDENCE

K. Kimura[*], *T. Matsushita, S. Tamehiro, K. Nakajima, and M. Suzuki*

Department of Micro Engineering, Kyoto University, Kyoto 606-8501, Japan

1. INTRODUCTION

Although the interactions of atomic ions with solid surfaces have been extensively studied, much less is known about the interactions of large polyatomic ions with solid surfaces. In this work, the interactions of slow C_{60}^+ ions with a KCl(001) surface, including charge exchange, energy loss and fragmentation of C_{60}^+ are studied under grazing angle incidence.

2. RESULTS AND DISCUSSION

A beam of 3 keV C_{60}^+ ions was produced by a 10-GHz ECR ion source. The beam was incident on a (001) surface of a KCl single crystal at a grazing angle θ_i. The charge state distribution of the scattered ions was measured by a two-dimensional position-sensitive detector with a pair of electric field plates. Although the velocity of 3 keV C_{60}^+ is as low as ~ 0.013 a.u., C_{60}^+ is dominant in the reflected beam, indicating that the neutralization of C_{60}^+ is suppressed because of the wide band gap of KCl. This allows us to measure the energy spectrum of the scattered ions using a simple electrostatic analyzer.

Figure 1 shows an example of the observed energy spectrum. The open circles show the energy spectrum of the incident beam and the black dots show that of the scattered ions. The spectrum consists of several peaks which are equally separated by ~ 105 eV. Such a multi-peak spectrum might be attributed to either *skipping motion* or *subsurface channeling*.

In order to clarify the origin of the observed multi-peak spectrum, energy spectra were measured at various θ_i. Figure 2 shows the observed energy losses of these peaks as a function of θ_i. The energy loss increases with θ_i, while the peak separation is almost constant. Such a behavior cannot be explained by either the skipping motion (energy loss ratio should be 1 : 2 : 3 ··· irrespective of θ_i) or the subsurface channeling (the energy loss ratio should be 1 : 3 : 5 ···). Moreover, the observed intensity of the second peak increases with θ_i, which is opposite to what expected in either the skipping motion or the subsurface channeling.

A possible explanation of the observed multi-peak spectrum is based on the fact that the peak separation is always about 1/30 of the incident energy. The observed peaks correspond to C_{60-2n}^+ ions produced by sequential C_2 emission, *i.e.* the second, third, fourth, ··· peaks correspond to C_{58}^+, C_{56}^+, C_{54}^+ ··· ions, respectively. Further evidence to support this explanation will be presented in the workshop.

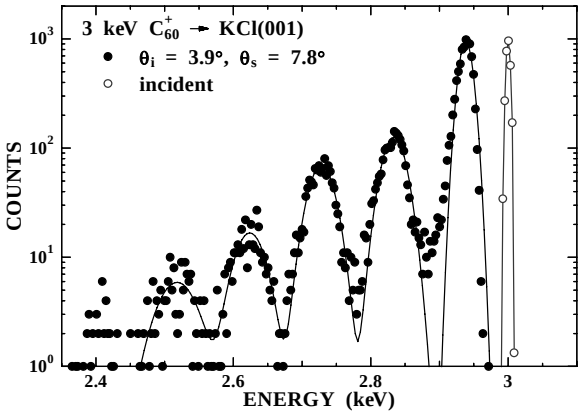

Figure 1: Observed energy spectrum of scattered ions when 3 keV C_{60}^+ ions are incident on a KCl(001).

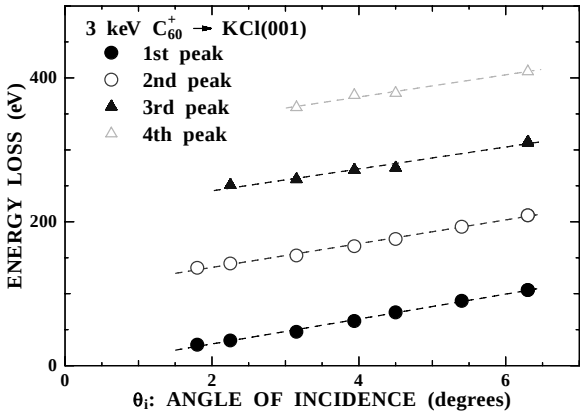

Figure 2: Observed energy losses of the peaks as a function of θ_i.

[*] E-mail: kimura@kues.kyoto-u.ac.jp

GRAZING COLLISIONS WITH INSULATOR SURFACES

M.S. Gravielle[*]

Instituto de Astronomía y Física del Espacio, CONICET, Casilla de Correo 67, Sucursal 28, 1428 Buenos Aires, Argentina,
and Departamento de Física, FCEN, Universidad de Buenos Aires

1. INTRODUCTION

Electronic transitions produced from insulator surfaces by grazing impact of fast ions are investigated, considering two different situations: planar and axial surface incidence. The planar incidence corresponds to a random orientation of the projectile trajectory with respect to the crystal axes, while the axial incidence is related to projectiles moving along precise strings of surface atoms. In both cases we employ distorted-wave methods to describe electron capture and emission processes.

2. THEORY

For axial incidence on insulator surfaces, the electronic transitions induced by the projectile can be seen as a collection of individual processes from the different ionic centers of the crystal. The corresponding transition amplitudes must be coherently added, giving rise to interference effects that reveal signatures of the periodic structure of the solid.

For electron capture, we extend the use of the eikonal-impulse (EI) approximation to describe the electron exchange from a surface state. The coherent transition amplitude reads

$$A_{i\mathbf{k}}^{(c)} = \sum_{nm} \exp\left[i(\mathbf{k}-\mathbf{W}) \bullet \mathbf{x}_{nm} \right] \; a_i^{(cap)}(\boldsymbol{\rho}_{nm}), \qquad (1)$$

where the wave vector **k** identifies a given crystal state within the initial surface band *i*, and **W** is the transferred momentum vector, parallel to the impact velocity. In Eq. (1), each atomic transition amplitude $a_i^{(cap)}(\boldsymbol{\rho}_{nm})$ is associated with the capture from a different lattice site $\mathbf{x}_{nm}$.

In similar way, for electron emission the coherent transition amplitude is derived from the continuum-distorted-wave -eikonal-initial-state (CDW-EIS) approximation. It reads

$$A_{i\mathbf{k}}^{(e)} = \sum_{nm} \exp\left[i(\mathbf{k}+\mathbf{Q}-\mathbf{k}_f) \bullet \mathbf{x}_{nm} \right] \; a_i^{(ion)}(\boldsymbol{\rho}_{nm}), \qquad (2)$$

where $\mathbf{k}_f$ is the final electron momentum, **Q** is the transferred momentum vector, parallel to the velocity, and $a_i^{(ion)}(\boldsymbol{\rho}_{nm})$ is the atomic transition amplitude corresponding to ionization from the lattice site $\mathbf{x}_{nm}$.

3. RESULTS

The method is applied to 100 keV protons grazing colliding with LiF(100) surfaces. Partial probabilities from initial crystal states with **k**=(0,0) are shown in Figs. 1 and 2, for capture and electron emission, respectively.

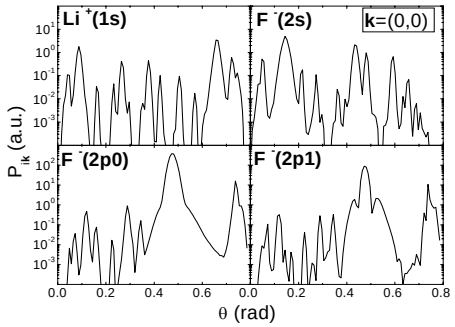

Figure 1: Partial capture probabilities from initial crystal states with **k**=(0,0), as a function of the orientation of the projectile trajectory.

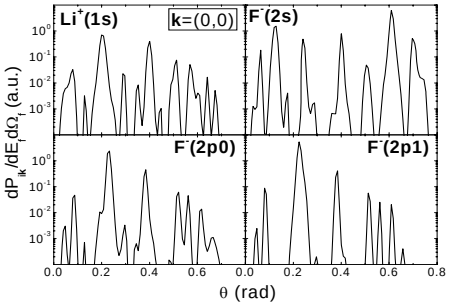

Figure 2: Similar to Fig. 1 for electron emission with final electron angle and energy, θ_f=20 deg. and E_f=92 eV, respectively.

For capture these structures almost disappear when the total contribution from the surface band is considered.

4. REFERENCES

[1] M.S. Gravielle and J.E. Miraglia, Phys. Rev. A **71**, 032901 (2005).

[*] E-mail: msilvia@iafe.uba.ar

CONVOY ELECTRON EMISSION AND ENERGY LOSS OF SWIFT PROTONS IN GRAZING COLLISION AGAINST LIF(001), CLK(100) AND IK(100) SURFACES

I. Aldazabal[1,*], *M.S. Gravielle*[2], *A. Arnau*[1,3], *J.E. Miraglia*[2], *and V.H. Ponce*[4]

[1] Departamento de Fisica de Materiales UPV/EHU, Apartado 1072, San Sebastian 20080, Spain
[2] Instituto de Astronomia y Fisica del Espacio, Facultad de Ciencias Exactas y Naturales, Universidad de Buenos Aires, C.C. 67, Suc. 28, 1428 Buenos Aires, Argentina
[3] Centro Mixto C.S.I.C.-UPV/EHU, San Sebastian, Spain
[4] Donostia International Physics Center D.I.P.C., San Sebastian, Spain and Centro Atomico Bariloche, Bariloche, Argentina

At grazing angles of incidence, electrons emitted in ion-surface collisions give information about the atomic and electronic structure of the surface. However, at high emision energies the details of the electronic structure of the target are not so relevant and two structures appear which have their origin in binary *ion-atom* collisions. They are the so-called *convoy* and *binary* electron peaks.

Electrons contributing to the convoy electron peak (CEP) arise on one side from the electrons extracted from the surface (*electron capture to the continuum* or *ECC* contribution) and on the other from the electrons ionized from the neutralized projectile (*electron loss to the continuum* or *ELC* contribution).

In the present work we calculate these two contributions to the CEP taking into account the charge state of the projectile. We also compute the projectile energy loss per unit path lenght, or stopping power, as well as the energy loss along the ion trajectory.

This trajectory is treated classically and, being a grazing collision, we approximate it as a series of discrete trajectories in which the projectil velocity is considered essentially parallel to the surface.

We consider that each surface atom contributes to the total electron emission on its own, and that only the top most layer contributes effectively to the emission process.

Thus, for the electron emission we can use the straight-line version of the impact parameter formalism within a binary collision model in *a)* first Born approximation[1, 2] for the ELC electrons contribution and *b)* continuum-distorted-wave-eikonal-initial-state (CDW-EIS) approximation for the ECC electrons[3, 4].

Furthermore, ELC/ECC electrons can only be produced while the projectile is in its neutral/ionized state respectively. Thus, in order to know the charge state of the projectile along the trajectory we *a)* integrate over all the projectile emitted electrons to compute the projectile ionization probability and *b)* use a distorted wave method[5] to calculate its neutralization probability.

From the previously described model we compute the electron emission cross section for different angles of emision, and analyze the relative contribution to the convoy peak of the ELC and ECC electrons for protons inpinging three different surfaces, namely LiF(001), ClK(100) and IK(100).

The energy loss along a given trajectory is also obtained by integrating the distance-dependent stopping power.

* E-mail: ialdazabal@ehu.es

1. REFERENCES

[1] M. McDowell and J. P. Coleman, *Introduction to the Theory of Ion-Atom Collisions* (North-Holland, Amsterdam, 1970).

[2] I. Aldazabal, V. H. Ponce and A. Arnau, phys. stat. sol. (b) **241**, 2374 (2004)

[3] P. D. Fainstein, V. H. Ponce and R. D. Rivarola, J. Phys. B **22**, 1207 (1989)

[4] I. Aldazabal, M.S. Gravielle, J.E. Miraglia, A. Arnau and V.H. Ponce, Nucl. Instrum. Methods Phys. Res. B **232**, 53 (2005).

[5] M. S. Gravielle, J. Miraglia, Phys. Rev A **44**, 7299 (1991)

ENERGY SPECTRUM SHAPE OF LOW ENERGY ION SCATTERING FROM INSULATORS AND ITS SIMILARITY TO ASYMMETRIC SPECTRUM SHAPE OBSERVED IN CORE LEVEL XPS

M. Kato[1*], *Y. Sakuma*[1] *and R. Souda*[2]

[1] Dept. of Quantum Engineering, Nagoya University, Nagoya 464-8603, Japan
[2] National Institute for Materials Science, Ibaraki 305-0044, Japan

1. INTRODUCTION

The line spectrum observed in x-ray photoemission spectroscopy (XPS) usually exhibits an asymmetric shape for metallic targets. This asymmetric shape can be satisfactorily fitted by Doniach-Sunsic lineshape function[1], referred to as DS-function:

$$DS(E) = \frac{\Gamma(1-\alpha)\cos\left[\frac{\pi}{2}\alpha + (1-\alpha)\arctan(E/\gamma)\right]}{\left(E^2+\gamma^2\right)^{(1-\alpha)/2}} \quad , \qquad (1)$$

where α is the singularity index, and γ is the line width.

In low energy ion scattering spectroscopy (LEIS) also, the experimental energy spectrum of scattered ions often shows an asymmetric shape(solid circles of fig.1).

The physical origin of the asymmetric lineshape of XPS is known as the infrared divergence of electron-hole pair excitations in metals. This infrared divergence occurs because of the electronic response to the core hole potential suddenly created by x-ray absorption.

In this regard, LEIS cannot observe this divergence, because the low energy ion does not behave as a sudden perturbation to the electronic system. However, surprisingly, we found that the asymmetric spectrum shape of LEIS also could be well fitted by the DS-function. In the present study, we have proven analytically that the asymmetric spectrum shape of LEIS can be well explained by the DS-function, and have clarified the physical implication of α and γ for the case of LEIS.

2. EXPERIMENT

We have carried out LEIS experiments, by using low energy H^+ ion (< 1 keV) for the rare gas solids of Ar, Kr and Xe. As shown in fig.1, the spectrum has a multi peak structure, and the peaks appear separately by equidistance of 15 eV on the energy axis. As this energy distance coincides with the bandgap energy between valence and conduction band of the solid Ar, this peak structure can be assigned to the inter-band electronic excitation in a close collision of H^+ with an Ar atom. The multiple peaks are explained as the sequential inter-band excitations in the collision sequence of H^+ with several Ar atoms.

3. RESULTS

Each peak of the experimental spectrum can be well fitted by DS-function(α =0.24, in fig.1). In the case of LEIS, the origin of the asymmetric shape has been assigned to the multiple elastic collisions between H^+ ions and target atoms, and in fact, α can be expressed in terms of inter-atomic potential, and the peak width γ is given by the bandwidth of the solid Ar.

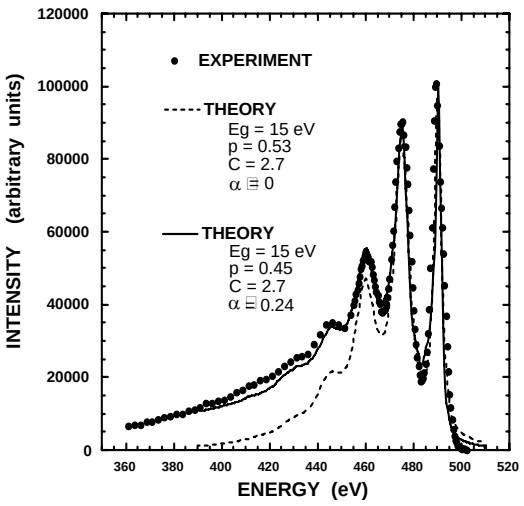

Fig. 1: Experimental energy spectrum and analysis. H^+ ions of 500 eV were incident on the solid Ar, grown on a substrate at a low temperature. The incidence angle was 15°(measured from the surface plane), and the scattering angle was 60°. The solid/dashed line is the best fitting curve to the experimental observation, when the multiple elastic collisions are taken into account, α=0.24/not taken into account, α =0. .

4. REFERENCES

[1] S. Doniach and M. Sunjic, J. Phys. C :Solid St. Phys. **3**, 285 (1970), and, G. D. Mahan, Phys. Rev. **163**, 612 (1967).

* E-mail: m-kato@nucl.nagoya-u.ac.jp

KINETIC EXCITATION OF SOLIDS: EXPERIMENT AND COMPUTER SIMULATION

A. Wucher[1,*], *S. Meyer*[1], *D. Diesing*[2], *and A. Duvenbeck*[1]

[1] Physics Department, University of Duisburg-Essen, Campus Duisburg, 47048 Duisburg, Germany
[2] Chemistry Department, University of Duisburg-Essen, Campus Essen, 45117 Essen, Germany

The electronic stopping of a projectile impinging onto a solid surface leads to kinetic excitation processes within the solid. Moreover, the collision cascade produced by nuclear stopping generates a large number of recoil atoms, which in turn can produce additional kinetic electronic excitation. In part, these excitations manifest in the emission of electrons into the vacuum, provided the energy transferred to an electron is large enough to overcome the surface barrier (work function). However, many excitation processes generate low energy electrons in states located between the Fermi level and the vacuum level, which are inaccessible by electron emission experiments. We have recently developed a new method to detect such hot electrons by means of a metal-insulator-metal (MIM) tunnel junction [1]. The outer metal film represents the actual target which is bombarded by the incoming ion beam. The thickness of this layer (~ 20 nm) is carefully selected to be large enough to completely stop the projectile and contain the collision cascade, but small enough to allow ballistic transport of hot electrons towards the underlying oxide interface. The thin (~2 nm) oxide layer represents a potential barrier which can be tunneled by these electrons, leading to the detection of a bombardment induced tunneling current into the metal base electrode. By applying a bias voltage across the junction, it is possible to modify the tunneling barrier in a controlled manner, thus opening the possibility for "spectroscopic" detection of the excited electrons.

We present first results for kinetic electronic excitation of metal surfaces obtained with this technique. It is shown that the bombardment induced tunneling current depends on the kinetic energy of the impinging projectiles in a characteristic way similar to that observed for kinetic electron emission. Moreover, it is demonstrated that the detected signal depends exponentially on the thickness of the target silver layer. Comparing the tunneling current measured under impact of ionized and neutral projectiles, we find consistently lower yields for neutral species, which are interpreted in terms of a charge state dependent electronic stopping power rather than an effect of the potential (ionization) energy carried by the projectile ions.

The excitation "spectra" measured by varying the bias voltage across the junction exhibit an a priori unexpected behavior. More specifically, the measured tunneling yield depends almost linearly on the applied potential difference rather than exponentially as expected for a tunnel junction. Moreover, the measured tunneling current is observed to change sign at bias voltages around 1 V. This behavior is discussed in terms of the band structure of the oxide layer. In addition to the excited electrons tunneling via the conduction band edge, hot holes can tunnel via the valence band edge of the oxide film, leading to a bias voltage dependent current of opposite sign which can counterbalance the electron current. The experimental results are interpreted in terms of a spectrum simulation, leading parameter of which is the bombardment induced electron temperature T_e generated in the metal film. Results show that T_e must be temporally raised to several thousand K following, e.g., the impact of a 10-keV Ar^+ ion in order to understand the measured spectra.

The experiments are complemented by computer simulations describing the kinetically induced electronic excitation of a solid after bombardment with fast projectiles [2]. In these model calculations, the particle kinetics following the projectile impact are described by classical molecular dynamics using an empirical many-body interaction potential. The electronic stopping of both the projectile and all moving recoil atoms is then used as a source term in a diffusive treatment of the transport of electronic excitation energy away from the point of original excitation. In addition to electronic friction, electron promotion in close collisions is included as another source of excitation. As an important feature of the model, the electronic heat diffusivity is allowed to vary as a function of electron and lattice temperature as well as the local lattice disorder introduced by the collision cascade. Results show that particularly the latter is extremely important, since it leads to an efficient trapping of excitation within the cascade volume during the lifetime of the collision cascade. Characterizing the excitation energy distribution by a spatially and temporally varying electron temperature, it is shown that the surface T_e is strongly time dependent and may reach several thousand K at times of hundreds of femtoseconds after the projectile impact. These values compare well with those deduced from the experiments.

[1] S. Meyer, D. Diesing, and A. Wucher, Phys. Rev. Lett. **93**, 137601 (2004).
[2] A. Duvenbeck, and A. Wucher, Phys. Rev. B **72**, 165408 (2005).

* E-mail: wucher@uni-essen.de

TRANSPORT AND STM MEASUREMENTS OF HCI MODIFIED MATERIALS

J.M. Pomeroy[1*], *H. Grube*[1], *and A.C. Perrella*[1,2]

[1] National Institute of Standards and Technology, Gaithersburg, MD, USA
[2] Army Research Laboratory, Adelphi, MD USA

While more than a decade of work has provided glimpses into the physics of highly charged ion (HCI) neutralization on surfaces, two prominent objectives remain unfulfilled: 1) a unified, quantitative model for separating the kinetic energy response of a wide range of materials classes from the effects of HCIs' potential energy effects, and 2) insertion of HCI technology(s) as a cost-effective processing tool in a high-volume market sector. The NIST EBIT facility has recently incorporated tools for preparing clean, atomically flat surfaces of single crystals from gold to tungsten to silicon, and for depositing and patterning thin films including high resistivity oxides, ferromagnetic metals, normal metals and superconductors. Current and ongoing activities are focused on utilizing this unique capability to simultaneously address both of the objectives above by utilizing a technologically important magnetic multi-layer systems to perform transport measurements that provide new insight into the fundamental processes that occur during HCI-surface neutralization. Specifically, we are producing Magnetic Tunnel Junctions (MTJs) critical to both magnetic field sensors (like next generation hard-drive read heads and MRAM) and superconducting Josephson junction devices and incorporating HCIs in the processing recipe to adjust critical electronic properties that are currently inhibiting their advancement. In return, the electrical response of the tunnel junction to the HCI processing provides a novel approach to performing ensemble measurements of HCI-surface interactions. By varying the construction of the tunnel junction, the target materials electron density is varied over many orders of magnitude providing critical tests of the role of electron density, densities of states, and electronic structure in the HCI-surface charge exchange.

[*] E-mail: joshua.pomeroy@nist.gov

Elektronenstrahlverdampfer

www.tectra.de/e-flux.htm

Plasmaquelle

www.tectra.de/plasma-source.htm

- Atomstrahlquelle
- Ionenquelle
- Atom-/Ionen-Hybrid-quelle

Atomic Hydrogen Source

www.tectra.de/hydrogen.htm

IonEtch sputter gun

www.tectra.de/sputter.htm

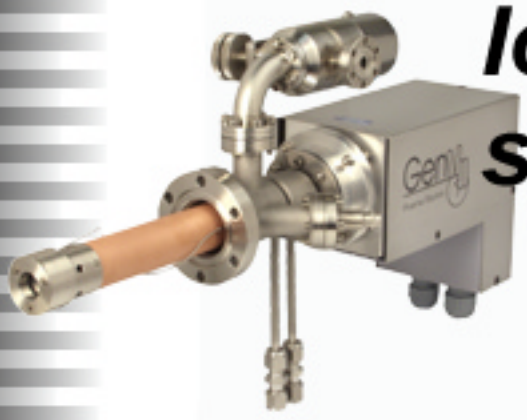

tectra GmbH

www.tectra.de

CHARGING AND DISCHARGING OF NANO-CAPILLARIES DURING ION-GUIDING OF MULTIPLY CHARGED PROJECTILES

M. Fürsatz, W. Meissl, S. Pleschko, M.C. Simon, I.C. Gebeshuber, N. Stolterfoht, HP. Winter, and F. Aumayr*

Institut f. Allgemeine Physik, TU Wien, A-1040 Vienna, Austria
* Hahn Meitner Institut Berlin, D-14109 Berlin, Germany

1. INTRODUCTION

Efficient guiding of slow (typ. keV) highly charged ions (Ne^{7+}) through insulating nano-capillaries has been observed even for cases where the capillaries were considerably tilted by up to 20° with respect to the ion beam direction [1]. Surprisingly, the majority of the projectile ions was found to survive the surface scattering events inside the insulating capillary in their initial charge state. Measured 1-dim. scattering distributions of the transmitted particles indicated propagation of the projectile ions along the capillary axis. As reason for this "guiding effect" a charging-up of the inner walls of the capillaries in a self-organized way due to impact of preceding projectile ions has been proposed [1-4].

Theoretical modelling of the experimental observations has so far proven to be a challenging task [1-3]. Difficulties arise especially due to the different characteristic times observed in the experiment for capillary-wall charging and discharging [3, 4].

2. EXPERIMENT

To gain more insight in this interesting phenomenon we have measured the 2-dim. scattering distribution of transmitted projectiles during the charging-up process. The capillary target for these experiments made of PET has been obtained from HMI-Berlin and was characterized with atomic force microscopy-AFM at TU Wien (mean capillary diameter of 180 nm ± 25%). The transmitted ions are registered on a 2-D position sensitive channel-plate detector. The variation of the scattering distribution during the charge-up process could be monitored as a function of time and total charge. As shown in fig.1 for a capillary tilt angle of 4° (with respect to the incident beam direction) the peak position of the transmitted ions starts at a deflection angle of only 2° and moves with increasing total charge until it saturates at a deflection angle nearly equal to the capillary tilt angle.

The obtained experimental results are compared to recent modelling calculations [3, 4] for self-organized charge-up. Good agreement between simulation and experiment is found.

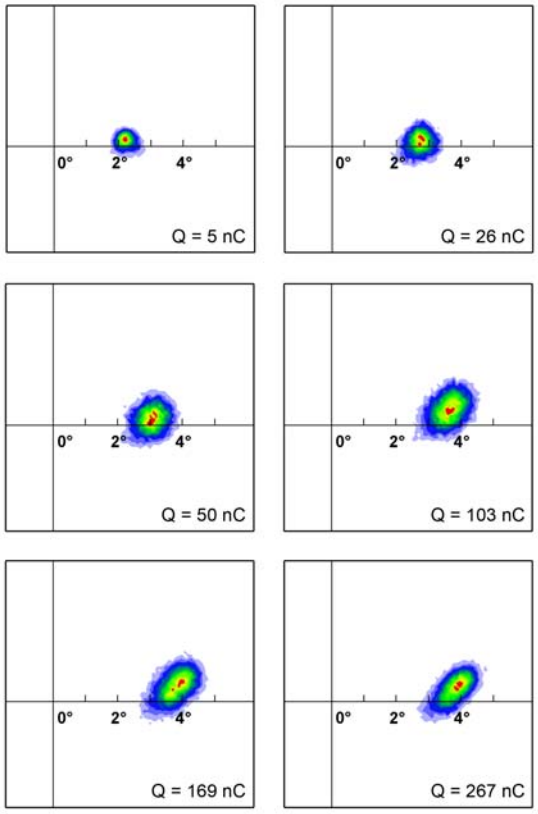

Fig. 1: Evolution of the measured 2-dim. scattering distribution for 0.3 keV/amu Ar^{8+} ions transmitted through PET capillaries (tilt angle 4° with respect to the incident ion beam direction) during the charging-up phase.

This work has been supported by Austrian Science Foundation FWF and was carried out within Association EURATOM-ÖAW.

3. REFERENCES

[1] N. Stolterfoht et al., Phys. Rev. Lett. **88** (2002) 133201
[2] N. Stolterfoht et al., Vacuum **73** (2004) 31
[3] K. Schiessl, et al. NIM B **232** (2005) 228
[4] K. Schiessl, et al. Phys. Rev. A **72** (2005) 62902

* E-mail: meissl@iap.tuwien.ac.at

TWO DIMENSIONAL IMAGES OF SLOW NEON IONS GUIDED BY NANOCAPILLARIES IN POLYMER FOILS

Y. Kanai[1,*], *M. Hoshino*[1,2], *T. Ikeda*[1], *T. Kambara*[1], *R. Hellhammer*[3], *N. Stolterfoht*[3], *and Y. Yamazaki*[1,4],

[1] RIKEN, 2-1 Hirosawa,Wako, Saitama 351-0198, Japan
[2] Sophia University, Chiyoda, Tokyo 102-8554, Japan
[3] Hahn-Meitner-Institut Berlin, Glienickerstr.100, D14109 Berlin,Germany
[4] The University of Tokyo, 3-8-1 Komaba, Meguro, Tokyo 153-8902, Japan

1. INTRODUCTION

Recent observation [1] has shown that slow highly charged ions are guided when transmitted through capillaries of large aspect ratio (100 nm in diameter and 10 μm in length) in a highly insulating polymer (PET: polyethylene terephthalate) foil. The guiding effect indicates that the inner walls of the insulator capillaries are charged in a self-organizing process so that close collisions with the surface are suppressed. In previous experiments[1], only horizontal distributions of transmitted ions were measured. In order to obtain more comprehensive information on the guiding effect, we started to measure the two-dimensional (2-D) images of transmitted ions through PET capillaries.

2. EXPERIMENTS AND RESULTS

The experiments were performed at the Slow Highly Charged Ion Facility at RIKEN [2]. Beams of 3.5-7 keV Ne^{7+} ions from a 14.5 GHz electron cyclotron resonance ion source were collimated to a diameter of 1 mm and a divergence of 0.5^o at a 10-μm-thick PET-foil target. Typical beam currents were 5-200 pA. The PET foil had capillaries with a diameter of 200 nm, whose density was 4×10^6 holes/cm^2. The front and exit sides of the PET foil were evaporated with Au, producing a conducting film of $\sim$ 20 nm thickness to avoid charge up. 2-D images of transmitted ions were measured using a position-sensitive detector with micro channel plates and a wedge-and-strip anode.
Intensity of transmitted ions was increased with time and saturated, as same as reported in previous works [1]. Figure 1 shows 2-D images of transmitted Ne^{7+} ions at different tilt angles of the PET foil relative to the beam with 7 keV Ne^{7+}, after the saturation of transmitted ion intensity. By rotating the target tilt angle from 0^o to 4^o, the peak positions of transmitted ions moved to the capillary axis direction; that is, the deflection angle is nearly equal to the tilt angle. This indicates that the ions were guided by the capillaries. As is seen in Fig. 1, the 2-D images of transmitted ions are rather isotropic and the angular widths of transmitted ions are $\sim 1^o$, which is in good agreement with the theoretical simulation [3], but different from the previous measurements [1][4], where a high-capillary-density (10^8 holes/cm^2) PET foil was used and the angular width of transmitted ions was $\sim 3^o$ for 7 keV Ne^{7+}. We have to mention that the peak position and peak shape of transmitted ions were changed along the tilted direction of capillaries during the intensity evolution of transmitted ions.
In our measurements, Ne^{7+} ions are guided larger than 5^o and the maximum intensity of guided ions around 0^o is about 100 ions/pC, which corresponds to about 20% of the incident Ne^{7+}ions for each capillary being transmitted by the guiding effect. This maximum efficiency does not depend on the beam energy and current under our experimental conditions; 3.5 - 7 keV and 5 - 200 pA.

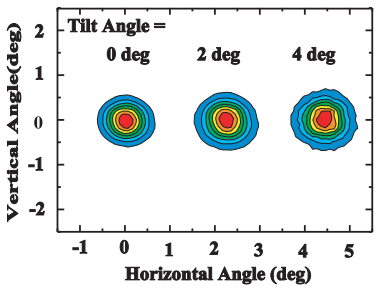

Figure 1: 2-D images of Ne^{7+}ions transmitted through PET capillaries at tilt angle = 0^o, 2^o, and 4^o after the saturation of transmitted ion intensity. The beam energy is 7 keV.

3. REFERENCES

[1] N. Stolterfoht et al.: Phys. Rev. Lett. **88**, 133201 (2002).

[2] Y. Kanai et al.: Phys. Scr. T **92**, 467 (2001).

[3] K. Schiessl et al.: Phys. Rev. A **72**, 062902 (2005).

[4] R. Hellhammer et al.: Nucl. Instrum. Methods Phys. Res. B **232**, 235 (2005).

* E-mail: kanai@rarfaxp.riken.jp

SCALING LAWS FOR ION GUIDING THROUGH NANOCAPILLARIES IN INSULATING PET

R. Hellhammer, D. Fink and N. Stolterfoht

Hahn-Meitner-Institut Berlin, Glienickerstr. 100, D-14109 Berlin, Germany

Experiments in our laboratory have shown that highly charged ions are guided through nanocapillaries in insulating PET polymers without changing their initial charge state [1,2]. The ion guiding was found to be significant when the capillary axis was inclined up to 20° by the tilt angle Ψ. This finding was interpreted as a deflection of the ions near the entrance region of a capillary, where a significant charge patch is produced in a self-organizing manner [1,4]. The patch is characterized by the potential U produced by the charge $Q=CU$ deposited in the patch, where the proportionality constant C may be considered as a capacity of the capillary.

Previous model calculations [2,3] have suggested that the fraction of transmitted ions is given by

$$f_p = f_0 \exp\left[-\left(\frac{E_p}{qU} + c_s\right)\sin^2\Psi\right] \qquad (1)$$

where E_p is the projectile energy, q is the incident charge state, $f_0 \approx 0.5$ is the fraction for $\Psi = 0$, and c_s is an adjustable correction. This expression is based on the assumption that the ions are lost by deposition in the entrance patch if the perpendicular energy $E_\perp = E_p \sin^2\Psi$ exceeds the deflection energy qU. Previous results from our laboratory [3] on the energy dependence of the transmission exhibited inconsistencies with Eq. (1), which we expect to be produced by the non-parallelism of the capillaries.

In this work, we present experiments with PET capillaries of 200 nm involving a significant improvement in the parallelism of the capillary axes. To verify Eq. (1), we first consider the dependence on the tilt angle

$$f_p = f_0 \exp\left[-\frac{\sin^2\Psi}{\sin^2\Psi_c}\right] \qquad (2)$$

This expression introduces the characteristic tilt angle Ψ_c, which can be taken as a measure for the *guiding power* of a capillary. In fact, the *guiding angle* Ψ_c is defined without model assumptions as the tilt angle for which the transmitted intensity drops by the factor 1/e.

We performed measurements using projectiles with different energies and charge states, i. e., Ne^{7+} and Ne^{9+} at 3-10 keV, Ar^{13+} at 7-13 keV, and Xe^{25+} at 25-40 keV. For each projectile the guiding angle Ψ_c was determined under equilibrium conditions, i. e, for sufficiently large times. For example, we obtain Ψ_c=5.4° for 3-keV Ne^{7+} and 2.8° for 25-keV Xe^{25+}. All results are plotted in Fig. 1 as a function of the ratio E_p/q of the projectile energy and charge state. It is seen that the data fall on a universal curve given by

$$\sin^{-2}\Psi_c = U_\infty^{-1} E_p / q + c_s \qquad (3)$$

with the fitted equilibrium potential $U_\infty = 1.75$ V and $c_s = -130$. Hence, the previous model assumptions [2,3], implied in Eq. (1), are essentially confirmed.

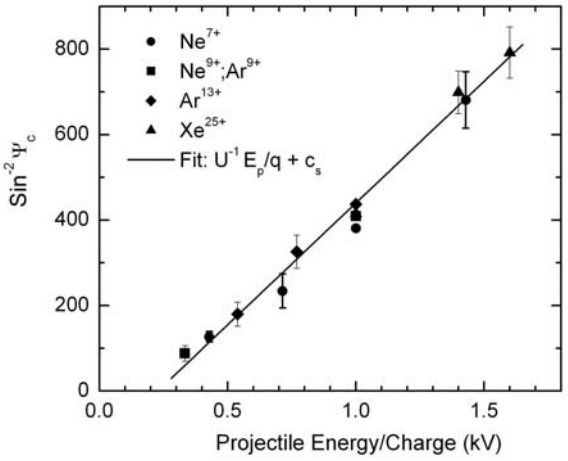

Fig. 1: The quantity $\sin^{-2}\Psi_c$ showing a linear dependence on the ratio E_p/q of the projectile energy and charge (see text).

It should be realized that the good representation of the data by a single curve suggests that the potential U_∞ at equilibrium remains constant when the projectile charge and energy is varied. This finding is in agreement with results of the present study and previous experiments [5] showing that the fraction of transmitted ions remains nearly constant when the current of the incident ions varies by more than an order of magnitude. It appears that U_∞ is a maximum voltage characteristic for the material and geometry near the capillary entrance.

1. REFERENCES

[1] N. Stolterfoht *et al*., Phys. Rev. Lett. **88** (2002) 133201
[2] N. Stolterfoht *et al*., Vacuum **73** (2004) 31
[3] R. Hellhammer *et al*., Nucl. Instr. Methods B **232** (2005) 235
[4] K. Schiessl, et al. NIM B **232** (2005) 228 and Phys. Rev. A **72** (2005) 62902
[5] Y. Kanai *et al.*, this conference (2006)

* E-mail: stolterfoht@hmi.de

ELECTRON GUIDING THROUGH NANOCAPILLARIES IN INSULATORS

B.S.Dassanayake, M.Winkworth, J.A.Tanis, and N.Stolterfoht[*]

Department of Physics, Western Michigan University, Kalamazoo, MI 49008, USA
(*) Hahn-Meitner-Institut Berlin, Glienickerstr. 100, D-14109 Berlin, Germany

In recent experiments the transmission of 3 keV Ne^{7+} ions through nanocapillaries etched in polymer foils has been investigated [1,2]. Though it was believed that highly charged particles would neutralize when travelling through capillaries due to scattering, the intensity of transmitted Ne^{7+} ions was found to be significant even when the foil was tilted to rather large angles (up to ~20^o) with respect to the incident ion beam. This enhanced ion transmission suggested that the inner walls of the capillaries collect charges so that electrostatic repulsion inhibits close collisions with the surface and, in turn, electron capture to the projectile [1,3].

To date, guiding through nanocapillaries has been studied only for positive ions such as Ne^{7+} and H^+ [1-4]. Inspired by the outcome of those experiments, we investigated the transmission of 500 eV and 1000 eV electrons through nanocapillary foils. The experiment was conducted at Western Michigan University using a scattering chamber designed for electron spectroscopy measurements. The electron beam was collimated to a diameter of about 1 mm and directed towards a polyethylene terephthalate (PET) sample, which had been etched with fast ion tracks to form the capillaries. The sample was mounted in a goniometer for precise positioning and a parallel-plate electron spectrometer located just behind the sample detected transmitted electrons.

First, the 'zero position' for transmission of electrons straight through the sample was located by varying the two goniometer angles in small steps, and also by varying the electron observation angle. Next, the sample was tilted with respect to the straight-through position. A significant intensity of transmitted electrons was found for tilted (sample) angles, and correspondingly shifted observation angles, similar to the results for highly charged ions [1-4]. Some of the results from the analysis are shown in Fig. 1.

Electron intensities were studied for several tilt angles from 1° to 10° (the 'zero' was at ~5.5^o) for both 500 eV and 1000 eV electrons. The electron observation angle varied linearly with the tilt angle in each case, as shown in Fig. 1a for 500 eV. Furthermore, the FWHM of the observation angle was found to be essentially constant and equal to ~2.7°, as shown in Fig. 1b, for both 500 eV and 1000 eV. This is to be compared with a FWHM of ~2.1° for the collimated electron beam with no sample in place. As the tilt angle was varied away from the straight-through position, the intensity of guided electrons decreased nearly linearly (results not shown), but this dependence needs further investigation.

These results indicate that electrons are guided through nanocapillaries in a manner similar to positive ions. Future studies of this ongoing work will focus on time dependences of the electron guiding, as well as variations in the capillary dimensions and capillary materials.

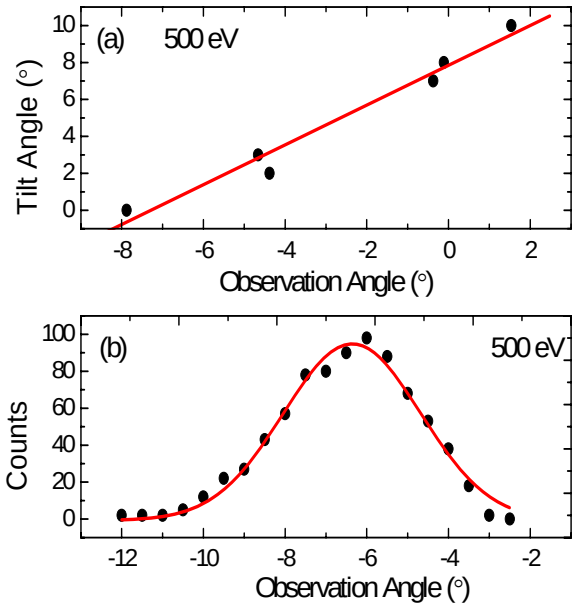

Fig. 1: Electron guiding in PET foils: (a) measured sample tilt angle as a function of electron observation angle, and (b) and measured electron intensity distribution for a tilt angle of 3°.

REFERENCES

[1] N. Stolterfoht et al.: Phys. Rev. Lett., 88, 133201 (2002).
[2] N. Stolterfoht et al.: Nucl. Instr. and Meth. B 225, 169, (2004).
[3] K. Schiessl et al., Phys. Rev. A **72**, 062902 (2005).
[4] M. B. Sahana et al., Phys. Rev. A **73**, 040901 (2006).

[*] E-mail: stolterfoht@hmi.de

Z_1 OSCILLATIONS IN THE SPIN POLARIZATION OF ELECTRONS EXCITED BY SLOW IONS IN A SPIN-POLARIZED ELECTRON GAS

R. Vincent[1,*], *J. I. Juaristi*[2]

[1] Donostia International Physics Center DIPC,
P. Manuel de Lardizabal 4, 20018 San Sebastián, Spain
[2] Departamento de Física de Materiales and Centro Mixto CSIC-UPV/EHU, Facultad de Químicas,
UPV/EHU, Apartado 1072, 20080 San Sebastián, Spain

A slow ion moving through the bulk of a metal with $v < v_F$ (where v is the velocity of the ion and v_F the Fermi velocity of the electrons of the metal) loses energy mainly creating single-particle excitations in the conduction band of the metal. If the energy of excited electrons overcomes the work function of the metal, this leads to the so-called kinetic electron emission.

Here, we present a study of the electronic excitation process when a ion travels through a spin-polarized free electron gas as a function of the atomic number (Z_1) of the projectile. In this case, the screening of the projectile by the medium electrons is more complex than in the paramagnetic case. Electrons of majority and minority spins respond in a different way to the projectile perturbation. Therefore, the screened potential of the incoming particle is spin dependent.

To describe the screening we use density functional theory for a static impurity in a Free Electron Gas (FEG), whose mean electronic density is $n_0 = 3/(4\pi r_s^3)$. Additionally, we consider that the unperturbed electron gas is spin-polarized. The FEG polarization is described by the fractional spin-polarization ξ_0 defined as follows: $\xi_0 = (n_0^{\uparrow} - n_0^{\downarrow})/(n_0^{\uparrow} + n_0^{\downarrow})$ where $n_0^{\uparrow}(n_0^{\downarrow})$ is the background density of majority (minority) spin electrons. We use the local spin density approximation for the exchange correlation potential . In order to calculate the number of electrons excited in projectile-electron collisions, we adopt a model developed in [1]. In this model, the distribution of electrons is directly obtained from the calculation of the scattering of conduction band electrons in the potential induced by the projectile. The scattering is calculated to all orders in the projectile charge using phase-shifts. Since, in our case, the potential is spin dependent due to the spin-polarization of the electron gas, we obtain separately the number of excited majority and minority spin electrons. The difference between these numbers allows us to calculate the spin polarization of the excitation (ξ_{EE}) .

As the most important result, we obtain that the calculated spin-polarization of the excited electrons (Figure 1) shows oscillations when varying Z_1.

* E-mail: waavivir@ehu.es

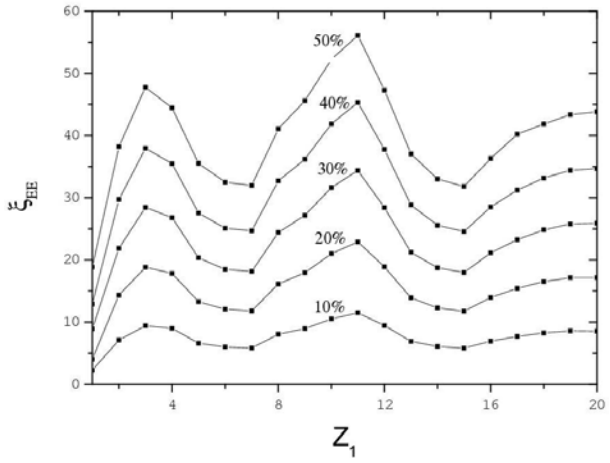

Figure 1: Spin-polarization of the excited electrons for different polarization of the medium and different atomic number of the projectile (Z_1). The velocity of the projectile is $v = 0.8$ (atomic units), r_s is $2a_0$, and ξ_0 is given in the figure.

1. REFERENCES

[1] J. I. Juaristi, M. Rösler, and F. J. García de Abajo, Phys. Rev. B **58**, 15838 (1998).

INFLUENCE OF SCREENING LENGTH CORRECTION ON LEIS-SPECTRA

*R. Kolarova, S.N. Markin, D. Primetzhofer and P. Bauer**

Institut für Experimentalphysik, Johannes Kepler Universität Linz, A-4040 Linz, Austria

1. INTRODUCTION

In the LEIS regime, e.g. for He ions in the energy range 1 – 10 keV, the scattering potential is given by a screened Coulomb potential

$$V(r) = \frac{Z_1 Z_2 e^2}{r} \cdot \Phi_{TFM}\left(\frac{r}{a}\right), \qquad (1)$$

with Z_1 and Z_2 the atomic numbers of ion and scattering centre, respectively, e the electronic charge and $\Phi_{TFM}(r/a)$ the screening function. For the screening length, a, various definitions are used, e.g.

$$a = \frac{0.8852 \cdot a_0}{\sqrt[3]{\left(\sqrt{Z_1} + \sqrt{Z_2}\right)^2}}, \qquad (2)$$

with the Bohr radius $a_0 = 0.529$Å. It is known that the screened potentials used are not equally appropriate for all ion-target combinations. Whenever corrections are required, one reduces a by a multiplicative screening correction factor c_a; which may be as small as 0.53 [1]. The electronic stopping cross section ε [2] is not precisely known in this regime either.

We investigate by means of Monte-Carlo simulations, how a LEIS spectrum is influenced by changes in the screening length or in the stopping cross section. For this purpose, the code TRBS was used, which calculates backscattering spectra allowing for multiple scattering and for electronic energy loss along the trajectory [3].

2. RESULTS AND DISCUSSION

Energy spectra were calculated for 1 – 10 keV He ions and Cu (2, 3 and 4 nm thick) on PET. First, c_a was varied in the range $0.5 \le c_a \le 1$. A strong influence on the scattered yield (neutrals plus ions) was observed, the scattered yield decreasing with decreasing c_a. In Fig.1, the scattered yield is shown for 2nm Cu and 2 keV He projectiles. In this case, not only the peak height but also the peak width is reduced, due to reduced multiple scattering for $c_a < 1$.

Then, for a fixed value $c_a = 0.6$, the stopping cross section was varied in the range $0.5 \cdot \varepsilon_{SRIM} \le \cdot\varepsilon \le 2.0 \cdot \varepsilon_{SRIM}$. In the single scattering model, the spectrum height would be proportional to ~ 1/[ε]. As shown in Fig. 2, the effect is less pronounced in the LEIS regime, due to multiple scattering.

From these simulations the optimum conditions to obtain information about nm Cu films by TOF-LEIS are deduced; the expected accuracy is discussed.

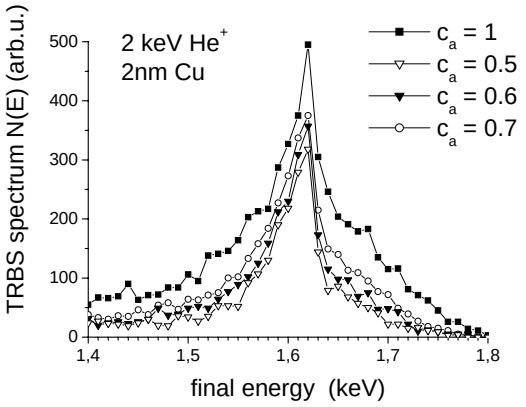

Figure 1: energy spectra simulated for 2 keV He ions and 2 nm Cu, using the TFM potential, for different screening correction factors ca (see insert).

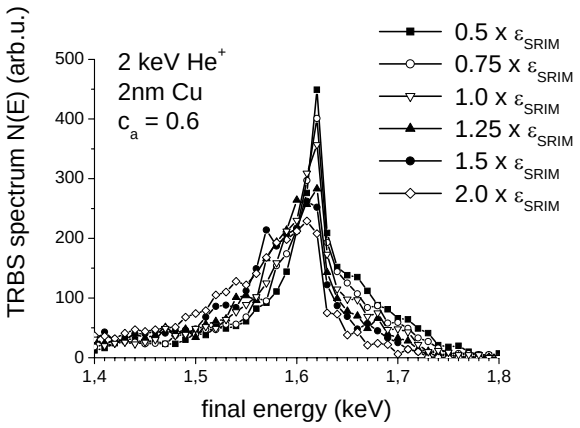

Figure 2: energy spectra simulated for 2 keV He ions and 2 nm Cu, using the TFM potential, for $c_a = 0.6$ and different stopping cross section values (see insert).

3. REFERENCES

[1] M. Draxler, presented at the Ion Beam Analysis conference in Sevilla, June 2005, and Nucl. Instr. Meth. B, in press.

[2] http://www.srim.org
http://www.exphys.uni-linz.ac.at/Stopping

[3] E. Steinbauer, P. Bauer and J.P. Biersack, Nucl. Instr. Meth. **45**, 171 (1990).

* E-mail: Peter.Bauer@jku.at

POLAR AND AZIMUTHAL SCANS FOR He^+ IONS AND A Cu(100) SURFACE

S.N. Markin, D. Primetzhofer, R. Kolarova and P. Bauer*

Institut für Experimentalphysik, Johannes Kepler Universität Linz, A-4040 Linz, Austria

1. INTRODUCTION

In the LEIS regime, i.e. for low energy ions, e.g. He^+ ions, in the energy range 1 – 10 keV, the scattering potential is given by a screened Coulomb potential

$$V(r) = \frac{Z_1 Z_2 e^2}{r} \cdot \Phi_{TFM}\left(\frac{r}{a}\right), \qquad (1)$$

with Z_1 and Z_2 the atomic numbers of ion and scattering centre, respectively, and $\Phi_{TFM}(r/a)$ the Thomas-Fermi-Moliere screening function. For the screening length a various definitions are used, e.g.

$$a = \frac{0.8852 \cdot a_0}{\sqrt[3]{\left(\sqrt{Z_1} + \sqrt{Z_2}\right)^2}}, \qquad (2)$$

with the Bohr radius a_0 = 0.529Å. It is known that the screened potentials used are not equally appropriate for all ion-target combinations and all impact parameter ranges. Whenever corrections are required, one reduces the screening length a by a multiplicative screening correction factor c_a; which may be as small as 0.53 [1]. A convenient way to explore the scattering potential is to study polar and azimuthal scans, I(ψ) and I(φ) respectively. In these scans, the widths of the channeling/blocking minima are quite sensitive to the strength of the scattering potential. By comparing experiment and simulations, the appropriate value of c_a can be obtained.

The scattered total intensity (positive ions plus neutrals), I, were recorded in polar scans for 15° ≤ ψ ≤ 110° and in azimuthal scans for 0° ≤ φ ≤ 110°. Cu(100) was used as a target surface, and 1.5 to 8 keV He^+ ions as projectiles. Note that the polar angle ψ is the complementary angle of the angle of incidence, α.

2. RESULTS AND DISCUSSION

In the polar scans, channeling minima were obtained for ⟨100⟩ and ⟨110⟩ directions (ψ = 90° and 45°, respectively). For the scattered yield a pronounced surface peak was observed in the polar scans at channeling conditions. The intensities in these minima, $I_0(\psi)$, depend on ψ as the number of visible surface atoms increases as 1/sinψ (suppression of contributions from deeper layers). At intermediate angles an increase in I_0 by about one order of magnitude was observed, indicating contributions from first, second and deeper layers (see Fig. 1a). The azimuthal scans exhibit the symmetry of the crystal as expected (see Fig. 1b).

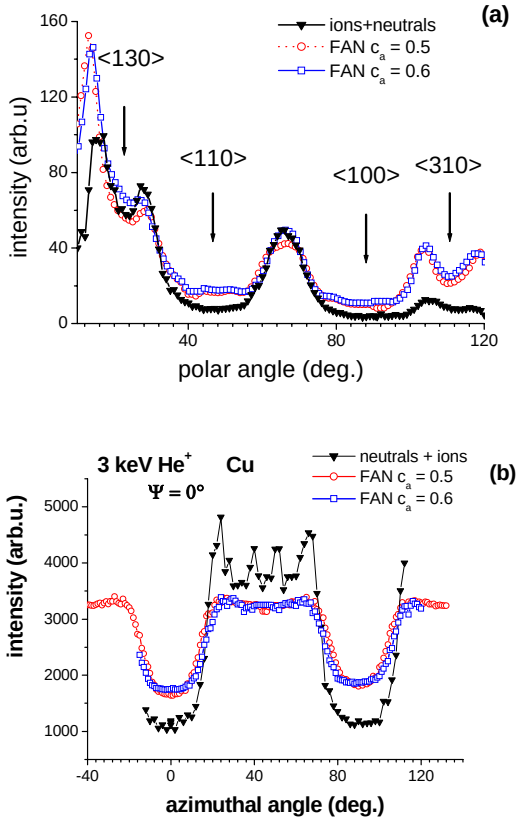

Fig.1: (a) experimental and simulated polar angle scans for 2 keV He ions and Cu(100) (see legend).

(b) experimental and simulated azimuthal angle scans for 3 keV He ions and Cu(100) (see legend).

In order to deduce quantitative information about the scattering potential, the angular scans I(ψ) and I(φ) are compared to simulations using the FAN code [2] (see Fig. 1). As a result, the potential is found to be weaker than given by 1 and 2, corresponding to $c_a \approx 0.5 \ldots 0.6$, in good agreement with literature [1].

3. REFERENCES

[1] M. Draxler, M. Walker and C.F. McConville, Nucl. Instr. Meth. B, in press.

[2] H. Niehus, W. Heiland and E. Taglauer, Surf. Sci. Rep. 17 (1993) 215.

* E-mail: daniel.primetzhofer@aon.at

MONTE CARLO SIMULATION OF CHARGE EXCHANGE PROCESSES IN THE SCATTERING OF 4 keV He^+ IONS BY AN AMORPHOUS SILICON SURFACE

K. Khalal-Kouache[*]

Faculté de Physique, Université des Sciences et Technologies Houari Boumedienne, B.P. 32, El Alia, Bab Ezzouar, Algiers, Algeria.

ABSTRACT

Charge exchange in the scattering of slow He^+ ions off an amorphous silicone surface is studied. For this purpose, numerical simulation based on a Monte Carlo method is used to calculate energetic spectra and positive charge fraction of the scattered particles. This simulation takes into account two charge exchange processes (Auger neutralization and charge exchange in close collisions) and the effect of image potential on ion trajectories in incoming and outgoing channels. Comparison is done with experimental results about the scattering of 4keV He^+ ions from a silicon surface. This method allows the determination of different parameters governing the particle-matter interaction at low energy.

[*] E-mail: kkouache@yahoo.fr

ON THE RELATIVE ROLE OF ELECTRON PROMOTION PROCESSES AND ELECTRONIC FRICTION IN ATOMIC COLLISION CASCADES

A. Duvenbeck[1,*], *O. Weingart*[2], *J. Bloemen*[3], *V. Buss*[2] *and A. Wucher*[1]

[1] Department of Physics, University of Duisburg-Essen, D-47048 Duisburg, Germany
[2] Department of Theoretical Chemistry, University of Duisburg-Essen, D-47048 Duisburg, Germany
[3] Department of Applied Computer Sciences, University of Applied Sciences Gelsenkirchen, D-45877 Gelsenkirchen

1. ABSTRACT

We present a computer simulation model for the space- and time resolved calculation of electronic excitation energy densities in atomic collision cascades. The model treats electronic friction as well as electron promotion as a source term of excitation energy that is carried away from the original point of excitation according to a nonlinear diffusion equation.
While the frictional sourceterm is treated within the Lindhard model of electronic stopping, electron promotion is described using diabatic correlation curves derived from ab-initio molecular orbital energy level calculations in combination with the Landau-Zener curve crossing model.
Results show that the electron promotion mechanism may contribute significantly to the time structure of the excitation energy density, giving rise to distinct and very short peaks of the local electron temperature at the surface. This contribution is essentially restricted to the first 100 fs after the projectile impact and may therefore be of significance for either external or internal kinetic electron emission. At later times, where the kinetics lead to the sputter ejection of material from the surface, the excitation is shown to be primarily governed by electronic friction. This finding is important in order to understand the excitation and ionization probabilities of sputtered particles.
The obtained results will be presented using the free and easy-to-use visualization software CINEMAMD, which has been developed in our group for the 3D-stereoscopic visualization of atomic collision cascades.

* E-mail: wucher@uni-essen.de

SURFACE-PLASMON-ASSISTED ELECTRON CAPTURE IN GRAZING INCIDENCE H^+/AL COLLISIONS

R. Sandoval[1], *F.A. Gutierrez*[1] *and H. Jouin*[2,*]

[1] Departamento de Física, Universidad de Concepción, Casilla 160-C, Concepción, Chile
[2] CELIA (UMR 5107 CNRS-Université Bordeaux 1-CEA),
Université Bordeaux 1, 351 Cours de la Libération, 33405 Talence Cédex, France

1. INTRODUCTION

In the surface-plasmon assisted electron capture mechanism, the energy released when a metal electron is captured in a bound state of the passing ion allows the collective excitation of surface electrons. This process has been found very relevant in order to explain the experimental angular distributions of neutralized He^+ ions after grazing incidence collisions with Al surfaces [1-2]. For the H^+/Al system, it is known [3] that in the frame of the fixed ion approximation (FIA), in which the ion is fixed at a given distance from the surface, this mechanism is forbidden since the energy given up by the captured electron is not enough to excite the surface plasmon of Al. Nevertheless, consideration of the ion's velocity allow to open this channel. Therefore, our first aim in the present work is to analyse the ion's velocity effect on the opening of the collective surface-plasmon channel. Furthermore, we have studied the importance of this process with respect to Resonant and Auger mechanisms in grazing incidence H^+/Al collisions. This latter analysis has been performed by computing the fractions and angular distributions of scattered species after collisions of protons with Al(111). Comparisons with experimental results for neutral fractions as a function of the projectile parallel velocity [3-4] show that the surface-plasmon assisted electron capture mechanism play a non negligible role at high impact velocities.

2. TRANSITION RATES

Velocity dependent transition rates for the surface-plasmon assisted electron capture process have been calculated for the H^+/Al system by means of the approach already presented in [2]. The main features of these rates with respect to velocity and distance to the image-plane dependence are as follows:
(a) For all finite velocities, the rates present a threshold distance s_T below which the process is forbidden due to energy and momentum conservation. For a given velocity and increasing distances from s_T, the rates increase up to a maximum and then decrease more or less exponentially. (b) For $v_\bullet \leq 0.1$ a.u. the rates are very weak (less than 10^{-9} a.u.) and the threshold distance is large (greater than 5 a.u.). For increasing velocities threshold distances decrease while the magnitude of the rates increases. At $v_\bullet = 1$ a.u., the threshold distance is around 0.5 a.u. and the rate reach a maximum of 3.10^{-3} a.u. for a distance of 1.5 a.u..

It must be noted that the magnitude of the rates for $v_\bullet \geq 0.5$ a.u. is comparable to the magnitude of the ones obtained in [2] for the $He^+(1s)$/Al system.

3. CHARGE FRACTIONS

It is well known that in the H^+/Al system the resonant processes (capture and loss) play an important role since the ground state of H is always resonant with occupied levels of the metal. Resonant transition rates have been calculated by means of various approaches within the FIA during the past decade [5]. Furthermore Auger process is also present for populating H(1s) [3]. Thus in order to study the interplay of these three processes (Resonant, Auger and Surface-Plasmon) in proton neutralization after grazing Al(111) surface scattering, we have used the ETISC1D simulation code [6] that allow to compute charge fractions and angular distributions of scattered species. Velocity dependence of Resonant [5] and Auger [3] rates is taken into account by means of the method proposed first by Mišković and Janev [7] and also used in [3]. In this approximate approach, Auger and Resonant velocity dependent rates are calculated by means of the FIA ones and by using the simplifying assumption that velocity dependent matrix elements are isotropic in the **k**-space. We find that the surface-plasmon-assisted electron capture process starts to play a role for $v_\bullet \geq 0.5$ a.u. for populating H(1s).

4. REFERENCES

[1] H. Jouin, F.A. Gutierrez and C. Harel, Phys. Rev. **A 63**, 052901 (2001); Phys. Rev. **A 66**, 019901(E) (2002).
[2] F.A. Gutierrez and H. Jouin, Phys. Rev. **A 68**, 012903 (2003).
[3] R. Zimny, Z.L. Mišković, N.N. Nedeljković and Lj. D. Nedeljković, Surface Science **255**, 135 (1991).
[4] H. Winter, Physics Reports **367**, 387 (2002).
[5] P. Nordlander and J.C. Tully, Phys. Rev. **B 42**, 5564 (1990); A. G. Borisov et al, Nucl. Instrum. and methods **B 78**, 51 (1993) ; F. Martín and M.F. Politis, Surface Science **356**, 247 (1995).
[6] S. Jequier, H. Jouin, C. Harel and F.A. Gutierrez, Surface Science **570**, 189 (2004).
[7] Z.L. Mišković and R.K. Janev, Surface Science **221**, 317 (1989).

* E-mail: jouin@celia.u-bordeaux1.fr

ENERGY LOSS AND ELECRON EMISSION DURING GRAZING SCATTERING OF FAST NOBLE GAS ATOMS FROM AN Al(111)-SURFACE

S. Lederer[1], *HP. Winter*[2], *and H. Winter*[1,*]

[1] Institut für Physik der Humboldt Universität Berlin (Germany)
[2] Institut für Allgemeine Physik der Technischen Universität Wien (Austria)

1. INTRODUCTION

Detection of the projectile energy loss in coincidence with the number of emitted electrons during grazing scattering of fast atoms or ions from metal surfaces allows one to perform detailed studies on the electronic excitation and emission processes in this collision regime [1]. In the work presented here we have scattered keV noble gas atoms from an Al(111)-surface under a grazing angle of incidence Φ_{in} of typically some degree and observed via a time-of-flight (TOF) setup the energy loss for specularly reflected projectiles. The energy loss spectra are recorded in coincidence with the number of emitted electrons which is obtained by means of a surface barrier detector biased to a high voltage of typically 25 kV.

2. RESULTS

A representative energy loss spectrum obtained in our studies is shown in Figure 1 for the scattering of 12 keV Ar atoms from an Al(111) surface under Φ_{in} = 2.2°. The full circles represent the experimental data, the curves are results from our computer simulations. In the theoretical description of data we assumed classical binary collisions of the projectile with conduction electrons where the differential cross sections for electron-atom scattering are taken from quantum mechanical calculations [2] showing preferential scattering in forward and backward directions. The number of effective collisions is used as a parameter and is fixed to about 50, electron emission is described assuming a probability of about 1 percent for excited electrons with sufficient energy to cross the vacuum-solid interface. A good overall agreement with the measured spectra is obtained for He and Ne atoms, for Ar atoms we find a slightly smaller energy loss than observed (dashed curve in Figure 1). The reason for this discrepancy is based on the energy transfer to lattice atoms during the scattering process which is substantially larger for Ar projectiles than for the lighter noble gas atoms. The dotted curve in Figure 1 represents results from computer simulations for this nuclear stopping. Incorporation of this additional energy loss channel via convolution of the simulation for the electronic excitations results in a fair agreement with the experiment (solid curve).
Comparison of spectra coincident with the emission of no and one electron reveals a systematic shift which is interpreted as the additional energy needed to eject an electron to vacuum. This shift is quantitatively reproduced in our calculations.

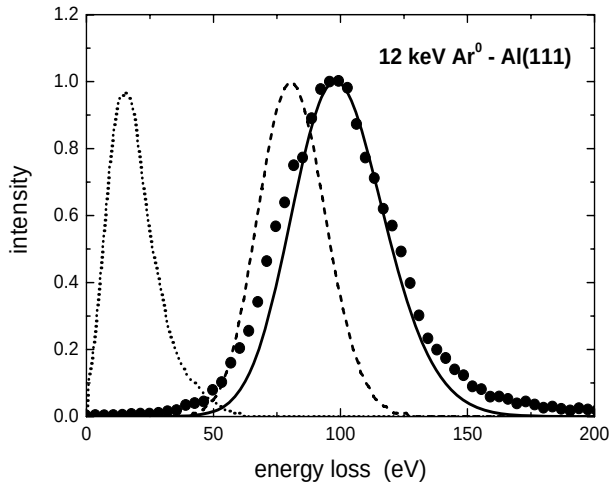

Figure 1: Energy loss for scattering of 12 keV Ar atoms from Al(111) under Φ_{in} = 2.2°. Full circles: experimental data, curves: computer simulations.

3. REFERENCES

[1] S. Lederer, K. Maass, D. Blauth, H. Winter, HP. Winter, and F. Aumayr, Phys. Rev. B **67**, 121405(R) (2003).
[2] A. Dasgupta and A. Bathia, Phys. Rev. A **32**, 335 (1985).

* E-mail: winter@physik.hu-berlin.de

COMPUTER SIMULATIONS OF GRAZING SCATTERING OF ATOMIC PROJECTILES FROM CRYSTAL SURFACES

S. Wethekam[*] *and H. Winter*

Institut für Physik der Humboldt-Universität zu Berlin, Newtonstr. 15, D-12489 Berlin, Germany

The structure of surfaces and thin films or the interaction of atomic projectiles with solid surfaces can be studied by scattering of atomic projectiles under a grazing angle of incidence [1]. The analysis of the data is based on trajectory calculations for the scattered projectiles as, e.g., for ion beam triangulation [1, 2], rainbow scattering to investigate interaction potentials [3], or probing defect structures and lattice vibrations via polar angular distributions [4].

In this work we concentrate on the aspect of incorporation of lattice vibrations of target atoms in molecular dynamics simulations for a meaningful comparison with experimental data. We performed classical 3D trajectory simulations by taking into account a rigid lattice and on the other hand thermal vibrations of target atoms. We studied the fraction of atoms that penetrate the first target layer as function of azimuthal orientation of the incoming beam (ion beam triangulation). Angular distributions are calculated for impact along random and low indexed azimuthal directions. Thermal vibrations are incorporated within the Debye model with no further approximations applied. The Debye model is used in molecular dynamics simulations by approximations: the high-temperature limit neglecting strong correlations in the vibrations of neighboring atoms [4]. The approximation of uncorrelated vibrations is also used in the KALYPSO code [5]. On the other hand, Jackson and Barrett [6] have pointed out that the incorporation of correlations of lattice vibrations is crucial for a realistic simulation of trajectories in the channeling regime. This raises the general question on the influence of correlation effects and thermal vibrations on the above mentioned quantities.

Based on computer simulations we will show that correlations of lattice vibrations have only a minor effect on ion beam triangulation studies and positions of rainbow peaks for scattering along low indexed directions. The shape of angular distributions, for low energies of motion normal to the surface of a few eV, however, turns out to be sensitive on correlations. In conclusion, ion beam triangulation data can be analyzed using uncorrelated thermal vibrations, while a realistic description of angular distributions requires a more detailed modeling. For rainbow structures thermal vibrations lead to only small shifts of the peak positions. A two-dimensional simulation, where the interaction potential is averaged along atomic strings [7] provides an adequate modeling of the scattering process.

Fruitful discussions with Prof. J.R. Manson (Clemson) and A. Schüller (Berlin) are gratefully acknowledged. This work is supported by the Deutsche Forschungsgemeinschaft (DFG) under contract Wi 1336.

[1] H. Winter, Phys. Rep. **367**, 387 (2002).
[2] T. Bernhard et al., Phys. Rev. Lett. **95**, 087601 (2005).
[3] A. Schüller et al., Phys. Rev. A **69**, 050901(R) (2004).
[4] R. Pfandzelter, Phys. Rev. B **57**, 15496 (1998).
[5] M.A. Karolewski, Nucl. Instr. and Methods B **230**, 402 (2005).
[6] D.P. Jackson and J.H. Barrett, Comp. Phys. Comm. **13**, 157 (1977). J. H. Barrett and D.P. Jackson, Nucl. Instr. and Methods **170**, 115 (1980).
[7] D. Gemmell, Rev. Mod. Phys. **46**, 129 (1974).

[*] E-mail: stephan.wethekam@physik.hu-berlin.de

TIME–DEPENDENT SIMULATIONS OF ELECTRON EMISSION IN GRAZING ION–SURFACE COLLISIONS

D.M. Mitnik[1], *I. Aldazabal*[2,*], *A. Arnau*[2,3], *M.S. Gravielle*[1], *J.E. Miraglia*[1], *and V.H. Ponce*[4]

[1] Instituto de Astronomía y Física del Espacio, and Departamento de Física, Universidad de Buenos Aires, Argentina
[2] Departamento de Física de Materiales UPV/EHU, Apartado 1072, San Sebastián 20080, Spain
[3] Donostia International Physics Center D.I.P.C., San Sebastián, Spain
[4] Centro Atómico Bariloche, Río Negro, Argentina

1. INTRODUCTION

Spectra of electrons emitted in grazing ion–surface collisions provide information about the structure of the surface, and have been the subject of intense research in the past years. In particular, it is interesting to study the electron distribution around the direction of the specular reflection of the projectile, where the spectrum displays a sharp peak[1], known as the *"convoy"* peak. However, the shape and position of the convoy peak are affected by the surface potential produced by the ionization of the target (the *"track potential"*). In this work, we developed a numerical method for treating the surface track potential, expanding it in spherical coordinates around the colliding ion. We assume that the ion captures an electron from the surface, leaving it in a particular continuum state. The formation of a charge distribution in the surface behind the projectile, breaks up the spherical symmetry of the captured electron distribution, producing an electron emission spectra that is not necessarily centered around the ion.

2. THEORETICAL METHOD

2.1. Surface track potential

We consider a heavy ion projectile impinging grazingly on a solid surface, with the following classical trajectory

$$Y(Z) = Y_0 \cosh Z \tag{1}$$

where Y is the perpendicular position and Y_0 is the closest distance of the projectile respect to the surface. The potential[2] generated by the ionization of target atoms in the surface is calculated, in the ion coordinates as

$$V(\vec{r}) = \int_{-\infty}^{Z} du \frac{n(u)}{r}, \tag{2}$$

where n is the charge density.
Assuming the projectile position $Z = Z_0 + v_Z t$, the potential becomes time dependent.

* E-mail: ialdazabal@ehu.es

2.2. Time dependent propagation

The track potential $V(\vec{r}, t)$ developed in the previous section is used in order to construct the Hamiltonian

$$\hat{H}(\vec{r}, t) = -\frac{\nabla^2}{2} - \frac{1}{r} + V(\vec{r}, t). \tag{3}$$

The time-dependent wavefunction and the track potential are expanded in spherical harmonics $Y_{\ell m}$:

$$\Psi_{\ell m}(\vec{r}, t) = \frac{1}{r} \sum_{\ell m} P_{\ell m}(r, t) Y_{\ell m}(\theta, \phi), \tag{4}$$

and

$$V(r, \theta, \phi, t) = \sum_{\ell m} A_{\ell m}(r, t)\, Y_{\ell m}(\theta, \phi), \tag{5}$$

where $P_{\ell m}(r, t)$ is the reduced radial wavefunction, and $A_{\ell m}$ are the expansion coefficients. Upon substitution of Eqs. (4) and (5) into the time-dependent Schrödinger equation we obtain the time dependent close–coupling equations for each ℓm symmetry. We use the techniques developed for the time dependent calculations of atomic collisions[3] to propagate an initial configuration along the projectile trajectory. By analyzing the final electron distribution around the incident ion, we can understand the mechanisms responsible for the acceleration or deceleration of the convoy electrons. In particular, the relationship between the position of the maximum of the electron distribution with the electron–capture processes, and with the track potential form.

3. REFERENCES

[1] K.O. Groeneveld, W. Meckbach, I. Sellin, and J. Burgdörfer, Comments At. Mol. Phys. **4**, 187 (1984).

[2] A. Arnau, M.S. Gravielle, J.E. Miraglia, and V.H. Ponce, Phys. Rev. A **67**, 062902 (2003).

[3] D.M. Mitnik, D.C. Griffin, and M.S. Pindzola, Phys. Rev. Lett. **88**, 173004 (2002); D.M. Mitnik, Phys. Rev. A **70**, 022703 (2004).

AR SCATTERING FROM SI (100) SURFACE AT GRAZING INCIDENCE: EXPERIMENT AND MD SIMULATION

F. Gou [1], *M. A. Gleeson* [2] *and A. W. Kleyn* [1,2,*]

[1] Gorlaeus Laboratories, Leiden Institute of Chemistry, 2300 RA Leiden, The Netherlands
[2] FOM Institute for Plasma physics, Rijnhuizen, 3430BE, Nieuwegein, The Netherlands

The interactions of low energy ions with surfaces have long been a topic of both theoretical and experimental interest. In the present study, we present molecular dynamics (MD) modeling of Ar scattering from perfect and defective Si (100) at grazing incidence with respect to the surface plane at 0 and 300 K. Inelastic energy loss is not included in these simulations. The simulated results demonstrate that with decreasing adatom density, the angular and energy distribution of the scattered particles broaden and the peak intensity decreases. The azimuthal angle distribution shows that (a) 90% adatom density is almost identical to the perfect crystal, (b) 10% adatom density significantly affects the scattering.

The experimental results shows the energy loss of 3 keV Ar^+ scattering at very grazing incidence is mainly contributed by inelastic energy loss. Therefore, a new electron stopping model based on the continuous model is included in the above simulations. The results show the simulated energy loss is in good agreement with the experiment.

* E-mail: A.W.Kleyn@rijnh.nl

DIFFERENTIAL MULTI-ELECTRON EMISSION INDUCED BY SWIFT HIGHLY CHARGED GOLD IONS PENETRATING CARBON FOILS

H. Rothard[1,*], *R. Moshammer*[2], *J. Ullrich*[2], *H. Kollmus*[3], *R. Mann*[3], *S. Hagmann*[3,4], *T.J.M. Zouros*[5]

[1] CIRIL-Ganil (CEA/CNRS/ENSICAEN/Université de Caen), BP5133, F-14070 Caen cedex 05, France
[2] Max-Planck-Institut für Kernphysik, Saupfercheckweg 1, D-69117 Heidelberg, Germany
[3] GSI, Planckstr. 1, D-64291 Darmstadt, Germany
[4] IKF, Johann Wolfgang Goethe-Universität, Max-von-Laue-Strasse 1, D-60438 Frankfurt am Main, Germany
[5] Department of Physics, University of Crete, PO Box 2208, 71003 Heraklion, Greece

Electron ejection from target atoms is one of the basic processes when ionizing radiation interacts with matter. The primary electrons and their subsequent secondary interactions lead to the deposition of energy around the ion trajectory. The detailed knowledge of the structure of these ion tracks is a key issue for our understanding of radiation effects in condensed matter, an important example being calculations of the RBE of heavy particles, where doubly differential electron ejection cross sections enter as input parameter.

Usually, data obtained from collisions with single atoms or molecules, i.e. with gas targets, are used, but condensed matter effects may considerably alter the emission patterns [1]. The emission of low energy electrons was up to now mainly studied by means of electrostatic electron spectrometers. Time-of flight-methods were used in some cases. Here, we present first results on swift heavy ion induced electron emission from solids obtained with a reaction microscope [2,3], a technique that is successfully used since quite some time to study electron ejection in ion-atom collisions [3]. For a recent review, see ref. [4].

This advanced technique combines the measurement of the time-of-flight of electrons with imaging techniques. A combination of electric and magnetic fields assures that more than 80% of all ejected electrons are guided onto a position sensitive detector [2]. This large area electron detector is capable to accept multi hits at an instantaneous count rate of more than 100 MHz. From position and time-of-flight measurement the full differential emission characteristics of up to 10 electrons per single incoming ion can be extracted.

Here, we present energy spectra (as shown in Fig. 1), angular distributions, and the multiplicity distribution of electrons from impact of Au^{24+} (11 MeV/u) on a thin carbon foil (28 μg/cm^2).

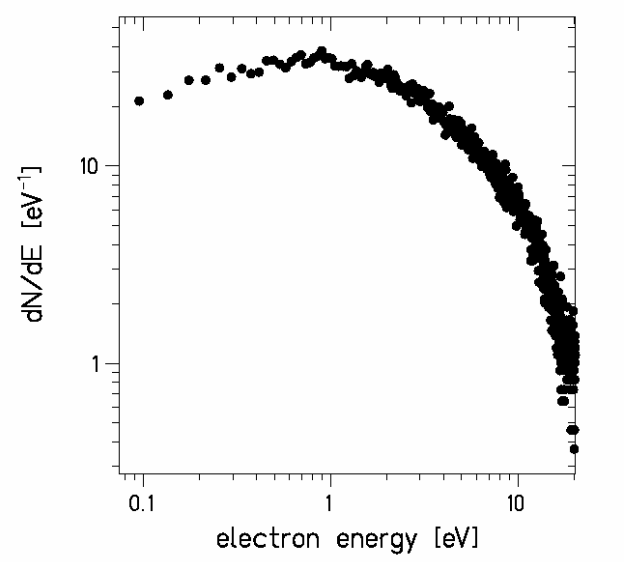

Figure 1: Energy distribution of low energy electrons emitted in collisions of Au^{24+} (11 MeV/u) on a thin carbon foil (28 μg/cm^2).

REFERENCES

[1] H. Rothard, Nucl. Instrum. Meth. B **225**, 27 (2004)
[2] R. Moshammer, M. Unverzagt, W. Schmitt, J. Ullrich and H. Schmidt-Böcking, Nucl. Instr. Meth., **B108**, 425 (1996).
[3] W. Schmitt, R. Moshammer, F.S.C. O'Rourke, H. Kollmus, L. Sarkadi, R. Mann, S. Hagmann, R.E. Olson and J. Ullrich, Phys. Rev. Lett. **81** , 4337 (1998).
[4] J. Ullrich, R. Moshammer, A. Dorn, R. Dörner, L.P. Schmidt and H. Schmidt-Böcking, Rep. Prog. Phys. **66**, 1463 (2003).

* E-mail: rothard@ganil.fr

ENERGY LOSS OF CARBON CLUSTER ION IMPACTED ON FOIL

T.Kaneko[*], *and S. Ikegami*

Faculty of Science, Okayama University of Science, 1-1 Ridaicho, Okayama 700-0005, Japan
...

1. INTRODUCTION

Since cluster ions were accelerated at high energies, they have been interested from the viewpoint that they present aspects, different from mono-atomic ion impacts, in electron excitation and atomic scattering. These are called cluster effects, which were found in the average charge per ion[1,2], in the energy-loss[3]. Recentry, reduction of the secondary electron yield under MeV/atom cluster impacts was also reported. Cluster ions moving in a foil tend to explode their mutual distances, resulting in the average charge. In this paper, we studied phenomena in collision of MeV/atom cluster ion with a target material, i.e., inelastic energy loss and the elastic collision. Regarding the former, we copare the existing data and give some prediction. As for the latter, we propose an approximated form of the screening length and discuss the charge state dependence. Knowledge obtained on the latter in included in estimation of the former quantity.

2. METHOD AND RESULTS

2.1. Energy-loss of a cluster ion

Here the charge and the size of the electron cloud accompanying a cluster in a material are important. The average charge is evaluated in a self-consistent manner on a basis of a statistical model, where the electric field of surrounding ions on an individual ion was taken into account. This leads to reduction of the average charge per ion, compared with a mono-atomic ion with an equivalent speed. The constituent ions in a cluster are described as partially stripped ions, whose electron clouds are described in a Thomas-Fermi-Moliere form. The number of the bound electrons is determined by the average charge. Electronic energy-loss of a cluster is estimated in a dielectric function method[4]. Here excitation of conduction electrons and the bound electrons are both taken into account. Coulomb explosion, cluster structure and wake effect are also included together with the ion-atom elastic collisions given below. The calculated energy-loss shows the cluster effect, depending on the speed.

2.2. Screening length

In order to take into account the deflection of ions in a cluster due to a repulsive interaction with a target atom, we consider the two-body ion(atom)-atom potential in a statistical model. Our interest is focused on rather swift projectiles so that weak attractive part of the potential is neglected. Then we treat the repulsive part of the potential. Employing a statistical model, we write the interaction in the form $V(r) = Z_1 Z_2 e^2 \Phi(r/a)/r$. If we describe the screening function $\Phi(r/a)$ in a Thomas-Femi-Moliere function, the screening length for neutral atom-atom collision is approximated as

$$a = 0.8853 a_0 xy(x+y)/(x^2 + y^2 + cxy)$$

where $x = Z_1^{-1/3}$, $y = Z_2^{-1/3}$, $c \approx 1.337$.

The values of for Li -> C, Al, Si, V, Cr, Fe, Co, and Ni targets are respectively 0.l717, 0.1462, 0.1439, 0.1282, 0.1269, 0.1245, 0.1233, and 0.1182 in units of 10^{-8}cm. The corresponding values from the small angle multiple scattering experiments[5] are 0.216, 0.156, 0.142, 0.110, 0.111, 0.093, 0.115, and 0.092 in the same units. We also derived the screening length for ion-atom collisions, which is used in collisions between a cluster ion and a target atom.

3. REFERENCES

[1] A. Brunelle, S. Della-Negra, J. Depauw, D. Jacquet, Y. Le. Beyec and M. Pautrat, Phys. Rev. A **59**, 4456(1999).
[2] A. Chiba, Y. Saitoh, and S. Tajima, Nucle. Instr. Meth. In Phys. Res. B **232**, 32(2005).
[3] K. Baudin, A. Brunelle, M. Chaobot, S. Della-Negra, J. Depauw, D. Gardes, P. Hakansson, Y. Le. Beyec, A. Billebaud, M. Fallavier, J. C. Poizat and J. P. Thoma, Nucl. Instr. Meth. in Phys. Res. B **94**, 341(1994).
[4] T. Kaneko, Phys. Rev. A **66**, 052901(2002).
[5] S. Schwabe et al., Phys. Stat. Sol(b) **47**, 111(1971)

[*] E-mail: kaneko@dap.ous.ac.jp

PRECISE ANALYSIS ON SHAVE-OFF DEPTH PROFILING

M. Nojima[1, 2,*], *T. Yamamoto* [2,3], *Y. Ishizaki*[2, 3], *M. Owari*[2], *and Y. Nihei*[1, 3]

[1] Research Inst. for Sci. & Tech., Tokyo University of Science, 2641 Yamazaki, Noda, Chiba 278-8510, Japa
[2] Inst. Industrial Sci., University of Tokyo, 4-6-1 Komaba, Meguro-ku, Tokyo 153-8505, Japan
[3] Fac. Sci. & Tech., Tokyo University of Science, 2641 Yamazaki, Noda, Chiba 278-8510, Japan

1. INTRODUCTION

Any analytical systems introducing probe or ray must come across charge problems when the systems are used for insulator or semiconductor samples. We have been developing nano-beam secondary ion mass spectrometry (SIMS) apparatus for shave-off depth profiling [1]. The nano-beam SIMS system equips Ga-focused ion beam (FIB) and sector typed mass analyzer (Mattauch-Herzog type) [2].

In shave-off depth profiling with dynamic micromachining with FIB, sample and its environment are supplied high voltage. The biased sample makes it difficult to solve the charge up problems with electron shower near ground leveled voltage.

In this presentation, we have developed an epoch-making flood gun system for the nano-beam SIMS apparatus and minimized charge up problem in shave-off depth profiling.

2. Flood gun system

The flood gun system is controlled by 3 power sources (for the emitter, the suppresser and the extractor) and can realize different voltages on each electrode. The introduction of the flood gun system will be enabled charge neutralization in the nano-beam SIMS system and can realize precise analysis on shave-off depth profiling.

3. REFERENCES

[1] Toi et al., Journal of Surface Analysis Vol.12 **No.2** p.170 (2005)
[2] Nojima et al., Applied Surface Science Vol. 231, p. 930 (2004)

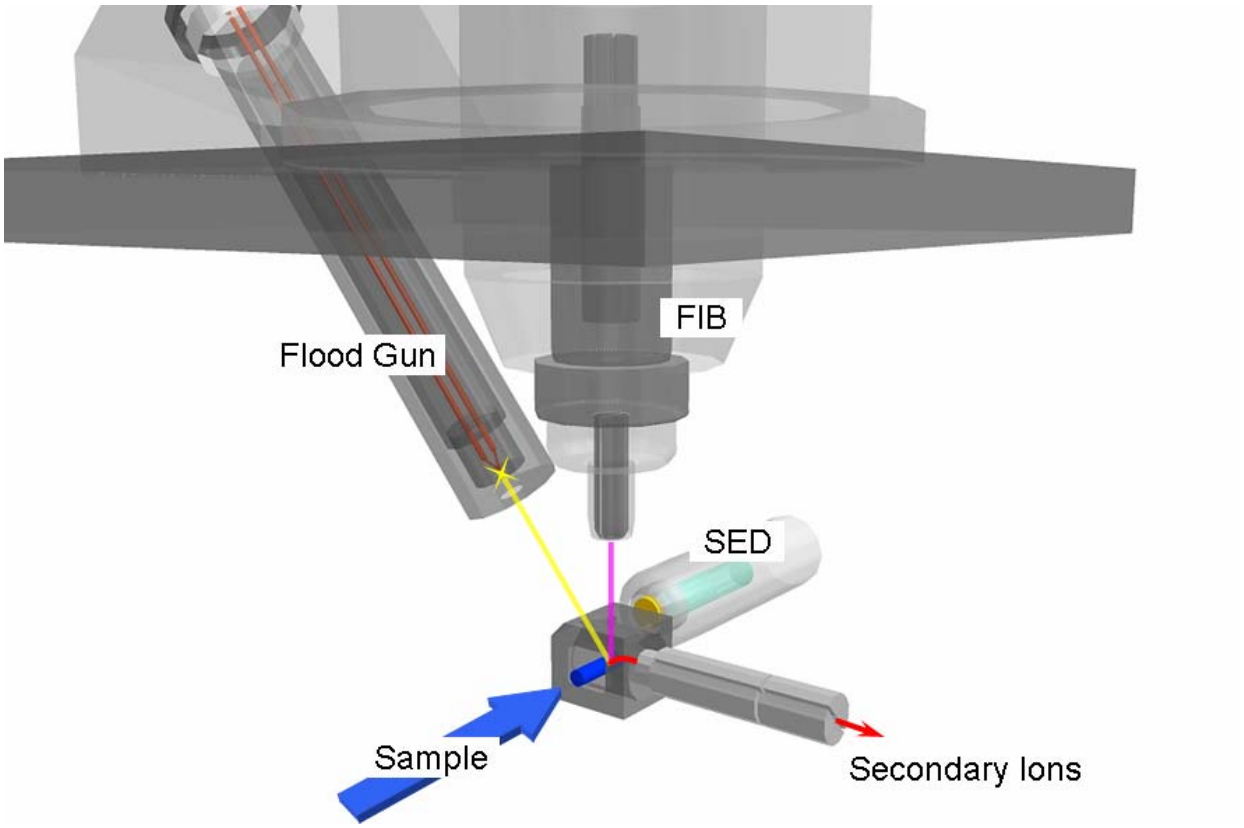

Fig. A schematic image of food gun system

* E-mail: mnojima@rs.noda.tus.ac.jp

TEMPERATURE DEPENDENCE OF THE D-H REPLACEMENT RATES IN D-IMPLANTED OXIDE CERAMICS EXPOSED TO H_2O VAPOR

K. Morita[1,*], *B. Tsuchiya*[2], *S. Nagata*[2], *K. Katahira*[3], *M. Yoshino*[4], *Y. Arita*[5], *T. Ishijima*[4] *and H. Sugai*[4]

[1]Department of General Education, Faculty of Science and Technology, Mejio University,
1-501 Shiogamaguchi, Tenpaku-ku, Nagoya 468-8502, Japan
[2]Institute for Materials Research, Tohoku University, Japan
[3]Advanced Materials Research Institute, TYK Co. Ltd., Japan
[4]Graduate School of Engineering,
[5]Institute for EcoTopia Science, Nagoya University, Japan

We have been systematically looking at the replacement of hydrogen isotopes (D-H and H-D) in hydrogen ion(H, or D)-implanted oxide ceramics exposed to water(H_2O, or D_2O) vapor at room temperature by means of the ion beam analysis technique. We have found from the data analysis that the hydrogen-implanted oxide ceramics provide with the catalytic function of dipole induced water splitting and hydrogen gas emitting, which originates from the attractive Coulomb interactions of dipole charge of water with charge of the lattice defects at the surface and from the bulk molecular recombination of hydrogen atoms in traps with hydrogen atoms absorbed from the surface, respectively [1.2]. The catalytic function provides a possibility of producing hydrogen gas from water vapor at room temperature at high energy-efficiency and the hydrogen gas emission rate is estimated to be 1 Nm^3/hr, when the surface area of the specimen is 500 m^2, based on the experimental champion data on the hydrogen gas emission. For practical use of the catalytic function, it is of essential importance to understand atomistic mechanism of the catalysis and to find higher rate materials in the hydrogen gas emission.

In this paper we have measured the temperature dependence of the hydrogen gas emission rates in D-implanted $BaCe_{0.9}Y_{0.1}O_{3-\delta}$ exposed to water vapor. It is found that the D-H replacement rate increases monotonically as the specimen temperature increases up to 50^{O}C. The concentration of H retained in the specimen decreases when annealed in the vacuum at the temperature, while it does not decrease when exposed to water vapor at the temperature. On the other hand, the hydrogen gas emission rate is shown to be closely connected to charging speed of the lattice defects which introduces donor and acceptor levels near the conduction and valence bands and which have been once neutralized by the Coulomb interactions [2]. The experimental result will be discussed in terms of the mass balance equations and also the optimal temperature for hydrogen production is also discussed.

This study was supported by Industrial Technology Research Grant Program in 05A0002c from New Energy Development Organization (NEDO) of Japan and also supported by Feasibility Study of Japan Science and Technology Agency (JST) Tokai Plaza.

References

[1] K. Morita, H. Suzuki and K. Soda: Nucl. Instru. Meth.B206(2003) 228.
[2] K. Morita, B. Tsuchiya, S. Nagata and K Katahira: Nucl. Instru. Meth. B(2006) in print.

* E-mail: kmorita@ccmfs.meijo-u.ac.jp

ANTISITE DEFECTS IN A CHEMICAL COMPOUND CRYSTAL CAUSED BY ION IRRADIATION

S. T. Nakagawa[1,*], *K. Hashimoto*[1], *and G. Betz*[2]

[1] Graduate School of Science, Okayama Univ. of Science, Okayama 700-0005, JAPAN
[2] Inst. f. Allgemeine Physik, Technische Universität Wien, Wiedner Hauptstraße 8-10, A-1040 Wien, AUSTRIA

1. INTRODUCTION

Silicon-carbide (SiC) is a wide band-gap semi-conductor, which has high carrier-mobility and high thermal-conductivity. This material has more than 100 politype-crystals, depending on the stacking form involved. Most investigations are for wurtzeit (2H-SiC), moissanite (4H-SiC or 6H-SiC), or zincblende (3c-SiC). In this case the periodic arrangement of "Si-C dimers" (which is parallel to the c-axis) determines each crystal structure. Here we discuss the zincblende structure (3c-SiC), which has the same ligand field for atoms as in the diamond structure.
Of wide-gap semiconductors, only SiC can adopt both types of dopants, e.g., boron implantation into 3c-SiC results in p-type devices with high resistivity. Although the defect formation is crucial in impurity doping by ion bombardment, it is still a promising way in device syntheses using annihilation. A peculiar defect called anti-site displacement can be produced in zincblende-type (AB) crystals, if atoms A and B exchange their sites. This means to reverse the position of atoms in a "Si-C dimer" in SiC. It is supposed that the planar defects called $\{311\}_A$ or $\{311\}_B$ [1] in zincblende-type semiconductors are produced by synergetic assembly of such pair replacements [1].
We have identified {311} defect formation in c-Si [2] caused by self-irradiation. In this article we mainly examine the intrinsic defects [3] including anti-phase boundaries ($\{311\}_A$ or $\{311\}_B$) for 3c-SiC crystal caused by boron, silicon, or carbon projectiles.

2. METHODS OF CALCULATION

2.1. MD (Molecular Dynamics)

Ion bombardment (B, C, Si) of 3c-SiC is simulated by molecular dynamics (MD) at a target temperature of 1000 K. Energetic ballistic collisions of particles following projectile injection are described by the repulsive ZBL potential. To describe low energy collisions and the equilibrium allocation of atoms the ZBL potential is splined to the Tersoff-4 potentials for Si-Si, Si-C and C-C [4].

Interatomic potentials for B-Si and B-C are determined by the ab-initio density functional method called B3LYP in Gaussian-03 [5]. (Becke type 3 parameter density functional method with the Lee-Yang–Parr correlation function). The numerical results are parameterized into the form of a Morse potential.

$$V(r) = D_e \left\{ e^{-2\beta(r-r_e)} - 2e^{-\beta(r-r_e)} \right\} \qquad (1)$$

These potentials are also splined to the ZBL potential for energetic collisions.

2.2. Defect analysis (Pixel Mapping)

We have proposed a method to analyze various types of defects in a diamond-type crystal, which we called the Pixel Mapping (PM) method [6]. PM can identify various types of microscopic, mesoscopic and macroscopic defects. Especially, definition of Miller indices of atomic planes is useful to identify planar defects and linear defects [2].
Here we apply the PM method to different compound crystals with cubic symmetry [7], where each cubic crystal is characterized mathematically in a PM table. Using the PM table, we can find the spatial distribution of various kinds of defects, identify whether a structure change from one to another crystal type has occurred, observe modified domain structures, etc. In this work we are mainly concerned with planar defects or anti-phase boundaries in the case of chemical compounds.

3. REFERENCES

[1] K. Morizane, J. Crystal Growth 38, 249 (1977).
[2] S. T. Nakagawa, H. J. Whitlow, and G. Betz, Nucl. Instr. Meth., in press (2006)
[3] A. Mattausch, M. Bockstedte, and O. Pankratov, Phys. Rev. B69, 045322 (2004).
[4] J. Tersoff, Phys. Rev, B39, 5566 (1989).
[5] Gaussian03; http://www.gaussian.com/
[6] S. T. Nakagawa, Phys. Rev. B 66, 094103/1-7 (2002).
[7] S. T. Nakagawa, (to be published in 2006)

* E-mail: stnak@physics.dap.ous.ac.jp

STOPPING POWER AND FINAL CHARGE FRACTIONS IN keV PROTONS TRAVERSING THIN C AND AlF_3 FILMS

L. Serkovic, E.A. Sánchez, O. Grizzi, N.R. Arista, J. Eckardt and G. Lantschner*

Centro Atómico Bariloche, Instituto Balseiro, CNEA, CONICET, 8400 S.C. de Bariloche, Río Negro, Argentina

The slowing down of light atomic projectiles traversing insulator materials at low velocities has raised some controversies regarding the expected departure from the linear velocity dependence[1] and the existence of a threshold velocity[2]. Two experimental approaches have been previously used to study these phenomena at low velocities: 1) grazing scattering of protons from flat LiF surfaces[3] and 2) reflection of protons from LiF films evaporated on Au substrates[2]. In this work we use the well known transmission method, with the energy analysis performed by the time of flight technique (TOF) in order to reduce the incident irradiation dose, and evaporate the AlF_3 films on one side of a self-supporting C foil, in the same scattering chamber and under UHV conditions. The initial stopping in the C foil allows measurements down to a few hundred eV, keeping the energy straggling small enough to deduce accurately the final outgoing energy (upper panel of Fig.1).

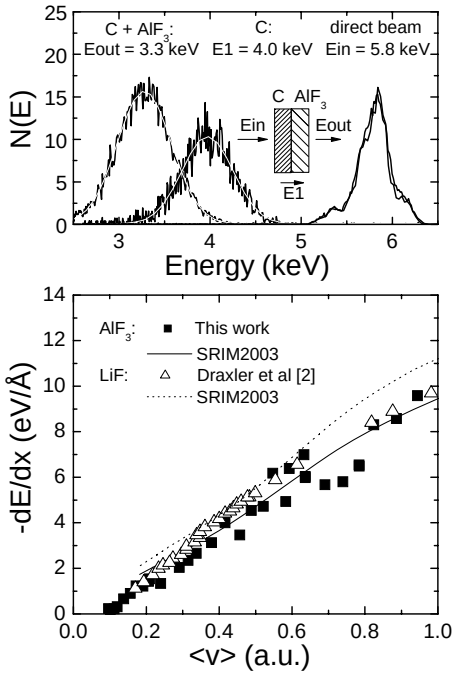

Fig.1: *Upper panel*: TOF spectra for protons transmitted through a 2 μg/cm^2 C foil and through the same C foil with a film of AlF_3 of 200 Å thick. *Lower panel*: Stopping power plotted versus the mean velocity in the insulator film.

Deflection plates located at the end of the drift tube allow measurements of the positive, negative and neutral emerging fractions. The capability of doing the measurements in the same evaporation chamber allows determination of stopping and charge fractions as a function of the film thickness (Fig. 2). The film composition is verified by TOF direct recoil spectroscopy, while the thickness is determined by a quartz balance and by atomic force microscopy performed *ex situ.*

For pure C foils at low energies the positive and negative ion fractions are comparable; however at higher energies the positive component becomes increasingly predominant.

The energy loss results in the C-foils are in good agreement with those measured with an electrostatic energy analyzer of our lab.

For AlF_3 films, the results show a trend similar to that measured by Draxler[2] in LiF. The stopping power plotted versus the mean velocity of the projectiles in the AlF_3 film has a threshold velocity of 0.1 a.u. (Fig.1, lower panel).

The positive ion fractions dominate in the whole energy range; however, in contradiction with the pure C case, they increase with decreasing proton energy. The ion fractions become stable for AlF_3 film thickness larger than 25 Angstroms (Fig. 2).

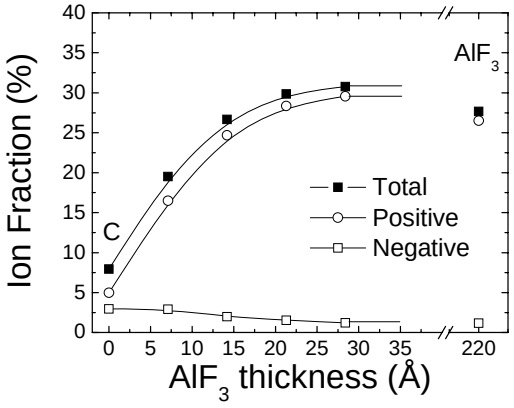

Fig.2: H^+ and H^- outgoing ion fractions versus AlF_3 film thickness measured for 5.8 keV incoming protons.

REFERENCES

[1] D. Semrad, Phys. Rev. A **33** 1646 (1986).
[2] M. Draxler et al., Phys. Rev. Lett. **95** 113201 (2005).
[3] C. Auth et al., Phys. Rev. Lett. **81** 4831 (1998).

* E-mail: grizzi@cab.cnea.gov.ar

ION BEAM INDUCED MAGNETIC CHANGE OF ULTRATHIN FE FILMS ON CU(100)

W. Rupp[*] , *B. Kamenik, M. Schmid, and P. Varga*

Institut für Allgemeine Physik, Technische Universität Wien, A-1040 Wien, Austria

1. Abstract

The structure and magnetism of ultra thin epitaxial Fe films grown on Cu(100) at 300 K (RT) have been investigated by STM (scanning tunnelling microscopy), low-energy electron diffraction (LEED) and by surface magneto-optical Kerr effect (SMOKE) [1]. Hysteresis loops in longitudinal and polar geometry can be determined. Depending on the film thickness, three regimes with different magnetic properties and different orientation of the magnetic anisotropy are known [2] and could be confirmed. Further it is also known that the fcc phase, which has no magnetic moment, can be achieved at room temperature (RT) only for a thickness of 5 to 10 monolayers (ML).

In these films small (needle-like) nuclei of the bcc structure were found by STM measurements [3, 4].

We have observed that in these Fe films the phase transition from the fcc phase to the bcc phase can be induced and promoted by ion bombardment (Fig. 1). By LEED measurements we observe the structural change from fcc to bcc-like structures after ion bombardment (e.g. ion dose around 0,4 Argon ions / surface atom). At RT, the structural transition is accompanied by a change of in-plane magnetization from paramagnetic to ferromagnetic behaviour. Additionally, our SMOKE data show the disappearance of the low temperature surface ferromagnetism (with perpendicular magnetic anisotropy) [2, 5] as the films becomes bcc during ion bombardment.

The magnetic properties and crystallographic structure of such treated films depending on ion dose, ion energy and ion mass will be discussed.

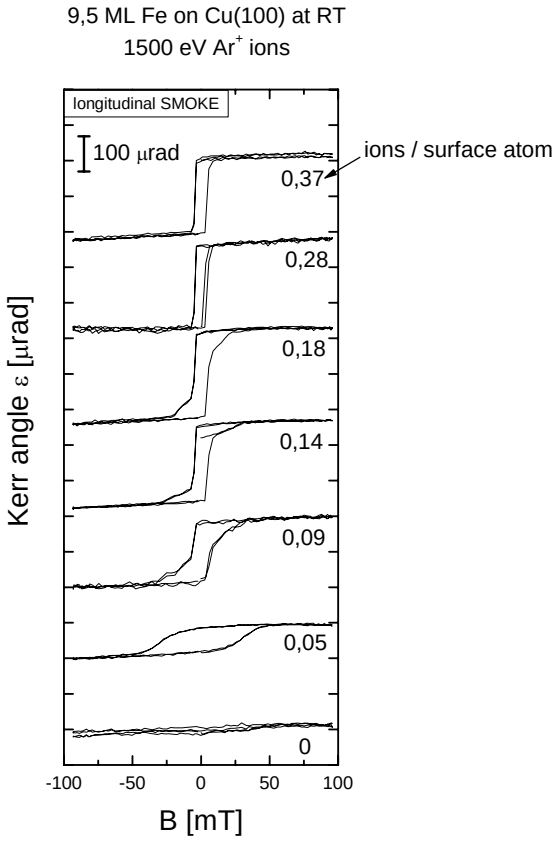

Figure 1: Evolution of the transformation with 1,5 keV Ar^+ ion bombardment.

2. REFERENCES

[1] S.D. Bader, J. Magn. Magn. Mater. 100, 440-454 (1991).

[2] J. Thomassen, F. May, B. Feldmann, M. Wuttig and H. Ibach, Phys. Rev. Lett. 69, 3831 (1992).

[3] A. Biedermann, M. Schmid and P. Varga, Phys. Rev. Lett. 86, 464 (2001).
A. Biedermann, R. Tscheließnig, M. Schmid and P. Varga, Phys.Rev.Lett. 87, 86103 (2001).

[4] A. Biedermann, R. Tscheließnig, Ch. Klein, M. Schmid and P. Varga, Surf. Sci. 563, 110-126 (2004).

[*] E-mail: rupp@iap.tuwien.ac.at

CAPILLARY GUIDING OF SLOW Ne^{6+} IONS IN ANODIC ALUMINA

Z. Juhász[1,*], *Gy. Víkor*[2], *S. Biri*[1], *É. Fekete*[1], *I. Iván*[1], *K. Tőkési*[1], *E. Takács*[2], *J. Pálinkás*[2], *S. Mátéfi-Tempfli*[3], *M. Mátéfi-Tempfli*[3], *L. Piraux*[3], *N. Stolterfoht*[4], *and B. Sulik*[1]

[1] Institute of Nuclear Research (ATOMKI), Bem tér, 18/c, H-4026 Debrecen, Hungary
[2] Department of Experimental Physics, University of Debrecen, Egyetem tér 1, H-4032 Debrecen, Hungary
[3] Unité de Physico-Chimie et de Physique des Matériaux, Université Catholique de Louvain (UCL), Place Croix du Sud, 1, B-1348 Louvain-la-Neuve, Belgium
[4] Hahn-Meitner Institute Berlin GmbH, D-14109 Berlin, Germany

The ion guiding ability of nanocapillaries etched in PET polymer foils has been discovered recently [1]. In this work, this phenomenon is investigated at ATOMKI for Al_2O_3 capillaries prepared by a two step anodization process at UCL.

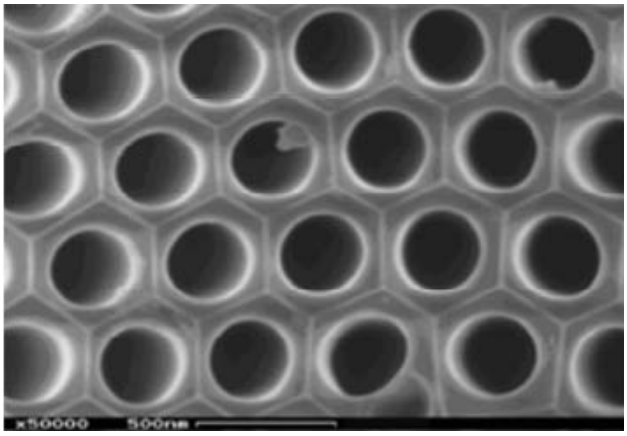

Figure 1: SEM view of an array of Al_2O_3 capillaries.

The experiments have been performed with slow Ne^{6+} ions of impact energies of 3 keV and 6 keV, which were transmitted through the highly ordered capillary arrays with pore diameter of 150 nm and 290 nm. It has been found that ions with larger incidence angles than the one belongs to the geometric transparency can pass through the Al_2O_3 capillaries similarly as for PET. The ions leave the capillaries along the capillary axis with a narrow angular distribution. Systematic measurements have been performed for different energies and incidence angles, which could be changed by tilting the capillary array. Time dependences of the transmission, charge and angular distributions of the transmitted ions are obtained. Angular distributions with FWHM of 3-4° have been found. Similar results have been found for PET capillaries [1], but in the case of SiO_2 the observed angular distributions were narrower [2]. The different behavior of SiO_2 can be caused by different material properties but structural differences may also play a role.

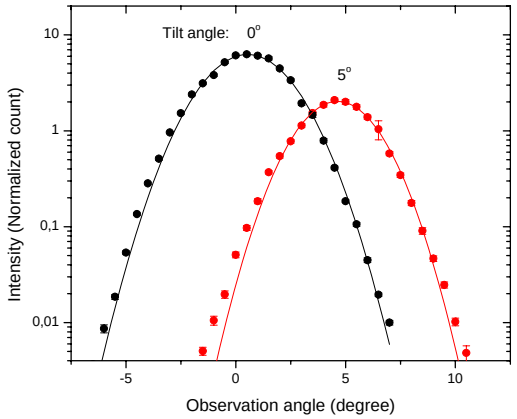

Figure 2: Angular distribution of 3keV Ne^{6+} ions transmitted through Al_2O_3 capillaries with pore diameter of 290 nm.

To explain capillary guiding different models have been developed [3, 4]. These are based on the assumption that the guiding effect is due to charge deposition on the capillary walls. The time and tilt angle dependences of the overall transmitted intensities can be understood within the framework of the models. The differences in the width of the angular distributions of the transmitted ions comparing observations for PET, SiO_2 and Al_2O_3 membranes are not yet understood. We are developing a model, in which individual local events of charge deposition and migration are traced. The calculation is performed for a single capillary, but the effects of the other capillaries are included. These effects seem to contribute to the widening of the angular distribution of the outgoing ions.

Acknowledgements

This work was supported by the Hungarian National Science Foundation OTKA (Grants: T046905, T046454, T042729 and PD 050000).

REFERENCES

[1] N. Stolterfoht et al., Phys. Rev. Lett. **88**, 133201, (2002).
[2] M. B. Sahana et al., Phys. Rev. A **73**, 040901, (2006).
[3] N. Stolterfoht et al., Vacuum **73**, 31 (2004).
[4] K. Schiessl et al., Phys. Rev. A **72**, 062902 (2005).

* E-mail: zjuhasz@atomki.hu

NONLOCAL PARTICLES KINETICS AND INELASTIC SURFACE COLLISIONS

*O.G. Bakunin**

RRC "Kurchatov Institute", Nuclear Fusion Institute, 123182 Moscow,Russia, Sq Kurkhatova 1.

1. INTRODUCTION

In the case of beam-matter interactions we deal with a strong non-equilibrium system, where the particles distribution function differs significantly from the Maxwellian one. In that case, it is important to obtain the relationship between the distribution function and correlation functions that describe long-range correlation effects [1-3]. Here, the classical kinetic equation in the diffusive form does not apply, because it describes only systems near equilibrium. In this paper, we offer to use the methods of anomalous diffusion in phase-space to describe the particle distribution function [4]. The correlation properties are described by the velocity correlation function of emitted particles. We suggest using a functional equation for collision probability instead of the conventional diffusive kinetic equation. In this case, we deal with "memory" effects due to the finite numbers of the collisions. This mirrors the direct relation between the distribution function and the correlation function. In case under consideration, we can apply the power approximations of correlation functions. The information about both kinetics and correlation properties is contained in the single functional equation. The solution of this equation was received in the form of Levy's function with different power tails, which are described by the correlation exponent α :

$$F(v) \propto \frac{1}{v^{\alpha}} \exp\left(-\frac{1}{v}\right).$$

Such solutions cannot be obtained by means of the asymptotic consideration of conventional kinetic equations. The asymptotic solution has the scale-invariant character $F(V) \propto \frac{1}{V^{a}}$ that gives the scalings, which describe suprathermal particle transport.

2. REFERENCES

[1] O. Bakunin *Plasma Physics Control. Nucl. Fusion*, **47** (2005) 1857

[2] O. Bakunin *J. Plasma Physics* **73,** part 2 (2005).

[3] O. Bakunin, *Physica A* **337** (2004) 27

[4] O. Bakunin, *Reports on Progress in Physics* **67** (2004) 965-1032.

[5] O.Bakunin O.G. 2003 *Pasmal.Phys. Cont. Fusion* **45** 1909

* E-mail: oleg_bakunin@yahoo.com

ELECTRON TRANSPORT ALONG ATOMIC CHAIN

K.K. Satarin[*], *I.K Gainullin, and I.F. Urazgildin*

Moscow State University Physics Faculty

1. INTRODUCTION

The charge exchange between a negative hydrogen ion and atomic chain is considered. The electron transfer problem was solved by the Wave Propagation Packets (WPP) method, which does not involve the perturbation theory. It was shown that interatomic potential barrier substantially affects on electron transport effectiveness; character of electron transport was described.

2. ELECTRON DYNAMICS

The electron transport along hydrogen atomic chain was calculated using the wave packet propagation method.

Initially electron's wave function taken in ion's electron wave function form. Average electron coordinate and electron most probability coordinate was calculated using wave function. Atomic chain consists of 10 hydrogen atoms. For small interatomic distances (8 a.u.) electronic transport along the chain was found to be very effictive.

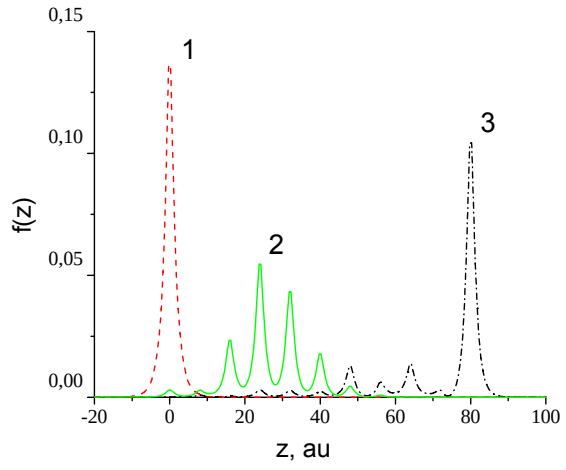

Figure 1 Line 1 – initial electron's density of distribution along Z axis. Line 2 – electron's density of distribution along Z axis in moment of time 350 au. Line 3 – electron's density of distribution along Z axis in moment of time 750 au.

On figure 1 one can see electron's density of distribution along Z coordinate in different moments of time. Initially electron located on hydrogen ion (figure 1, line 1). As a result of resonant charge transfer electron propagates to following chain atoms (figure 1, line 2). Electron is not localized on a single atom, it's distributed among several neighbore atoms. Electron's density of distribution at the end of transition displayed on figure 1, line 3, one can see that electron localized on remote chain boundary.

At figure 2 electron position was shown as function of the time. Electron distribution along atomic chain is discrete, but average electron's coordinate changes droningly and continiously.

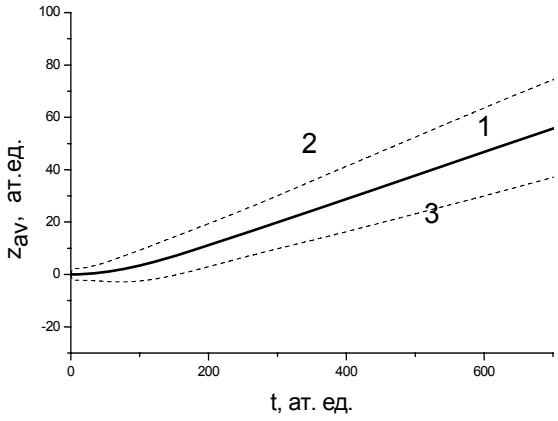

Figure 2, Line 1 – average electron's coordinate in dependace on time. Line 2, Line 3 – standart derivation of average electron's coordinate in dependence on time.

Also the electron transport along aluminium chain was calculated. The electron transition rate was found to be more eficient than for free metal case.

3. REFERENCES

[1] P. Nordlander, J. C. Tully, Phys. Rev. Lett. **61**, 990 (1988).

[2] V.A. Ermoshin, A.K. Kazansky Phys. Lett. A **218**, 99 (1996).

[3] T. Hecht, H. Winter, A. G. Borisov, J. P. Gauyacq etc. Phys. Rev. Lett. **84**, 2517 (2000).

[4] E.Yu. Usman, I.F. Urazgildin, A.G. Borisov, J.P. Gauyacq Phys. Rev. B **64**, 205405 (2001).

[*] E-mail: satarin@ph-elec.phys.msu.su

RESONANCE TUNNELING POSITRONS NEAR METAL SURFACES

Abdalaziz A. Almulhem
Department of Physics, King Faisal University
P. O. Box 1759, Alahssa 31982 Saudi Arabia

When bombarding a metal surface with ions, the ions will interact with the surface resulting in a specific distribution of the charge state. This is due to the fact that some of the ions will pick up electrons to be neutralized. Neutralization of positrons scattered from metal surfaces via resonance tunneling is considered. In this mechanism a positron is neutralized by picking up an electron that tunnel through the potential barrier at the surface $e^+ + e^- (Al\ metal) \rightarrow Ps(1s)$. The problem is similar to what happen when a proton is being scattered from a metal surface. There the mechanisms that produce neutralized atoms upon scattering of ions from metal surfaces are three. Those are: resonance tunneling; Auger neutralization and surface plasmon-mediated ion neutralization. The third mechanism namely surface plasmon-mediated ion neutralization was applied for the case of positron neutralization in an earlier work. There, a unitary transformation was introduced to the second quantized Hamiltonian. This transformation proved very useful in tackling problems of reactive scattering that included composite particles. The bound state was described by a state orthogonal to all conduction band states of the metal. The theory is applied to the case of a positron capturing an electron from a metal surface. The neutralization rate is calculated as a function of distance from the surface. Also the ratio of positroniums created to the positrons scattered is calculated. The figure shows the neutralization rate P as a function of the distance s from the surface. From the figures it is evidently clear that the transition rate decays exponentially with distance from the surface. The general behavior is similar to the ion neutralization at metal surface. At small distances the transition rate is greatly affected in the important region for neutralization namely small distances from the surface. In this region the repulsive potential due to the positive background of the metal has large values. This decreases the total potential (attractive and repulsive) and consequently the transition rate. The effect of lowering the transition rate is accomplished in our theory by the orthogonalization term in the matrix element, which is subtracted from the original matrix element. The attractive potential (positron charge with the electron density) also increases at small distances from the surface. The two effects add up to a potential that give rise to the turnover region. The incident positron will penetrate into the turnover region when the electron density on the surface is such that the attractive potential rate of increase is greater than that of the repulsive potential.

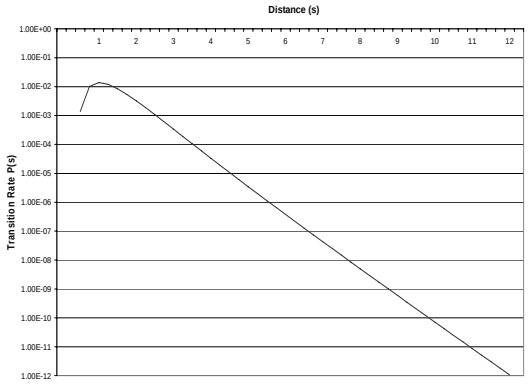

Resonance tunneling neutralization rate P as a function of the distance s from the metal surface for a positron scattered from aluminum surface.

REFERENCES

[1] H.D. Hagstrum, Phys. Rev. 96 (1954) 336.

[2] A.A. Almulhem and M.D. Girardeau, " Theory of Ion Neutralization at Metal Surfaces by Surface Plasmon Excitation", Surface Science 210 (1989) 138.

[3] Almulhem A.A., "Resonance Tunneling Neutralization of Low-energy Ions near Metal Surfaces", Surface Science, 304 (1994) 191.

[4] Akira ISII, "Theory of Positronium formation on Solid Surfaces, I. General theory and its application to positronium formation probability", Surface Science. 147 (1984) 227.

[5] Akira ISII, "Theory of Positronium Formation on Solid Surfaces, II. Velocity distribution of re-emitted positronium", Surface Science. 147 (1984) 295.

STRUCTURALLY STABLE HIGHER-ORDER OPTICAL VORTICES GENERATED BY THE DIELECTRIC WEDGES SYSTEM

Ya. V. Izdebskaya, V. G. Shvedov, A.V. Volyar*

Taurida National V.Vernandsky University, Vernadsky av.4, Simferopol, Ukraine

1. INTRODUCTION

We experimentally showed that higher-order optical vortices generated by the system of dielectric wedges subjected to focusing do not lose its structural stability.

It is proved to be quite natural now to see a variety of new optical applications based on unique properties of the vortex-bearing singular beams. The microparticle traps and spanners and also needs of nonlinear optics take up one of the first places among them. The greater is the vortex topological charge, the greater is the angular momentum of the beam to twist the particles and to perform different self-action operations. To that end it is necessary to focus the singular beam into a small area. However, higher-order optical vortices can be structurally unstable ones to such transformation. Soskin[1] et al pointed out that even transmission of a Gaussian beam with the double-charged optical vortex through a relatively wide circular aperture results in breaking out the vortex into two single-charged ones. Helseth extended such conclusion onto all higher-order optical vortices in a focal region. Is this characteristic inherent in all types of singular beams or only in Gaussian beams bearing the higher-order optical vortices? Are there any exceptions from this rule?

In this article we investigate the focusing of the higher-order optical vortices nested in singular beams generated by the optical wedge.

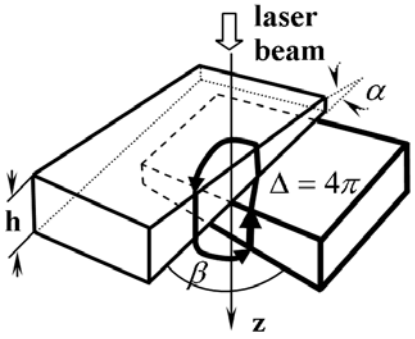

Figure 1: Generation of the double-charged vortex by the SW, *l*=2

We have recently shown[2] that the optical mask consisting of a consecution of the optical wedges is able to produce the singular beam carrying over the optical vortex whose topological charge is equal to the number of the wedges in the system (Fig.1). At the same time, geometry of such beam is different from that of the initial beam incident upon the system. This is the consequence of the fact that each isotropic dielectric wedge produces two partial beams. One of them is inclined at some angle to the optical axis of the initial beam while the other one propagates along the axis. Such wave superposition of two beams with non-coplanar axes will make up a complete resulting beam provided that the diffracting divergence of the initial beam is greater then the angle of the wedge.

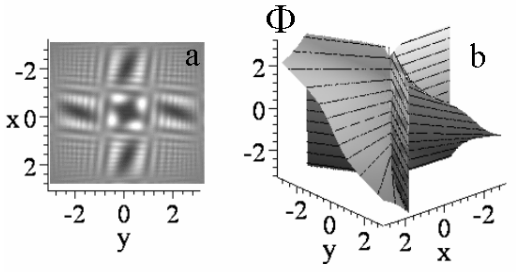

Figure:2 Theoretical intensity I (a) and phase Φ (b) distribution of the wedge-generated vortex with *n=2*

It is important to note that the vortex-bearing beam structure near the focus depends essentially on the diameter of the focal spot of the initial beam at the plane of the mask and the angle of the wedge.

Thus, we have experimentally revealed that the wedge-generated singular beam with the double topological charge (Fig.2) subjected to focusing does not lose its structural stability. Moreover, the vorticity of the beam rises near the focus. The wedge-generated beams can be presented as a superposition of some pars of partial off-axis non-singular beams. A number of such beam pairs is equal to a vortex topological charge.

REFERENCES

[1] I. Basistiy I., V. Bazenov, M. Soskin, M. Vasnetsov, Opt. Comm., Vol. 103, P. 422, (1993).

[2] Ya. Izdebskaya, V. Shvedov, A. Volyar, Optics Letters, Vol. 30, № 18, P. 2472, (2005).

* E-mail: izdebskaya@mail.ru

AUGER EFFECT IN ATOMS AND SOLIDS: CALCULATION OF THE AUGER DECAY CHARACTERISTICS

A. Glushkov[1,*], *E. Gurnitskaya*[2] , *D. Sukharev*[1] *and L. Nikola*[2]

[1] Dept. Atomic Physics, Odessa University, P.O.Box 24a, Odessa-9, ukraine
[2] Computer Physics Centre, Odessa University, P.O.Box 24a, Odessa-9

1. INTRODUCTION

Auger spectroscopy is the powerful tool for investigation of the surface chemical composition and near surface layer in solids [1]. Here a new approach to studying the Auger decay in the complex atomic systems and solids within S-matrix Gell-Mann and Low formalism (energy approach)[2] is carried out. The cross-sections of ionization of the internal shells for a number of atoms (*Na,Si, Au*) and energies of Auger electron transitions in solids (*Na,Si,Ge,Ag*) are calculated with account of the correlation effects. There are also examined the possibilities of the chemical analysis with the use of the relations between the core and valence Auger - lines intensities.

2. METHOD AND RESULTS

2.1. Method

Within energy approach the Auger transition probability and intensity are defined by the interelectron interaction matrix element:

$$V^{\omega}_{1234} = [(j_1)(j_2)(j_3)(j_4)]^{1/2} \sum_{\lambda\mu} (-1)^{\mu} \begin{pmatrix} j_1 & j_3 & \lambda \\ m_1 & -m_3 & \mu \end{pmatrix} \times \mathrm{Re}\, Q_{\lambda}(1234)$$

$$Q_{\lambda} = Q^{\mathrm{Qul}}_{\lambda} + Q^{\mathrm{Br}}_{\lambda}.$$

The values $Q^{\mathrm{Qul}}_{\lambda}, Q^{\mathrm{Br}}_{\lambda}$ are corresponding to the Coulomb and Breiht parts. The Coulomb part is expressed through the radial integrals R_{λ} ,and angular coefficients S_{λ} [2]:

$$\mathrm{Re}\, Q^{\mathrm{Qul}}_{\lambda} = \frac{1}{Z}\mathrm{Re}\{R_l(1243)S_{\lambda}(1243) + R_{\lambda}(\tilde{1}24\tilde{3})S_{\lambda}(\tilde{1}24\tilde{3}) + R_{\lambda}(1\tilde{2}\tilde{4}3)S_{\lambda}(1\tilde{2}\tilde{4}3) + R_{\lambda}(\tilde{1}\tilde{2}\tilde{4}\tilde{3})S_{\lambda}(\tilde{1}\tilde{2}\tilde{4}\tilde{3})\}.$$

The Auger decay probability is defined by the matrix elements $\mathrm{Re}Q_{\lambda}(1243)$:

$$\mathbf{Re}\, R_{\lambda}(1243) = \iint dr_1 r_1^2 r_2^2 f_1(r_1) f_3(r_1) f_2(r_2) f_4(r_2) Z^{(1)}_{\lambda}(r_<) Z^{(1)}_{\lambda}(r_>).$$

Heree f – large component of radial part of the Dirac one-electron state function, Z – Bessel function. The Auger width is derived from the adiabatic Gell-Mann and Low formula [2]. Contribution of diagram A_d 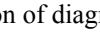 to the Auger width of level with vacancy $n_{\alpha}l_{\alpha}j_{\alpha}m_{\alpha}$

$$\sum_{\lambda} \frac{2}{(\lambda)(j_{\alpha})} \sum_{\beta\gamma\le f} \sum_{k>f} Q_{\lambda}(\alpha k\gamma\beta) Q_{\lambda}(\beta\gamma k\alpha),$$

and contribution f or diagram A_{ex} 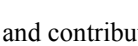 :

$$\frac{2}{(j\alpha)} \sum_{\lambda_1\lambda_2} \sum_{\beta\gamma\le f} \sum_{k>f} Q_{\lambda_1}(\alpha k\gamma\beta) Q_{\lambda_2}(\beta\gamma k\alpha) \begin{Bmatrix} j_{\alpha} & j_{\gamma} & \lambda_2 \\ j_k & j_{\beta} & \lambda_1 \end{Bmatrix}$$

An energy of electron, which is created due to transition *jkl*, is defined by a difference of energies of the atom with a hole on level j and twice ionized atom on levels *kl* in final state and can be written for solid as:

$$E^S A(jkl, {}^{2S+1}L_J) = E_A(jkl, {}^{2S+1}L_J) + \Delta E^S + R_{rel} + eF$$

Here ΔE^s – correction on changing bond energy in solid, R_{rel} – correction due to the outside atomic relaxation; eF accounts for the output work.

2.2. Results

In table 1 we present calculated and experimental data on the Auger electrons energies for some solids: a-experimental data; b – data are obtained within semiempirical calcultion with using an equvalent core approximation of Larkins [1]; c – our results.

Table 1.

	Auger line	a	b	c
Na	$KL_{2,3}L_{2,3}\ ^1D_2$	994,2	993,3	994,1
Si	$KL_{2,3}L_{2,3}\ ^1D_2$	1616,4	1614,0	1616
Ge	$L_3M_{4,5}M_{4,5}\ ^1G_4$	1146,2	1147,2	1146
Ag	$M_5N_{4,5}N_{4,5}\ ^1G_4$	353,4	358,8	353,3

3. REFERENCES

[1] F.P.Larkins, J.Phys.: Solid State Phys. **C10** , 2453 (1977); W.Raith, In: Photonic, electronic and Atomic Collisions, Eds. F.Aumayr and H.Winter. –World Scientific, Singapore (1997);
[2] A.V.Glushkov , L.N.Ivanov, Phys. Lett. A**170**,36 (1992); J.Phys.CS. **178**, 188 (2005); **178**, 198 (2005); J.Phys.CS **35,** 420 (2006); **35**, 425 (2006).

* E-mail: glushkov@paco.net

SUPERINTENSE LASER FIELD ACTION ON SURFACE WITH FORMING THE FEMTO-SECOND PLASMA AND A NEW TYPE OF THE HYDRODYNAMIC ABLATION WITH THE EXPLOSION CHARACTER. NEW LASER SPECTROSCOPY OF NUCLEAR ISOMERS

A. Glushkov[1,*], *S. Malinovskaya*[2] *and Yu. Dubrovskaya*[2]

[1] Dept. Atomic Physics, Odessa University, P.O.Box 24a, Odessa-9, ukraine
[2] Computer Physics Centre, Odessa University, P.O.Box 24a, Odessa-9

It's known that using super intense short light pulses changes principally a character of interaction of a laser radiation with substance [1-3]. For laser intensities more than 10^{15} Wt/cm^2 electrons get energy of 100-1000eV and it is realized a process of forming the femto-second laser plasma. We consider possibilities of governing by processes, which are taken a place in the femto-second laser plasma in nano-structured porous materials (Si). The nano-structured porous materials consist of the separated clusters set with the fractal structure. The key mechanism of the hot electrons generation in plasma is provided by oscillation of electron on the border "plasma-vacuum" or resonant absorption of laser radiation. One may wait for the sharp increasing the hot electrons generation and X-ray radiation. For large laser intensity it is observed a new type of the hydrodynamic ablation with the explosion character. Besides ususal mechanism of the ambipolar accelerating ions by electrons another mechanism begin to play an essential role. Speech is about the Coulomb repulsion of the chargied particles inside a cluster. The separation of charges inside a microplasma of the single cluster became possible as an amplitude of electron oscillations in a field of the light wave (~10nm for intensity I~10^{16} Wt/cm^2) is more than the size of cluster. Besides, a laser radiation wavelength is more essentially the cluster size. So, microplasma is in the homogeneous iscillating field and all electrons of plasma move in the phase. Our theoretical and independent experimental estimates show that a velocity of the plasma flying away for the strongly porous samples Si (I~3x10^{16}W/cm^2) is ~10^8cm·s^{-1}, that is ~ to energy 2±1 MeV. Let us note for comparison [2] that the velosity of flying away for usual Si is not more than $3\cdot10^7$ cm/s. For time ~ 500 fs a plasma in the nano-structured porous materials became homogeneous with decreased density and its forming is accompanied by essential heating the ion component due to the transformation of energy of translational movement of the ions to heated energy during collision of the jets of different clusters. Estimate is shown that the kinetic energy of ions in the flying away plasma is ~ 30keV for the electron temperature ~ 1keV and the plasma ionization degree Z~12 [3]. The collisional length of free runing for ion is ~ 30 nm and frequency of
the ion-ionic collisions is ~ 10^{13}s^{-1}. Under collison of two plasma jets an energy of the kinetic movement of ions trasfers to the thermal energy during 50-100 fs and reachss dozens of keV [3]. We carried out the modelling of femto-second laser plasma forming in the porous materials on the basis of the energy balance equations and Green functions method [3-5]. The energy and heat balance equations approach is used for modeling the process of plasma flying away and the hydrodynamic ablation with the explosion character [2]. The special attention is devoted to the modelling the system: nano-structured porous materials with clusters, on surface of which there is a great number of bonds with H and OH groups. In a case of D-and OD group's one can wait for realization of the cluster explosion process and reaction D+D→α+n (3,8MeV). Our theoretical modeling indicates on the non-tirivial behaviour of this process [5]. Besides non-trivial features of the explosion process one can wait simulteniously an appearance of the powerful flow of neutrons in plasma under intensity of heating pulse ~ 10^{16} Wt/cm^2. In the high density plasma there is possible an excitation of the low lying isomers (level energy less 20 keV) by means of the channels: photo excitation by own X-ray plasma radiation, the electron impact excitation, electron conversion, the excitation for isomer nuclear level in laser plasma. We calculated properties of stable and long lived nuclei low lying isomers characteristics (energy, decay channels etc.), using methods [3].

REFERENCES

[1] *Superstrong Fields in Plasmas*. Eds. M.Lontano etal, AIP Proc., **426**, N.-Y. (1998); V.M.Gordienko, A.B.Saveliev, UFN, **169**, 78 (1999); A.V.Andreev et al., JETP Lett. **66**, 312 (1997).
[2] A.V.Glushkov et al, Int. J.Quant. Chem. **104**, 512 (2005); Progr. Theor. Phys. (2006); J. Phys. CS **178**, 188 (2005); Int. J.Quant. Chem. **104**, 512, 562 (2005); J. Phys. CS **178**, 198 (2005).
[3]. A.V.Glushkov, L.N. Ivanov, Phys. Lett. A.**170**, 33 (1992); A.Glushkov etal, In*: New Projects and New Lines of research in Nuclear Physics.* Eds. Fazio G. and Hanappe F., World Sci., Singapore, 146 (2003); Nucl. Phys. A. **734**, e21 (2004).

* E-mail: glushkov@paco.net

ENERGY APPROACH TO QED THEORY OF CALCULATING POSITRON IMPACT IONIZATION OF MULTIELECTRON ATOMS AND ENERGY LOSS AT SURFACES

A. Glushkov[1,*], *A. Loboda*[2], *and O. Khetselius*[3]

[1] Dept. Atomic Physics, Odessa University, P.O.Box 24a, Odessa-9, ukraine
[2] Computer Physics Centre, Odessa University, P.O.Box 24a, Odessa-9
[3] Dept. Quantum Optics, Odessa University, P.O.Box 24a, Odessa-9

1. INTRODUCTION

Considered will be processes, which lead to single (outer shell) ionization of the multielectron atom. Positron impact can lead to ionization via two reaction channels usually called break up (of the atom into an electron and ion) and transfer (of one atomic electron to the projectile to form positronium. The most accurate positron ionization cross sections for example, for helium are presented in [1] and analysed in comparison with that for electron impact ionization. It should be noted that the features of particular interest are the merging of the cross sections above 600 eV when the first Born approximation is valid, the positron cross section exceeding the electron cross section at medium energies and a cross over of the cross section curves near threshold [1]. The problem of energy loss of positrons at surfaces is of a great importance and far from adequate solution.

2. METHOD AND RESULTS

2.1. Method

We suppose that a uniform theoretically comprehensive approach to considered problems solving must base on the quantum electrodynamics (QED). In this paper the energy approach to consistent qauge-invariant QED description of positron and electron collision (ionization) processes of the atom and defining the energy loss of positrons at surfaces is presented. It is based on the QED perturbation theory approach and S-matrix Gell-Mann and Low formalism (c.f.[2]), which has been used earlier in solving the nuber of atomic ionization and xollision problems [3]. As example we consider the positron impact ionization of helium. We consider $a_{in}^{+}\Phi_0$ as the initial state. In general form a scattered part for imaginary energy shift *Im ΔE* appears at first in the second order of the atomic perturbation theory in the form of integral over the scattered positron energy ε_{SC}

$$\int d\varepsilon_{SC} G(\varepsilon_{iv},\varepsilon_{ie},\varepsilon_{in},\varepsilon_{SC})/(\varepsilon_{SC}-\varepsilon_{iv}-\varepsilon_{ie}-\varepsilon_{in}-i0)$$

with $$Im\Delta E=\pi G(\varepsilon_{iv},\varepsilon_{ie},\varepsilon_{in},\varepsilon_{sc}).$$

Here ε_{in} *and* ε_{sc} are the incident and scattered energies respectively to the incident and scattered positron; *G* is a definite squired combination of the Coulomb and Breit inter particle interaction integrals [3]. We use further the optimized basis's of Dirac orbitals, which is got from minimization principle for contribution of the fourth QED perturbation theory diagrams into the imaginary part of energy shift, i.e., radiative width of atomic level [2]. Our numerical code [2-4] is used.

2.2. Results

We present preliminary results on positron impact ionization of the atoms and the energy loss of positrons at surfaces. In particular the results on positron impact ionization of helium are presented in table below and compared with results: A-Knudsen etal and B-Bielefeld (c.f.[1]).

Impact energy, eV	Measured A σ, (Å^2)	Measured B σ, (Å^2)	Calculated σ Present (Å^2)
50	0,23	0,29	0,24
100	0,52	0,45	0,51
200	0,45	0,40	0,46

3. REFERENCES

[1] W.Raith, In: Photonic, electronic and Atomic Collisions, Eds. F.Aumayr and H.Winter. –World Scientific, Singapore (1997); F.M.Jacobsen, N.P. Frandsen, H.Knudsen, U.Mikkelsen and D.M.Schrader, J.Phys.B. **28**, 4691 (1995);

[2] L.N.Ivanov, E.P.Ivanova, L.N.Knight, Phys.Rev.A **48**, 4365 (1993)A.V.Glushkov , L.N.Ivanov, Phys. Lett. A**170**,36 (1992); J.Phys.B: At.Mol.Opt.Phys. **26**, L379 (1993); Preprint of Institute of Spectroscopy of RAS, NAS-5,Moscow-Troitsk (1992);

[3] A.V.Glushkov et al, Nucl.Phys.A. **734**, e21 (2004); Int.J.Quant.Chem. **99**, 936 (2004); 99, 879 (2004); 104, 512 (2005); 104, 562 (2005); Prog.Theor.Phys. and Chem. , in print (2006); J.Phys.CS. **178**, 188 (2005); **178**, 198 (2005); J.Phys.CS **35,** 420 (2006); **35**, 425 (2006).

[4] E.Ivanova, L.N.Ivanov, A.Glushkov, A.Kramida, Phys.Scr. **32**, 524 (1985); A.V.Glushkov, E.P.Ivanova, J.Quant.Spectr.Rad.Tr. **36**, 127 (1986).

* E-mail: glushkov@paco.net

NEW OPTIMAL SCHEMES OF THE LASER PHOTOIONIZATION TECHNOLOGIES FOR CLEANING THE SEMICONDUCTOR MATERIALS AND PREPARING THE FILMS OF PURE COMPOSITION AT ATOMIC LEVEL

A. Glushkov[1,*], *S. Ambrosov*[2], *and I. Shpinareva*[2]

[1] Dept. Atomic Physics, Odessa University, P.O.Box 24a, Odessa-9, ukraine
[2] Computer Physics Centre, Odessa University, P.O.Box 24a, Odessa-9

1. INTRODUCTION

The paper is devoted to the search and computer modeling the optimal schemes of laser photo ionization processes and technologies for control, separation, cleaning the semiconducting substances and preparing the films of pure composition on example of creation of the 3-D hetero structural super lattices (layers of GaAs). Photo ionization process of obtaining the Ga^+ ions and optimal technology for preparing the films of pure composition are considered. New models for calculation of the optimal realization of the first step excitation and further ionization of the Ga^+ ions in Rydberg states by electric field are used and optimal parameters of the photo ionization process are found.

2. METHOD AND RESULTS

2.1. Laser ionization of atoms in mixtures at surface

The corresponding processes are described by the standard master system of equations for density matrice [1]:

$$d\rho_0/dt=-W_1(\rho_0-\rho_1)+\rho_1T_1+K_1\rho_0'\rho_1,$$
$$d\rho_1/dt=-W_1(\rho_0-\rho_1)-\rho_1T_1-R\rho_1-K_1(\rho_0'\rho_1-\rho_1'\rho_0),$$
$$d\rho_0'/dt=-W_1(\rho_0'-\rho_1')+\rho_1'T1+K_1\rho_0\rho_1',$$
$$d\rho_1'/dt=-W_1(\rho_0'-\rho_1')-\rho_1' T1-R\rho_1'-K_1(\rho_0\rho_1'-\rho_1\rho_0'),$$
$$dn/dt=R\rho_1-n_1(K_2^{(o)}\rho_0'-K_2^{(1)}\rho_1')+n'(K_2^{(0)}\rho_0-K_2^{(1)}\rho_1)-n/\tau,$$
$$dn'/dt=R\rho_1'-n_1'(K_2^{(o)}\rho_0-K_2^{(1)}\rho_1)+n(K_2^{(0)}\rho_0'-K_2^{(1)}\rho_1')-n/\tau$$

where ρ_0, ρ_0'- concentrations of atoms of substance and admixture in a ground state; ρ_1, ρ_1'- in excited state; n,n'- concentrations of their ions; R- the ionization probability; coefficients K_1,K_2 define the velocity of process of resonant transfer for excitation energy correspondingly ($K_1=\sigma_w v$; σ_w–the Wysckopf cross section, v- velocity of atoms) and the velocity of process of the re-charging ($K_2=\sigma_{ch}(v_i)v_i$; $\sigma_{ch}(v_i)$- cross section of resonant re-charging, v_i- velocity of ions relatively of neutral atoms; W_1, W'_1 – probabilities of radiative transitions, which are expressed through intensities of field I_1 of the resonant radiation and transverse relaxation time T_2 . Cited system can be simplified and transferred to linear one under some conditions, in particular, a laser radiation acts on the admixtured atom and concentration of admixtures is quite little. The photoionization scheme includes at first step an excitation of atoms by laser field and their transition into Rydberg states and then ionization by electric field. A creation of the films of pure composition (our problem is creation of the 3-D layers of $Ga_{1-x}Al_xAs$ with width 10Å and GaAs of 60Å)is directly connected with using photo ion pensils of Ga^+,Al^+,As^+.Similar pensils can be created by means of the selective photoionization method with ionization by electric field. Then electromagnetic focusing and deflecting systems will provide a creation the 3-D supper lattices.

2.2. Results

The photoionization scheme of obtaining the Ga^+ ions with transition scheme: $4p^2P_{3/2}\rightarrow(\lambda_1=417,2nm)\rightarrow 5s^2 S_{1/2}\rightarrow(\lambda_1=420\text{-}440nm)\rightarrow np^2P_{1/2}$.(n=14-70) is studied. In fig. 1 we present results of modeling the Ga atoms separation process from two atomic mixture at surface and search of optimal laser pulse form. In simple case δ -pulse provides maximum possible level of excitation and the parasite processes such as spontaneous relaxation, resonant reexchange etc. can't change an achieved excitation during a little time

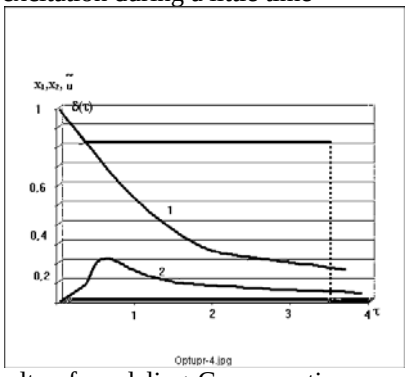

Fig.1 Results of modeling Ga separation process from Ga-X mixture (δ+dashed – laser pulse optimal form; 1, 2 are ~ to populations of ground and excited states).

3. REFERENCES

[1] A.V.Glushkov, Int.J.Quant.Chem. **99**, 879 (2004); **104**, 562 (2005; J.Phys.CS. **178**, 188 (2005); **178**, 198 (2005);); Prog.Theor.Phys. and Chem. in print (2006);

* E-mail: glushkov@paco.net

SPATIAL AND ANGULAR CHARGE DISTRIBUTION OF CHANNELED HEAVY IONS

V.S. Malyshevsky[*], *S.V. Rakhimov*

Rostov State University, Rostov-on-Don, 344090, Russia

Recently in Refs. [1-2], it has been shown, that the penetration of heavy ions through crystals is accompanied by a breaking of the isotropy of the angular distributions of an originally isotropic ion beam. The systematic experimental research for various crystals has shown the existence of so-called "cooling" or "heating" of ion transmitted through the crystal along a major crystallographic direction. These effects depend not only on the type of a target, but also on the energy of ions.

Compared to usual channeling calculations, the statistical description of the charge exchange effects is complicated by the introduction of an additional dimension, a new discrete variable Q indicating the charge state. In this case the kinetics of ions in an oriented crystal is described by a set of kinetic equations whose number is equal to the ion atomic number Z_1. The kinetic equations describing diffusion and charge exchange processes of channeled ions in space of transverse momentums in a single-electron approximation can be written as “generalized” diffusion equation in which there is a change of a transverse momentum due to multiple scattering and change of a charge state of ion [3]. The theory gives an adequate description of observed angular distributions of heavy ions transmitted through a crystal, allows calculation of the partial angular distributions of the various charge states, and gives a physical explanation of the cooling maxima and the heating minima in the angular distributions. The occurrence of cooling or heating effects and the detailed structure of the angular distribution depend on both the impact parameter dependence of the probabilities for electron capture and loss and on the relative contributions from different charge states.

The evolution with depth of the charge state distribution leads to a redistribution of the flux of ions in the crystal and, finally, changes the character of their interaction with the crystal. The dependence of the average ion charge on the depth of penetration into a crystal and the normalized distribution of charge states are calculated in Ref. [3]. The calculated equilibrium charge in the above-barrier (random) area for 48 MeV and 13.5 MeV is equal to $\simeq 10.4$ and $\simeq 8.7$, respectively.

The results of the calculations of angular and spatial distribution for channeled Al^{+Q} ions with different energy and crystal thickness 0.1 μm are shown in Figure 1 and Figure 2. Thus, at a reduction of the ions energy the average charge of the channeled ions appears less then for random ions. It can be explained to that ions with smaller energy have smaller speed and according to the Bore criterion can capture of a crystal electron from higher orbits. That is efficiency of electron capture becomes more, and as results it lead to the reduction of an average charge. The similar results have been observed experimentally in Ref. [2].

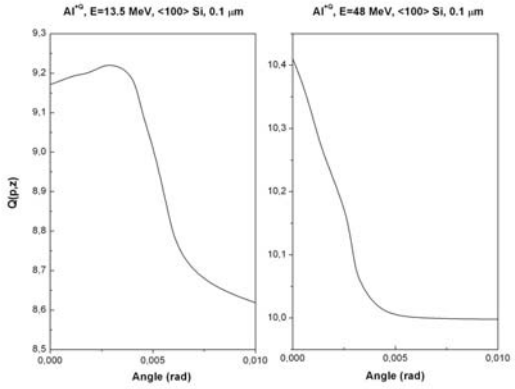

Figure 1: The density of the angular charge distribution of ions.

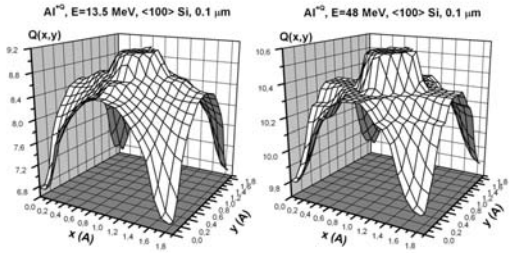

Figure 2: The spatial charge distribution. The mean charge in the under-barrier (channeled) area for 13.5 MeV and 48 MeV is equal to $\simeq 8.3$ and $\simeq 10.3$, respectively.

REFERENCES

[1] M. Schubert, F. Gruner, W. Assmann, F. Bell, A. Bergmaier, L. Goergens, O. Schmelmer, G. Dollinger, S. Karamian, Nucl. Instr. and Meth. in Phys. Res. **B 209,** 224 (2003).

[2] F. Gruner, W. Assmann, F. Bell, M. Schubert, J.U. Andersen, S. Karamian, A. Bergmaier, G. Dollinger, L. Gorgens, W. Gunther, M. Toulemonde, Phys. Rev. **B 68**, 174104 (2003).

[3] V.S. Malyshevsky, Phys. Rev. **B 72**, 094109 (2005).

[*] E-mail: gvidon@aaanet.ru

Wednesday, 20.9.2006

PLASMA-WALL-INTERACTION: IMPORTANT ION INDUCED SURFACE PROCESSES AND STRATEGY OF THE EU TASK FORCE

Joachim Roth[1 *], *Emmanuelle Tsitrone*[2], *Alberto Loarte*[3]

[1] Max-Planck-Institut für Plasmaphysik, EURATOM-Association, 85748 Garching, Germany
[2] Association Euratom-CEA, CEA/DMS/DRFC CEA Cadarache, 13108 Saint Paul lez Durance, France
[3] EFDA-Close Support Unit Garching, 85748 Garching, Germany

1. INTRODUCTION

In future thermo-nuclear fusion devices, such as ITER the interaction of the plasma with surrounding materials Plasma-Wall interaction constitutes the main remaining engineering problem. Issues, such as the lifetime of plasma-facing components under high particle and heat load and radioactive tritium inventory in the vacuum vessel determine directly the material choice of ITER The resolution of these issues requires intense efforts aimed at the understanding of low-energy ion-surface interaction.

2. SCIENTIFIC WORK PROGRAMME

The European Task Force on Plasma wall interaction has been installed by EFDA in the fall 2002 and was motivated scientifically by
"the need to provide ITER with information concerning lifetime-expectations of the divertor target plates and tritium inventory build-up rates in the foreseen starting configuration and to suggest improvements, including material changes, which could be implemented at an appropriate stage."
These aims outline the needs for quantitative data and fundamental understanding in the work programme of the EU Task Force on:

- erosion yields under low energy (1-500 eV) and high flux ($>10^{24}$ /m^2s) hydrogen ion bombardment of fusion relevant surfaces, including physical sputtering and chemical erosion,
- hydrogen implantation, retention and release in fusion relevant materials,
- material modification under intense hydrogen and impurity ion bombardment associated with high heat loads.

The presentation will provide examples and the present status of knowledge for erosion yields, hydrogen retention efficiencies and material mixing for the choice of ITER materials Be, C and W.

3. TASC FORCE STRATEGY

Also, the presentation will concentrate on the strategies and organisation tools of the EU Task Force.
In its second 3-year period starting at the beginning of 2006, 26 European associations have joined their efforts in a common work programme. Seven Special Expert Working Groups have been created on critical issues such as

- Chemical erosion, transport and deposition
- Gas balance and fuel retention
- Transient power loads (ELMs, disruptions)
- High-Z materials
- Tritium removal
- Dust in fusion devices
- ITER-like Material Mix

Where important experimental or modelling efforts are needed research can be stimulated through financial support of well defined EFDA Tasks in the EFDA technology Programme.

In the first period these three organisational tools have proven effective in reaching valuable advancements. Highlights from the first three year period will be given.

* E-mail: Joachim.Roth@ipp.mpg.de

CHEMICAL SPUTTERING OF GRAPHITE BY LOW ENERGY DEUTERIUM PROJECTILES

F. W. Meyer, L. I. Vergara, H. F. Krause*

[1] Physics Division, Oak Ridge National Laboratory, Oak Ridge, TN 37831-6372 USA

Because of its high thermal conductivity, excellent shock resistance, absence of melting, low activation, and low atomic number, there is significant technological interest in using graphite as a plasma-facing component on present and future fusion devices. This interest extends to the use of different types of graphite or carbon fiber composites (CFC's), together with tungsten, beryllium, or other refractory metals, in the ITER divertor. Although these materials have outstanding thermo-mechanical properties, they can suffer significant chemical erosion and sputtering by low energy hydrogen ion impact, which determines in large part the carbon-based-material lifetime.

Due to evolving divertor design, the interest in the erosion characteristics of the carbon surfaces is shifting to progressively lower impact energies. Results are presented of chemical sputtering yields of ATJ graphite at room temperature by impact of D^+, D_2^+, and D_3^+ in the energy range 5-250 eV/D. We have also investigated methane and acetylene production at elevated sample temperatures [1].

Our experimental approach [2] is based on the use of a quadrupole mass spectrometer (QMS) to monitor partial pressure increases of selected mass species resulting from ion impact on the graphite surface. Due to the high D^+ currents obtainable with our ECR ion source, and the highly efficient beam deceleration optics employed at the entrance to our floating scattering chamber, comparison between same velocity atomic and molecular ion impact was possible with our apparatus at energies as low as 10 eV/D, and permitted testing of the commonly made assumption that isovelocity atomic and molecular species lead to identical sputtering yields when normalized to the D constituent number of the incident projectiles.

We observed a systematic trend of the methane yields for the different molecular species compared at the same impact energy/D: while all three species lead to methane yields that coincide within the experimental uncertainty at the high energy end of the investigated range, at lower energies the yields diverge by progressively larger amounts, with the incident triatomic molecular ion leading to the largest yields per atom, and the atomic ion to the smallest [4]. The difference at the lowest investigated energy (10 eV/D) is about a factor of two. Our measurements also serve as benchmarks for new MD simulations [5] of the chemical sputtering process that seek to incorporate more realistic many-body potentials and to expand the reaction pathway to include vibrational and/or electronic excited states.

ACKNOWLEDGEMENTS

This research was sponsored by the Office of Fusion Energy Sciences and the Office of Basic Energy Sciences of the U.S. Department of Energy under contract No. DE-AC05-00OR22725 with UT-Battelle, LLC. LIV was appointed through the ORNL Postdoctoral Research Associates Program administered jointly by Oak Ridge Institute of Science and Education and Oak Ridge National Laboratory.

REFERENCES

[1] L. I. Vergara, F. W. Meyer, H. F. Krause, J. Nucl. Mat. 347, 118 (2005).
[2] F. W. Meyer, H. F. Krause, L. I. Vergara, J. Nucl. Mat. **337- 339**, 922 (2005).
[3] F. W. Meyer, L. I. Vergara, and H. F. Krause, Phys. Scripta **T124, 44** (2006) .
[4] L. I. Vergara, F. W. Meyer, H. F. Krause, P. Träskelin, K. Nordlund, and E. Salonen., to be published in J. Nucl. Mat (2006).
[5] C. O. Reinhold, P. S. Krstic, and S. J. Stuart, this conference.

* E-mail: meyerfw@ornl.gov

ENHANCED ROOM TEMPERATURE EROSION OF ULTRA THIN CARBON FILMS ON TITANIUM, TANTALUM AND BERYLLIUM BY DEUTERIUM IONS

M. Reinelt, Ch. Linsmeier , and K.U. Klages*

Max-Planck-Institut für Plasmaphysik, Boltzmannstrasse 2, D-85748 Garching b. München, Germany

Most present fusion devices use carbon as a first wall material. Due to high particle loads, especially hydrogen from the plasma, wall material is eroded and redeposited at different positions. This leads to the formation of surface layers, which are themselves subject to erosion. It is known that carbon exhibits chemically enhanced erosion by low energy hydrogen ions or elevated temperatures [1]. However, erosion of room temperature carbon by keV ions should be governed by a pure kinematic sputtering process. We found that this is not necessarily the case for carbon surface layers of few nanometer thicknesses.

To investigate the basic mechanisms governing the enhanced erosion of carbon, carbon layers in the range of several nm thickness are evaporated on clean metal substrates. The films are irradiated with 1 or 4 keV deuterium ions and the surface composition is analysed by X-ray photoelectron spectroscopy (XPS). The C 1s photoelectron peak at around 285 eV binding energy can be deconvoluted into three chemically and structurally different carbon states. Two of them can be assigned to elementary carbon and one to carbide [2]. In that way, the effect of carbidisation by ion beam mixing can be included in the quantification of the measurements.

To the erosion process both chemical (by carbon-hydrogen reactions) and physical mechanisms (by different collision cascades, depending on the substrate) contribute. The kinematic process is influenced by substrates of different atomic mass. For our studies we choose carbon films on tantalum, titanium and beryllium. Our experimental data is compared to Monte Carlo calculations using the TRIDYN code which takes into account kinematic interactions and adjusts the sample composition dynamically [3]. We find significant faster erosion of carbon on titanium irradiated with 4 keV D^+ ions in the experiment than calculated (Fig. 1a). For carbon on tantalum, a slightly enhanced erosion is measured (Fig. 1b). In the case of beryllium, the erosion of carbon is dominated by carbidisation via ion beam mixing, which is significantly faster than the removal of carbon from the surface by sputtering.

We discuss the results with respect to the kinematic collision interaction and the ion-induced chemical phase formations.

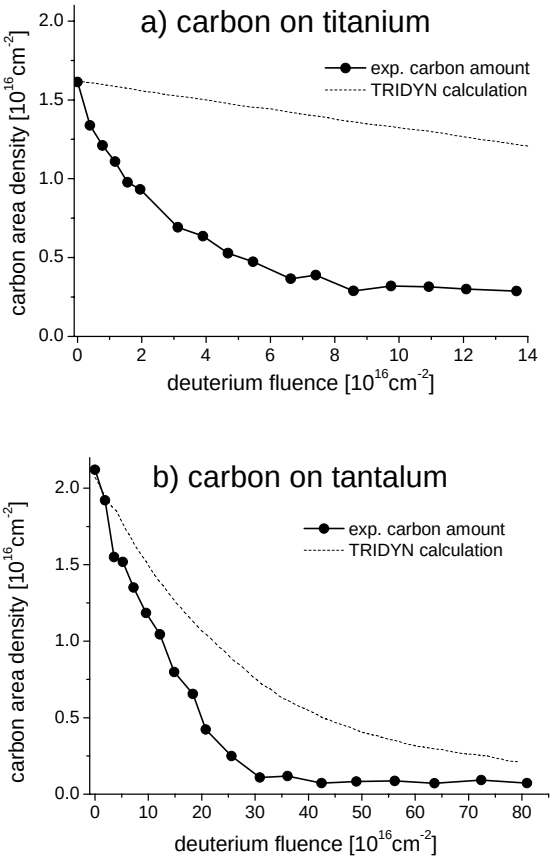

Figure 1: Erosion of ultra thin carbon films on titanium (a) and tantalum (b) by increasing deuterium fluences and comparison to TRIDYN calculations.

REFERENCES

[1] M. Balden, J. Roth, J. Nucl. Mater. **280**, 39 (2000).

[2] K. U. Klages, A. Wiltner, J. Luthin, and Ch. Linsmeier, J. Nucl. Mater. **313-316**, 56 (2003).

[3] W. Eckstein, *Computer Simulation of Ion-Solid Interactions, Springer Series in Materials Science, vol. 10,* (Springer, Berlin, 1991).

* E-mail: linsmeier@ipp.mpg.de

SURFACE AND INTERFACE STRUCTURE ANALYSIS BY USING HIGH RESOLUTION ION SCATTERING AND LEEM/PEEM

*T. Koshikawa**

Fundamental Electronics Research Institute, Osaka Electro-Communication University
18-8 Hatsu-cho, Neyagawa, Osaka 572-8530, Japan

The structure analysis at the surface and the interface will be demonstrated in some systems, e.g., Cu/Si(111), by using the high resolution medium ion scattering, which can analyze the structure with almost layer-by-layer. The Cu/Si(111) "5x5" structure analysis has been tried at the glancing exit angle (2-5 degree) from the surface. The simulation is necessary to carry the analysis, in which there are some not well known parameters, i.e., straggling, electronic surface concerned with the surface plasmon energy loss etc. These parameters have been decided after the analysis of the well known surface which is Si(111)7x7 structure. The distance between each layers of Cu and Si has been estimated with the above high resolution Cu and Si scattering spectra and the simulation calculation.

Low energy electron microscope and photo-emission electron microscope are intensively attracted in the field of the dynamic surface reaction observation. These technique has also been applied to the Cu thin film and nano-structure formation on Si(111). The video rate movie images and low energy electron diffraction can help a lot to surface reaction and the structure analysis. The advantage of such technique will be shown in the presentation.

* E-mail: kosikawa@isc.osakac.ac.jp

SECONDARY ION MASS SPECTROMETRY OF MCs_n^+ MOLECULAR ION COMPLEXES

P. Chakraborty[*]

Surface Physics Division, Saha Institute of Nuclear Physics, 1/AF Bidhannagar, Kolkata 700 064, India

Excellent detection sensitivity, high dynamic range and good depth resolution make the SIMS technique extremely powerful for the analysis of surfaces and interfaces. However, a serious problem in SIMS analysis is its "matrix effect" that hinders the quantification of a certain species in a sample and therefore, the applicability of SIMS to probe complex chemistry at surfaces or interfaces is greatly hindered. Therefore, appropriate corrective measures are needed to calibrate the secondary ion currents into respective concentrations for accurate compositional analysis. Working in the MCs^+ -SIMS mode (M – element to be analyzed, Cs^+ - bombarding ions) can circumvent the matrix effect. The quantitative potential of the MCs^+-SIMS method is understood by assuming that an MCs^+ ion is generated by the combination of a secondary neutral M^0 atom with a re-sputtered Cs^+ ion in the near-surface region. Consequently, the emission process for the species M^0 is decoupled from the subsequent MCs^+ ion formation process, in analogy with the ion formation in secondary neutral mass spectrometry (SNMS), resulting in a drastic decrease in matrix effect. Although this technique has found its applicability in direct quantification, it generally suffers from a low useful yield. In such cases, detection of MCs_n^+ (n= 2, 3, ...) molecular ions offers a better sensitivity as the yields of such molecular ion complexes have often been found higher than that of MCs^+ ions. This is true in most of the cases where the elements are strongly electronegative with respect to cesium.

Although several works have been reported on the emission of MCs_n^+ molecular ions in the SIMS process, a complete understanding on the formation mechanisms of these ion complexes is still lacking. In view of the fact that the energy distribution of secondary ions is an effective diagnostic to understand the kinematics of the emitted species, we have done a thorough and systematic experimental study on the energy distributions of MCs_n^+ species emerging from various metal targets and tried to estimate the local instantaneous surface work function changes under various conditions. The present talk will address a brief review on the SIMS study of MCs_n^+ molecular ion complexes including our phenomenological approaches on the subject.

[*] E-mail: purushottam.chakraborty@saha.ac.in

WAVE PACKET STUDY OF THE SECONDARY EMISSION OF NEGATIVELY CHARGED, MONO-ATOMIC IONS FROM SPUTTERED METAL SURFACES.

A. Sindona[*], *P. Riccardi, S. Rudi, S. Maletta and G. Falcone*

Dipartimento di Fisica dell'Università della Calabria and Istituto Nazionale di Fisica Nucleare (INFN), gruppo collegato di Cosenza, via P. Bucci, Cubo 30C, 87036 Rende (CS), Italy

1. DESCRIPTION OF THE MODEL.

Negative ionization of low energy, mono-atomic, and singly charged secondary ions, ejected during sputtering of metals, is studied by the model sketched in Fig. 1, where the ejected particle (a) is instantaneously probed either by an ideal flat surface or by its nearest neighbor substrate particle (b), that provides the impulse for ejection. A less accurate version of the theory was proposed in previous works [1], dealing with ionization of secondary $Cu^{\pm}$ ions sputtered from jellium surfaces, in which the role played by quasi-molecular orbitals, transiently formed, during ejection, between a and b atoms, was discussed. In the present paper, the metal surface is described by a one-dimensional, semi-empirical, single-electron effective potential, constructed from pseudo-potential local density calculations [2]. A Crank-Nicholson wave-packet propagation approach [3] is used to determine the inverse evolution of the affinity orbital of the negative ion, being isolated at distances of the order of $\sim 10^2$ a.u. from the surface. The overlap of the evolved atomic state with a metal band state yields the probability amplitude that an electron, occupying the band state at the instant of ejection, will eventually tunnel to the ejected atom.

2. RESULTS

The inverse velocity distributions of Cu^-, Ag^-, and Au^- ions, sputtered from $Cu(100)$, $Ag(100)$, and $Au(100)$ surfaces, respectively, are obtained with a simple analytical model for the motion of both a and b atoms, initially placed outside the surface. Good agreement is found with the experiments of Ref. [4]; specifically, the anomalous increase of the population of Ag^- ions, with increasing inverse velocities, above $\sim 10^{-6}$s/cm, is correctly reproduced.

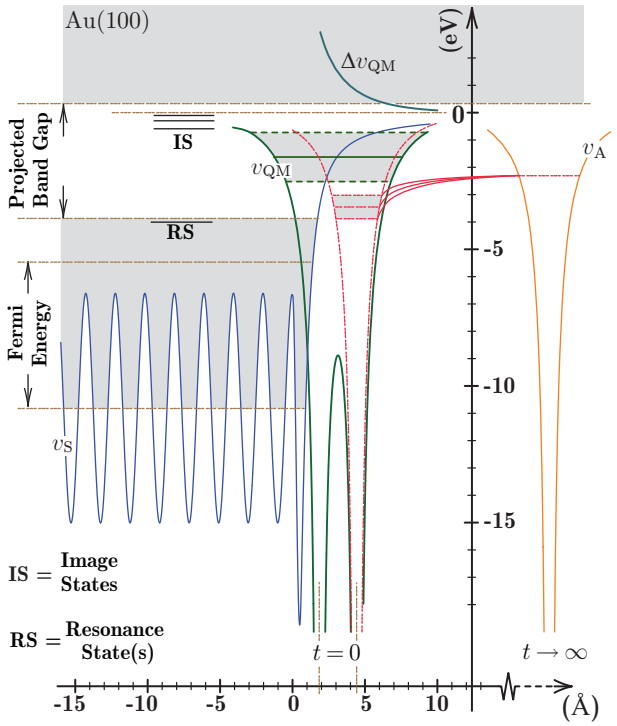

Figure 1: Schematics of the problem with the parameters of the $Au^-/Au(100)$ system: the effective one-electron potential includes the electron-surface interaction, v_S, the contribution of the diatomic system, v_{QM}, and the image potential, Δv_{QM}.

3. REFERENCES

[1] A. Sindona and G. Falcone, Surf. Sci. **529**, 471 (2003); A. Sindona, P. Riccardi, and G. Falcone, Nucl. Instr. & Meth. B**230**, 449 (2005).

[2] E. V. Chulkov, V. M. Silkin, and P. M. Echenique, Surf. Sci. **437**, 330 (1999).

[3] A. G. Borisov, A. K. Kazansky, and J. P. Gauyacq, Phys. Rev. Lett. **80**, 1996 (1998); H. Chakraborty, T. Niederhausen, and U. Thumm, Phys. Rev. A**69**, 052901 (2004)

[4] P. A. W. van Der Heide, Nucl. Instr. & Meth. in Phys. Res. B**157** (1999), 126

[*] E-mail: sindona@fis.unical.it

Thursday, 21.9.2006

ELECTRONIC EXCITATIONS INDUCED BY MOLECULE-SURFACE INTERACTIONS

Alec M. Wodtke

Dept. of Chemistry and Biochemistry UCSB

When molecules with low levels of vibrational excitation collide with metal surfaces, vibrational coupling to electron-hole pairs is not found to be strong unless incidence energies are high. However, there is accumulating evidence that coupling of large amplitude molecular vibration to metallic-electron degrees-of-freedom can be much stronger even at the lowest accessible incidence energies. This can occur due to the large changes in electron binding energetics as a bond undergoes large amplitude vibrational motion. As reaching a chemical transition-state also involves large amplitude vibrational motion, we pose the basic question: are electronically non-adiabatic couplings important at transition-states of reactions at metal surfaces? We have indirect evidence in at least one example that the dynamics and rates of chemical reactions at metal surfaces may be strongly influenced by electronically non-adiabatic coupling. This implies theoretical approaches relying on the Born-Oppenheimer approximation may not accurately reflect the nature of transition-state traversal in reactions at metal surfaces.

Developing a predictive understanding of surface reactivity beyond the Born-Oppenheimer approximation represents one of the most important challenges to current research in chemical dynamics. This lecture will present recent experimental results from our group that bear on this topic. Of particular interest are the questions: How can we directly detect Born-Oppenheimer breakdown in Molecule-Surface interactions and how general is it.

RELATED REFERENCES

[1] Chen, J.; Matsiev, D.; White, J. D.; Murphy, M.; Wodtke, A. M. Chem. Phys. (Netherlands) 2004, 301, 161.
[2] Wodtke, A. M.; Huang, Y.; Auerbach, D. J. J. Chem. Phys. 2003, 118, 8033.
[3] Matsiev, D.; Chen, J.; Murphy, M.; Wodtke, A. M. J. Chem. Phys. 2003, 118, 9477.
[4] Huang, Y. H.; Rettner, C. T.; Auerbach, D. J.; Wodtke, A. M. Science 2000, 290, 111.
[5] J. White, J. Chen, D. Matsiev, D.J. Auerbach and A.M. Wodtke, Nature 433(7025),503-505, (2005).

* E-mail: wodtke@chem.ucsb.edu

PROGRESS REPORT: CHARGE-TRANSFER RATES FOR XENON RYDBERG ATOMS AT METAL AND SEMICONDUCTOR SURFACES†

*F. B. Dunning**

Department of Physics and Astronomy, Rice University MS 61
6100 Main St., Houston, TX 77005

Charge exchange between atoms and surfaces is an important precursor to many surface reactions and forms the basis of several practical surface spectroscopies. Because of their large physical size and weak binding, Rydberg atoms provide a particularly sensitive probe of such charge exchange. Even relatively far from the surface, the motion of the electron is strongly influenced by image charge interactions which distort the electronic wavefunctions, leading to strong hybridization, and shift the atomic energy levels. Furthermore, the electron can tunnel into the surface leading to ionization and broadening of the atomic levels. These processes are the subject of continuing interest.

Recent experiments have employed xenon Rydberg atoms which are directed at near grazing incidence ($\theta \sim 4$ °) onto the target surface. Ions formed by tunneling are attracted to the surface by their image charge fields. These fields are large and rapidly accelerate an ion to the surface where it is neutralized by an Auger process. To prevent this an ion collection field is applied perpendicular to the surface. Because the initial image-charge field experienced by an ion, and thus the critical field required to counteract it, depends on the atom-surface separation at which ionization occurred, this can be inferred from measurements of the surface ionization signal versus applied field.

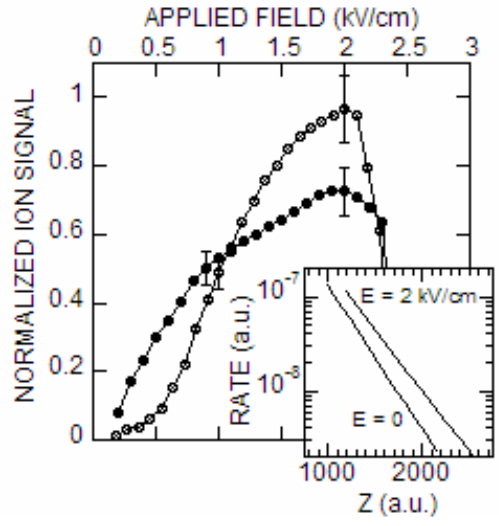

Figure 1. Applied field dependence of the surface ion signal when Xe(n=20) atoms are incident on Au(111) and hydrogen-passivated p-type Si(100). The inset shows the inferred ionization rate for Au(111) as a function of atom-surface separation for applied fields of 0 and 2 kV cm^{-1} .

Figure 1 shows the applied field dependence of the surface ion signal when Xe(n=20) Rydberg atoms are incident on Au(111) and hydrogen-passivated p-type Si(100) targets. In each case, the ion signal increases steadily with applied field and, for sufficiently large fields, a sizable fraction of the incident ions are detected as ions (The sharp cut off in the ion signal is associated with field ionization of the Rydberg atoms before they can strike the surface.)

The Au(111) data can be well fit by assuming that the ionization rate simply increases exponentially as the surface is approached, yielding the rates shown in the inset. While the resulting most probable ionization distance, ~3.4n^2 (a.u.), is in good agreement with hydrogenic theory, the characteristic exponential decay length is substantially larger. This can be attributed to the avoided crossings that occur between different (xenon) atomic levels as the ion collection field is applied and as the atom approaches the surface. Calculations show these levels have a wide variety of spatial characteristics, the electron probability densities for some being maximal towards the surface, others towards vacuum. If these avoided crossings are traversed adiabatically as recent dynamical calculations suggest, an incident atom will successively assume the character of a number of different states and lose much of its initial identity. If the calculated ionization rates for these various states are "averaged" by an exponential the resulting decay lengths are in reasonable accord with the measured values.

The differences between the Si(100) and Au(111) data are indicative of localized stray electric fields at the Si(100) surface. Although hydrogen passivation was used to remove the initial oxide layer, metastable atom impact leads to destruction of the passivation layer allowing growth of an oxide film. Taking into account the reduced image charge interactions at a dielectric surface, the data can be reasonably well fit by assuming an ionization rate similar to that for Au(111) and the presence of stray fields with values of up to ~±1 kV cm^{-1}.

†Research undertaken in collaboration with H. R. Dunham, S. Wethekam and J. C. Lancaster and supported by the NSF and the Robert A. Welch Foundation

* E-mail: fbd@rice.edu

IONISATION OF RYDBERG ATOMS COLLIDING ON METAL SURFACES

J.P.Gauyacq, J.Sjakste, and A.G.Borisov*

Laboratoire des Collisions Atomiques et Moléculaires, Bât.351, Université Paris-Sud, 91405 Orsay, France

The electronic levels of Rydberg atoms approaching a metal surface are usually located well above the Fermi level of the metal so that the Rydberg atoms can be ionized by a one-electron energy conserving transition, the Resonant Charge Transfer process. When polarized by the surface potential and/or by an external field, the electronic clouds of Rydberg atoms exhibit very different shapes, pointing toward the surface or away from it. As a consequence, one can expect different polarizations to lead to very different properties of the Rydberg atoms with respect to ionization and in particular to very different ionization distances from the metal surface[1]. Recently, an elegant method has been proposed to measure the distance of ionization of a Rydberg atom approaching a metal surface[2]. It is based on the presence of an external electric field repelling the ions formed by ionization. Surprisingly, Xe Rydberg atoms polarized toward the surface and away from it exhibit similar ionization properties[3], in apparent contradiction with the common knowledge on these systems.

We report on a theoretical investigation of the Xe* Rydberg states (n=7-8) ionization during a low energy collision on a metal surface. The aim is to determine the ionization dynamics of a Rydberg atom approaching a metal surface in the presence of an external electric field and the dependence of the ionization process on the initial state. The time evolution of the Rydberg electron is studied using a wave packet propagation approach[4]. It consists in solving the time-dependent Schrödinger equation for the active Rydberg electron on a grid of points, the core of the Rydberg ion being assumed to move along a classical trajectory. This allows to study the Rydberg atom ionization, taking into account all the dynamical non-adiabatic effects of the atom-surface collision.

As the main result of this study, the ionization of a Rydberg atom is strongly influenced by the presence of an external field. The initial state of the collision is a Stark hybrid defined in the external field, it can be oriented toward the surface or toward vacuum. As expected, the *static* (fixed atom-surface distance) ionization rate of the Rydberg atom is strongly dependent on the electronic cloud polarization. However, the dynamical study of the collision situation revealed the existence of significant non-adiabatic transitions. These concern both mixing inside a given n-manifold and inter-manifold transitions. In particular, as the atom approaches the surface, transitions between surface-oriented and vacuum-oriented states can occur that deeply affect the ionization properties.

Our results allow a detailed discussion of the experimental results of Dunning et al[3] and of the apparent absence of a polarization dependence of the ionization process. We find that, due to the strong perturbation introduced by the external field, the proposed method can yield a measure of the ionization distance only in some specific cases. For the vacuum-oriented states, the experimental procedure determines the threshold for mixing with a surface-oriented state, leading to the apparent absence of a polarization effect.

REFERENCES

[1] J.Hanssen, C.F.Martin and P.Nordlander Surf. Sci.Lett. **423** , L271 (1999).
[2] S.B.Hill, C.B.Haich, Z.Zhou, P.Nordlander and F.B.Dunning Phys.Rev.Lett. **85**, 5444 (2000).
[3] F.B.Dunning, H.R.Dunham, C.Oubre and P.Nordlander Nucl.Inst.Meth.B **203**, 69 (2003).
[4] A.G.Borisov, A.K.Kazansky and J.P.Gauyacq Phys. Rev.B **59**, 10935 (1999).

* E-mail: gauyacq@lcam.u-psud.fr

NANOSTRUCTURES BY GRAZING INCIDENCE IONS: RIPPLE PATTERNS, ATHERMAL COARSENING AND SUBSURFACE CHANNELING

T. Michely[*]

I. Physikalisches Institut, RWTH Aachen University, 52056 Aachen, Germany

The recent years showed significant progress in our ability to use ion beams for the controlled patterning of surfaces. New applications of patterned substrates as functional surfaces or of patterned thin films emerge. Nevertheless, our present understanding of the atomic scale mechanisms governing pattern formation through ion beams is still poor. Here we present results of temperature dependent scanning tunneling microscopy investigations of ripple pattern formation on Pt(111) by a 5 keV Ar^+ ion beam incident at angles between 78° and 86° with respect to the surface normal. These results combined with corresponding single impact molecular dynamics simulations allow a few steps towards a better understanding of metal surface patterning.

Two different regimes of pattern formation are clearly distinguished. The athermal regime between 250 K and 450 K with a temperature independent wavelength and the thermal regime between 500 K and 700 K exhibiting a strong increase of wavelength with temperature.

In the athermal regime elongated vacancy structures - vacancy grooves - form due to the selective erosion of ascending steps illuminated by the ion beam. These structures interact athermally through the adatoms produced by the ion impacts hitting the illuminated tips of the vacancy grooves. Consequently the initial wavelength is set by the lateral length scale of influence of a single ion impact, which is around 5 nm.

In the thermal regime step edge diffusion becomes efficient and keeps the vacancy islands formed compact, i.e. close to their minimum energy shape. Surprisingly, in this regime pattern formation depends crucially on the angle of incidence of the ions. As soon as this angle allows subsurface channeling of the ions, pattern regularity and alignment with respect to the ion beam greatly improves. These effects are traced back to the positionally aligned formation of vacancy islands through the damage created by the ions at dechanneling locations (compare Fig.1). Vacancy groove interaction in this regime is dominated by diffusion processes of adatoms and vacancies. Pattern formation is delayed compared to the athermal regime.

Pattern formation ceases both at low and high temperatures. Although the wavelength in the athermal regime is set by the length scale imposed by the ion beam, vacancy groove formation relies on diffusion of surface point defects and low coordinated atoms. Consequently, with vacancy diffusion frozen out below 200 K pattern formation ceases. Above 700 K ripple formation is impeded due to the onset of step atom detachment.

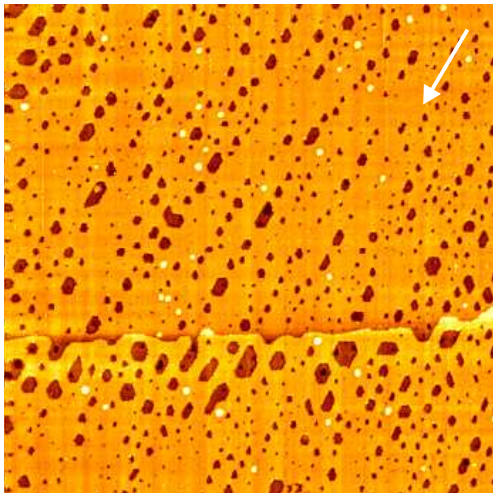

Figure 1: STM topograph after 5 keV Ar^+ ion bombardment of Pt(111) at 550 K and at an angle of 83° with respect to the surface normal. If viewed at grazing angle the alignment of the monolayer deep vacancy islands along the projection of the ion beam direction onto the surface (white arrow) is visible. Image size is 170 nm × 1700 nm.

The long term pattern evolution is characterized by a power law increase of the pattern amplitude and a characteristic increase of the ripple pattern wavelength with the ion fluence. The pattern amplitude increases through the action of a step edge barrier for vacancies. The coarsening of the pattern is due to annihilation reactions of defects in the pattern, which travel in the ion beam direction. The same formal description as used for the coarsening of dune fields can be applied to this athermal ripple pattern coarsening.

The contributions of Alex Redinger, Henri Hansen, Sebastian Meßlinger, Georgiana Stoian, Oliver Ricken, Herbert Urbassek and Yudi Rosandi to this work are acknowledged.

[*] E-mail: michely@physik.rwth-aachen.de

ION INDUCED NANOPATTERNS ON SEMICONDUCTORS: FORMATION AND APPLICATION

A. Keller[*], *S. Roßbach, S. Facsko, and W. Möller*

Institute of Ion Beam Physics and Materials Research, FZ Rossendorf, P. O. Box 51 01 19, 01314 Dresden, Germany

1. INTRODUCTION

It is well known that under certain conditions, low and medium energy (typically 0.1 – 100 keV) ion sputtering can induce the formation of self-organized patterns on the irradiated surface [1]. Periodic ripple patterns and hexagonally ordered dot arrays form for oblique and normal ion incidence, respectively. The periodicity of the patterns depends on the sputtering conditions and ranges from some ten nanometres up to several microns. These structures were found on a large variety of materials, such as semiconductors, metals, and insulating surfaces [2]. The first attempt to describe the formation process was made by Bradley and Harper and led to a continuum model based on sputter theory [3]. In this framework, the patterns result from the interplay between curvature dependent sputter yield and diffusion.

2. NANOPATTERNS

2.1. Formation

To investigate the process of pattern formation, semiconductor surfaces are eroded by sub-keV Ar ions. The topography of the sputtered surfaces is studied by *ex-situ* atomic force microscopy (AFM).
Off-normal ion erosion of Si creates ripple patterns with a wavelength ranging from 20 nm to 60 nm and amplitude of approximately 2 nm. An example is given in Figure 1.

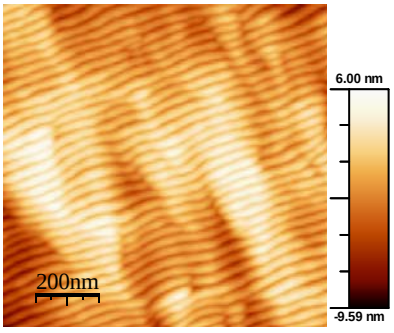

Figure 1: Si after 500 eV Ar sputtering; incidence angle 67°.

By means of normal incidence bombardment, well ordered dot arrays are fabricated on GaSb. These arrays exhibit hexagonal symmetry and a periodicity of the order of 40 nm. The amplitude is of the same magnitude as the periodicity. Figure 2 shows an AFM image of the sputtered GaSb surface.

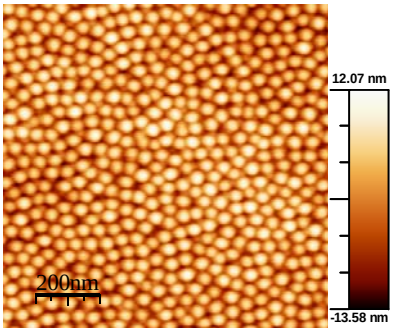

Figure 2: GaSb after 500 eV Ar sputtering; normal incidence.

The formation process will be discussed in detail and recent results of our studies on pattern evolution and the influence of boundary conditions are presented.

2.2. Application

As a promising application, erosion induced surface patterns can be used as templates in further processes such as molecular beam epitaxy or sputter deposition. The morphological anisotropy of the surface can influence the process significantly. Recent findings of investigations on ripple induced anisotropies in metallic thin films are presented.

3. REFERENCES

[1] M. Navez, D. Chaperot and C. Sella, C. R. Acad. Sci. **254**, 240 (1962)
[2] U. Valbusa, C. Boragno and F. Buatier de Mongeot, J. Phys.: Condens. Matter **14**, 8153 (2002)
[3] R. Bradley and J. Harper, J. Vac. Sci. Technol. A **6**, 2390 (1988)

[*] E-mail: a.keller@fz-rossendorf.de

NANOPATTERN FORMATION WITH FOCUSED ION BEAMS

E. Bertagnolli[*]

Vienna University of Technology, Institute for Solid State Electronics, Vienna, Austria

1. INTRODUCTION

A Focused Ion Beam (FIB) system is a scanning microprobe technique similar to a Scanning Electron Microscope (SEM). However, in contrast to a SEM, in a FIB system, an ion beam of a few ten keV is rastered over a surface for surface modificaton. The beam correlated secondary electrons are used to image simultaneously the target area under irradiation. Thus, surface modifications on a nanometric scale can be made under direct control. The FIB functionalities rely on the application of ion beam interactions with the target surface. Due to its strict confinement, nanoscale level research is the dominant application of FIB. Application of Focused Ion Beams cover a wide range of activities, from basic ion-surface interaction research, over local processing for removal or deposition of layers up to device fabrication and 3-D-Nanofabrication.

2. BEAM PROFILE OF NANOSCALE FIB

The correct beam profile at the targeted surface is a crucial parameter for any proper solid-beam interaction investigation. Therefore our group developed a new approach to extract the specific beam profile by a material insensitive approach. Fig. 1 shows typical focused ion beam profiles.

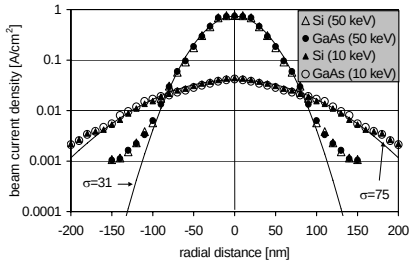

Fig. 1: Radial distribution of beam current density for a 50 keV and a 10 keV focused ion beam, respectively. Symbols mark measured data; the solid curves represent Gaussian fits.

3. FIB PROCESSING AND RADIATION DAMAGE

Any FIB based modification of electronic devices is endangered by radiation damage. Therefore, a quantification of the impact of FIB on specific parameters of devices during beam exposure is essential. By an in situ sensing of an active device (n-channel MOSFET) we found, that progressive degradation of the device starts when long-range damage cascades begin to extend into the inversion channel regions. The device degradation can be attributed to charge mobility decrease in the channel region, and can be quantified by a semi-empirical mobility model.

4. NANOFABRICATION

Nanofabrication by FIB issues both, direct, that means maskless nanoscale patterning, and target insensitive material engineering. As an example of nanofabrication by FIB, fig. 2 shows a GaAs/AlGaAs quantum cascade laser with monolithic one-dimensional photonic-band gap mirrors formed at the end of the laser ridge by FIB.

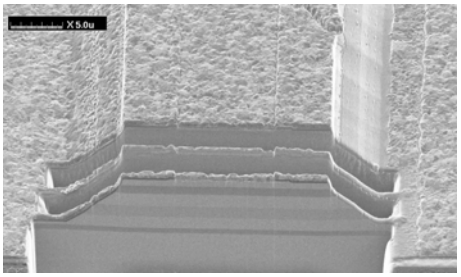

Fig.2: Photonic-band-gap-mirror on a QCL laser ridge.

5. FIB FOR DOTS AN NANOWIRES

Recently, quantum dots and nano-wires have gained much interest, since they promise solutions for the foreseeable onset of the quantum regime at downscaled devices. In this nanoscale fields, FIB processing is a primary choice, due to the combination of maskless patterning with nanoscale critical dimensions. As an example, in fig 3 an array of nanodots on a preformed semiconductor surface is shown.

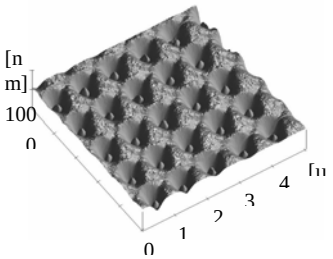

Fig. 3: AFM image of an array of entrenched Gallium dots in 80nm deep cavities generated by FIB.

In summary, in this paper most of the specific applications of FIB for nanoscale patterning are presented.

6. REFERENCES

[1] A. Lugstein, B. Basnar, G. Hobler, and E. Bertagnolli, Journal of Applied Physics 92, 4037 (2002).
[2] W. Brezna, H. Wanzenböck, A. Lugstein, E. Bertagnolli, E.Gornik, J. Smoliner, Sem. Sci. Technol. 18, 195 (2003)
[3] C. Schoendorfer, A. Lugstein and E. Bertagnolli, Microelectronic Engineering, 83, 1491 (2006).

[*] E-mail: emmerich.bertagnolli@tuwien.ac.at

NANO-SCALE EFFECTS OF SWIFT HEAVY ION IRRADIATION OF SIO_X LAYERS AND MULTILAYERS

W.M. Arnoldbik[1,], D.Knoesen[2] and F.H.P.M. Habraken[1]*

[1] Surfaces, Interfaces and Devices, Dept. Physics & Astronomy, Faculty of Sciences, Utrecht University, P.O. Box 80.000, NL-3508 TA Utrecht, The Netherlands
[2] Dept. of Physics, University of the Western Cape, Bellville, ZA-7530 South Africa

1. ABSTRACT

Since a long time the interaction of swift heavy ions, i.e. ions with a kinetic energy ~1 MeV/a.m.u. or larger, with solids is considered to be an interesting subject of research in physics and materials science. For the swift ions the electronic stopping dominates above the nuclear stopping, and in the interaction the first step is the electronic excitation of the solid along the so-called ion track. The next step is the transfer of the energy from the electronic system to the atomic system in a cylindrical region of the solid around the ion path, which results in a strong heating and subsequent fast cooling of the material in and around the ion track [1,2]. The interaction is a nanometer scale phenomenon [3], since the diameter of the ion track is of the order of a few nanometers. Despite the individual nature of the occurrence of every ion track, it appears that the repeating occurrences of these ion tracks in solid structures can give rise to interesting coherent phenomena, recent examples being the modification of the shape of silica colloids [4].

Irradiation of SiO_x layers and multilayers ($0 \leq x \leq 2$) with swift heavy ions shows many examples of interesting materials modifications.
We consider the Si/SO_2 phase separation in SiO_x films during irradiation with 50 MeV Cu^{8+} ions [5]. In this work, the particle current density was such low that indeed every ion impact and concomitant ion track occurrence can be considered as one individual event.
Figure 1 shows for various x in SiO_x the position of the maximum of the infrared absorption in the region of the Si-O-Si stretching mode (750-1400 cm^{-1}). This maximum shifts from about 950 cm^{-1} for an isolated Si-O-Si bond in amorphous silicon up to about 1050 cm^{-1} in low-temperature deposited, disordered SiO_2.
For every x-value we note a shift of the absorption peak towards higher wave numbers, indicating that the oxygen atoms in the network are increasingly more present in oxygen rich regions (with nanometer dimensions), and since the x-value remains constant, this implies that simultaneously oxygen poor regions come into existence.

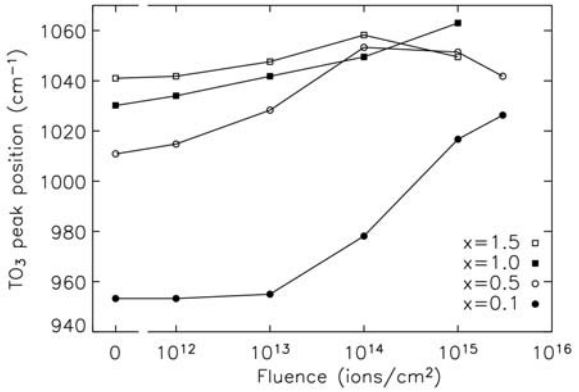

Figure 1: IR Si-O-Si stretching mode absorption peak position as a function of swift heavy ion fluence [5] .

We consider the observed evolution of the IR peak shape [5] to be further proof that SiO_x fulfills the conditions for spinodal decomposition [6].

Our contribution discusses the material modifications as a result of swift heavy ion irradiation in Si/SiO_2 multilayers with SiO_x thin layers at the interfaces between distinct Si and SiO_2 films.

2. REFERENCES

[1] M. Toulemonde, C. Dufour, A. Meftah and E. Paumier. Nucl. Instrum. Methods. B 166, 903 (2000)
[2] E.M. Bringa and R.E. Johnson, Phys. Rev. Lett. 88, 165501 (2002).
[3] G. Schiewitz, E. Luderer, P.L. Grande, Appl. Surf. Sci. 182, 286 (2001)
[4] T. van Dillen, E. Snoeks, W. Fukarek, C. van Kats, K.P. Velikov, A. van Blaaderen and A. Polman, Nucl. Instrum. Methods. B 175, 350 (2001)
[5] W. M. Arnoldbik, N. Tomozeiu, E. D. Hattum, R. W. Lof, A. M. Vredenberg, and F. H. P. M. Habraken, Phys. Rev. B, 71 125329 (2005)
[6] J.J. van Hapert, A. M. Vredenberg, E. E. van Faassen, N. Tomozeiu, W. M. Arnoldbik, and F. H. P. M. Habraken, Phys. Rev. B 69, 245202 (2004)

* E-mail: w.m.arnoldbik@phys.uu.nl

SFM INVESTIGATIONS OF DISCONTINUOUS ION TRACKS

Thorsten Peters[1,*], *Ender Akcöltekin*[1], *Ralf Meyer*[1] *Henning Lebius*[2] *and Marika Schleberger*[1]

[1] Universität Duisburg-Essen, FB Physik, 47048 Duisburg, Germany
[2] CIRIL / GANIL, Blvd. Henri Becquerel, 14070 Caen, Cedex 5, France

1. INTRODUCTION

In recent years the interaction between ions and solid surfaces has been studied intensively. For obvious reasons this interaction has been investigated almost exclusively above the surface and previous to the impact. The processes and modifications at and below the surface are another part of the story. These complicated and not yet fully understood processes still offer a broad field to experimental as well as theoretical physics. It is experimentally well established that the ions create a track of amorphous material when travelling through the solid. This results in surface modifications which can be observed. Within a few femtoseconds the majority of the kinetic and potential energy is dissipated into the bulk. On many non-metallic materials hillock like surface modifications with heights and diameters of a few nanometer were found after irradiation. Despite these experimental results Monte-Carlo-simulations predict craters instead of hillocks [1]. A phenomenological approach is given by the so-called thermal spike model [2]. Detailed microscopic and quantitive explanations or numerical simulations are however still missing. Experimentally the investigation of latent tracks requires the application of different techniques. Tracks below the surface can be made visible by transition electron microscopy or the amorphous material can be selectively etched away. In our experiments we apply scanning force microscopy.

2. EXPERIMENTAL

The irradiations were performed at the beamline IRRSUD of the GANIL in Caen, France. To ensure that no enviromental effects would have any influence on the irradiation effects some measurements were performed *in situ* in an UHV-AFM (base pressure $2 \cdot 10^{-10}$ mbar) right after the irradiation. In addition, measurements were performed at different SFMs under ambient conditions in contact mode, tapping mode as well as in non-contact mode to ensure that the tip would not modify the hillocks. SFM images of every sample were taken before irradiation to check the cleanliness and morphology of the surfaces. As targets we used oxide surfaces ($SrTiO_3$, TiO_2, MgO_2, Al_2O_3), fluorides (CaF_2, LiF) and salts (KaCl, NaCl, KBr) as well as HOPG. HOPG was cleaved, all other samples were cleaned with aceton. No further preparation techniques were necessary. The irradiation was done with Pb^{28+} at 0.521 MeV/u and Xe^{20+} at 0.55 MeV/u and 0.71 MeV/u typically at a fluence of about $2{\cdot}10^9$ ions/cm^2. This fluence yields a density of about 10 impacts/μm^2 which allows us to investigate single impacts without overlap of two defects. The angle of incidence was varied from 90° (with respect to the surface) down to $< 10°$.

3. RESULTS

Under normal incidence the defects appear hillock like with ca. 5 nm height and a round base, 25 nm in diameter. The number of defects directly corresponds to the number of impacts so we conclude that in the chosen regime every ion creates a single hillock.

After decreasing the angle significant changes of the hillocks begin to occur. From 60° down to 30° the structures become elongated along the direction of incidence. Further decreasing the angle produces no longer elongated, but periodically discontinuos defects like pearls on a chain. The length of the chain can be as long as several microns.

In this energy regime electronic stopping (19.1 to 24.3 keV/nm, calculated with SRIM[3]) is dominant. Therefore, this unexpected behaviour may due to the anisotropic electron densities in the crystal. A comparison of experimental results with theoretical calculations of the electronic densities will be presented.

4. REFERENCES

[1] E.M. Bringa, E. Hall, R.E. Johnson and R.M. Papaleo, Nucl. Instr. Methods B **193**, 734 (2002).

[2] M. Toulemonde and F. Studer, Solid State Phenom. **477**, 30-31 (1993).

[3] J.F. Ziegler and J.P. Biersack (1984-2003).

* E-mail: thorsten.peters@uni-duisburg-essen.de

THE MEDAUSTRON PROJECT

E. Griesmayer[1,*], *T. Schreiner*[2], *and M. Pavlovič*[3]

[1] University of Applied Sciences Wiener Neustadt
[2] Fotec – Forschungs- und Technologietransfer GmbH
[3] Slovak University of Technology, Faculty of Electrical Engineering and Information Technology

ABSTRACT

The Austrian government has approved its financial contribution to the MedAustron project in October 2004. MedAustron, the Austrian ion therapy and cancer-research centre, should be set into operation in 2010. MedAustron combines medical cancer treatment & cancer research and non-clinical research.

For medical treatment and cancer research active scanning of a proton and a carbon-ion beam is provided. The beam energy must correspond to the desirable residual range of the beam in the patient body, which translates into the energy interval of 60 MeV to 220 MeV protons and 120 MeV per nucleon to 400 MeV per nucleon carbon ions. The beam intensity is limited to 10^{10} protons per second and 4 times 10^8 carbon ions per second which is equivalent to an electrical beam current of 1.6 nA for protons and 0.38 nA for carbon ions.

Although the machine parameters must be optimised for therapy needs, additional beam features can be offered by a modern medical accelerator for non-clinical research. Various ions with energies up to 400 MeV per nucleon can be used for irradiation purposes. For synchrotrons such as proposed in the Design Study the proton energy can be increased to 1.18 GeV when using a dedicated RF-system. Two beam lines are proposed for non-clinical research, such as biomedicine, medical physics, physics or industrial technological research. The experimental facility of MedAustron will be offered to research institutes and to industry on an international level.

* E-mail: eg@fotec.at

Member of UniCredit Group

Bank Austria Creditanstalt

Banking for success.

What would the big successes be
without the little victories?

FUSION RELEVANT ION - SURFACE COLLISION PROCESSES

A. Golczewski, G. Kowarik, S. Figueira da Silva, S. Cernusca, HP. Winter and F. Aumayr*

Institut f. Allgemeine Physik, TU Wien, A-1040 Vienna, Austria

1. INTRODUCTION

Numerical codes are nowadays available to model the behavior of the boundary of fusion plasmas and the plasma wall interaction. These codes are based on our knowledge on heat and particle loads and re-emission, various surface processes (physical and chemical sputtering, electron emission and reflection, etc.) and transport processes. However, there are large uncertainties in the present day predictions due to the lack of detailed knowledge about the involved processes. We therefore study the interaction of ions with fusion relevant surfaces, in particular processes of ion - induced electron emission and sputtering/erosion, and investigate their importance for a successful modeling of the plasma boundary and plasma-wall-interaction.

2. ELECTRON EMISSION

Electron emission due to the interaction of slow singly and multiply charged ions with clean or gas covered conducting surfaces including graphite tiles from the Tokamak experiment TORE SUPRA in CEA-Cadarache/France, highly oriented pyrolytic graphite [1,2] and tungsten surfaces has been studied (see fig. 1). Projectiles range from low Z to heavy ions. Investigations are carried out in the eV to keV impact energy region as typical for fusion edge plasma conditions. The underlying mechanisms for kinetic and potential electron emission are being identified. Implications of the experimental results for plasma-edge modeling are studied in collaboration with the University of Innsbruck, based on a newly developed plasma sheath theory with ion-induced electron emission from the cathode side [3]. These calculations demonstrate that the presence of electron emission can lower the sheath potential from the usual value 3kT to almost 2kT. These results could be of relevance for impurity ion-induced sputtering of W surfaces.

3. SPUTTERING

Our group has longstanding experience in measuring ion-induced sputter yields by means of a sensitive quartz crystal microbalance [4]. We have started to apply this method to surfaces which are already used or considered as divertor or wall materials for JET and ITER (e.g., a-C:H and W).

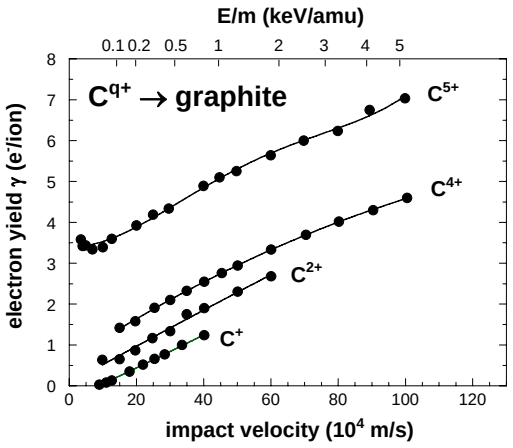

Figure 1: Total electron yields for impact of singly and multiply charged carbon ions on clean graphite, vs. ion impact velocity

In addition we plan to investigate whether the impact of multiply charged ions (e.g. C^{q+}) on such surfaces leads to increased erosion due to the process of potential sputtering [5-7].

This work has been supported by Austrian Academy of Sciences (Project KKKÖ 1-2005) and was carried out within Association EURATOM-ÖAW.

4. REFERENCES

[1] S. Cernusca, et al., Int. J. Mass Spectrom. Ion Proc. **223-224** (2003) 21; A. Qayyum, et al., J. Nucl. Mat. **313-316** (2003) 670;
J. Lörincik, et al., Surf. Sci. **504** (2002) 59
[2] S. Cernusca, M. Fürsatz, HP. Winter, and F. Aumayr, Europhys. Lett. **70** (2005) 768
[3] N. Schupfer, et al., Plasma Phys. Contr. Fusion (2006) in print
[4] G. Hayderer, M. Schmid, P. Varga, HP. Winter and F. Aumayr, Rev. Sci. Instrum. **70** (1999) 3696
[5] M. Sporn, et al.,Phys. Rev. Lett. **79** (1997) 945
[6] G. Hayderer, et al., Phys. Rev. Lett. **83** (1999) 3948; G. Hayderer, et al., Phys. Rev. Lett. **86** (2001) 3530
[7] F. Aumayr and HP. Winter, Phil. Trans. Royal Soc. London A **362** (2004) 77

* E-mail: golczewski@iap.tuwien.ac.at

CHEMICAL SPUTTERING OF DEUTERATED CARBON BY D AND D_2 IMPACT

C.O. Reinhold[1,*], *P.S. Krstić*[1], *and S.J. Stuart*[2]

[1] Physics Division, Oak Ridge National Laboratory, P.O. Box 2008, Oak Ridge, TN 37831-6372, USA
[2] Department of Chemistry, Clemson University, Clemson, SC 29634, USA

1. INTRODUCTION

Bombardment of carbon-based surfaces by low-energy (E<50eV) D atoms and D_2 molecules (and ions) induces chemical reactions which ultimately lead to emission of stable hydrocarbons. Because such chemical sputtering processes are an important source of erosion of plasma-facing materials (limiters/divertor plates, vacuum vessel walls) of fusion reactors, there is a strong need within the fusion community for quantitative predictions of the corresponding yields. Motivated by this need and recent experiments at ORNL [1,2], we have undertaken a series of large-scale classical molecular dynamics (MD) simulations of chemical sputtering of carbon surfaces.

2. RESULTS

We have performed MD simulations of D and D_2 impinging on deuterated amorphous carbon surfaces in the energy range of 5-30 eV/D using REBO [3] potentials. Figure 1 shows that the calculated sputtering yields per deuteron obtained for D and D_2 agree quantitatively with each other (within the statistical uncertainty) and that the methane sputtering yields are in very good agreement with experiment [1].

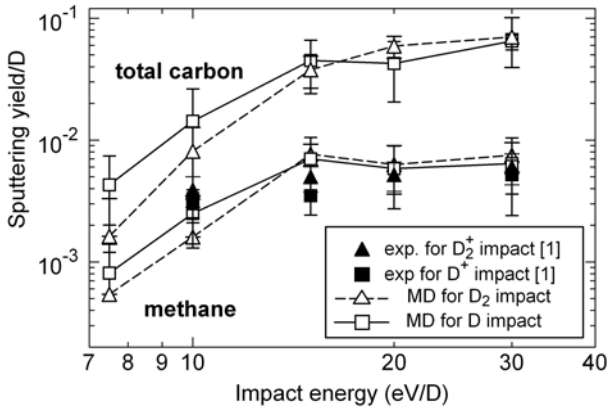

Figure 1: Total and methane sputtering yield (per D) of deuterated carbon surfaces at room temperature as a function of the energy per D.

While previous MD simulations have focused on the total sputtering yield of carbon [4], we have centered our work on the description of the methane yield. Mimicking the experimental conditions requires careful control of the time scales of the sputtering process; specifically the fluence and the relaxation time after each impact. Surfaces were prepared by D or D_2 impact of up to 2000 deuterons on an initial deuterated simulation cell of about 2500 atoms for a time period of up to 2ns. For a constant D flux a "quasi steady state" in the hydrocarbon sputtering yield is reached which depends on the particular hydrocarbon. The quasi-steady-state result fluctuates considerably, the error bars in the figure providing the standard deviation of such fluctuations. Remarkably, we find that the sputtering yield in the quasi-steady-state regime differs considerably from that obtained for a non-irradiated simulation cell, emphasizing the importance of modeling the experimental system, rather than an idealized one. The calculated yields of methane are directly related to the sp^2/sp^3 densities at the topmost layers. We also find that after each impact the particle emission process can require a considerably long time of ~5ps.

3. ACKNOWLEDGEMENTS

PSK and COR acknowledge the support from the US DOE OFES and OBES with UT-Battelle under contract DE-AC05-00OR22725. SJS acknowledges support by US DOE (DE-FG02-01ER45889) and the NSF (CHE-0239448).

4. REFERENCES

[1] L.I. Vergara, F.W. Meyer, H.F. Krause, P. Traskelin, K Nordlund, and E. Salonen, J. Nucl. Mat. (2006), in press.
[2] F.W. Meyer, L.I. Vergara, and H.F. Krause, this conference.
[3] S. J. Stuart, A. B. Tutein and J. A. Harrison, *J. Chem. Phys.* **112** 6472-6486 (2000).
[4] E. Salonen, K. Nordlund, J. Keinonen, and C.H. Wu, Phys. Rev B 63, 195415 (2001).

* E-mail: reinhold@ornl.gov

ION SURFACE COLLISIONS ON SURFACES RELEVANT FOR FUSION DEVICES

N. Endstrasser[*] *,L. Feketeova , F. Zappa, B. Rasul,V. Grill, P. Scheier, and T.D. Märk*

Institut für Ionenphysik und Angewandte Physik, LFU Innsbruck, Technikerstr. 25, A-6020 Innsbruck, Austria

1. INTRODUCTION

One of the great challenges of fusion research is the compatibility of reactor grade plasmas with plasma facing materials coating the inner walls of a fusion reactor. The question of which surface coating should be used is of particular interest for the design of ITER.
The impact of energetic plasma particles leads to sputtering of wall material into the plasma. The lower the atomic number Z of the wall material, the smaller is the number of electrons lost by ionization in the plasma by inelastic scattering processes. As a consequence this disturbing effect should be held as small as possible. The produced ions may impact into other reactor walls and perform further ion-surface collisions.
Due to the low Z-value and the high thermal resistivity graphite is often used in Tokamak fusion reactors. But experiments showed that graphite migrates in the reactor and the graphite dust produced by sputtering absorbed hydrogen very effectively. Therefore graphite should be replaced by other materials and one of the surface materials under consideration is Beryllium. The absorption of hydrogen in the surface leads to appearance of blisters and damage in Beryllium which could be reduced by the use of tungsten. Relatively low vapour pressures at high temperatures, a low sputtering rate and high thermal resistivity make tungsten attractive for fusion experiments.
Another possible solution for the coating of plasma facing walls would be the use of special carbon surfaces. Nanocristalline diamond surfaces were granted by Rho-Best coating company in Innsbruck for our experiments. Investigations of these various surfaces have been started at BESTOF ion-surface collision apparatus in Innsbruck to ease the choice of materials to be used for ITER.

2. EXPERIMENTAL

A beam of singly charged molecular ions of hydrocarbon molecules, i.e. $C_2D_4^+$, is generated in a Nier-type electron impact ionization source at an electron energy of about 70 eV. In the first double focusing mass spectrometer the ions are mass and energy analyzed and afterwards refocused onto a surface. The secondary reaction products produced after ion surface collisions with collision energies up to about 50 eV are monitored using a Time Of Flight mass spectrometer.
The secondary ion mass spectra are recorded as a function of the collision energy for different projectile ions and different surfaces. A comparison of these spectra show for example distinct changes in the survival probability of the same projectile ion $C_2D_4^+$ for different surfaces as can be seen in Figure 1.

Figure 1: Effective survival probability of $C_2D_4^+$ ions, i.e. the yield of scattered parent ions divided by the total

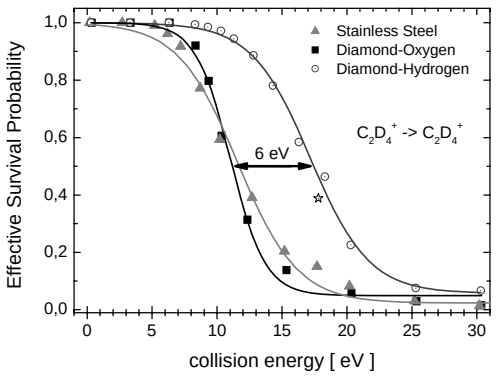

yield of all scattered ions for a stainless steel, an oxygen terminated and a hydrogen terminated diamond surface. The solid line reflects a nonlinear least square fit with a sigmoidal function.

2.1. Acknowledgement:

Work supported by FWF, Wien and the EURATOM/ÖAW Association, Wien. We thank ρ-BeSt coating, Tirol for their contribution of diamond samples used in this work. Thanks to Dr. Erwin Seidl, Atomic Institute of the Austrian universities, for cutting the beryllium surfaces. Postdoctoral fellowship grant from Brazilian agency CNPq, and PhD fellowship granted from HEC, Pakistan, is gratefully acknowledged.

[*] E-mail: nikolaus.endstrasser@uibk.ac.at

STICKING COEFFICIENT AND SIMS OF HYDROCARBONS ON FUSION RELEVANT PLASMA – SPRAYED TUNGSTEN SURFACES

W. Schustereder[1,*], *N. Endstrasser*[2], *V. Grill*[2], *P. Scheier*[2], *T.D. Märk*[2]

[1] Max-Planck-Institut für Plasmaphysik, EURATOM Assoziation, Boltzmannstraße 2, D-85748 Garching, Germany
[2] Institut für Ionenphysik und Angewandte Physik, Universität Innsbruck, Technikerstr. 25, A-6020 Innsbruck, Austria

1. INTRODUCTION

Tungsten and Carbon are foreseen as plasma facing material for the divertor of ITER [1]. Naturally erosion and redeposition will occur and influence the fusion plasma purity as well as the Tritium accumulation in first wall materials. Tungsten surfaces will help to minimize this critical effect. A promising method for covering such a large area like a fusion reactor divertor with tungsten is plasma spraying of tungsten (PSW) on some feasible substrate. The advantages of PSW in comparison with other deposition methods are homogeneously distributed voids, which stop crack propagation under high heat loads.

Laboratory data on hydrogen interaction with PSW are very scarce [2], the same is true for hydrocarbons. Here we concentrate on data of energy analyzed CD_3^+ ions impinging on a PSW sample as used in the divertor of ASDEX Upgrade. We investigate the sticking coefficient and the secondary ion mass spectra as function of the incident energy from 10eV to 100eV which is the energy range of hydrocarbons expected in the ITER divertor.

2. EXPERIMENTAL

2.1. Methods

Deuterated hydrocarbon ions are produced by a 2.45 GHz ECRH and a Nier-Type ion source. They are extracted and accelerated for mass- and energy-analysis by a double-focusing two-sector-field mass spectrometer. A beam of CD_3^+ ions is selected and refocused in front of the PSW surface. The incident ions are undergoing elastic and inelastic collisions. A Time-Of-Flight mass spectrometer collects the reaction products coming off the surface. Another fraction of incident ions keeps sticking on the PSW. After exposure the retrieved probes are analyzed ex-situ using Rutherford Back-Scattering (RBS) and Nuclear Reaction Analysis (NRA) employing a 800kV $^3He^+$ beam. Thereby areal densities of C and D are measured.

2.2. Laboratory Experiments

After collision of incident CD_3^+ ions with the PSW surface dissociation products of the projectiles, reflecting the loss of a D atom or a D_2 molecule, can be observed. Moreover also product ions formed in chemical reactions with the surface material are expected to be seen. These studies are compared to previous investigations on stainless steel and graphite tiles from TORE SUPRA.

After exposure to the CD_3^+ ion beam the PSW sample is retrieved and analyzed. Comparison of the areal density of C and D at the surface with the incident flux will allow to calculate the sticking coefficient and draw conclusions about the D/C ratio, that in turn indicates the nature of the deposited hydrocarbon film. The sticking probability of hydrocarbon species to the surface strongly influences the transport of hydrocarbon molecules in the edge plasma of fusion experiments [3].

2.3. Results From ASDEX Upgrade

It is foreseen in the 2006 campaign of ASDEX Upgrade to expose Tungsten coated probes to the divertor plasma. After some dedicated discharges with strike point position at the sample the erosion of the tungsten layer as well as deposition of hydrocarbons and other impurities are measured.
Also time resolved measurements of tungsten collected by a pyrolytic graphite probe at the midplane edge plasma of ASDEX Upgrade are presented.

3. REFERENCES

[1] G. Janeschitz, ITER JCT and HTs, J. Nucl. Mat. 290-293, 1 (2001)
[2] A. Golubeva, PhD Thesis at IPP Garching, to be finished in 2006
[3] D. Naujoks, D. Coster, H. Kastelewicz, and R. Schneider, J. Nucl. Mat. 266 (1999) 360

* E-mail: Werner.Schustereder@ipp.mpg.de

ANGULAR STUDIES OF ELECTRON EMISSION IN THE INTERACTION OF SLOW NA^+ WITH AL SURFACES

*M. Commisso, M.Minniti, A. Sindona, P. Barone, A. Bonanno, A. Oliva, and P. Riccardi**

Laboratorio IIS, Università della Calabria and INFN - gruppo collegato di Cosenza - 87036 Rende , Cosenza - Italy

In this work, we deal with the complexity of the interactions leading to electron emission induced by atomic particles by studying electron emission in the interaction of Na^+ ions with Al surfaces.
We measured energy spectra of electrons emitted by 300 eV and 1 keV Na^+ ions impacting Al surfaces as a function of ion incidence angle. Our measurements show evidence of several interplaying emission processes, including inner shell excitation of projectiles and target atoms , bulk plasmon excitation, and recently investigated sub-threshold KEE [1]. The role of the observed emission mechanisms in determining the intensity of electron emission will be discussed.

1. REFERENCES

[1] Z. Sroubek, X. Chen, Y. Yarmoff, Phys. Rev. B 73, 045247 (2006).

* E-mail: riccardi@fis.unical.it

ELECTRON EMISSION FROM INSULATOR SURFACES INDUCED BY IMPACT OF SLOW HIGHLY CHARGED IONS

W. Meissl[1,*], *M.C. Simon*[1], *HP. Winter*[1], *F. Aumayr*[1]
B. Solleder[2], *C. Lemell*[2], *J. Burgdörfer*[2]
J.R. Crespo López-Urrutia[3], *H. Tawara*[3], *J. Ullrich*[3]

[1] Institut f. Allgemeine Physik, TU Wien, A-1040 Vienna, Austria
[2] Institute f. Theoretical Physics, TU Wien, A-1040 Vienna, Austria
[3] EBIT group, Max-Planck Institut für Kernphysik, D-69029 Heidelberg, Germany

1. INTRODUCTION

Interaction of slow highly charged ions (HCI) with metal surfaces, which leads to the formation of so-called "hollow atoms", has been studied extensively over the past 20 years [1-2]. Due to the dielectric response of insulator surfaces (less image charge acceleration, low hole mobility), results for the interaction of HCI with insulator surfaces are difficult to interpret by available theoretical models.

2. EXPERIMENT

We have constructed an experimental setup which allows to compare electron emission from conducting Au(111) and insulating LiF(001) single-crystal targets (mounted on the same target holder). As projectile ions we used HCI from the Heidelberg-EBIT where Xe projectile charge states up to 52+ and W projectile charge states up to 64+ can be delivered. Measurements of the electron emission statistics have been performed under UHV conditions, and atomically clean target surfaces have been prepared by sputter cleaning and heating. Total electron emission yields have been recorded as a function of ion impact angle (between 0° - 70°) with respect to the surface normal.
As a typical example, in fig. 1 we show the impact angular dependence of the electron emission yield for 2.6 keV/amu Xe^{50+} impact on Au(111) and LiF(001) single-crystal surfaces.

3. MODEL CALCULATIONS

A simulation code has been recently developed [3] for the prototype insulator surface LiF that allows to explicitly treat the multi-electron dynamics of interactions of highly charged ions with insulator surfaces. It includes a large number of one – and two-electron processes that play an important role in the neutralization of HCI. Among them are (i) resonant capture and loss, (ii) multiple sequential electron transfer form and to the same fluorine site (iii) intra-atomic and inter-atomic Auger transitions, and (iv) hole transport in the surface. Our simulations are based on a Liouville - master equation which we solve by Monte-Carlo event-by-event sampling.

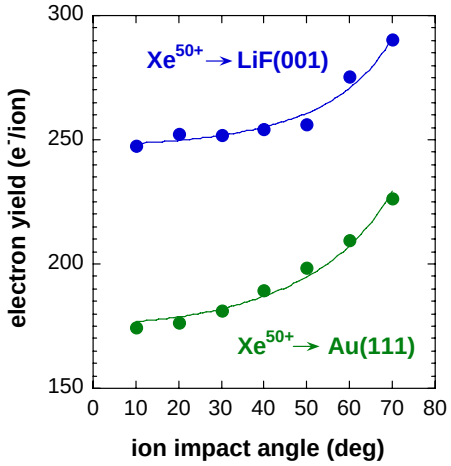

Fig. 1: Total electron emission yield for impact of 2.6 keV/amu Xe^{50+} ions on Au(111) and LiF(001) single-crystal surfaces as a function of ion impact angle (measured with respect to the surface normal).

This description goes well beyond previously employed rate equations for single-particle expectation values, as it deals directly with the joint probability density of projectile and target degrees of freedom. This method allows us to make quantitative predictions for multi-electron and multi-hole dynamics.
This work has been supported by Austrian Science Foundation FWF (Project No. P17449-N02) and was carried out within Association EURATOM-ÖAW. The experiments were performed at the distributed LEIF-Infrastructure at MPI Heidelberg Germany, supported by Transnational Access granted by the European Project HPRI-CT-2005-026015.

4. REFERENCES

[1] J. Burgdörfer, et al., Phys.Rev.A **44** (1991) 5674
[2] A. Arnau, et al., Surf. Sci. Rep. **27** (1997) 113;
F. Aumayr and HP. Winter NIMB **233** (2005) 111
[3] L. Wirtz, et al., Phys.Rev.A **67** (2003) 12903

* E-mail: meissl@iap.tuwien.ac.at

PROJECTILE CHARGE AND ANGLE OF INCIDENCE EFFECT ON SECONDARY ELECTRON YIELD

B. Ban-d'Etat, P. Boduch, F. Haranger, H. Lebius, L. Maunoury and H. Rothard.*

Centre Interdisciplinaire de Recherche Ions Laser CIRIL,
UMR 6637 (CEA, CNRS, ENSICAEN, Université de Caen), BP 5133,
Boulevard Henri Becquerel, F-14070 Caen Cedex 05, France

1. INTRODUCTION

The sputtering of uranium dioxide (UO_2) was studied at CIRIL-GANIL both at perpendicular and oblique incidence. Angular distributions and total sputter yields were measured by means of the catcher technique [1] with Xe^{q+} ions (q = 10 , 15, 25) at different kinetic energies. Also, cluster emission was studied by a TOF technique [2]. Here, we present measurements of the secondary electron emission yields, which provide further information about the interaction of Xe^{q+} ions with UO_2. At normal and at oblique incidence, a strong increase of the secondary electron yield is observed with increasing charge state of the projectile. In addition, we note that at normal incidence, there is no variation of the electron yield with the projectile kinetic energy.

2. EXPERIMENT AND RESULTS

Differential current measurements were realized at normal incidence for Xe $^{10+,\ 15+,\ 25+}$ impinging a UO_2 surface at various kinetic energies (0.3 keV < E_k < 81 keV) and at oblique incidence the kinetic energy of Xe^{q+} was equal to 81 keV.
Although UO_2 is an insulator its relatively small resistivity (ρ= 1000 Ω.cm) allows the measurement of the intensity of electric charge current through the target. The current can be written as:

$$I_{Target} = I_{Beam} + I_{Sec\ e-} - I_{Sec\ I-} - I_{Sec\ I+} \quad (1)$$

As the secondary ion emission is very small [2, 3], the last two terms of eq (1) can be neglected. Then the secondary electron yield, i. e. the number of secondary electrons emitted from the surface per incident ion, Γ_e can be deduced from the current measured at the target.

$$\Gamma_e = q\,(I_{Target} - I_{Beam}) / \ I_{Beam} \quad (2)$$

The first set of results concern the interaction at normal incidence. As shown in Figure 1, Γ_e increases strongly with the charge state of the projectile but there is no dependence on the velocity of the projectile.

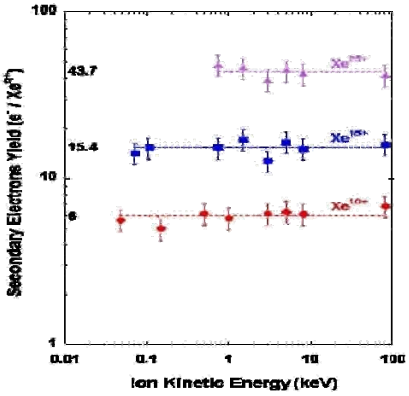

Figure 1: Projectile charge and velocity effect on the secondary electron yield et normal incidence

A second set of experiments concerns the measurement of Γ_e at oblique incidence. Finally, we will present a comparison between Γ_e and the total sputter yield Γ previously measured.
These results will be compared to Γ_e measurements obtained by Aumayr et al [4].

3. REFERENCES

[1] F. Haranger, B. Ban-d'Etat, Ph. Boduch, S. Bouffard,
H. Lebius, L. Maunoury and H. Rothard, Eur. Phys. J. D (2006) available on line.
[2] S. Boudjadar, F. Haranger, T. Jalowy, A. Robin, B. Ban d'Etat, T. Been, Ph. Boduch, H. Lebius, B. Manil, L. Maunoury, H. Rothard, Eur. Phys. J. D **32**, 19 (2005).
[3] T. Schenkel, A. V. Hamza, A. V. Barnes, D. H. Schneider, J. C. Banks, B. L. Doyle, Phys. Rev. Lett. **81**, 2590 (1998).
[4] F. Aumayr, "Electron emission from insulator surfaces by ions in extremely high charge states" http://www.ganil.fr/ciril/IRSIB/irsib.htm

* E-mail: bandetat@ganil.fr

CHANGING CARBON FILMS BY HIGHLY CHARGED IONS

S. Facsko[1,*], *T. Som*[2] , *and W. Möller*[1]

[1] Institute of Ion Beam Physics and Materials Research, Forschungszentrum Rossendorf e.V., Bautzner Landstr. 128, 01328 Dresden, Germany
[2] Institute of Physics, Sachivalaya Marg, Bhubaneswar 751 005, India

1. INTRODUCTION

Carbon films exist in a variety of modifications ranging from soft amorphous carbon film (a-C) to hard diamond-like carbon (DLC) films [1]. Due to their diverse properties carbon films are technologically important materials, especially for protective, biomedical, or field emission coatings. In addition, special forms such as fullerene-like films have attracted the scientific interest for their special structure. Many of the properties of the carbon films are intrinsically related to their nanostructure which in turn is strongly related to the existence of sp2 and sp3 hybridized phases.
The nanostructure of the carbon films depend strongly on the preparation conditions but are as well modified by the irradiation with ions. Irradiation with single charged heavy ions at high energy normally turns the films amorphous reducing the amount of sp3 and sp2 hybridized phases [2]. Here, we present systematic studies of irradiation of carbon films by highly charged argon and xenon ions with low kinetic energy.

2. EXPERIMENTS

2.1. Ion irradiation

Carbon films with different nanostructure have been prepared by magnetron sputter deposition and molecular beam epitaxy. The irradiation of the films is done at the Two Source Facility in Rossendorf. Argon ions with charge state from 1+ to 16+ and xenon ions with charge state up to 46+ are produced in an ECR ion source and in an Electron Beam Ion Source. The irradiation is done with kinetic energy ranging from a few keV to 200 eV. At low kinetic energy the interaction with the carbon films is supposed to be dominated by the potential energy of the ions.

2.2. Characterization

In order to fully characterize the interaction of the HCIs with the carbon films the irradiated target as well as the sputtered material which is caught on a Si surface is analyzed by means of micro-Raman spectroscopy, Rutherford Backscattering Spectroscopy, and Atomic Force Microscopy. The Raman spectroscopy allows not directly the determination of sp2/sp3 ratio but gives information about the medium-range sp2 ordering [3]. Raman spectroscopy of the irradiated film shows the disorder induced by the irradiation. In the case of the sputtered material it reveals the sputtering of carbon clusters with still intact sp2 phases. In addition, Transmission Electron Microscopy of the sputtered carbon caught on a TEM grid supports this finding. Figure 1 shows a large scale TEM image of carbon clusters sputtered with Ar^{8+}. The inset in Fig. 1 shows graphitic sheets which survived the sputtering process with 400 eV Ar^{8+}. Mechanisms induced by the potential energy in the carbon films are proposed.

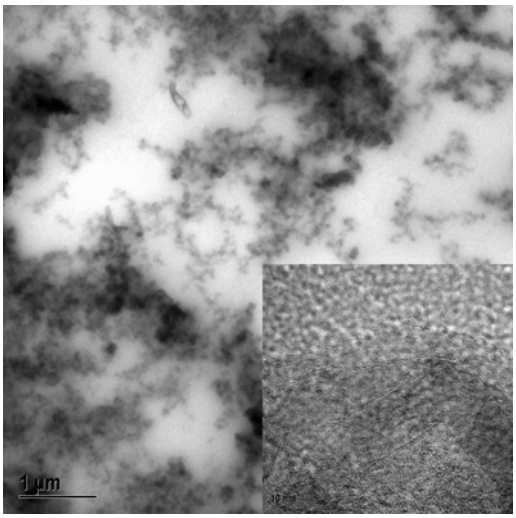

Figure 1: Transmission Electron Microscope Image of carbon clusters sputtered from fullerene films irradiated with 400 eV Ar^{8+}. The inset shows graphitic sheets which survived the sputtering process.

3. REFERENCES

[1] D.R. McKenzie, Rep. Prog. Phys. **59**, 1611 (1996).
[2] R. Kalish et al., Phys. Rev. B. 48, 18235 (1993).
[3] G. Abrasonis, R. Gago, M. Vinnichenko, U. Kreissig, A. Kolitsch, and W. Möller, Phys. Rev. B **73**, 125427 (2006).

* E-mail: S.Facsko@fz-rossendorf.de

PRODUCTION OF HIGHLY CHARGED IONS FOR ION-SURFACE INTERACTION STUDIES

G.Zschornack[1,*], *F.Grossmann*[2], *R.Heller*[3], *U.Kentsch*[2], *M.Kreller*[1], *S.Landgraf*[1], *V.P.Ovsyannikov*[2], *M.Schmidt*[2], *and F.Ullmann*[2]

[1] Technische Universität Dresden, Institute of Applied Physics, Mommsenstr. 13, 01062 Dresden, Germany
[2] Leybold Vacuum Dresden GmbH, Zur Wetterwarte 50, 01109 Dresden, Germany
[3] Forschungszentrum Rossendorf, Institute of Ion Beam Physics and Materials Research, PF 510119, 01314 Dresden, Germany

Highly charged ions are promising tools to modify surfaces and can be applied effectively in surface analysis techniques. For applications in surface reaction studies the most common ways to produce highly charged ions are accelerator based production techniques and ion sources, such as micro-wave heated ECR plasma sources and electron-impact ion sources, i.e. EBIT and EBIS. In the present work we give an overview about the production of highly charged ions in different generations of compact room-temperature EBIT which have been developed for different areas of application in the past years [1,2,3].

With the Dresden EBIT [1] and Dresden EBIS / EBIS-A [2] (see Fig. 1) ion sources are available able to produce beams of highly charged ions in pulsed regimes in the order of up to μA per pulse at pulse lengths of some μs. The ion output in DC mode (continuous) reaches up to tens of pA. For instance, with the Dresden EBIT argon beams of about $1*10^6$ Ar^{16+} ions per second can be extracted. Typical ion charge states range from bare nuclei of light elements ($Z \leq 28$) to helium-like ions of higher Z-elements and up to neon-like ions for heavy elements. Some typical charge state spectra of ions extracted from the Dresden EBIT are shown.

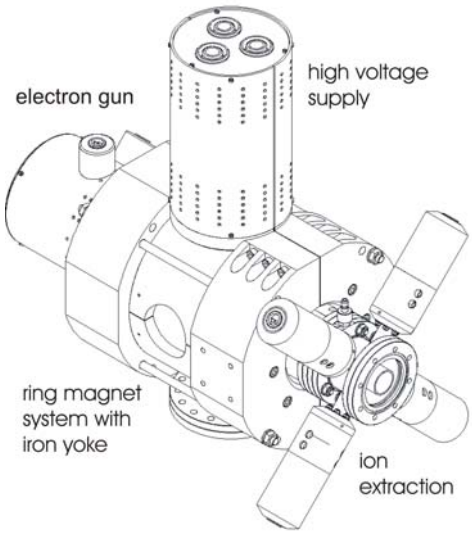

Figure 1: 3D drawing of the Dresden EBIS-A.

Highly charged ions have unique features. For instance, the potential energy stored during the ionization process can achieve 100 keV or more for an individual ion. This in connection with the small spatial extend of such an ion allows nanometer-scale structures generated at the interaction process of slow highly charged ions with solid surfaces. We report on a corresponding experiment with argon ions on HOPG surfaces. The interaction produced nano-patterns, which were analyzed with a scanning tunnelling microscope (STM).

For surface analysis techniques highly charged ions show properties which favour them for certain applications in comparison to low charged classical ions. The high yield of secondary ions [4] and molecule ions produced by highly charged ions during the interaction process with surfaces is an excellent prerequisite for time-of-flight analyse techniques, for instance. The production of noble gas beams ("non-toxic" particles) with a wide variety of charge states is a further distinctive feature of the Dresden EBIS/T, which is interesting for applications in surface analysis or FIB devices. Furthermore, the Dresden EBIS/T is also a stable source for beams of low charged molecule fragments.

The work is supported by the EFRE fund of the EU and by the Freistaat Sachsen (projects 8945/1450 and 8946/1450), respectively.

REFERENCES

[1] V.P.Ovsyannikov and G.Zschornack, Review of Scientific Instruments **70**, 2646 (1999).
[2] G.Zschornack, R.Heller, M.Kreller, S.Landgraf, F.Grossmann, U.Kentsch, V.P.Ovsyannikov, M.Schmidt and F.Ullmann, Review of Scientific Instruments **77**, 1 (2006).
[3] http://www.dresden-ebit.de.
[4] G.Hayderer, S.Cernusa, V.Hoffmann, D.Niemann, N.Stolterfoht, M.Schmid, P.Varga, HP.Winter and F.Aumayr, Nuclear Instruments and Methods **B182**, 143 (2001)

* E-mail: g.zschornack@fz-rossendorf.de

DYNAMICS OF SPUTTERING BY HIGHLY CHARGED HEAVY IONS INVESTIGATED BY THE XY-TOF TECHNIQUE

J. Lenoir, P. Boduch, H. Rothard, B.Ban d'Etat, A. Cassimi, H. Lebius, B. Manil*

Centre Interdisciplinaire de Recherche Ions Laser CIRIL,
UMR 6637 (CEA, CNRS, ENSICAEN, Université de Caen), BP 5133,
Boulevard Henri Becquerel, F-14070 Caen Cedex 05, France

1. INTRODUCTION

The combination of imaging techniques (XY) and time-of-flight (TOF) spectroscopy was applied to sputtering of secondary ions from solid surfaces with LiF and UO_2. Ion-surface collisions in two different velocity regimes were investigated: high velocity (e.g Ca^{17+}, 9 MeV/u), where the electronic energy loss is dominant, and low velocity (Xe^{21+}, 350 keV). In the latter case, nuclear stopping is most important. Possibly, further effects related to the high projectile charge (high potential energy leading to potential sputtering) can occur. In order to study whether the physics of energy deposition is different in these two energy regimes, we determined the energy and angular distributions for the secondary sputtered ions.

2. RESULTS

As an example, we show in fig. 1 the energy distribution of Li^+ at low and high projectile velocity. Clearly, it can be seen that the two energy distributions are rather different thus showing that the physical processes are different in these two cases.
With the XY-TOF technique, we are now able to extract the following information:

- energy distributions (see fig. 1)
- angular distributions (which can be compared to angular distributions of neutral ejecta)
- a comparison of energy and angular distributions for monoatomic ions versus ejected cluster ions [e.g. Li^+ vs. $(LiF)_nLi^+$: fig. 2]
- correlated detection of two or more ions.

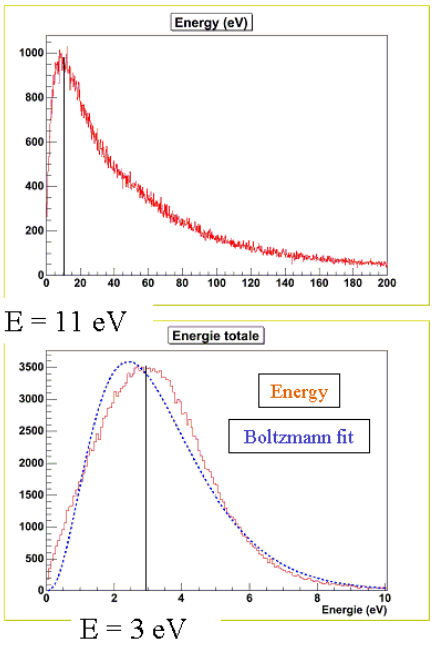

Figure 1: Energy distributions of $^7Li^+$ for low [350 keV (top)] and high [9 MeV/u (bottom)] projectile velocity.

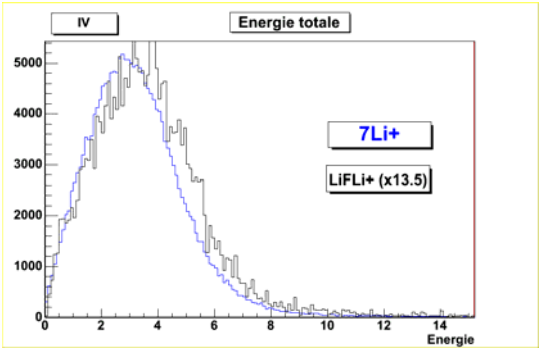

Figure 2: Energy distribution of Li^+ and $LiFLi^+$ induced by Ca^{17+} (9 MeV/u)

* E-mail: lenoir@ganil.fr

EFFECT OF RESIDUAL OXYGEN IN SI(111)-7×7 SURFACE ON SI^+ AND SI^{2+} SPUTTER YIELDS

Y. Sakuma[*], *N. Shinde, M. Kato, S. Yagi and K. Soda*

Department of Quantum Engineering, Nagoya University, Furo-cho, Chikusa-ku, Nagoya 464-8603, Japan

1. INTRODUCTION

Secondary ion mass spectroscopy (SIMS) is one of the powerful techniques for surface-composition analysis, although the charge states of sputtered particles strongly depend on the condition of the surface and its ambient. It is well known that the secondary positive ion yields from oxidized surfaces are considerably enhanced in comparison to those from clean surfaces. However, the impurity (oxygen) effect on the sputter yield as well as the involved physical processes is still unclear.

For example, a study on the formation of Si^{2+} ions sputtered from a clean Si(111) surface reported an anomalously large Si^{2+} yield [1]. It is considered that this Si^{2+} ion is created by intra-atomic Auger transition after the production of an inner-shell hole, mainly Si 2p hole, via energetic atomic collisions inside a cascade. However, the effect of residual oxygen impurity on the Si^{2+} ion yield has not yet been systematically studied.

In the present study, we have investigated the sputter yields of Si^{2+} and Si^+ ions from a 'clean' Si(111)-7×7 surface bombarded with a pulsed Ar^0 beam and the effect of residual oxygen impurity on the secondary ion yields.

2. EXPERIMENT

Specimens of Si were cut from a n-type, 3 Ω-cm Si(111) wafer. The SiO_X layers on the sample surface was removed by using several repetitive cycles of 7 keV Ar^0 sputtering and annealing at ~1100 K, thus controlling the concentration of oxygen impurity in the near surface region. Before the measurements of the sputter yields, the 'cleanness' of Si(111) surface was evaluated by low-energy electron diffraction (LEED) observation and Auger electron spectroscopy (AES). Observed LEED images showed a clear 7×7 reconstruction pattern of Si(111) and all impurities, viz, C and O were below the AES detection limit of 0.01ML. The well characterized and clean Si(111)-7×7 surface was irradiated by 11keV Ar^0 at an angle of 45° and the secondary ions ejected to the surface normal direction were detected by a time-of-flight (TOF) technique.

3. RESULTS AND DISCUSSION

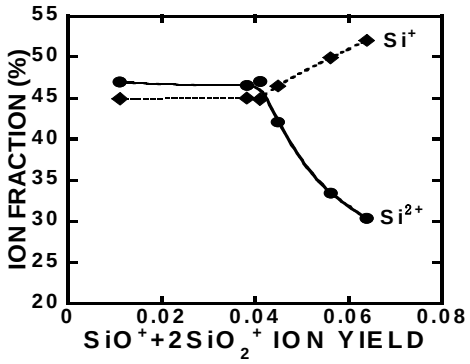

Fig.1: Ion fractions vs. the amount of residual O.

Fig.1 shows the fraction of Si^{2+} and Si^+ ions yields vs. the amount of residual O impurity. As mentioned already the AES measurements could not detect any O impurity. Hence, by assuming that the yield of secondary oxidized ion species is proportional to the amount of O impurity, we regard a sum of the SiO^+ yield and twice the SiO_2^+ yield as the relative impurity level of O. Even at the low concentration of O impurity, the Si^+ and Si^{2+} yields are significantly sensitive to the residual O impurity. As seen from fig.1, the Si^+ yield is enhanced and the Si^{2+} yield is reduced, with increasing O impurity. The enhancement of Si^+ yield could be ascribed to the fact that O has the large electron affinity in comparison to that of Si [2], and the decrease in the Si^{2+} yield can be explained on the basis of the inter-atomic Auger transition between O and a precursor Si^+* forming Si^{2+} (Si^+ having a 2p-hole), which efficiently interferes the production process of Si^{2+}.

4. REFERENCES

[1] N. Shinde, K. Morita, S.D. Dhole, D. Ishikawa, Nucl. Inst. Meth. in Phys. Res. B, **182** (2001) 135.
[2] G. Blaise, A. Nourtier, Surf. Sci. **90** (1979) 495

[*] E-mail: h056403d@mbox.nagoya-u.ac.jp

FRAGMENTATION OF C_{60} IONS DURING GRAZING SCATTERING FROM AN Al(100) SURFACE

S. Wethekam[*], *A. Schüller, and H. Winter*

Institut für Physik der Humboldt-Universität zu Berlin, Newtonstr. 15, D-12489 Berlin, Germany

C_{60}^{+} and C_{60}^{2+} ions with energies ranging from 1 to 80 keV are scattered under grazing angles of incidence of typically 1° from a clean and atomically flat Al(100) surface. Scattering proceeds in the regime of surface channeling with well defined trajectories and negligible nuclear energy losses. By means of a position sensitive micro-channelplate detector and biased electric field plates, cluster fragments, angular distributions, and charge states of scattered projectiles are recorded. Based on the experimental information, fragmentation, elasticity, distances of resonant charge transfer, and angular guiding along low index directions of C_{60} are studied. The results are compared with computer simulations.

Under our scattering conditions only fragments with even numbers of C atoms are observed which result from sequential evaporation of C_2 clusters from the vibrationally excited clusters. The fragmentation turns out to be independent of the energy of motion parallel to the surface and C_{60} clusters with energies of up to several 10 keV can survive the scattering event with the surface. For low energies of the motion normal to the surface of a few eV the projectiles are scattered elastically without fragmentation whereas for larger normal energies subspecular reflection and an efficient transfer of normal energy to vibrational excitations of the cluster is found in accord with our computer simulations. This coincides with the onset of fragmentation due to an increase of internal energy of the cluster.

Measurements of angular distributions for scattered C_{60}^{+} and C_{60}^{2+} projectiles reveal differences in the outgoing normal energy of about 1 eV. Making use of the approximation of the classical image potential, distances of charge transfer are deduced.

The angular distributions of C_{60} clusters scattered with azimuthal angles close to a low index direction show an azimuthal shift toward the low indexed direction. This finding can be understood from trajectory calculations which reveal that scattering from low index chains introduces a rotation of the cluster with angular momentum parallel to the chains. This reduces the energy of motion normal to the chains and leads to a guiding effect of clusters along low indexed directions.

[*] E-mail: stephan.wethekam@physik.hu-berlin.de

THE DYNAMICS OF He^+ ION NEUTRALIZATION AT RARE GAS FILMS: ENERGY- AND SPIN-RESOLVED STUDIES[†]

*F. J. Kontur, J. C. Lancaster, and F. B. Dunning**

Department of Physics and Astronomy, Rice University MS 61, 6100 Main St., Houston, TX 77005

The processes responsible for He^+ ion neutralization at rare gas films are being investigated over the ion energy range 10-500 eV by both measuring the number and energy distribution of ejected secondary electrons and by using spin labeling techniques in which the polarization of electrons ejected by incident electron-spin-polarized He^+ ions is determined.

In the present work polarized He^+ ions extracted from an optically-pumped rf-excited helium discharge are formed into a beam and directed onto the target surface at an angle of incidence of ~45˚. The number and energy distribution of the ejected electrons is measured using a retarding-potential analyzer. Their average polarization is determined using a Mott polarimeter. The target surfaces are grown on a clean Au(100) substrate that is cooled to ~25 K and exposed to the selected rare gas at pressures of $\sim 10^{-7}$-10^{-6} torr. Assuming a sticking coefficient of one, an exposure of 10^{-6} torr s, *i.e.*, 1 Langmuir (L), will result in the deposition of ~0.2 to 0.25 of a monolayer.

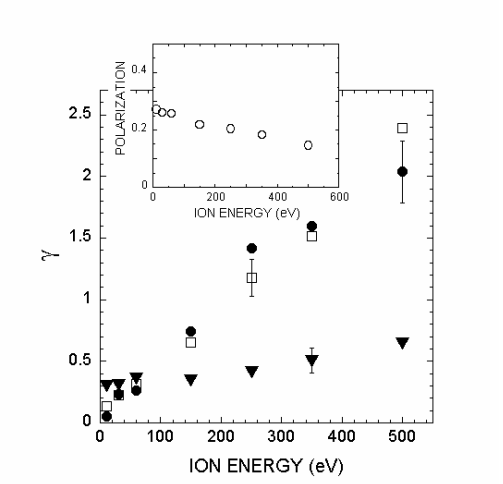

Figure 1. Ion energy dependence of the secondary electron ejection coefficient γ for He^+ ions incident on (▼) xenon, (□) krypton , and (●) argon films with estimated surface coverages of 4, 5, and 8 monolayers, respectively. Inset: ejected electron polarization for a xenon surface coverage of ~2 monolayers.

The ion energy dependence of the secondary electron ejection coefficient γ, *i.e.*, the number of electrons ejected per incident ion, is shown in Fig. 1 for a variety of rare gas films. The data are normalized by comparing the ejected electron signals with that from the clean Au(100) substrate for which γ (~0.15) is known. In each case the electron yield increases with ion energy pointing to a growing contribution from kinetic ejection.

For xenon, the inferred values of γ are sizable even at low ion energies. The corresponding ejected electron polarizations are shown in the inset, normalized to the polarization of the incident ions. At low ion energies, a strong spin correlation is evident. The electron polarization, ~0.3, is similar to that seen at a variety of clean metal surfaces and is consistent with that expected if neutralization proceeds by Auger neutralization. Earlier photoemission studies of xenon films have shown that the outermost valence electrons are delocalized, the width of the resulting band being ~3 eV with its top lying ~10 eV below the vacuum level. The increase in electron yield relative to Au(100) can be attributed to more efficient backscattering of Auger electrons that are initially produced traveling into the surface. The decrease in polarization observed at the higher ion energies is consistent with an increasing contribution from unpolarized electrons associated with kinetic ejection.

Somewhat different behavior is observed for krypton and argon films. The electron yield at low ion energies is very small. This is not unexpected as Auger neutralization is essentially energetically forbidden at both surfaces. In consequence, incident ions can penetrate the film without neutralization where they suffer strong inelastic scattering which leads to creation of electron-hole pairs and secondary electron emission. Such inelastic scattering can account for the large increases in electron yield seen at the higher ion energies. At high energies, the yields are substantially larger than those seen at xenon films. For xenon, however, incident ions are efficiently neutralized at the surface and penetrate the film as neutrals which do not excite electron-hole pairs as strongly.

[†]Research supported by the US DoE and by the Robert A. Welch Foundation

* E-mail: fbd@rice.edu

COMPARATIVE STUDY OF POLYATOMIC SECONDARY ION EMISSION FROM SILICON WITH Au_m^-, Si_m^- AND C_m^- PROJECTILES

*S. Morozov, U. Rasulev**

Arifov Institute of Electronics, 700125 Tashkent, Uzbekistan

Great perspectives of using cluster ion bombardment in SIMS stimulate search for optimal species of cluster projectiles. More significant enhancement of secondary emission of molecular ions was obtained with the Au_m, Bi_m and C_{60} ions. The most important field of SIMS application remains depth profiling of semiconductors, particularly silicon. It is evident that in this case Si_m cluster ions may be more preferable as projectiles because the process will not be accompanied by impurity atoms implantation capable of distorting the analysis results. Moreover, in the self-sputtering mode the efficiency of sputtering of upper layer is maximal, which is important for ultra-shallow depth profiling.

Besides, there is no clear understanding of the physical nature of the molecular bombardment. Therefore, further fundamental studies in this field are required. The overwhelming majority of studies was carried out with cluster projectiles containing atoms of heavy elements. At present, practically there is no experimental data for comparative studies of non-additivity of secondary emission under bombardment by cluster ions containing atoms of light and heavy elements under identical conditions of experiment and within a wide energy range.

Therefore, the comparative studies of the effect of mass and energy of primary cluster ions are important to understand a mechanism of secondary ion emission under cluster bombardment, define more precisely the range of non-linear collision cascades and to reveal new physical phenomena connected with those cascades.

In the present work the comparative studies of the emission of cluster Si_n^+ ions (n=1–11) and polyatomic Si_nX^+ ions (X is B, C, N) under bombardment of single crystalline silicon (containing impurities) by cluster ions of Au_m^- (m = 1–9), Si_m^- (m =1–6) and C_m^- (m=1–11) with energy E_0 = 4–18 keV have been carried out.

Significant non-additive enhancement of the yield of Si_n^+ cluster ions and most polyatomic ones has been observed with an increase in the number of atoms in the cluster projectiles. In spite of the fact that the yield of secondary cluster ions under C_m^- and Si_m^- bombardment was less than that under Au_m^- bombardment, the nonadditivity factors were approximately the same values for all projectiles with the same number of atoms – m.

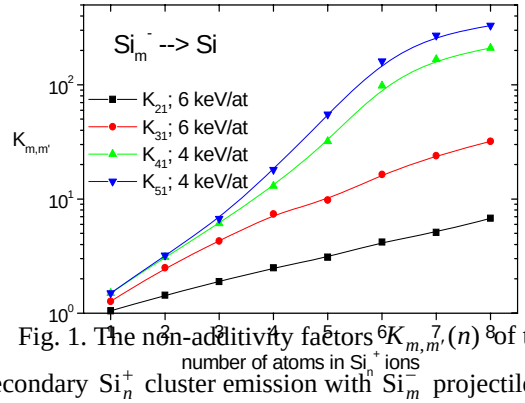

Fig. 1. The non-additivity factors $K_{m,m'}(n)$ of the secondary Si_n^+ cluster emission with Si_m^- projectiles.

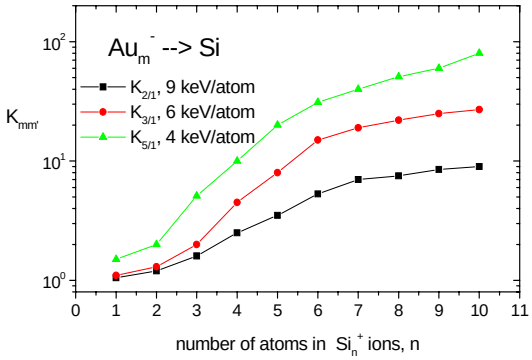

Fig. 2. The non-additivity factors $K_{m,m'}(n)$ of the secondary Si_n^+ cluster emission with Au_m^- projectiles

Sharp increase in the yield of Si_3B^+, Si_3C^+, Si_2N^+ ions by 100 – 1000 times has been observed when both Si_m^- and Au_m^- projectiles with m = 5 – 9 instead of atomic ones were used. These results confirm the advantages of analysis by the cluster-SIMS-cluster mode.

The high values of the non-additivity factors $K_{m,m'}(n)$ and their increase with decrease in energy within the keV range of kinetic energy of primary ions and the weak dependence of non-additivity on mass of the atoms in cluster projectiles are unexpectedly from the point of view of the traditional concepts about sputtering from dense non-linear cascades.

* E-mail: rasulev@ariel.uzsci.net

SPUTTERING SOURCE OF CLUSTER IONS AND SURFACE-IONIZATION SOURCE OF POLYATOMIC IONS OF ORGANIC COMPOUNDS

U. Rasulev[*], *S. Morozov,U. Khasanov and D. Usmanov*

Arifov Institute of Electronics, Tashkent, Uzbekistan

In recent time a great interest in sources of polyatomic ions is caused by possibilities of practical application of polyatomic ion beams [1]; for example for Secondary Ion Mass Spectrometry (SIMS) or ion modification of materials, as well as for revealing the fundamental aspects of non-linear non-additive effects of the secondary processes of polyatomic ion interaction with solid surface. The atoms of a polyatomic ion are incident practically simultaneously (~ 10^{-14} s) onto a small area (~ nanometer) of the solid surface thus simulating interaction of atomic beams of super-high density with surface practically inaccessible with beams of atomic ions. It is important that each atom of the molecular ion interacts with an area of the surface already excited or being excited by other atoms of the same polyatomic ion. Therefore, the density of energy released by the molecular ion containing *m* atoms and yields of the secondary processes (e.g., sputtering, secondary ion emission etc.) can be much greater than those caused by *m* separate atoms with the same velocity as that of the molecular ion. Now the various methods of ionization from liquid-metallic and sputtering ones to a classical method of electron ionization are used to produce cluster and molecular ions. More perspective for applying as primary ions for SIMS of materials of micro- and nano-electronics are considered the cluster ions of Au_m^- and Bi_m^+ and for SIMS of organic and bioorganic materials also the fullerene ions C_{60}^+ and polyatomic ions of large organic molecules [1].

The results of development of sputtering sources of cluster ions of Au_m^-, Si_m^-, $Si_mO_{2m+1}^-$ and C_m^- and surface-ionization sources of polyatomic ions of organic nitrogen bases are presented in the report.

A sputtering source of cluster ions consists of a surface-ionization source of the Cs^+ ions which beam (~ 1 μA) with energy 4.5 keV at an angle 45° bombards a target under sputtering. Produced as a result of target sputtering, the negative cluster ions are formed and separated in a sector magnetic field and further the preset species of cluster ions are focused onto a target under sputtering. The values of cluster and molecular ion currents (nA) obtained after separation in the sector magnetic field are presented in Table. The cluster Si_m ions may be more preferable as projectiles because the process will not be accompanied by impurity atom implantation capable of distorting the analysis results. Moreover, in the self-sputtering mode the efficiency of sputtering of the upper layer is maximal. One can suppose that the presence of electronegative atoms of oxygen in the $Si_mO_{2m+1}^-$ ions ought to lead to additional increase in secondary ion emission.

Table. Cluster and molecular ion currents (nA).

Ion \ m	1	2	3	4	5	6	7	8	9
Au_m^-	3.9	0.91	1.6	-	0.2	-	0.08	-	0.04
Si_m^-	4.2	5.8	1.5	0.4	0.16	0.08			
$Si_mO_{2m+1}^-$	0.7	0.05	0.04	0.02	0.04				
C_m^-	15.5	54.5	-	10	-	2.3	-	0.7	

The report also consider possibilities of a simply designed effective surface-ionization (SI) source of polyatomic ions of organic compounds [2], its advantages, particularly possibilities of focusing the SI ions having the Boltzman distribution in energy corresponding to SI ionizator temperature into a micro-probe. The operation modes of the SI ion source are also presented allowing producing with no separation the effective beams of polyatomic ions of a practically similar composition. For example, the surface ionization of papaverine produces the $C_{20}H_{21}N^+O_4$ and $C_{20}H_{20}N^+O_4$ ions, that of carbamazepine $C_{14}H_{10}N^+$ only and SI of drotaverine the $C_{24}H_{30}N^+O_4$ and $C_{24}H_{28}N^+O_4$ ions. According to an operation mode of the source, the current density of these ions can be from 10^{-10} to 10^{-7} A/cm^2; duration of stable emission can reach tens of hours.

REFERENCES

[1] Proceedings of XIV International Conference on SIMS and Related Topics, San Diego, California, VS1, 2003, Editors A. Benninghoven, J.L. Hunter Jr., B.W. Schueler, H.E. Smith, H.W. Werner. Appl. Surf. Sci. **231-232** (2004).

[2] U. Kh. Rasulev and E. Ya. Zandberg. Surface Ionization of Organic Compounds and Its Applications. Prog. Surf. Sci. **28**, 182-412 (1988).

[*] E-mail: Rasulev@ariel.uzsci.net

ASPHALTENE INTERACTION WITH METALLIC SURFACES

W. Abdallah[*] *and S. Taylor*

Schlumberger Reservoir Fluid Centre
9450–17 Ave. Edmonton, Alberta, Canada T6N 1M9

1. INTRODUCTION

In the production of conventional and heavy oil reservoir fluids, changes in temperature, pressure, and/or composition can lead to formation and deposition of undesirable organic and inorganic solids. The least understood of these solids is asphaltenes, a black solid material that may be precipitated from oil or bitumen by pressure depletion or addition of paraffinic solvents.

Asphaltene formation and deposition may result in reduced reservoir productivity because of restricted or plugged flow lines, fouling of production facilities, and damage to the reservoir. The precipitation and deposition of asphaltenes from reservoir fluids is one of the more challenging issues facing oil producers because there is a relatively poor understanding of asphaltenes. Asphaltenes are commonly defined as a solubility class material, a blend of complex molecules that are known to have H/C ratios of 1.15 ± 0.05 with variations proportional to the hetero-elements contents (O, S, N) and metals (iron, nickel, and vanadium); typical molecular weight is about 2000 ± 500.

Current research has led to limited descriptions of asphaltene precipitation models. However, there is a tremendous lack of knowledge about how asphaltene molecules interact and deposit on surfaces, owing to asphaltene molecular structure complexity. The objective of this research is to investigate the interactions of asphaltene molecules with metallic surfaces and to identify the active site that could be responsible for its adsorption.

2. EXPERIMENTAL

Axis 165 X-ray photoelectron spectrometer (XPS) and X-ray imaging are used for surface characterization. Currently, energy survey spectra (0–1,200 eV) are used to estimate surface composition, while high-resolution spectra (within 10–20 eV) provide information about the chemical bonds. The XPS instrument is equipped with an ion source for surface sputtering, which allows for depth profile analysis. Depth profile data is coupled with our adsorption procedures to establish a minimum adsorbed film of asphaltene. Once surface preparation is accomplished, XPS spectra with elemental mapping on the surface will provide us with surface composition, oxidation states, and the lateral distribution of the corresponding elements on the surface. Furthermore, a high-resolution electron energy spectroscopy is utilized to determine the vibrational frequencies of asphaltene film. The elastic peak showed excellent resolution coming off the surface and now is tuned to collect energy losses for the inelastic peaks once surface preparation is accomplished.

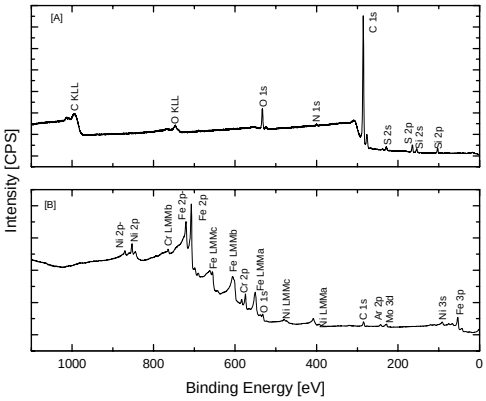

Figure 1: XPS survey of asphaltene stainless steel surface, [A] before sputtering, [B] after sputtering.

3. PRELIMINARY RESULTS

Preliminary survey spectra for adsorbed asphaltene film on a stainless steel surface were obtained for different film thickness before and after surface sputtering. The spectrum before sputtering clearly did not show any metal elements, which indicates complete surface coverage, while after sputtering surface metal elements started to appear. Further, depth profiling were collected for C 1s, O 1s, N 1s, S 2p, Ni 2p, Fe 2p, Cr 2p to monitor the elemental concentration profile through the film and to relate sputtering rate with asphaltene film on the surfaces. Figure 1 shows the survey spectrum of the same surface before and after sputtering.

[*] E-mail: wabdallah@slb.com

SIMS DEPTH PROFILE STUDY USING METAL CLUSTER COMPLEX ION BOMBARDMENT

M. Tomita[1,*], *T. Kinno*[1], *M. Koike*[1], *H. Tanaka*[1], *S. Takeno*[1], *Y. Fujiwara*[2], *K. Kondou*[2], *Y. Teranishi*[2], *H. Nonaka*[2], *T. Fujimoto*[2], *A. Kurokawa*[2], *and S. Ichimura*[2]

[1] Corporate Research & Development Center, Toshiba Corporation, 8 Shinsugita-cho, Isogo-ku, Yokohama 235-8522, Japan

[2] National Institute of Advanced Industrial Science and Technology (AIST), Tsukuba Central 2, 1-1-1 Umezono, Tsukuba-shi, Ibaraki-ken 305-8568, Japan

1. INTRODUCTION

Ion-beam sputtering analysis, including secondary ion mass spectrometry (SIMS), has been utilized for depth profiling of chemical composition and impurity in thin films and shallow junctions in silicon devices. Scaling down of silicon device dimensions calls for thinner films and shallower junctions and it is difficult to analyze these depth profiles accurately using conventional ion beams (O_2^+, Cs^+, Ar^+ etc.), because of degradation of depth resolution caused by atomic mixing. One of the solutions to improve the depth resolution is cluster ion bombardment [1]. Since the energy of the constituent atoms of a cluster ion that includes many atoms is low, the use of cluster ions is expected to reduce atomic mixing. In order to analyze such silicon devices, we have developed a prototype cluster ion source using the metal cluster complex of $Ir_4(CO)_{12}$ [2]. The ion source emits uniform-size cluster ion beam of $Ir_4(CO)_7^+$ (molecular weight: 964.9), which has 18 atoms including heavy atoms of iridium. SIMS analyses of delta-doped sample were carried out using the cluster ion, and the depth profiles that depend on primary ion conditions were investigated.

2. RESULTS and DISCUSSIONS

SIMS measurements were carried out with Atomika 4000 SIMS instrument equipped with the cluster ion and oxygen ion (O_2^+) sources. For the purpose of evaluating depth resolution and sputtering rate variation during SIMS analyses, boron multi-delta-doped sample (four B delta-layers with 20-nm intervals followed by four delta-layers with 5-nm intervals were deposited on silicon (100) substrate) was measured [3]. Figure 1 indicates SIMS depth profiles of the delta-doped silicon sample measured by the cluster ion and oxygen ion with the energies of 10 keV, the incident angle of 45 degrees and oxygen flooding. Obviously depth resolution by the cluster ion bombardment (depth resolution defined by 1/e decay length: 2.2 nm) is better than that by oxygen ion (4.9 nm). The improvement of depth resolutions may be caused by suppression of atomic mixing. Although the good depth resolution is obtained by the cluster ion bombardment, strange sputtering rate variation appears in the near surface region (5-nm intervals of the delta-layers increased once, and decreased). This phenomenon may be attributable to different implantation-range of the constituent atoms of the cluster ions (C, O and Ir). In this presentation, we will discuss the cluster-ion SIMS profiles that indicate strange transient region, and depth resolution that depends on the primary ion conditions.

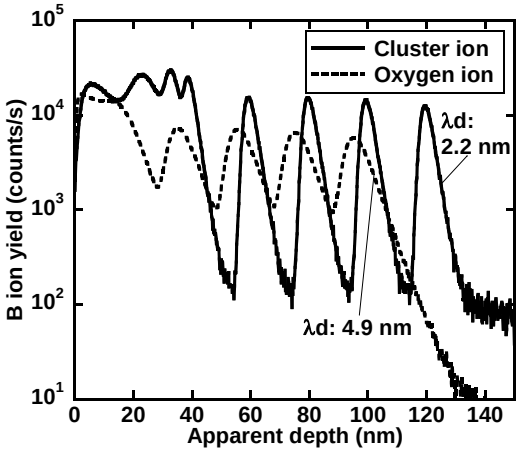

Figure 1: SIMS depth profiles of the boron delta-doped sample measured by the cluster ion and oxygen ion with the energies of 10 keV, the incident angle of 45 degrees and oxygen flooding. Depth scales were adjusted using the distance of the known 20-nm interval of deep delta-layers.

3. REFERENCES

[1] G. Gillen, M. Walker, P. Thompson, and J. Bennett, J. Vac. Sci. Technol. **B18**, 503 (2000).

[2] Y. Fujiwara, K. Kondou, Y. Teranishi, H. Nonaka, T. Fujimoto, A. Kurokawa, S. Ichimura, and M. Tomita, submitted to J. Appl. Phys.

[3] M. Tomita, C. Hongo, M. Suzuki, and M. Takenaka, J.Vac. Sci. Technol. **B22**, 317 (2004).

* E-mail: mitsuhiro.tomita@toshiba.co.jp

ON THE FORMATION MECHANISM OF MCs_2^+ MOLECULAR IONS UNDER VARYING OXYGEN ENVIRONMENT

B. Saha[*] *and P. Chakraborty*

Surface Physics Division, Saha Institute of Nuclear Physics, 1/AF, Bidhannagar, Kolkata 700 064, India.

ABSTARCT

Secondary emission of MCs_n^+ molecular ions under Cs^+ bombardment has shown its low sensitivity to matrix effect and applicability to quantification in secondary ion mass spectrometry (SIMS). Potential of the MCs^+ molecule is realized by assuming that it is formed via a recombination of neutral M^0 atom with Cs^+ ion in the near-surface region [1]. In case of electronegative elements, detection of MCs_2^+ molecules has been reported to offer even better sensitivity. As these molecular ions can form via different routes depending on the nature of the element M, the formation mechanism is a complex one. Although there are few proposed mechanisms, a universal formation mechanism is yet to be ascertained.

Two proposed combination processes for MCs_2^+ are [2]:

$$M^0 + Cs_2^+ \rightarrow MCs_2^+ \quad (1)$$

$$MCs^0 + Cs^+ \rightarrow MCs_2^+ \quad (2)$$

In the present work we have done a systematic study of MCs_2^+ molecular ions emitted from pure silver under varying oxygen environments. Silver was chosen for its fairly high atomic polarizability that plays an important role in MCs_n^+ molecular ion formation. Kinetic energy distributions of Cs^+, Cs_2^+, $AgCs^+$ and $AgCs_2^+$ were measured for different oxygen pressures. The changes in instantaneous local surface work function, measured from the changing slopes of the energy distributions [3] of the above species, strengthened the existing believe that an MCs^+ molecular ion is formed via recombination of a neutral M^0 atom with a Cs^+ ion. A phenomenological approach based on the analysis of mean emission energies, estimated from the energy distributions, favors that the formation of an MCs_2^+ molecular ion via recombination of a neutral MCs^0 molecule and a Cs^+ ion (process 2) is more probable in the present situation.

REFERENCES

[1] S. Sarkar, P. Chakraborty and H. Gnaser, Phys. Rev. B **70**, 195427 (2004).

[2] Y. Marie, Y. Gao, F. Saldi and H.N. Migeon, Surf. Interface Anal., **23**, 38 (1995).

[3] S. Sarkar and P. Chakraborty, Nucl. Instrum. Meth. **232**, 153 (2005).

[*] E-mail: biswajit.saha@saha.ac.in

INTERACTIONS OF LIQUID CLUSTER ION BEAMS WITH METAL SURFACES

*G. H. Takaoka**, M. Kawashita, K. Nakayama and T. Okada,*

Ion Beam Engineering Experimental Laboratory, Kyoto University,
Nishikyo, Kyoto 615-8510, Japan

1. INTRODUCTION

The physical and chemical properties of clusters, which consists of a few tens to several thousands atoms, are not the same as those of bulk state matter. Clusters represent a new phase of matter, and they have attracted much interest.[1,2] Furthermore, cluster ion beams are useful tools for the investigation of the fundamentals of solid-state physics, chemistry and related materials science. The impact of accelerated cluster ion beams on the solid surfaces exhibits unique characteristics such as multiple collision and low-energy irradiation effect, which are not obtained by monomer ion beams. [3,4] We have developed a liquid cluster ion beam system, [5,6] in which cluster ions of ethanol and water can be produced by an adiabatic expansion phenomenon. In this article, sputtering effects of the ethanol and water cluster ions on metal surfaces are investigated in order to clarify various applications of the liquid cluster ion beam process. Furthermore, the surface state after sputtering is discussed based on atomic force microscope (AFM) and contact angle measurements.

2. RESULTS

The cluster size was measured by a time-of-flight (TOF) method. The cluster size was calculated based on the drift time ranging from micro- to milliseconds, which was different depending on the cluster size. The liquid cluster ions such as ethanol and water cluster ions were produced at the vapor pressures larger than 1 atm, and the intensity of the cluster ions increased with increase of the vapor pressures. The peak size was about 500 to 1000 molecules-per-cluster for the ethanol cluster ions and about 2500 molecules-per-cluster for the water cluster ions, respectively.

In order to investigate the interactions of liquid cluster ion beams with metal surfaces, titanium (Ti) substrates were irradiated at different acceleration voltages. The ion dose was kept at 1.0×10^{16} ions/cm^2. The sputtered depth increased with increase of the acceleration voltage. The sputtering yield of Ti at an acceleration voltage of 9 kV for the ethanol cluster ions was approximately 100 times larger than that by argon (Ar) ion beams. This is ascribed to the enhancement of the chemical sputtering by the ethanol cluster ion beams. On the other hand, for the case of the water cluster ion irradiation, the sputtering yield was a few tens times larger than that for Ar monomer ion irradiation. This is due to the physical sputtering by the water cluster ion beams. In addition, the AFM observation showed that the sputtered surfaces by the ethanol and water cluster ion beams had an average roughness of less than 1 nm.

Furthermore, the wettability of the Ti surfaces irradiated by the ethanol and water cluster ion beams were investigated by measuring the contact angles for water droplet, which was put on the samples immediately after their removal from the vacuum chamber. The contact angle for the unirradiated surface was 30 degrees. For the surfaces irradiated by the ethanol cluster ion beams, the contact angle decreased with increase of the acceleration voltage, and it became about 10 degrees at higher acceleration voltages. However, for the case of the water cluster ion irradiation, the contact angle increased with increase of the acceleration voltage, and it became about 80 degrees at higher acceleration voltages. Thus, the wettability of the Ti surfaces was changed drastically with the species of the cluster ions as well as the acceleration voltage.

3. REFERENCES

[1] M.A. Duncan and D.H. Rouvray, Scientific America (December Issue), 110 (1989).
[2] M.E. Mack, Nucl. Instr. Meth. B**237**, 235 (2005).
[3] I. Yamada and G.H. Takaoka, Jpn. J. Appl. Phys. **32**, 2121 (1993).
[4] G.H. Takaoka, H. Shimatani, H. Noguchi and M. Kawashita, Nucl. Instr. Meth. B**232**, 206 (2005).
[5] G.H. Takaoka, H. Noguchi and Y. Hironaka, Nucl. Instr. Meth, B**242**, 100 (2006).
[6] G.H. Takaoka, H. Noguchi and M. Kawashita, Nucl. Instr. Meth, B**242**, 417 (2006).

* E-mail: gtakaoka@kuee.kyoto-u.ac.jp

ULTRASONICALLY-ENHANCED DIFFUSION AND CLUSTERING OF IMPLANTED COPPER IN SILICA

A. Romanyuk[1,*], *V. Melnik*[2], *R. Kurps*[2] *and P. Oelhafen*[1]

[1] Institute of Physics, University of Basel, Klingelbergstrasse 82, CH-4056 Basel
[2] IHP-Microelectronics, Im Technolgiepark 25, D-15236 Frankfurt (Oder)

1. INTRODUCTION

Ion implantation is a suitable technique for the synthesis of nanoparticles in dielectric matrices due to its high degree of controllability of dopant concentration and space distribution. Until now, studies on formation of metal nanoparticles in silica have been mainly concentrated on the influence of ion dose, dose rate, substrate and implant temperature on cluster formation and growth kinetics. Only little is known about the effect of ultrasonic waves generated in crystal during ion implantation on impurity diffusion and clustering mechanisms. Ultrasound waves propagating through the solid during ion implantation can affect the generation and motion of point defects leading to different defect reactions [1, 2]. In this work we report on the influence of ultrasound treatment (UST) applied during implantation of copper into thermally grown silicon oxide.

2. RESULTS

We observed that ultrasonically induced lattice excitations during ion implantation result in an enhanced copper diffusion towards the oxide surface as detected by secondary ion mass spectrometry (SIMS). Corresponding SIMS profiles together with distribution of generated vacancies are presented on Fig. 1. We propose that crystal excitations by ultrasound enhance the diffusion of interstitials towards the bulk of the substrate and result in the accumulation of vacancies thus substantially increasing the diffusivity of copper atoms.

In order to understand the influence of ultrasound vibrations on clustering processes the silicon oxide films were implanted with/without UST with different doses. Transmission electron microscopy (XTEM) demonstrates that *in situ* applied ultrasonic treatment leads to a lowering of the clustering threshold and an increased precipitate size after post-implantation annealing. Similar results have been reported by our group before for the case of silver implantation [3].

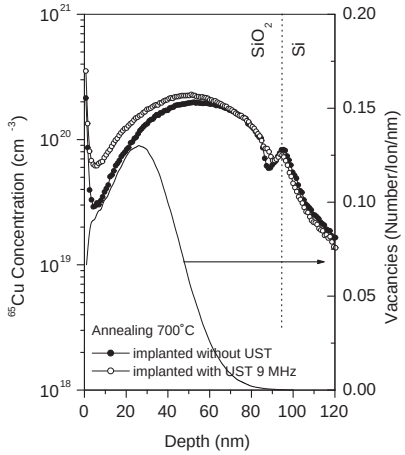

Figure 1: SIMS profiles of Cu^+ implanted SiO_2 with applied UST and without UST after annealing at 700° for 20 min. The distribution of generated vacancies as calculated with SRIM software package is shown with solid line.

3. CONCLUSIONS

We have shown that *in situ* applied ultrasonic treatment leads to an enhanced copper diffusion and increased precipitate size after post-implantation annealing. The physical mechanism of this effect is attributed to the spatial redistribution of point defects and vacancies accumulation in the precipitation region. The observed effects open new possibilities in nanomaterials engineering and provides additional understanding of physical mechanisms of sonochemical reactions in solid.

4. REFERENCES

[1] V.N. Pavlovich, Phys. Stat. Sol. B, **180**, 97 (1993).

[2] W.H. Franklin and T. Sengupta, IEEE J. Quantum Electronics **8**, 393 (1972).

[3] A. Romanyuk, V. Melnik, V. Spassov, J. Appl. Phys. **99**, 034314 (2006).

* E-mail: andriy.romanyuk@unibas.ch

AB-INITIO STUDY OF THE ADSORPTION OF CH_3SH MOLECULE ON AU(111)

P. G. Lustemberg[1,2], *M. L. Martiarena*[1,2,*], *A. E. Martinez*[3] *and H. F. Busnengo*[3,†]

[1]Instituto Balseiro - 8400 Bariloche
[2]Consejo Nacional de Investigaciones Científicas y Técnicas
[3]Instituto de Fíisica de Rosario (CONICET-UNR) Facultad de Ciencias Exactas, Ingeniería y Agrimensura, Universidad Nacional de Rosario - Argentina

Gold surfaces and anchor sulfur organic groups such as thiols (HSR) and disulfides (RSSR) (where R is an alkyl chain) are the prototype components of supramolecular systems using self-assembled monolayers (SAMs)[1] for the functionalization of extended surfaces and for the preparation of monolayer *protected* clusters. Given the wealth of potential technological aplications, including corrosion inhibition, lithography, lubrication, catalysis, and molecular recognition, the interest in the underlying chemistry and physics of such systems has been steadily growing during the past decade (see[1, 2, 3, 4, 5] and references therein). However, how thiols bind to gold surfaces to form SAMs is a long-standing open question.

The first (and maybe the simplest) step for the formation of SAMs is the initial adsorption on the clean surface. Stable SAMs are usually made of *long* alkyl chain thiols. However, the complexity of the molecule-surface potential energy surfaces (PES) of polyatomic molecules makes that short chain thiols (typicaly $HSCH_3$) are often used as model systems for theoretical studies.

Nuzzo and co-workers [6] estimated a very small value of the reactive sticking coefficient of $HSCH_3$ on Au(111) ($\sim 10^{-5}$ at 300 K), in agreement with a recent study which has found no evidence of S-H (or C-S) bond cleavage during the adsorption [7]. To explain such a small dissociative adsorption probabilities for H-SCH_3/Au(111), the existence of a barrier to dissociation of ~ 0.26 eV has been proposed [6]. However, to our knowledge, this energy barrier has never been computed through DFT calculations. This is certainly due to the extremely complex PES of $HSCH_3$/Au(111) which makes the search of possible dissociation pathways computationally demanding.

The main goal of this work is to investigate several possible reaction pathways for the cleavage of the H-S bond of $HSCH_3$ on a perfect (defect free) Au(111) surface to try to understand the origin of the small reactive sticking probability obtained in experiments.

We investigate the adsorption of methanethiol on Au(111) with Density Functional Theory DFT [8] calculation within the slab supercell-approach. We study the energies and the most stable geometries for both, the molecular and dissociatively adsorbed. We consider seven dissociation pathways and the value of the minimum energy barrier for H-S bond cleavage is estimated. These results confirm that the nondissociative molecular adsorption of methanethiol on Au(111) is due to the existence of an activation barrier of 0.6 eV. Therefore, a dissociative adsorption of methanethiol could only be achieved with an energetic molecular beam.

1. REFERENCES

[1] J.C. Love, L. A. Estro, J.K. Kriebel, R.G. Nuzzo, and G.M. Whitesides. Chem. Rev., 105:1103, 2005.

[2] A. Ulman. Chem. Rev., 96:1533, 1996.

[3] F. Schreiber. Prog. Surf. Sci., 65:151, 2000.

[4] F. Schreiber. J. Phys.: Condens. Matter, 16:R881, 2004.

[5] C. Vericat, M.E. Vela, and R.C. Salvarezza. Phys. Chem. Chem. Phys., 7:3258, 2005.

[6] L. Dubois, B.R. Zegarski, and R.G. Nuzzo. J. Chem. Phys., 98:678, 1993.

[7] I.I. Rzeznicka, J. Lee, P. Maksymovych, and J.T. Yates Jr. Phys. Chem. B, 109:15992, 2005.

[8] W. Kohn and L. J. Sham. Phys. Rev. A, 140:1133, 1965.

IMPULSIVE SURFACE-VOLKOV APPROACH FOR PHOTOELECTRON EMISSION FROM SURFACES

M.N.Faraggi[1,*], *M.S.Gravielle*[1,2], *and V.M. Silkin*[3]

[1] IAFE, CONICET, C.C. 67, Suc. 28, 1428 Buenos Aires, Argentina.[2] Depto. de Física, FCEN, UBA.
[3]Donostia International Physics Center DIPC, P. Manuel de Lardizabal 4, 20018 San Sebastián, Spain.

1. INTRODUCTION

Photoelectron emission from surfaces, induced by short laser pulses, can be employed as a tool to determine the characteristics of the pulse [1]. In a recent work [2] we proposed a distorted wave method -the *Surface-Volkov* (SV) approximation- to describe the electron emission produced by the interaction of an intense few-cycle laser pulse with a metal surface. In the model the surface is represented within the *Band-Structure-Based* (BSB) formalism [3], while the action of the electric field is described with the Volkov phase [4].
As an improvement in the previous theory, in this work we develop the *Impulsive Surface-Volkov* (ISV) approach, which incorporates the effect of the quiver amplitude in the Volkov phase.

2. THEORY

Taking into account that the BSB surface potential depends only on the coordinate *z* perpendicular to the surface, we consider a lineal polarized field *F(t)*, oriented along the *z*-axis. The temporal profile is defined as:

$$F(t) = F_0 \sin(\omega t + \varphi) \sin^2(\pi t / \tau) \qquad (1)$$

for $0 < t < \tau$ and 0 elsewhere, with τ the pulse duration, ω the carrier frequency, φ the carrier-envelope phase, and F_0 the maximum field strength.
Within the ISV model the quiver amplitude $\alpha^-(t)$ is included in the Volkov phase of the final distorted wave function. It reads:

$$\alpha^-(t) = \frac{1}{c} \int_{+\infty}^{t} A^-(t')\, dt' \quad , \qquad (2)$$

where *c* is the light velocity and $A^-(t)$ represents the vector potential at the time *t*.

3. RESULTS

The ISV approach is applied to evaluate the differential probability of electron emission from Al(111). In the figures, results for the ejection angle $\theta_e=90^o$ (measured with respect to the surface) and for a symmetric pulse ($\varphi=\pi/2-\omega\tau/2$) are displayed for two different values of τ.

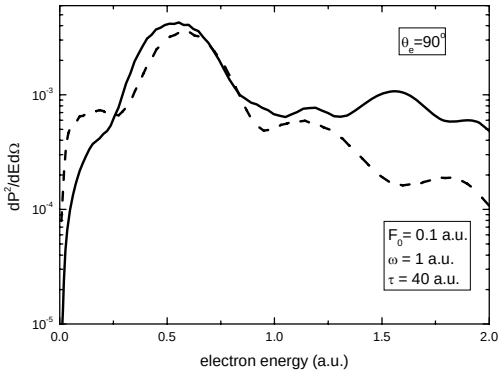

Figure 1: Electron distribution as a function of the final electron energy. The laser parameters are: F_0= 0.1 a. u., ω =1 a. u., and τ = 40 a. u. Solid line, ISV model; dashed line, SV approach.

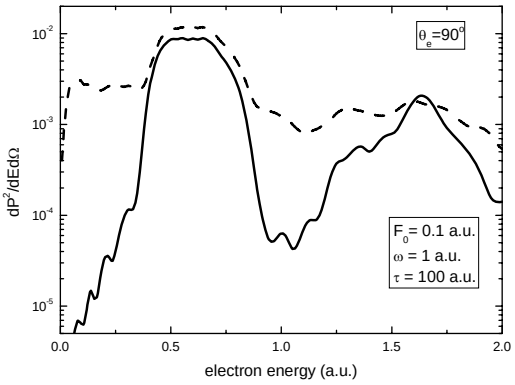

Figure 2: Similar to Fig.1 for τ = 100 a. u

We conclude that the incorporation of the quiver amplitude leads to a significant modification of the differential probability of electron emission.

4. REFERENCES

[1] Lemell *et al*., Phys. Rev. Lett **90**, 076403 (2003); Apolonski *et al*., **92**, 073902 (2004).
[2] M. N. Faraggi *et al*., Phys. Rev. A **73**, 032901 (2006).
[3] Chulkov *et al*., Surf. Sci. **391**, L1217 (1997) ; **437**, 330 (1999).
[4] Volkov, Z. Phys. 94,250 (1935).

* E-mail: faraggi@iafe.uba.ar

TOPOGRAPHYCAL INVESTIGATION OF SOFT LANDED IONIC PEPTIDES ON ATOMICALLY FLAT SURFACES

O. Hadjar[1*], *J. Green*[2], *R. G. Cooks*[2], *J. H. Futrell*[1] *and J. Laskin*[1]

[1] Pacific Northwest National Laboratories, Richland, WA 99354 USA

[2] Department of Chemistry Purdue University West Lafayette, IN 47907 USA

1. INTRODUCTION

Interaction of hyperthermal ions (1-100eV) with surfaces results in several processes[1] such as scattering, surface induced dissociation[2] (SID) and soft landing[3]. Soft-landing of biomolecular ions with known mass and composition on specially prepared surfaces presents a highly specific approach for surface modification and preparation of novel substrates with very high purity using only a fraction of material utilized in conventional approaches. Our previous studies suggested that a significant fraction of soft-landed peptide ions remain charged on inert SAM surfaces. First observation of soft landed peptides on self assembled monolayer (SAM) using ex-situ Atomic Force Microscopy (AFM) technique will be presented.

2. EXPERIMENT AND RESULTS

Protonated peptides are produced using electrospray ionization technique and efficiently transferred into the vacuum system of a mass spectrometer using an electrodynamic funnel. Ions are thermalized in a collisional quadrupole, mass selected using an RF/DC quadrupole, transferred into the UHV region of the ion deposition instrument via a series of electrostatic lenses and collided with a surface at normal incidence. The size of the ion beam is monitored using a phosphorus screen type detector and the spot size can be varied in the range from 1.5 to 5 mm. SAMs of dodecanelthiol on gold (HSAM) were prepared using a standard procedure.

AFM images of surfaces following soft-landing was performed using atomically flat gold on mica substrates. Figure1a shows the AFM image of the HSAM/gold surface obtained in the tapping mode, Atomically flat terraces of about 300nm size are clearly observed. Fig.1b shows the image of the HSAM surface obtained following 5 min exposure to 90 pA of a mixture of +1, +2, and +3 charge states of substance P corresponding to ca. 10% of a monolayer. Soft-landed species are clearly visible as small spots on atomically flat terraces. An expanded region of one of the terraces (fig.1c) shows features of two sizes: small (1 nm height) spots and larger 2-4 nm features. Force calculations provide an important insight on the differences in the sizes of spots observed in AFM images. The size of small features is consistent with force calculations between the neutral peptide and the AFM tip, while 2-4 nm height of larger features correspond to peptides that preserved their charge following soft-landing. Because of the stronger interaction potential between the AFM tip and a charged particle, ionic species are observed as bright spots on the atomically flat surface. This study presents a first direct observation of soft-landed ions on SAM surfaces.

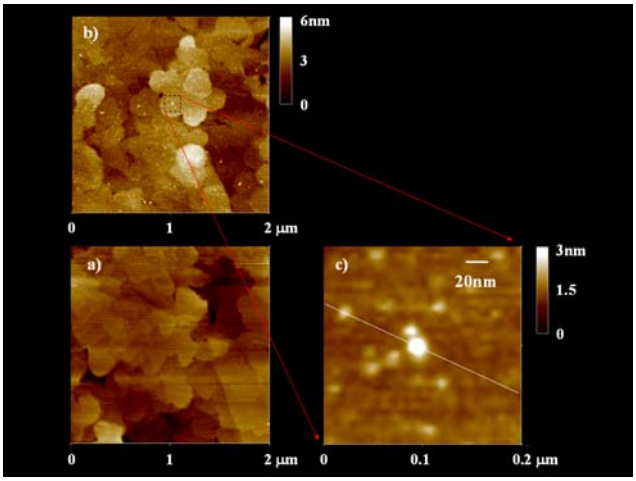

Figure 1: AFM images of H-SAM –AU-Mica surface in a tapping mode. a) Before soft landing. b) After soft landing and c) 200 nm range zoom showing individual peptides.

3. REFERENCES

[1] R. G. Cooks, S. C. Jo, J. Green, Apl. Sur. Sci. 231-232, 13 (2004).

[2] J. Alvarez, R. G. Cooks. S. E. Barlow, D. J. Gaspar, J. H. Futrell, J. Laskin, J. Anal. Chem. 77, 3452 (2005).

[3] S. A. Miller, H. Luo, S. J. Pachuta, R. G. Cooks, Science 275, 1447 (1997).

* E-mail: omar.hadjar@pnl.gov

NANO- FABRICATION USING POINT DEFECTS INDUCED BY ION IRRADIATION

N. Nitta, S. Morita, D. Kikkawa and M. Taniwaki

Kochi University of Technology, Kami-City, Kochi, Japan

The authors found that an anomalous cellular structure, which consists of cylindrical cavities, is developed on the GaSb surface ion-implanted at a low temperature [1-2], and verified experimentally that this structure is formed by the behavior of the point defects induced by ion implantation [3-4]. These cavities have about 50 nm diameter, 300 nm depth and partitioning wall with 10 nm thickness, whose fineness and high aspect ratio are very favorable for application to a variety of nano-devices. However, their shapes are irregular and their arrangement is random, then, it is needed to control the shape and the arrangement of the cavities for application to electronic or optical devices. This irregularity in the cellular structure comes from the random process of the point defects. In order to produce more minute structure on the surface of materials than that by photo-lithography technique, the authors proposed a new nano-fabrication technique which consists of two processes; the first process is to produce an ordered initial structure artificially and the second is to develop it self-organizationally but without disturbing the regularity [5-6]. In this presentation, the idea and experiment using FIB (focused ion beam) is reported and the new technique is proved to be available for application to nano-fabrication.

The experiment was performed by the following procedures. First, the initial pattern of ordred structure was fabricated on a (100) GaSb wafer by ion irradiation using milling mode of FIB. Then the structure was developed by ion irradiation using imaging mode of FIB, when the ion doses was determined by the number of scanning times. The ion dose of one scanning was 2.8×10^{15} ions/cm^2 and the maximum number of scanning was 20 times. The surface morphology of the initial structure and the developed structure after each scan was observed by a field emission type scanning electron microscope.

Two kinds of experiment, which were different in the fabrication of the initial structure, were performed. The pattern of an initial structure is shown in Fig. 1. Nine matrices of dots at constant intervals are created in the area of 10×10 μm^2. The area of a matrix is 2.4×2.4 μm^2 and the dot intervals (I_d) are 30, 50, 80, 100, 120, 150, 200, 240 and 300 nm. In the experiment A, the initial pattern was fabricated by irradiating 30 keV Ga^+ to the constant ion dose per unit area (10^{15} ions/cm^2), therefore, the number of ions irradiated on one dot differs between the matrices. In the experiment B, the initial pattern was fabricated irradiating 30 keV Ga^+ so that the number of ions per one dot became equivalent in an initial pattern, then the ion doses differed between the matrices. The there initial patterns were fabricated by irradiations of 2.25×10^4, 1.125×10^5, 2.25×10^5, 1.125×10^6, and 2.25×10^6 ions/dot. In fabrication of initial patterns and a spot interval and the times of imaging mode were changed. Initial structure and imaging mode used 30 kV Ga^+ like the experiment A. The dose per one scannig of 2.8×10^{15} ions/cm^2 and the scan is 1- 20 times

The resuts are as follows. The initial structure with cell interval more than 50 nm is able to be fabricated by FIB. The ordered structures whose dot interval is 80 – 150 nm are developed into the ordered cell structure. The structures with smaller intervals than 30 nm are not orderly developed by coalesce of the cascades, and the regularity of the structure with larger intervals than 180 nm is lost by the formation of the secondary structure (elevation).

REFERENCES

[1] N. Nitta, M. Taniwaki, T. Suzuki, Y. Hayashi, Y. Satoh and T. Yoshiie, J. Jpn. Inst. Met. **64**, 1141(2000).

[2] N. Nitta, M. Taniwaki, T. Suzuki, Y. Hayashi, Y. Satoh and T. Yoshiie, Mater. Trans. **43**, 674(2002).

[3] N. Nitta, M. Taniwaki, Y. Hayashi and T. Yoshiie, J. Appl. Phys. **92**,1799(2002).

[4] N. Nitta, M. Taniwaki, Y. Hayashi and T. Yoshiie, Physica **B 376-377**, 881 (2006).

[5] N. Nitta and m. Taniwaki, Physica **B 376-377**, 872 (2006).

* E-mail: taniwaki.masafumi@kochi-tech.ac.jp

DEPENDENCE OF DEFECT FORMATION IN Si NANOCRYSTALS ON ION ENERGY LOSSES

G.A.Kachurin, S.G.Cherkova, D.V. Marin, A.G.Cherkov, A.K.Gutakovsky

Institute of Semiconductor Physics SO RAN, 630090 Novosibirsk, RUSSIA

Recently, the investigation of ion beam modification of Si nanostructures has received considerable attention. This attention is motivated by the following moments – continuous down scaling of the microelectronic device dimensions, the ability of quantum-size Si nanocrystals to emit strong visible light, that opens the door to the Si-based integrated optoelectronics, and the well known advantages of ion beam processing. The ion-induced defects in bulk Si have been studied extensively for many years, because this material dominates microelectronics. However, Si nanocrystals (Si-ncs) essentially differs from the bulk crystals in remarkably increased surface-to-volume ratio and in impossibility for the mobile defects, confined in a nm-size volume, to diffuse away from each other. The resulted from the atomic collisions interstitials and vacancies have to annihilate, to form defect complexes or to interact with the Si-ncs surface. Few data are available now on the behavior of point defects in the nanocrystals. It was supposed in [1] the fate of such defects should depend on the collision cascade density, i. e. on the ion energy loss rates. In order to study these issues more in detail, we have synthesized the light-emitting Si nanocrystals (Si-ncs) by implantation of Si^+ ions in the thermally grown SiO_2 layers, followed by anneals at 1100 ^oC in a neutral ambient. Si-ncs have been formed at different distances from the sample surface by varying the Si^+ ion energy. To investigate the defect behavior the irradiation with 200 keV F^+ ions within the dose range of 10^{12}-10^{14} cm^{-2} was performed. Due to the difference in depth location of Si-ncs the ion energy loss rates in them were different, ranging between 0,5 and 5 displacement/nm. The rates have been evaluated using the TRIM-95 code with 15 eV as an atom displacement threshold in silicon. Photoluminescence (PL) and HREM were employed for the characterizations. The experiments have shown even individual atom displacements in Si-ncs quench their PL band near 800 nm, caused by the quantum-size effect. However, the PL quenching efficiency rapidly decreases with an increase in energy loss rate over ~ 1 displacement/nm, i.e. in more dense displacement cascades only a part of the introduced point defects form the non-radiative recombination centers. Usually such centers are ascribed to the dangling bonds resulted from the sink of the point defects to the Si-ncs surface. HREM has shown the Si-ncs size to be of 3-5 nm, thus ion energy loss rates of ~ 1 displacement/nm provide simultaneously multiple Frenkel pairs in the crystallites, enabling complex formation and/or annihilation of the produced vacancies and interstitials.

However Raman spectroscopy and HREM have revealed Si-ncs render amorphous at very low damage levels –

about 10% of the atoms displaced. To compare, for amorphization of bulk Si by ion bombardment ~ 100% of atoms should be displaced. HREM has shown that for higher ion energy loss rates the defects are accumulating not at the Si-ncs shells only, but in the cores too, disturbing their crystal lattice. Fast amorphization of Si-ncs and nearly complete sink of the point defects to the Si-ncs surface, seen from the PL quenching at the early stages of irradiation, indicate the vacany–interstitial annihilation does not a dominant process, as might be expected for the volumes of 10^{-7}cm size. The obtained results are in agreement with recent theoretical calculations and computer modeling, which predict existence of ~1,1 eV annihilation barrier for the Frenkel pair and high probability to form vacancy and interstitial complexes by the bond switching without leaving the dangling bonds [2-6].

1. REFERENCES

[1] G. A. Kachurin, S. G. Cherkova, V. A. Volodin, D. M. Marin, D. I. Tetel'baum, and H. Becker. Semiconductors, **40**, 72, (2006).

[2] Y. Q. Wang, R. Smirani, G. G. Ross. Appl. Phys. Left. **86**, 221920, (2005).

[3] M. Tang, L. Colombo, J. Zhu, T. Diaz de la Rubio. Phys. Rev. **B 55**, 14279, (1997).

[4] T. Motooka. Phys. Rev. **B 49**, 16367, (1994).

[5] D. M. Stock, B. Weber, K Gaertner. Phys. Rev. **B 61**, 8150, (2000).

[6] L. Marques, L. Pelaz, J. Hernandez, J. Barbolla. Phys. Rev. **B64**, 045214, (2001).

* E-mail: kachurin@isp.nsc.ru

ANOMALOUS INTERDIFFUSION AT ANISOTROPIC INTERFACES

*P. Süle**

MTA-MFA, Budapest, Hungary, Konkoly-Thege 29-33

Intermixing has been studied at interfaces in various systems during vapor deposition (atomic layer growth) and under forced conditions such as low-energy ion-sputtering (bombardment) using atomistic computer simulations. It has been shown that the anisotropy of the bilayers governs the phase instability of the systems. The atomic transport superdiffusive in strongly size and mass-anisotropic heterophases. In bilayers Pt/Ti (mass-anisotropic) and in Co/Ti (size-anisotropic) we find anomalously strong interdiffusion during ion-sputtering. The enhancement of intermixing is explained by a specific backscattering mechanism at the interface (reversed recoils). In anisotropic growing systems we also find anomalous atomic transport. Depositing Pt on Al(111), Pt is injected to the Al phase nearly freely via an oscillatory interaction with the substrate. Morever during the submonolayer growth of the intermixed phase the cascading ejection of Al towards the surface is observed.
These finding are commonly explained by the anomalous interdiffusion phenomenon.

REFERENCES

[1] P. Süle, M. Menyhárd, Phys. Rev., **B71,** 113413 (2005).
[2] P. Süle, Surf. Sci., **585**, 170 (2005).
[3] P. Süle, M. Menyhárd, L. Kótis, J. Lábár, W. F. Egelhoff Jr., submitted to Phys Rev., cond-mat/0510077.
[4] P. Süle, M. Menyhárd, K. Nordlund, Nucl Instr. and Meth. in Phys. Res., **B226**, 517 (2004).

* E-mail: sule@mfa.kfki.hu

MATERIALS SURFACE TREATMENT BY PULSED PLASMA FLOWS

A. Zhukeshov, A. Gabdullina, and A. Amrenova

Science Research Institute of Experimental and Theoretical Physics
Tole bi str. 96a, Almaty, 050012, Kazakhstan
e-mail: zhukeshov@physics.kz

1. INTRODUCTION

The pulsed plasma accelerators are used for obtaining of the powerful concentrated fluxes. The features of accelerators construction allow to obtain plasma flows in a wide range of energy: from several units up to hundreds kev. It gives the possibility to use them for a wide range of applications in various fields of plasma physics and material science. In the present work the pulsed plasma accelerator KPU with coaxial electrodes is used. The technological applications of this accelerator for updating structure of a semiconductors surface were submitted by the authors in work [1]. For improvement of a surface properties of constructional materials, such as carbon and stainless steels, method of plasma processing most acceptable. This work is devoted to investigation of the influence of plasma flows on a various constructional materials.

1.1. Apparatus

The accelerator KPU has two cylindrical electrodes with diameters of 90 mm (external) and 24 mm (internal). Energy of the capacitor bank is 32 kJ. The discharge current of 100-500 κA represents a increased harmonically signal with the period 14 μs. The work of this accelerator in two modes is in detail investigated. In the first mode, the gas is filled through the pulse fast valve, in the second mode the working chamber is filled by gas up to the pressure in a range 0,01-100 torr. Plasma flow energy density has made 2-60 J/sm^2. The concentration of electrons in plasma, determined by various methods, has made ~10^{12}-10^{15} sm^{-3} in different modes. The detailed description of this accelerator is given in work [2].

1.2. Experimental results

The physical properties and changes in structure of vanadium alloy, common quality carbon and stainless steels were investigated. The formation of the modified

layer on a surface is usual for metals. However, the large density of energy results in formation of a non-uniform relief of a surface and blisters. This undesirable phenomenon can be removed if to use small density of energy. In all cases at achievement of melted energy by 15-25 J/sm^2, there are recrystallization of the surface area on depth 10-30 microns (it depends on materials) and the structure modification. The character of structural changes in metals depends on the energy density and the introduced doze. Also character of structure changes depends on used working gas and from accelerators operation mode. For carbon steel which basic structure is the ferrite, the formation of austenitic and martensitic phases is observed after processing. At the same time for stainless steel the formation of nitride hardening phases is usual at processing by nitric and air plasmas. The metals microhardness of plasma processed steels can grows in 1,5-4 times at increasing of the energy density. In any case, the degree of hardening is proportional to the introduced doze. Wear resistance of steel after plasma processing increased up to 4 times.

The reason of a structure changes consists in of short action of a pulse and of enough high energy density that results to fast heating of a material surface. Thus, the most important factor, which is responsible for structure-phase changes, is energy density delivered to the sample surface by an incident plasma stream. The materials, processed by pulsed plasma, undergo essential changes of surface properties. It allows on the basis of researches to develop technologies for industrial application.

2. REFERENCES

[1] F. B. Baimbetov, B. M. Ibraev, and A. M. Zhukeshov, Semiconductors. V. 36, N. 2, (2002).
[2] B.M. Ibraev, Thermophysics. V.12., N.2, (2003)

SURFACE MODIFICATION OF ELECTROSPUN PVA NANOFIBERS BY LOW TEMPERATURE PLASMA

M.Damercheli[1,], M.Ghoranneviss[1] ,R.Damercheli[2], R.Khajavi[3], K.Yasserian[1]*

[1]Plasma Physics Research Center, Science and Research Campus, I.Azad University, Tehran (14736), Iran
[2]Faculty of engineering , Science and Research Campus, I.Azad University, Tehran, Iran
[3]Post Graduate Faculty South Branch, I. Azad University,Tehran,Iran

1. ABSTRACT

Electrospinning is a useful technique to produce nanofiber webs. Nanofibers with amazing characteristics such as very large surface area to volume ratio, high flexibility and superior mechanical performance takes a lot of interest. Ultrafine Polyvinyl Alcohol (PVA)nanofibers, which may have potential applications in filtration and medical.

In this research, Low Temperature Plasma (LTP) was used to deposit of copper thin film on Polyvinyl Alcohol (PVA) nanofibers prepared by electrospinning to modify the surface of sample. Atomic Force Microscopy (AFM) was employed to study the surface characteristics of the fibers before and after coating. For investigating the percentage of crystallinity and size of crystals on the surface we used X-Ray Diffraction (X-RD).Morphology of electrospun nanofiber was investigated with Scanning Electron Microscope (SEM). Also we examined wetability of nanofibers before and after coating.

* E-mail: maasoomeh.damercheli@gmail.com

ELECTRICAL CHARACTERISTIC OF MAGNETIZED PLASMA IN A DC CYLINDRICAL MAGNETRON SPUTTERING DEVICE

K.Yasserian [1,*], *M.Ghoranneviss* [1], *A.Anvari* [2], *H.R.Pourbalasi* [1] *and H.Hosseini* [1]

[1] Plasma physics Research Center, Science and Research Campus, I.A. University, P.O.Box: 14665-678, Tehran, Iran
[2] Physics Department, Sharif University of Technology, Tehran, Iran

1. INTRODUCTION

The first paper on the magnetron as a sputtering device was reported in the 1960s, but the physical basis originates back to the late [1]. Since then, magnetrons have known a continuous development in various industrial fields, specially microelectronic and surface processing and widely used for thin film deposition. They are commonly classified among physical vapour deposition (PVD) [2] devices although they offer also advantage for sputtering studies [3] or etching [4]. Monograph dedicated to plasma processing contain parts or chapters devoted to magnetron [2, 4, 5]. Basically magnetrons utilize an external magnetic field parallel to the cathode (target). The component of this field parallel to target traps energetic electrons in their travel from the cathode to the anode leading to an amplification of gas ionization.

In this study a DC cylindrical magnetron sputtering device was used to investigate the electrical behaviour of cold magnetized plasma. DC cylindrical magnetron sputtering is capable of generating magnetized plasma and has been used for development of high-rate, low pressure, high efficiency processing machines. This system consists of two coaxial cylinders with 10 and 21 cm in radius and 72 cm in length. The cathode was edged. The distance between cathode and anode was 20 cm. The inner one was cathode. A magnetic coil mounted around the outer cylinders generated a nearly uniform axial magnetic field up to 600 G. The region between two cylinders was evacuated by means of a mechanical and also a turbo-molecular pump up to 10^{-6} torr. The dependences of the breakdown voltage, current-voltage characteristic of the system and power absorbed by plasma on the gas pressure, the type of working gas and the magnitude of magnetic field were studied. The effects of the various gas working were introduced into this system. The experiment shows that the magnetic field plays role of the collision in perpendicular of its direction and the magnitude of magnetic fields has optimum value. The detailed of the experiments and the results will be discussed in the full paper.

2. Reference

[1] Wasa K and Hayakawa S 1969 Rev.S. Instrum. 40 693-7 Pening FM 1939 US Patent 2146025.
[2] Thornton J A and Penfold A S 1978 Thin film Processes vol I, ch 2.2, ed L Vossen and K Kern (New York: Academic)
[3] Minea T M, Bretagne J, Gousset G, Magne L, Pagnon D and TouzeauM 1999 Surf.coat. Technol. 116-119 558-63.
[4] Manos D M and Flamm D L 1989 Plasma Etching-An introduction ch 3 (New York: Academic)
[5] Lieberman M A and Lichtenberg A J 1994 Principles of plasma Discharges and material processing (New York: Wiley)

* E-mail: kyasserian@yahoo.com

THE EFFECT OF PRESSURE AND MAGNETIC FIELD OF A DC SPUTTERING MAGNETRON ON PROPERTIES OF COPPER THIN FILM

M. Ghoranneviss, K. Yasserian, D. Dorranian, H. Hosseini , H.R. Pourbalasi

Plasma Physics Research center, Science and Research Branch, I.Azad University, P.O.Box 14665-678, Tehran, Iran

Deposition of thin films may be achieved by the following methods.
Reactive thermal evaporation deposition, RF & DC magnetron sputtering, electron beam evaporation, ion-assisted deposition techniques, electro less chemical growth techniques, spray pyrolysis, chemical vapor deposition, vacuum evaporation and laser-assisted deposition techniques [1].
Sputtering techniques are commonly used to deposit metal thin film on insulating and conducting substrates. The growth parameters, such as thickness of thin film and sputtering power usually play significant roles in governing the properties of metal films [2].
Plasma sources are nowadays widely used for sputtering and film deposition application [2, 3]. A dc magnetron sputtering device plasma is essentially a glow discharge produced between two cylindrical electrodes as anode and cathode. A magnetic coil located outside the cylinders creates a field configuration acting as a magnetic trap for the electrons [4], which typically have a temperature of a few eV.

A dc cylindrical magnetron sputtering device consists of two copper cylinders with 1.5 and 5 cm in radius and 20 cm in length. A magnetic coil mounted around the outer cylinder generates an axial magnetic field up to 550 G.
The effect of different magnetic field on the ionization rate of the discharge is observed. It is shown that the electrical behavior of the discharge strongly depends on the values of the magnetic field and shown an optimum value at which the power absorbed by the plasma is maximum. The effect of different pressure on the ionization rate is also studied and the results are reported.

Thin films produced in different condition.
The morphology, conductivity and structure of thin films are analyzed by X- ray diffraction (XRD), Rutherford Back Scattering (RBS) and Atomic Force Microscopy (AFM)
Dependence of the conductivity, thickness and roughness of thin film on deposition condition is investigated

1. REFERENCES

[1] Topic in Applied physics, volume 64, sputtering by particle bombardment (III), 1991.
[2] B. Window and Savvides N 1986 J. Vac. Sci. Technol. A **4** 196 (1986).
[3] M.J. Jung, K.H. Nam, L.R. Shagiyan and J.G. Han, Thin Solid Films 435 145 (2003).
[4] J.A. Bittencourt, Fundamental of Plasma Physics

CORROSION BEHAVIOUR SURFACE CHARACTERISATION OF ARGON BOMBARDMENT ON AUSTENITIC STAINLESS STEEL

A.Shokouhy[1*], *M.Ghoranneviss*[1], *M.M.Larijani*[1, 2]
M.Yari [1], *A.H. Sari* [1]

[1] Plasma Physics Research Center, Science and Research Campus, Islamic Azad University, P.O.Box 14665-678, Tehran, Iran
[2] Nuclear research center for Agriculture and Medicine, Atomic Energy organization of Iran, P.O.Box:31585-498, Karj, Iran

1. INTRODUCTION

Ion bombardment has been used to modify the physical properties of a wide range of metals and super-alloys using plasma techniques for ion sources and plasma surface treatment [1-2]. High dose ion bombardment is also a well-known technique to improve the mechanical properties of metals [3-4]. There have been number of investigations about increasing of microhardness, wear resistance and finally improvement of the fatigues life. Nitrogen ion implantation as a non-equilibrium process can produce amorphous, metastable and stable crystalline phases.
The influence of grain size has great role on the properties of the real widely used material, specially on austenitic-ferritic stainless steel, is of great interest.

2. MATERIALS AND EXPERIMENTAL TECHNIQUES

This work presents the results of low energy argon ion implantation on AISI 304 type stainless steel (SS) at moderate temperatures of about 400°C [5-8]. The argon ions are extracted from plasma ion source at a voltage of 30 keV and the ion current density was 100μA /cm^2. The range of doses was from 5×10^{16} to 1×10^{18} Ar^+/cm^2. The given values are the average of concentration measured at center of each sample.
The corrosion behavior was studied in acid solutions by potentiodynamic measurements. Also the effect of ion implantation on surface morphology was investigated by AFM technique.

3. REFERENCES

[1] H.Parchami, M.Ghoranneviss, A.Shokouhy, J.Plasma Fusion Res.**Vol.5** (2002) 000.
[2] A.H. Sari, Hantehzadeh, M.R, Ghoranneviss, M., 25th ICPIG, Nagoya, Japan, July 2001, paper 17a52.
[3] M.Ghoranneviss , A.Shokouhy ,Amir H.sari , H.Hora , M.Talebi Taher and A.E.Abhari, Proceeding of XXVI International Conference Phenomena in Ionized Gases (ICPIG) July 15-20,2003,Greifswald,Germany
[4]Warren, B.E. (1969).X-ray Diffraction, pp. 251-314.New York: Addison-Wesely.
[5] M. Cartier, Proceedings of ATTT 95, Paris, 37-57.
[6] C. Gautier, H. Moussaoui, F. Elstner, J. Machet, Surf. Coat. Technol. **86-87** (1996) 254-262.
[7] W. Herr, B. Matthes, E. Broszeit, M. Meyer, R. Suchentrunk, Surf. Coat. Technol. **57** (1993) 77-80.
[8] J. Creus, H. Idrissi, H. Mazille, F. Sanchette, P. Jacquot, Surf. Coat. Technol. **107** (1998) 183-190.

[*] E-mail: a_shokouhy@yahoo.com

AUGER CASCADE STIMULATED ION SPUTTERING OF COVALENT AND IONIC CRYSTAL UNDER ELECTRON AND MULTIPLE CHARGED ION BOMBARDMENT

B. Atabaev[1*]

[1] Arifov Institute of Electronics, Uzbek Academy of Sciences, Tashkent 700125, Uzbekistan

The secondary ion sputtering of covalent SiC and ionic LiF crystal under slow electron and multicharged ion bombardment are investigated. It is shown the non-elastic emission of silicon and carbon positive ions is proportional to potential energy of impact multicharged argon ion and has energy threshold at near Si 2p ionization level under triple charged argon ions bombardment. The energy threshold of non-elastic emission of lithium and fluorine ions equal potential energy of double charged argon ion. The SIMS mass-spectra of SiC and LiF content only single charged atomic and molecular ions. The covalent crystal can not sputtering by decay of self-trapped exiton. Also potential sputtering of KCl crystal under multicharged ion leads to planar surface erosion. This phenomena cannot be explained by model of decay of self-trapped exiton. In case of double charged argon ion impact of LiF at least one electron-hole pair rather than only a hole in valence band is generated by resonant neutralization. For explaining of experimental data we use model two hole formation in valence band at Auger neutralization of bombarding multicharged ion. We propose localized two hole stimulated non-elastic ion sputtering of covalent and ionic crystals by Coulomb repulsion of single charged ions under multicharged ion bombardment. The life time of localized two hole in silicon carbide valence band longer than recoil formation time at elastic collision . The evidence of cooperative potential and kinetic sputtering of silicon carbide by multicharged ion are shown.
The ESD mass-spectra of SiC and LiF content single and double charged atomic and molecular ions. The energy threshold of secondary double charged silicon ions close to 100 eV energy of bombarding electron and has same threshold for molecular SiC ions.

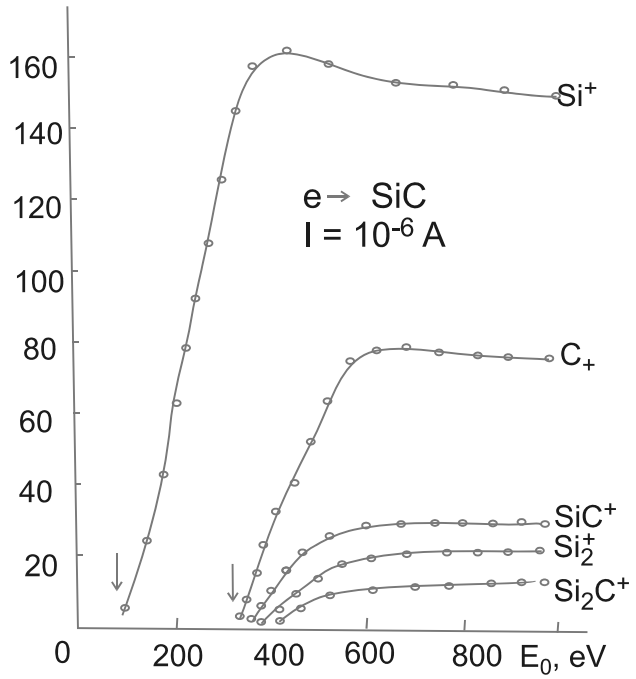

Figure 1: Energy threshold of Auger ESD of SiC.

For explaining of experimental evidence of soft potential sputtering of silicon carbide by electron we propose model of Coulomb explosion of double charged silicon and carbon ions under electron bombardment. It is known CsI crystal has weak properties for potential sputtering under highly charged ions bombardment. But in case of electron bombardment of CsI crystal secondary ion mass-spectra content single and multiple charged Cs^{q+} and I^{q+} (q=2-6) ions. This experiment can be explained by formation localized multiple hole state in valence band leading to CsI potential sputtering.

* E-mail: atabaev@ariel.uzsci.net

RADIATION-INDUCED LUMINESCENCE FROM Au, Pt/TiO_2 BY O^+ AND N^+ ION IRRADIATIONS

Sin-iti Kitazawa[1,*], *Shunya Yamamoto*[2], *Masaharu Asano*[2], *and Yuichi Saitoh*[2]

[1] Tokai Research Establishment, Japan Atomic Energy Agency, 2-4 Shirakata-Shirane, Tokai, Ibaraki 319-1195, Japan
2 Takasaki Research Establishment, Japan Atomic Energy Agency, 1233 Watanuki, Takasaki, Gunma 370-1292, Japan

ABSTRACT

The ion irradiations to solid targets produce excitation states, which are relaxed by radiation or non-radiation transitions. The light emission from the target due to the energy relaxation via radiation transition is called radiation-induced luminescence (RIL), and it is known that it has characteristic wavelengths for the band structures, the lattice defects and the impurity levels. Many researches have done for titanium dioxide in the optical properties by the difference of the crystal structure, lattice defects, impurity doping, and so on. However they are mainly performed for photo absorbance, since the photocatalysis in the sun light is the most important for the study of titanium dioxide. For the RIL of titanium dioxide by 10 keV oxygen ion irradiations, the existence of UV band and visible bands are observed at room temperature [1]. The range of 10 keV oxygen ions into titanium dioxide is about 30 nm. Therefore, the surface effect must be considered for the study. In this work, the RIL of titanium dioxide with gold or platinum thin layer on the surfaces, which consist nano-photochemistry diodes, by irradiations of 10 keV oxygen ions and nitrogen ions were observed. Some of the observed spectra are shown in Figure 1. Other than various atomic lines, three bands at 2.0 and 2.6 eV (visible bands) and 3.9 eV (UV band) are observed. There are few differences in each spectrum, therefore the influence of the surface was observed on neither gold nor platinum. It shows that the influence by the solid where the kinetic energy of ions mainly damped is larger than that of the surface. A part of the mechanism of the luminescence phenomenon by particle beams of the titanium dioxide expected application as an optical catalyst material was made clear by this research.

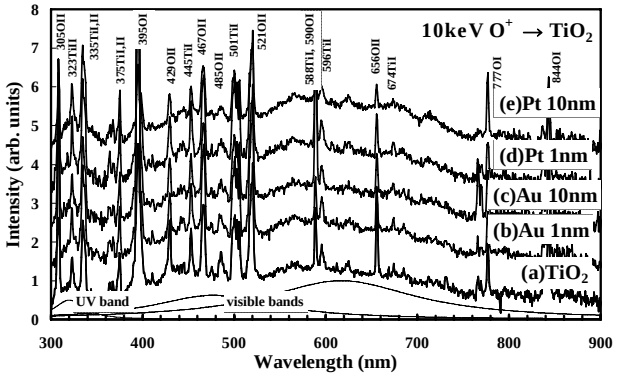

Figure 1: RIL spectra by 10 keV O^+ irradiation onto TiO_2 with no layer (a), 1 nm Au (b), 10 nm Au (c), 1 nm Pt (d) and 10 nm Pt (e) on the surfaces. Some atomic peaks are assigned and identified on the top. The three bands were fitted by Lorentz curves at the bottom.

REFERENCE

[1] S. Kitazawa, S. Yamamoto, M. Asano, Y. Saitoh and S. Ishiyama, Nucl. Instrum. Methodes Phys. Res. B 232, 94 (2005).

* E-mail: kitazawa.siniti@jaea.go.jp

ELECTRON-HOLE EXCITATIONS IN METAL NANOCLUSTERS UNDER LOW-ENERGY ION SCATTERING

V.A.Kurnaev, V.V. Lebid'ko, M.A. Pushkin, V.I. Troyan,
Moscow Engineering Physics Institute

1. INTRODUCTION

Size-dependent electronic properties of metal nanoclusters are of interest both for base physics and practical applications. These properties can be studied experimentally by measurement of cluster's electrons response to a sudden appearance of the uncompensated charge, resulting in many- and single-particle excitations, particularly, creation of low-energy electron-hole (*e-h*) pairs near Fermi surface ("infrared catastrophe"). Such excitations are known to result in the singularity (asymmetry) of the X-ray core-levels photoelectron spectra (XPS).
We present the results of investigation of *e-h* pairs generation in metal nanoclusters with the help of low-energy ion scattering spectroscopy (LEIS).

2. RESULTS AND DISCUSSION

1-10 nm size nanoclusters of Au, Co and Mo deposited on the surface of highly oriented pyrolitic graphite by pulsed laser are studied *in situ* by He^+ LEIS in the energy range E_0 = 0.3-1.5 keV.
The shape of the observed ion spectra for the investigated primary energies range is found to be asymmetric (see Fig.1), and can be well fitted by singular Doniach-Sunjic line-shape convoluted with Gaussian broadening of the initial ion flux.

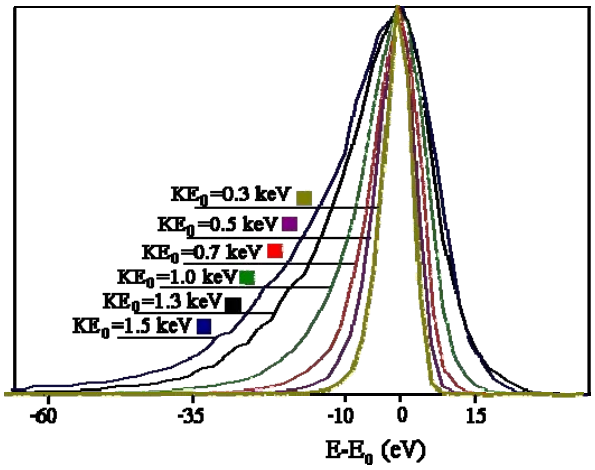

Figure 1: Energy spectra of He^+ ions with different primary energies scattered from HOPG target after 5000 pulses of Au laser deposition.

Anderson singularity index α characterizing spectra asymmetry is determined and found to increase with energy of ions that is attributed to the excitation of single-particle electron states. In contrast to XPS, LEIS spectra asymmetry is independent on the cluster size (Fig.2) and has higher values for bulk metals, indicating the difference in the electronic states of surface and bulk atoms.

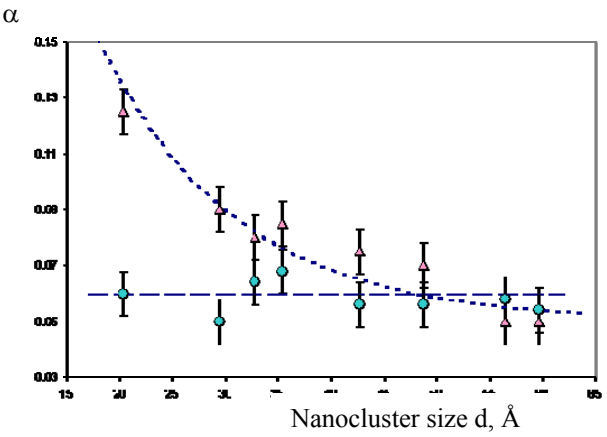

Figure 2: Experimental values of ISS Anderson singularity index α as function of Au/HOPG nanoclaster's size (*d*) in comparison with results measured with x-ray photoelectron spectroscopy (XPS): circles – ISS (E_{kin}=0.3 keV), triangles – XPS/

The details of the experimental technique and procedure are also presented. The results are discussed indicating that measured values of Anderson singularity index allow to determine phase shifts of screening *s*-, *p*- and *d*-electrons and thus to analyze the band structure and electron-state density of nanoclusters.

Friday, 22.9.2006

AUGER-ELECTRON EMISSION IN HEAVY ION -SURFACE COLLISIONS

G. Schiwietz [1,*], *F. Staufenbiel* [1], *M. Roth* [1], *K. Czerski* [1], *and P.L. Grande*[2]

[1] Hahn-Meitner-Institut Berlin, Division SF4, Glienicker Str. 100, D-14109 Berlin, Germany
[2] Universidade Federal do Rio Grande do Sul, 91500 Porto Alegre, Brazil

1. INTRODUCTION

Fast heavy ions penetrate the surface of any material without an appreciable kinetic energy loss, internal excitation or angular deflection. Notwithstanding this behavior, experiments can be performed in a surface-sensitive way by proper choice of the measured quantity. Here we have concentrated on ion-induced ejected Auger electrons. These electrons at low energies correspond to a mean free path between 0.3 nm (at ejection energies of about 50 eV) and 5 nm (at about 1500 eV). The mean free path on the other hand is directly related to the information depth covered by Auger-electron detection.

In this contribution, we review short-time effects in ion tracks and report on non-linear effects related to the extremely dense energy deposition of heavy ions at velocities around 10% the speed of light. In contrast to individual photons or electrons, swift heavy ions can produce highly excited electronic target systems [1] with multiply overlapping excitations such as excitons or plasmons. In fact, the power deposition by a single highly charged ion is comparable to a focused multi-photon pulse of future free-electron hard-x-ray lasers.

2. CONTENTS

Qualitative and quantitative results on electronic short-time effects in ion tracks are deduced from high-resolution Auger-electron spectra for different inner-shell configurations. The investigation of these different configurations corresponds to Auger-decay times of 1–10 fs (10^{-15} to 10^{-14} s) and yields snapshots of the initial time evolution of ion tracks.

The Auger peak intensity and energy contains information on the ionization degree and on collective electrostatic potentials [2]. The energy width of the Auger peak contains information about the populated density of states in the valence/conduction bands [3] and may yield the corresponding electron temperatures if a local thermal equilibrium is achieved. Complete ionization of all light atoms along the ion track results from the penetration of an individual ion. The remaining as well as the charge neutralizing electrons will rapidly equilibrate at electron temperatures of up to 100 000 K. Thus, locally there is extremely strong excitation accompanied by the breaking of all bonds inside a nanometer radius along the straight ion path. This excited solid-state volume may reach a length of hundreds of μm, corresponding to a very high aspect ratio of the electronically distorted cylinder.

The high electron temperatures should have an influence also on the angular distribution of emitted Auger electrons, since the electron transport to the surface will be affected. Such an influence will be reported at the workshop for 592 MeV Au^{48+} ions at normal incidence on atomically clean beryllium (Be) and aluminum (Al) surfaces.

3. REFERENCES

[1] G. Schiwietz et al., NIM-B225, 4 (2004).
[2] G. Xiao et al., Phys. Rev. Lett.79, 1821 (1997); G. Schiwietz et al., Phys. Rev. Lett.69, 628 (1 992).
[3] F. Staufenbiel et al., NIM-B230, 426 (2005); G. Schiwietz et al., Europhys. Lett.47, 384 (1999).

* E-mail: schiwietz@hmi.de

ION BEAM-INDUCED ELECTRON EMISSION FROM CARBON-BASED MATERIALS

*A.M.Borisov**

Institute of Nuclear Physics, Moscow State University, 119992 Moscow, Russia

1. INTRODUCTION

In this overview, the regularities of ion beam-induced electron emission from modified surface layers of different carbon-based materials under high-dose irradiation are outlined. The materials considered here are those whose bonding is sp^2 – that is, polygranular graphites (PGG), highly oriented pyrolytic graphites (HOPG) and glassy carbons (GC) [1,2]. The results are discussed in terms of accumulation and annealing of the radiation damage and its effect on electron transport in carbon-based materials. The electron transport is known plays essential role in a truck formation and inelastic sputtering in heavy ion-surface collisions [3]. Discovered decrease of secondary electron path length under ion-induced disordering of crystal lattice is the first experimental confirmation of the difference of electron interaction with amorphous solids and crystals.

2. EXP. RESULTS AND DISCUSSION

For all carbon-based materials a step-like increase of ion-induced electron emission yield γ with increasing target temperature (T = 20 – 350°C) under high-dose (10^{18} – 10^{19} ion/cm^2) tens keV ions (N_2^+, Ar^+) normal incidence at an certain annealing temperature T_a takes place, see fig.1 [4-8]. It has been appeared that the step-like $\gamma(T)$-dependencies are due to the ion-induced structure transition in carbon-based materials from a high degree of disorder at $T<T_a$ into a relatively ordered structure at $T>T_a$. The secondary electrons before their escape from a solid experience flux attenuation due to scattering on a lattice, the implanted particles and the radiation defects. The radiation damage annealing results to an increase of γ at T_a due to a decrease of electron flux attenuation in the ordered structure of carbon materials. For different types of materials T_a is different. For GC ion-induced disordering is observed only for materials with sufficiently high temperature of the treatment due to fullerene-related nanostructures [2]. An analysis based on the theory of kinetic ion-induced electron emission connects the behavior of $\gamma(\theta, T)$ to the dependence of both secondary electron path length λ and primary ion ionizing path length R_e on lattice structure that is drastically changed due to damage creation.

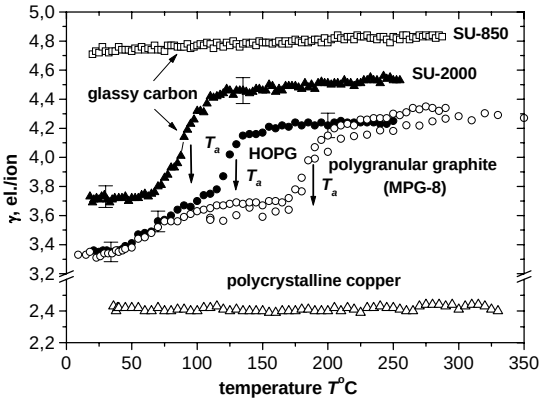

Figure 1. The temperature dependencies of γ for the carbon-based materials under 30 keV N_2^+ ion irradiation at normal incidence (θ = 0). For Cu_{poly} γ is independent of target temperature.

In particular, it was found that for HOPG at grazing ion incidence when the recovery of its structure takes place electron path length λ_p across the graphite layers is less than λ_{poly} in PGG. Moreover, the experimental evidence is now found, that λ_n along the graphite layers in HOPG two folds more than λ_p [9].

3. REFERENCES

[1] T. D. Burshell, MRS Bulletin **22,** 4, 29 (1997)
[2] P.J.F. Harris, Phil. Mag. **84**, 3159 (2004).
[3] D. Fink, L. T. Chadderton, Rad. Effects Def. Solids **160,** 67 (2005)
[4] A. M. Borisov, W. Eckstein, E. S. Mashkova, J Nucl Mater **15**, 304 (2002).
[5] A. M. Borisov, E. S. Mashkova, A. S. Nemov, Vacuum **73**, 1, 65 (2004).
[6] A. M. Borisov, E. S. Mashkova, A. S. Nemov, E. S. Parilis, Vacuum **80**, 295 (2005).
[7] A. M. Borisov, E. S. Mashkova, A. S. Nemov, E. S. Parilis, Nucl Instrum Methods B **230**, 1-4, 443 (2005).
[8] A. M. Borisov, Yu. S. Virgilev, E. S. Mashkova, A. S. Nemov, E. S. A.I.Sorokin, Fisika i chimia obrabotki materialov **1**, 27 (2005) (in Russian)
[9] S. Cernusca, M. Fürsatz, HP. Winter, F. Aumayr, Europhysics Letters, **70**, 6, 768 (2005).

* E-mail: borisov@anna19.npi.msu.su

ELECTRON EJECTION IN COLLISIONS BETWEEN SWIFT HEAVY IONS AND ATOMS

P. Sigmund[1] *and A. Schinner*[2]

[1] Department of Physics and Chemistry, University of Southern Denmark, DK-5230 Odense M, Denmark
[2] Institut für Experimentalphysik, Johannes-Kepler-Universität, A-4040 Linz-Auhof, Austria

1. GENERAL

The energy spectrum of electrons ejected from ion-atom collisions is an essential ingredient in the understanding of kinetic electron emission from solids under ion bombardment as well as other radiation effects such as formation of particle tracks. Existing theory has been summarized in refs. [1, 2].

We have applied the physical model underlying our binary theory of heavy-ion stopping [3] to the calculation of single-differential cross sections for energy transfer and electron ejection [4]. Binary stopping theory is essentially classical and, hence, applicable to the range of beam velocities $v < 2Z_1 v_{\rm Bohr}$, which is complementary to the Born regime.

Binary theory has been applied successfully to the stopping of heavy ions [5]. In comparison with conventional binary-encounter theory, binary stopping theory incorporates a realistic description of the binding of target and projectile electrons and higher-order Z_1 effects, as well as a realistic model for screening of the projectile charge. In comparison with classical-trajectory Monte Carlo simulation, the present model allows prediction of scaling laws and requires moderate computation times.

2. RESULTS

We present differential cross sections as well as ionization cross sections for a number of ion-target combinations and charge states. Emphasis is laid on scaling laws and their experimental verification as well as quantitative comparison with pertinent measurements.

Figure 1 shows, as an example, calculated differential cross sections for energy transfer T to electrons of atomic helium under bombardment with bare carbon and anticarbon ions. Numbers denote the value of the Bohr variable

$$\xi = mv^3/Z_1 e^2 \omega, \tag{1}$$

where $\omega = I/\hbar$ is related to the mean logarithmic excitation energy I, the 'I-value'. The plot makes use of the scaling variables

$$t = \frac{T\xi^2}{2mv^2} \tag{2}$$

* E-mail: psi@dou.dk

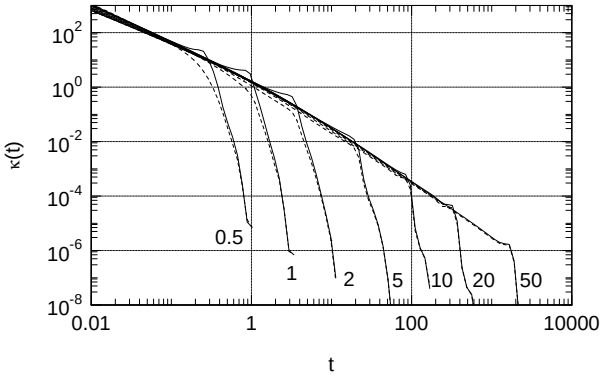

Figure 1: Calculated differential cross sections for energy transfer to electrons of atomic helium under bombardment with bare carbon and anticarbon ions. Solid lines: Bare carbon ions; broken lines: anticarbon ions. Labels indicate the value of the Bohr variable ξ, eq. (1).

and

$$\kappa(t) = \left(\frac{\omega}{v}\right)^2 \frac{d\sigma}{dt}. \tag{3}$$

The difference between carbon and anticarbon (Barkas effect) is most pronounced at the lowest beam velocities and vanishingly small for $\xi > 10$.

3. REFERENCES

[1] ICRU, *Secondary electron spectra from charged particle interactions*, Vol. 55 of *ICRU Report* (International Commission of Radiation Units and Measurements, Bethesda, Maryland, 1996)

[2] N. Stolterfoht, R.D. DuBois, R.D. Rivarola, *Electron emission in heavy ion-atom collisions*, Springer Series on Atoms and Plasmas (Springer, Berlin, 1997)

[3] P. Sigmund, A. Schinner, Europ. Phys. J. D **12**, 425 (2000)

[4] M.S. Weng, A. Schinner, A. Sharma, P. Sigmund, Europ. Phys. J. D p. online first (2006)

[5] ICRU, *Stopping of ions heavier than helium*, Vol. 73 of *ICRU Report* (Oxford University Press, Oxford, 2005)

X-RAY EMISSION FROM HOLLOW ATOMS

G. Xiao[1,*], *Y. Zhao*[1], *X. Zhang*[1], *Z. Yang*[1], *X. Chen*[2], *F. Li*[3], *Y. Zhang*[1], *and W. Zhan*[1]

[1] Institute of Modern Physics, Chinese Academy of Science, Lanzhou 730000
[2] Institute of Physics, Lanzhou University, Lanzhou 730000
[3] Department of Applied Physics, Xi'an Jiaotong Uiversity, Xi'an 710049

1. INTRODUCTION

Detecting the X-rays in the collision of highly charged ions with solid surface is of significance in the investigation of the inner-shell charge transfer reactions between the projectile ions and the target atoms. The X-ray spectra can both supply the test of theoretical models and provide sensitive diagnostic means for the hot plasma [1-4].

In this paper, the recent measurements of X-rays induced in the interaction of highly charged ions with a beryllium surface are reported. The character of the X-ray spectra and the two electrons, one photon (TEOP) transitions from hollow atoms are discussed.

2. RESULTS AND DISCUSSIONS

2.1. The character of the X-ray spectra from hollow atoms

In Fig.1, the X-rays induced by Ar^{17+} ions interacting with the beryllium surface is compared with the X-rays induced by the same ions interacting with the residual gases. It is obvious that the X-ray spectrum of hollow atoms (upper) is lower in energy and broader in width than that of highly charged ions (below).

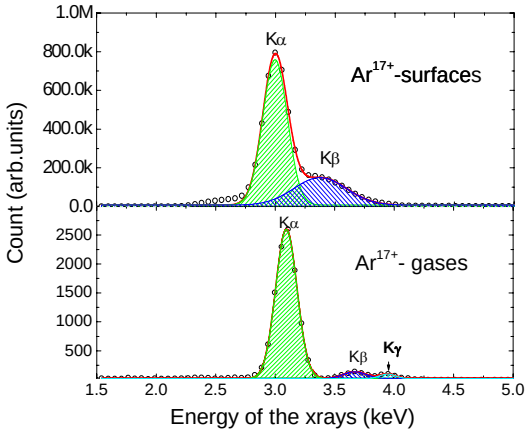

Figure 1: X-rays in the Ar^{16+} ion-surface collisions

2.2. TEOP transitions from hollow atoms

The Kαα and Mαα TEOP transitions in the collisions of $Ar^{17+, 18+}$ and $Xe^{28+, 29+, 30+}$ ions with a beryllium surface are shown as Fig.2 and Fig.3, respectively.

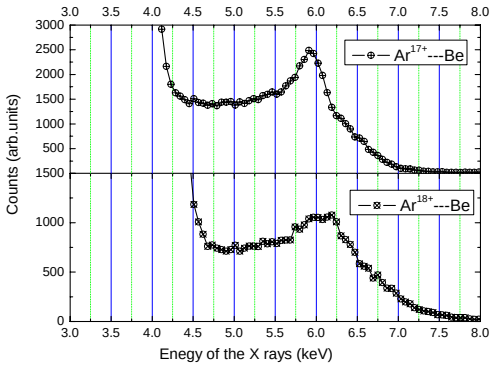

Figure 2: TEOP transitions in the Ar^{q+}-surface collisions.

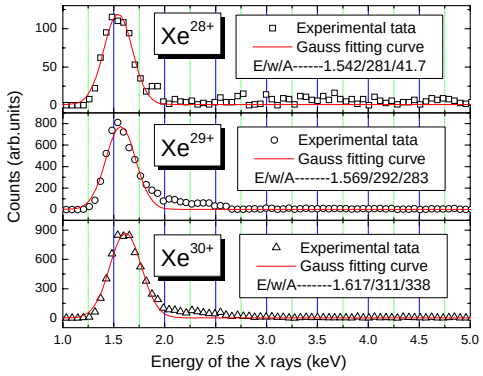

Figure 3: TEOP transitions in the Xe^{q+}-surface collisions.

3. REFERENCES

[1] J.-P. Briand, G. Giardino and G. Borsoni et al., Phys. Rev.A, 1996(54): 4136-4139.
[2] W. Wölfli, Ch. Stoller and G. Bonani et al., Phys. Rev. Lett. 1975(35): 656-659.
[3] Y. Zhao, G. Xiao, X. Zhang et al., Nucl. Inst. Meth. B, 2006(245):72-75.
[4] F.B. Rosmej et al., Phys. Rev. A, 2001(63): 032716.

* E-mail: xiaogq@impcas.ac.cn

LOCAL SPIN POLARIZATION AT SURFACES PROBES BY HOLLOW ATOMS

M. Unipan[*], *A. Robin, R. Morgenstern and R. Hoekstra*

KVI, Atomic Physics, Rijksuniversiteit Groningen
Zernikelaan 25, 9747 AA Groningen, The Netherlands

1. INTRODUCTION

Auger electron emission from hollow atoms formed in front of surfaces can be used as a probe of surface spin polarization, by linking the spectral peak intensities to the capture probability of parallel or anti-parallel spins. Realizing that slow, multiply charged ions capture electrons from a surface area of a few $Å^2$, this new method is suitable for determining the local spin ordering of magnetic surfaces. The potential of the technique is illustrated by He^{2+} and N^{6+} ions impinging on a ferromagnetic Ni(110) surface.

2. MULTIPLE ELECTRON CAPTURE SPECTROSCOPY

In recent years, highly spin polarized materials, like e.g half-metals, have been intensively studied for their potential in spin electronics. A direct access to the degree of surface spin polarization is indispensable in understanding the properties of these materials. Here we introduce a new method for probing the spin polarization of the top-most surface layer, namely MECS (Multiple Electron Capture Spectroscopy). We used KLL Auger electron emission originating from the interaction of slow He^{2+} and N^{6+} ions with a Ni(110) surface. The neutralization of multiply charged ions in front of a surface can be described by the classical over-the-barrier model [1]. The capture probability of electrons into specific spin states depends on the density of surface majority and minority electrons. For a highly spin polarized surface, on average high spin states will be more likely to be populated, while for a low surface spin polarization occupation of low spin states becomes more probable. Subsequently, the excited atoms fill their inner shell vacancies by Auger electron emission. The relative peak intensities in the Auger spectra will change as the polarization of the surface changes (e.g, by varying the temperature of a ferromagnetic surface). For illustration, a series of KLL Auger spectra from 20 eV He^{2+} ions impinging under 20° incidence on a Ni(110) surface is shown in Fig. 1, for different temperatures of the target. The lower energy peak, at $\sim$ 34.5 eV, has a triplet contribution, while the peak at $\sim$ 36 eV is purely singlet. As the temperature of the surface increases (thus its polarization decreases), the (relative) intensity of the triplet peak decreases drastically, consistent with the suppression of the electron capture probability into triplet states. The peak intensity ratio can be linked to the electron capture probability into singlet or triplet states, and the temperature dependency of the surface spin polarization can be extracted by making use of an atomic model [2].

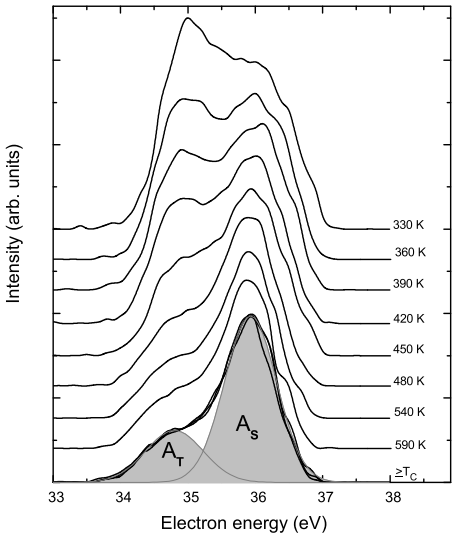

Figure 1: Normalized KLL Auger spectra from 20 eV He^{2+} ions impinging under 20° incidence on Ni(110), for different temperatures of the target crystal.

3. REFERENCES

[1] J. Burgdörfer,P. Lerner and F.W. Meyer, Phys. Rev. A **44**, 5674 (1991).

[2] M. Unipan, A. Robin, R. Morgenstern, R. Hoekstra, Phys. Rev. Lett. **96**, 177601 (2006).

[*] E-mail: unipan@kvi.nl

ELECTRON EMISSION DURING SCATTERING OF N^{6+} IONS FROM A MAGNETIZED IRON SURFACE

B. Solleder[1,*], *C. Lemell*[1], *K. Tőkési*[2], *and J. Burgdörfer*[1]

[1] Institute for Theoretical Physics, Vienna University of Technology, A-1040 Vienna, Austria
[2] Institute of Nuclear Research of the Hungarian Academy of Sciences (ATOMKI), H-4001 Debrecen, P.O. Box 51, Hungary

A detailed understanding of the properties of magnetized surfaces is important in view of many technical applications. Spectroscopy of such surfaces using highly charged ions (HCI) has emerged only recently [1, 2]. We focus on extracting information on spin polarization by electron emission during HCI-surface interaction.

We investigate the impact of N^{6+} ions on a magnetized iron surface using Monte Carlo simulations. Our calculations include potential emission of electrons as well as production and transport of secondary electrons in the solid. Potential emission is modelled using the Classical-Over-the-Barrier (COB) model [3]. Several channels for electron exchange during the ion-surface interaction are implemented, such as resonant transfer, autoionization, Auger processes, and peeling-off of outer shell projectile electrons. Electron transport in the solid is simulated as a stochastic sequence of elastic and inelasting scattering processes [4]. Cross sections for elastic scattering were based on Dirac partial-wave analysis [5], for inelastic collisions the dielectric function formalsism was used [6]. In addition to spin conserving scattering, Stoner excitations are taken into account leading to an enhancement of the polarization for very low emission energies in agreement with measurements by J. Kirschner *et al.* [7].

Spin flip in elastic scattering is neglegible because of vanishing values of the Sherman function in the energy range considered.

We apply the present theory to an experiment performed by R. Pfandzelter *et al.* [1], investigating 150 keV N^{q+} ions ($q \leq 6$) scattered from a magnetized Fe(001) surface under a grazing angle of incidence of $\Phi = 1.5°$. For K-Auger electrons of N^{6+}, polarization values are close to the mean polarization of the conduction band electrons in magnetic iron (27%). For low energies an increase of the polarization up to 70% is detected. Especially for high energies, where potential emission provides the only relevant contribution to the electron yields, our results show good agreement with the experimental values.

This work has been supported by Austrian Science Foundation FWF (Project No. P17449-N02).

E-mail: beate@concord.itp.tuwien.ac.at

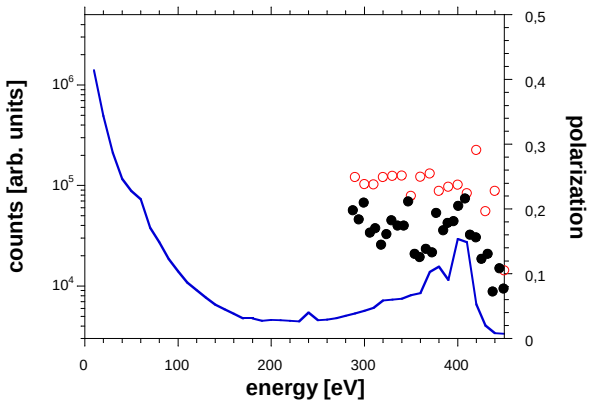

Figure 1: energy spectrum (solid line, left axis) and polarization (full circles: experiment [1], open circles: our calculation, right axis) of electrons emitted during the impact of N^{6+} ions on a magnetized Fe surface

1. REFERENCES

[1] R. Pfandzelter, T. Bernhard and H. Winter, Phys. Rev. Lett. **86**, 4152 (2001)

[2] M. Unipan, A. Robin, R. Morgenstern, and R Hoekstra, accepted for Phys. Rev. Lett. (2006)

[3] J. Burgdörfer, P. Lerner and F. W. Meyer, Phys. Rev. A **44**, 5674 (1991)

[4] K. Tőkési, D. Varga, L. Kövér, and T. Mukoyama, Journal of Electron Spectroscopy and Related Phenomena **76**, 427 (1995)

[5] F. Salvat, A. Jablonski, and C. J. Powell, Comp. Phys. Comm. **165**, 157 (2005)

[6] K. Tőkési, L. Wirtz, C. Lemell, and J. Burgdörfer, Phys. Rev. A **64**, 042902 (2001)

[7] J. Kirschner and K. Koike, Surf. Sci. **273**, 147 (1992)

Conference Outing to Schneeberg, the highest mountain in Lower Austria (Alt. 2076m)

Beginning at the Puchberg am Schneeberg train station, our train takes you up into the high alpine region of the Schneeberg mountain. As you ascend rich green meadows, the luscious scent of pine forests and the magnificent breathtaking panorama of the Alps pass by at a leisurely pace. Finally you will reach your destination at 1,795 metres above sea level, the highest train station in Austria.

Going there....

Departure of buses at conference site (lunch box will be provided):	12h15 (sharp)
Departure of rackrailway train in Puchberg (Alt. 577m):	13h30
Possible exit at station “Baumgartner” (Alt. 1400m, Map: [2]),	
to hike up the rest guided by Hannspeter Winter:	14h05
This hike to station Hochschneeberg (Map: [1]) takes about 60 min one-way	
Arrival of the train at station Hochschneeberg (Alt. 1795m, Map: [1]):	14h20

At Schneeberg, possibilities to go to:

- Visit the Mountain restaurant “Damböckhaus” (Map: [3]): ~15 min walk one-way
- Stay close to station Hochschneeberg (Map: [1]), the nearby Hotel Hochschneeberg and the chapel “Elisabethkirchlein”, commemorating the former Empress of Austria, Kaiserin Elisabeth I., better known as “Sissy”
- For experienced hikers: hike up to the summit “Klosterwappen” (Alt. 2076m, Map: [4]): ~55 min walk one-way
- Hike down again to station “Baumgarten” (50 min walk) and wait for the train to pick you up

WARNING:

Though well connected to the valley by the railway, the Schneeberg is an alpine mountain region, with possible hazards e.g. in case of unexpected weather changes.
We recommend to stay in a group with one of the local organizers or stay at the footpathes depicted in the map. In case of emergency call with your cell phone one of the local organizers (e.g. +43 – 650 - 7552466) or the international emergency number 112.
In any case, watch the time to be back for train departure at 16h30 (sharp) !!

Getting back...

Departure at station Hochschneeberg (Map: [1]):	16h30 (sharp)
Be on time, the train *will not wait* !!	
Pickup of downhill hikers at station “Baumgartner” (Map: [3]):	16h35
Arrival in Puchberg:	17h20
Departure of buses from the railway station in Puchberg:	17h30
Arrival at the Heurigen “Weiszbart” in Leobersdorf, Mariazellergasse 5:	18h30
Buses back to conference site at Schloss Hernstein:	21h30

Alternative Outing (bad weather)
Medieval Forchtenstein Castle

Timetable:

Departure of buses at conference site in Hernstein:	12h45
Arrival at the castle:	13h45
Guided Tour of Forchtenstein Castle:	14h00
Departure of buses from the Castle:	17h15
Arrival at the Heurigen “Weiszbart” in Leobersdorf:	18h00
Buses back to conference site:	21h30

List of participants and accompanying persons

1	**Abdallah**	Wael	Canada
2	**Aldazábal**	Inigo	Spain
3	**Arnold-Bik**	Wim	Netherlands
4	**Aumayr**	Friedrich	Austria
5	**Ban-d'Etat**	Brigitte	France
6	**Bauer**	Peter	Austria
7	**Bertagnolli**	Emmerich	Austria
8	**Borisov**	Anatoly	Russia
9	**Burgdörfer**	Joachim	Austria
10	**Chakraborty**	Purushottam	India
11	**Crichton**	Hilary	Great Britain
12	**Dunning**	Barry	USA
13	**Dunning**	Christine	USA
14	**Duvenbeck**	Andreas	Germany
15	**Echenique**	Pedro	Spain
16	**El-Said**	Ayman	Austria
17	**Endstrasser**	Nikolaus	Austria
18	**Facsko**	Stefan	Germany
19	**Gauyacq**	Jean-Pierre	France
20	**Golczewski**	Artur	Austria
21	**Gou**	Fujun	Netherlands
22	**Gravielle**	Maria	Argentina
23	**Griesmayer**	Erich	Austria
24	**Grizzi**	Oscar	Argentina
25	**Gutierrez**	Fernando	Chile
26	**Heiland**	Tilde	Germany
27	**Heiland**	Werner	Germany
28	**Hoekstra**	Ronnie	Netherlands
29	**Huber**	Bernd	France
30	**Husinsky**	Wolfgang	Austria
31	**Ikegami**	Seiji	Japan
32	**Insepov**	Zeke	USA
33	**Jouin**	Hervé	France
34	**Juaristi**	Joseba Inaki	Spain
35	**Kanai**	Yasuyuki	Japan
36	**Kaneko**	Akemi	Japan

37	**Kaneko**	Toshiaki	Japan
38	**Kato**	Masahiko	Japan
39	**Keller**	Adrian	Germany
40	**Khalal-Kouache**	Karima	Algeria
41	**Kimura**	Kenji	Japan
42	**Koshikawa**	Ryuko	Japan
43	**Koshikawa**	Takanori	Japan
44	**Laskin**	Julia	USA
45	**Lebius**	Henning	France
46	**Lemell**	Christoph	Austria
47	**Lemell**	Julia	Austria
48	**Lenoir**	Jérome	France
49	**Linsmeier**	Christian	Germany
50	**Marik**	Manuela	Austria
51	**Märk**	Tilmann	Austria
52	**Markin**	Sergey	Austria
53	**Martiarena**	Maria	Argentina
54	**Meissl**	Walter	Austria
55	**Meyer**	Fred	USA
56	**Michely**	Thomas	Germany
57	**Morgenstern**	Reinhard	Netherlands
58	**Morita**	Kenji	Japan
59	**Nakagawa**	Sachiko	Japan
60	**Nojima**	Masashi	Japan
61	**Peters**	Thorsten	Germany
62	**Pomeroy**	Josh	USA
63	**Primetzhofer**	Daniel	Austria
64	**Rasulev**	Utkur	Uzbekistan
65	**Reinelt**	Matthias	Germany
66	**Reinhold**	Carlos	USA
67	**Riccardi**	Pierfrancesco	Italy
68	**Romanyuk**	Andriy	Switzerland
69	**Roncin**	Philippe	France
70	**Roth**	Joachim	Germany
71	**Rothard**	Hermann	France
72	**Sakuma**	Yasuhiro	Japan
73	**Schiessl**	Klaus	Austria
74	**Schiwietz**	Gregor	Germany
75	**Schleberger**	Marika	Germany
76	**Schruff**	Johanna	Germany
77	**Schustereder**	Werner	Germany
78	**Sigmund**	Peter	Denmark
79	**Sindona**	Antonio	Italy

80	**Skog**	Patrik	Sweden
81	**Solleder**	Beate	Austria
82	**Stolterfoht**	Nikolaus	Germany
83	**Takaoka**	Gikan	Japan
84	**Terasawa**	Emiko	Japan
85	**Terasawa**	Mititaka	Japan
86	**Tomita**	Mitsuhiro	Japan
87	**Tona**	Masahide	Japan
88	**Unipan**	Mirko	Netherlands
89	**Vernhet**	Dominique	France
90	**Vincent**	Remi	Spain
91	**Wethekam**	Stephan	Germany
92	**Winter**	Hannspeter	Austria
93	**Winter**	Helmut	Germany
94	**Wodtke**	Alec	USA
95	**Wucher**	Andreas	Germany
96	**Xiao**	Guoqing	P. R. China
97	**Yamazaki**	Yasunori	Japan
98	**Zech**	Julia	Germany
99	**Zeijlmans van**	Pedro	Netherlands
100	**Zschornak**	Günter	Germany

Map of Hernstein

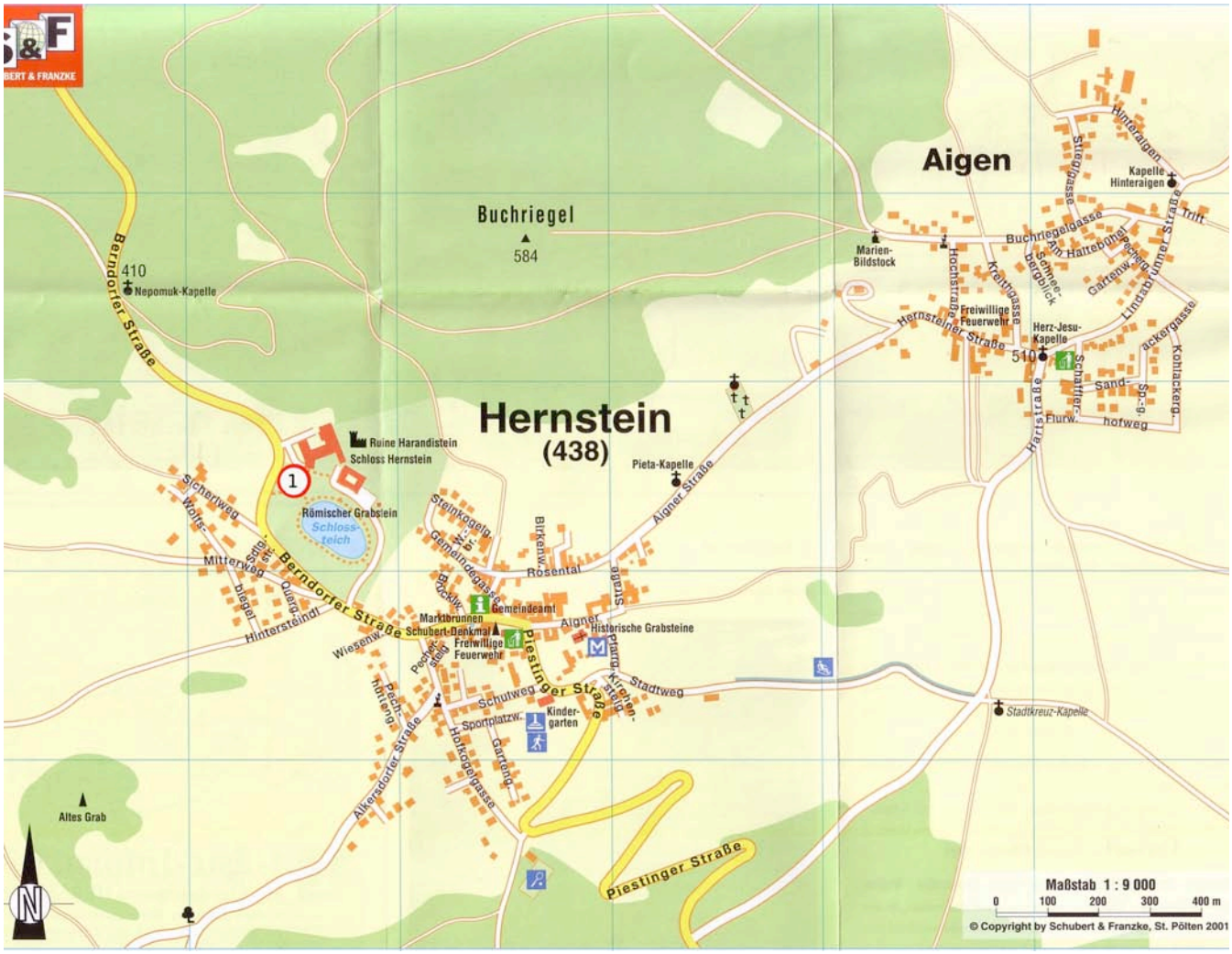

The conference location "Schloss Hernstein" is marked by a circle numbered 1.

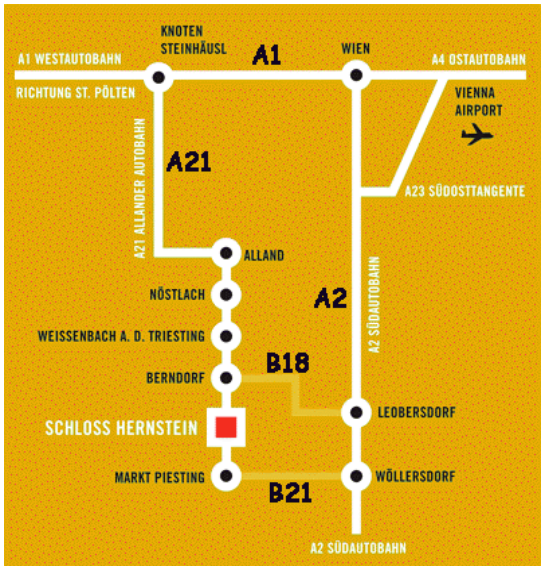

16th International Workshop on Inelastic Ion-Surface Collisions (IISC-16)

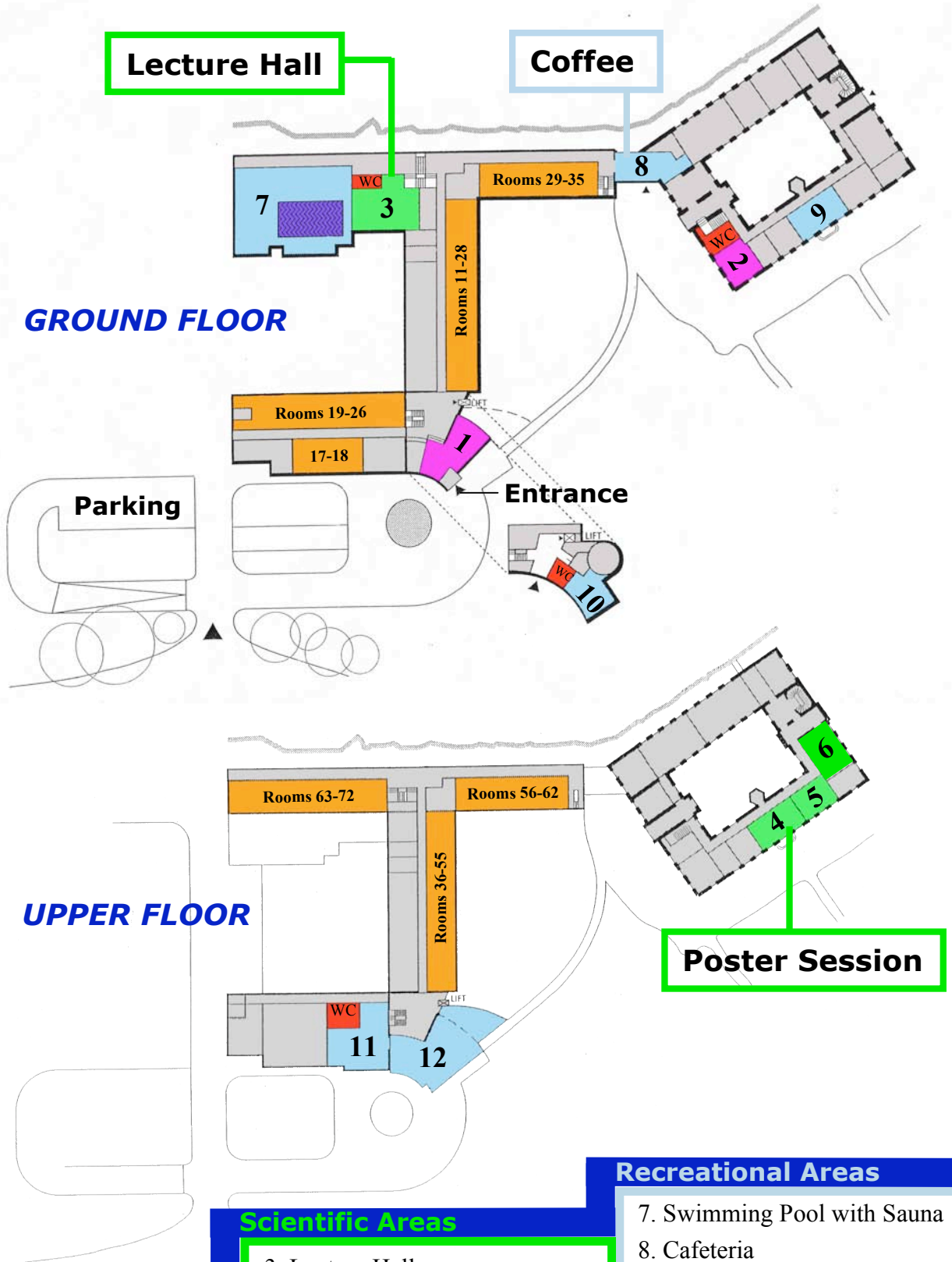

Administrative Areas

1. Registration
2. Office of the Local Organizing Committee, Editorial Office

Scientific Areas

3. Lecture Hall
4. Poster Session Room 1
5. Poster Session Room 2
6. Scientific Committee Meeting (Monday Evening)

Recreational Areas

7. Swimming Pool with Sauna
8. Cafeteria
9. Lounge
10. Fitness Room
11. Bar/Club
12. Restaurant with Terrace

16th International Workshop on Inelastic Ion-Surface Collisions (IISC-16)

Sept. 17 - 22, 2006
Schloss Hernstein, A-2560 Hernstein, Austria

organized by TU Wien
Friedrich Aumayr (chairman)

PL 40‘+5‘
I 25‘+5‘
O 15‘+5‘

Sunday, 17. Sept. 2006

15:00	REGISTRATION
17:30	WELCOME RECEPTION
18:30	DINNER

Monday, 18. Sept. 2006

07:15	BREAKFAST
08:30 - 08:45	OPENING
08:45 - 09:30	YAMAZAKI (PL)
09:30 - 10:00	SKOG (I)
10:00 - 10:20	SCHIESSL
10:20	COFFEE
10:50 - 11:20	WETHEKAM (I)
11:20 - 11:40	RONCIN
11:40 - 12:00	MARKIN
12:15	LUNCH
14:00 - 14:30	TONA (I)
14:30 - 14:50	EL-SAID
14:50 - 15:20	INSEPOV (I)
15:20 - 15:40	ROTHARD
15:45	COFFEE
16:15 - 16:45	MÄRK (I)
16:45 - 17:15	GRIZZI (I)
17:15 - 17:35	LASKIN
17:35 - 17:55	MARTIARENA
18:30	DINNER
20:00	COMMITTEE MEETING

Tuesday, 19. Sept. 2006

07:15	BREAKFAST
08:30 - 09:15	ECHENIQUE (PL)
09:15 - 09:45	HUBER (I)
09:45 - 10:15	VERNHET (I)
10:15	COFFEE
10:45 - 11:15	KIMURA (I)
11:15 - 11:45	GRAVIELLE (I)
11:45 - 12:05	ALDAZABAL
12:05 - 12:25	KATO
12:30	LUNCH
14:00 - 14:30	WUCHER (I)
14:30 - 14:50	POMEROY
14:50 - 15:50	POSTER INTRODUCTION A
15:50	COFFEE
16:00 - 18:30	POSTER SESSION A
18:30	DINNER
20:00	SPECIAL SESSION

Wednesday, 20. Sept. 2006

07:15	BREAKFAST
08:30 - 09:15	ROTH (PL)
09:15 - 09:45	MEYER (I)
09:45 - 10:05	REINELT
10:05	COFFEE
10:35 - 11:05	KOSHIKAWA (I)
11:05 - 11:35	CHAKRABORTY (I)
11:35 - 11:55	SINDONA
12:00	LUNCH
13:00 - 18:30	CONF. OUTING
18:30	“ HEURIGER“

Thursday, 21. Sept. 2006

07:15	BREAKFAST
08:30 - 09:15	WODTKE (PL)
09:15 - 09:45	DUNNING (I)
09:45 - 10:15	GAUYACQ (I)
10:15	COFFEE
10:45 - 11:15	MICHELY (I)
11:15 - 11:35	KELLER
11:35 - 12:05	BERTAGNOLLI (I)
12:15	LUNCH
14:00 - 14:30	ARNOLDBIK (I)
14:30 - 14:50	PETERS
14:50 - 15:20	GRIESMAYER (I)
15:20 - 16:15	POSTER-INTRO. B
16:15	COFFEE
16:30 - 19:00	POSTER SESSION B
19:30	CONFERENCE DINNER

Friday, 22. Sept. 2006

07:15	BREAKFAST
09:00 - 09:30	SCHIWIETZ (I)
09:30 - 10:00	BORISOV (I)
10:00 - 10:20	SIGMUND
10:20	COFFEE
10:45 - 11:15	XIAO (I)
11:15 - 11:45	UNIPAN (I)
11:45 - 12:05	SOLLEDER
12:05	CLOSING
12:15	LUNCH
	DEPARTURE